Towards improved predictions of growth and metabolism in the animal kingdom

by

Laura Lee

Thesis submitted in accordance with the requirements of the University of Liverpool for the degree of Doctor in Philosophy.

December 2020

Dedication

For my grandad, James Lee, whose passion for science will forever inspire me.

Acknowledgements

I would like to thank my supervisor Professor David Atkinson and my secondary supervisors, Professor Andrew Hirst and Doctor Stephen Cornell, for their continued support, guidance and help throughout my PhD. David and Andrew, thank you both for your insight and mentoring into the subject matter. Stephen, thank you for your time and patience in teaching me how to become R-fluent. I am grateful to the Natural Environment Research Council who funded this PhD, and without which this research would not be possible. A huge thank you to my friends and family for their support throughout my PhD. To my parents, Julie and John, thank you for always supporting me and nourishing my passion for science. My sister, Katie, thank you for always being there for me and humouring all my science facts. Lastly, I would like to thank my husband, Laurence, for his encouragement and positivity – you have been my rock throughout this roller coaster of a journey.

Contributions statement

This complete thesis was written by Laura Lee (LL) and was developed with comments and feedback from supervisors David Atkinson (DA) and Andrew Hirst (AH) which helped to improve the thesis throughout. The research aims and hypothesis for Chapter 2 were developed by LL, DA and AH, and the methods by LL and Stephen Cornell (SC). Specifically, SC carried out the mathematical derivations, and LL and SC both contributed to writing the R code for the growth models. LL performed all data collection and data analysis for Chapter 2.

The research aims, hypotheses and methods for Chapters 3 were developed by LL, DA and AH. LL conducted the data collection for all growth data and performed all analyses reported in Chapter 3. For Chapter 4, the research aims, hypotheses and methods were developed by LL and DA. LL solely conducted the laboratory experiment and data analysis. Chapter 5's aims, hypotheses and methods were developed by LL and DA. Data collection and analysis was solely conducted by LL.

Abstract

Towards improved predictions of growth and metabolism in the animal kingdom

By

Laura Lee

Metabolism is a fundamental process of life that fuels vital biological processes including growth. The rates of metabolism and growth often correlate with other biological and ecological traits, including body size, in distinct ways. Thus, understanding variation in the body mass-scaling of growth and metabolic rate is an important area of research when studying the ecology, evolution and life histories of organisms. The overall aim of this thesis is to improve predictions of animal growth and metabolic rates, and to explain variation in these processes. Many methods for estimating individual growth rates (rate of mass increase over time) impose invalid assumptions, such as isomorphic (shape-invariant) growth. This thesis proposes a new growth curve fitting framework that relaxes the assumption of isomorphy and can capture marked diversity of growth curves, including exponential and supra-exponential body mass change. Furthermore, because growth is fuelled by metabolism, the mass-scaling exponent of growth (A) and the mass-scaling exponent of metabolic rate (b_R) are predicted to positively correlate. This was explored across pelagic invertebrate species and within two oligochaete species over ontogeny. No significant relationship between A and b_R was found, suggesting organisms may differ in their proportion of metabolised energy allocated to growth and to other processes, such as locomotion, over ontogeny. In addition, I explored the relationship between A and known predictors of b_R: (i) the mass-scaling of body surface area (b_A), which may capture changes in surface area-mediated resource uptake over ontogeny for integument breathing organisms, and (ii) ambient temperature, which often correlates with body size at maturity in ectotherms and may correlate with b_R by influencing the energetic demand of locomotion over ontogeny. No significant correlations between A and b_A, or between A and temperature, were found for pelagic invertebrate species

or two oligochaete species, suggesting that the rates of growth and metabolism may differ in their response to different intrinsic and extrinsic factors. To improve current understanding of the variation in metabolic rate, I explored potential predictors of b_R for pelagic invertebrate species and two oligochaete species (b_A), and mammal species (ambient temperature and reproductive parity). Ambient temperature, but not reproductive parity, was shown to be a predictor of variation in basal metabolic rate responsible for curvature patterns across mammals. A significant correlation between b_R and b_A was found for an aquatic, but not a terrestrial oligochaete species or diverse species of pelagic invertebrates. A positive relationship between b_R and b_A suggests surface area-mediated changes in resource uptake over ontogeny may be shaping metabolic scaling relationships within an aquatic oligochaete. Overall, this research highlights the importance of considering both intrinsic (e.g. body shape and size) and extrinsic factors (e.g. ambient temperature) when exploring variation in the scaling of growth and metabolic rate. Ultimately, this perspective differs from previous approaches that focus on a single-cause mechanistic explanation or universal law; rather this thesis applies a multi-mechanistic approach by considering multiple correlates, theories and mechanisms to provide a more comprehensive understanding of the diversity in metabolic and growth scaling relationships.

Table of contents

Chapter 1. General introduction

1.1. Introduction to the body-mass scaling of metabolic rates

Living organisms occur in a wide range of body masses that span 24 orders of magnitude (Demetrius, Legendre and Harremöes, 2009). Many physiological, ecological and evolutionary traits have been shown to vary with body mass (Davies, 1966; Green, 2015; Gutowsky *et al*., 2015; Holm *et al*., 2006; Illius & Gordon, 1992; Kwapich *et al*., 2018; Mayer *et al*., 2016; Mirth *et al*., 2016; Woodward *et al*., 2005). Hence, understanding how organismal traits, including biological rates, vary with body size – a phenomenon known as scaling – is imperative to understanding the biology, ecology and evolution of organisms. Commonly, biological traits (R) are proposed to vary with body mass (m) according to the equation:

$$R = am^b \tag{1.1}$$

where a is the scaling coefficient and b is the scaling exponent. Equation (1.1) is often subjected to logarithmic transformation to achieve a linear relationship between R and m, and to normalise the distribution of data points around the regression line (White and Seymour, 2003):

$$\log(R) = \log(a) + b\log(m) \tag{1.2}$$

Traditionally, it has been reported that metabolic rate varies with body mass according to equations (1.1) and (1.2) (Brody and Procter, 1932; Glazier, 2005; Kleiber, 1932; Kooijman, 2010), although deviations from this linear relationship have been reported and will be discussed below. Metabolism is a fundamental process of all life, and fuels vital physiological and biochemical activities. Within an individual, the process of metabolism involves the uptake of energy and resources from the environment and its conversion into new biomass. Within an organism, metabolism process involves both anaerobic (in the absence of oxygen) and aerobic (requires oxygen) pathways to convert resources into metabolised energy (Clarke, 2019). Individual rates of metabolism are most commonly estimated as the rate of aerobic respiration (specifically as oxygen consumption rate) or heat production. Several methods of measuring an organism's metabolic rate can be used and result in different types of

metabolic rate. These can include: (i) basal metabolic rate (BMR), where individuals are in a post-absorptive state under thermo-neutral conditions and are non-reproducing (where thermo-neutral conditions, or thermoneutral zone, is defined as the range of ambient temperatures where no regulatory changes in metabolic heat production or evaporative heat loss occurs (Kingma and Frijns, 2012)), (ii) field metabolic rate (FMR) of individuals in the natural field environment (Speakman and Król, 2010a), (iii) standard metabolic rate (SMR) where individuals are in a resting and post-absorptive state in darkened conditions (Rosenfeld *et al*. 2015), (iv) routine metabolic rate where individuals are in a resting, post-absorptive state and normal random activity is allowed to occur (Killen, Marras and McKenzie, 2011), (v) active metabolic rate (AMR) for active individuals (Norin and Malte, 2011) and (vi) maximal metabolic rate (MMR) which represents the maximum metabolic rate that can be achieved by an individual at a given temperature (Norin and Malte, 2011). Thus, metabolic rate of an unfed individual can be classified as routine, resting or active depending on activity level.

Considering that organisms are a product of natural selection, it can be predicted under life history theory that organisms will have evolved the highest metabolic rates possible as a result of maximising the benefits from fuelling high rates of biological processes that affect fitness (e.g. growth and production) and minimising the costs of obtaining energy, such as an increased exposure to predators when foraging (McPeek, Grace and Richardson, 2001). Thus, understanding and explaining variation in the body mass-scaling of metabolic rate (the change in metabolic rate with body size) within (intra-specific, or ontogenetic, metabolic scaling) and across (inter-specific metabolic scaling) species is important to studies concerning the life history, ecology or evolution of organisms. Metabolic rate varies with body mass often in very distinct ways and explaining the causes and consequences of the variation in the relationship between these two terms has become an important field of study (Banavar *et al*., 2012; Brown *et al*., 2004; Glazier, 2005, 2010, 2020; Kolokotrones *et al*., 2010; Kooijman, 2010, West, Brown and Enquist, 1997, 1999).

Widespread variation in mass-scaling exponent of metabolic rate (b_R, see Figure 1) is observed both intra- and inter-specifically (see Glazier, 2005 for a review). Reported b_R values range between near-zero to greater than one, but generally

hypoallometry (where $b_R < 1$) is observed with b_R values mainly between $\frac{2}{3}$ and 1 (Glazier, 2014a,b). For example, there is significant variation in the inter-specific metabolic scaling exponents across major taxonomic groups of animals including mammals, birds and reptiles (White, Phillips and Seymour, 2006), and also within taxonomic groups such as mammals (Clarke, Rothery and Isaac, 2010; Griebeler and Werner, 2016a). The fact that widespread diversity in the scaling of metabolic rate is observed both across and within living organisms is both a puzzling and important topic to biology that has been intensely debated (Ballesteros *et al.*, 2018; Banavar *et al.*, 2010; Glazier, 2005b; Kooijman, 2010; Speakman and Król, 2010a,b; van der Meer, 2006a; West, Brown and Enquist, 1997, 1999). For example, a mechanistic explanation as to why smaller-sized species have evolved higher mass-specific metabolic rates than larger-sized species (hyperallometry of metabolic rate) is important for understanding coexistence of small- and large-sized species, and hence their fitness and evolution (Kozlowski, Konarzewski and Czarnoleski, 2020). Furthermore, because body size covaries with a plethora of physiological, ecological and evolutionary traits (Davies, 1966; Green, 2015; Gutowsky *et al*., 2015; Holm *et al*., 2006; Illius and Gordon, 1992; Kwapich *et al*., 2018; Mayer *et al*., 2016; Mirth *et al*., 2016; Woodward *et al*., 2005) and much of the variation in metabolic rate is linked to body size (Calder, 1985) providing a mechanistic explanation for the observed diversity in b_R is imperative to biology.

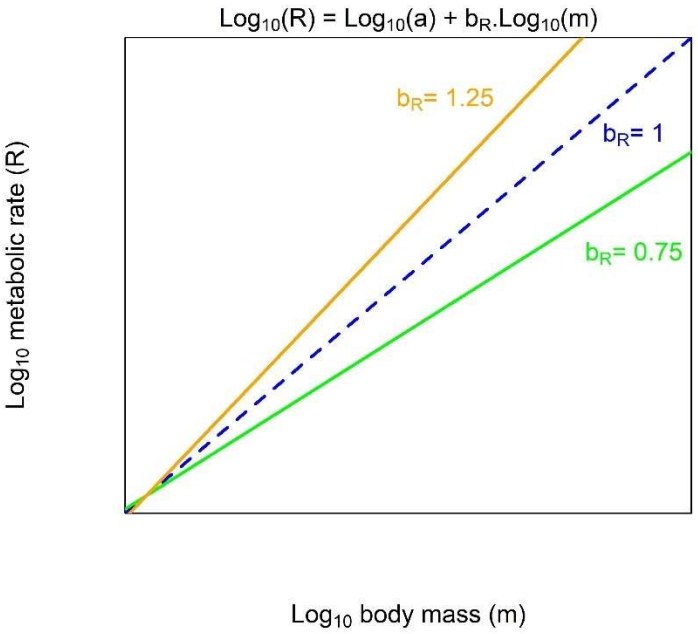

83

84 **Figure 1**. An illustration of the mass-scaling exponent of metabolic rate, b_R, which is
85 determined as the slope of a log-log plot of metabolic rate (R) versus body mass (m),
86 where $\log(R) = \log(a) + b_R \log(m)$ and a is the scaling coefficient. The dashed
87 blue line represents isometric scaling of metabolic rate with body size ($b_R = 1$). The
88 solid green and orange lines represent deviations from isometry, where $b_R = 0.75$ and
89 $b_R = 1.25$, respectively.

90

91 Despite widespread diversity in the scaling of metabolic rate within and across
92 organisms, it is commonly assumed that metabolic rate (R) scales with body mass (M)
93 to the $\frac{3}{4}$ power, a value that has been argued to be a universal metabolic scaling
94 exponent (West, Brown and Enquist, 1997). Such $\frac{3}{4}$ power scaling of metabolic rate
95 originated from the inter-specific comparisons of mammal and bird species which
96 revealed a metabolic scaling exponent of $\frac{3}{4}$ (Brody and Procter, 1932; Kleiber, 1932),
97 known as 'Kleiber's law'. Kleiber's law contrasted existing views of $\frac{2}{3}$ power scaling
98 of metabolic rate as proposed by Sarrus & Rameaux (1839), which was supported by
99 intra-specific metabolic scaling relationships of mammal and bird species reported by
100 Rubner (1883), which posited that maintenance (basal metabolic) costs scaled in

proportion to body surface area for endothermic organisms. The $\frac{2}{3}$ power scaling of metabolic rate has since been coined the 'surface area law' (Kleiber, 1932). Since its conception, Kleiber's $\frac{3}{4}$ power law has received much attention from biologists with numerous models and theories proposed to provide a mechanistic explanation of $\frac{3}{4}$ power scaling (Banavar *et al.*, 2010; Brown *et al.*, 2004; Brown, West & Enquist, 2005; Dodds, 2009; West, Brown and Enquist, 1997)

However, theories and models based on Kleiber's law often fail to capture the marked diversity in metabolic scaling relationships that exists across organisms. Empirical data shows numerous taxa deviate from the predicted $\frac{2}{3}$ or $\frac{3}{4}$ – power 'rule', including mammals (Speakman, 2000), amphibians (Hillman and Withers, 1979), birds (Schleucher and Withers, 2002), reptiles (Andrews and Pough, 1984) and invertebrates (Glazier *et al*., 2015), emphasising the widespread diversity of metabolic scaling exponents. A review article by Glazier (2005) highlights the observed diversity in both inter-specific and ontogenetic metabolic scaling exponents that deviate from the $\frac{3}{4}$ – power 'rule' for animals, plants and unicells. The plethora of existing models highlights the fact we lack a universally applicable model capable of predicting metabolic scaling slopes both within and across animal life. Most variation in metabolic rate can explained by body size, but it has been shown that other intrinsic and extrinsic factors may influence variation in the metabolic rates, for example, temperature (Clarke, Rothery and Isaac, 2010; Connor *et al.*, 2009), resource availability (Connor *et al.*, 2009), geography (Begum *et al.*, 2009; Mcnab, 2010), taxonomy (Griebeler and Werner, 2016; White, Blackburn and Seymour, 2009), musculature (McNab, 2019), diet (Clarke and O'Connor, 2014; McNab, 2000) and body shape (Glazier, Hirst and Atkinson, 2015; Hirst, Glazier and Atkinson, 2014). Metabolic rate is linked to other rates of biological processes and to body size, which in turn is related to numerous other biological traits including those determining fitness (e.g. production and growth) (Armstrong *et al*., 2017; Bouchard and Winkler, 2018; Bruce, 2016; Charnov, 2008; Lester *et al*., 2004; Moore and Farrar, 1996; Quesnel *et al*., 2018; Rollo, 2002), making it a relevant rate to study when exploring organism fitness (Pardo *et al*., 2013). Therefore, the need for further description and explanation of observed diversity in metabolic scaling is imperative to biology.

Furthermore, log-metabolic rate versus log-body mass relationships or allometries have traditionally been reported as a linear relationship but evidence for non-linear, or curvilinear metabolic scaling, has been reported and is especially prevalent for mammals. Upward curvature (where there is an acceleration of the metabolic scaling slope with body size) of the inter-specific metabolic scaling of mammals was originally reported by Hayssen and Lacy (1985) and later followed by many others for mammals (Bueno and López-Urrutia, 2014; Capellini, Venditti and Barton, 2010; Clarke, Rothery and Isaac, 2010; Kolokotrones *et al.*, 2010; Kozlowski and Konarzewski, 2005; Painter, 2005; Savage, Deeds and Fontana, 2008). Curvature of mammalian metabolic scaling received significant attention following the publication of Kolokotrones *et al.* (2010) who reported a superior fit of a quadratic metabolic scaling model in comparison to a linear model. The implications of curvilinear scaling are important because they imply different metabolic scaling laws exist across different sized species. For example, the upward curvature of mammalian basal metabolic rate (BMR, the metabolic rate of non-reproducing individuals in a post-absorptive state under thermo-neutral conditions) allometry means small-sized species have shallower scaling ($b \sim \frac{2}{3}$) than the accelerated scaling of large-sized species ($b \sim \frac{3}{4}$) (Clarke, Rothery and Isaac, 2010; Kolokotrones *et al.*, 2010).

1.2. Major theoretical approaches in metabolic scaling

Many models and theoretical explanations have been proposed to explain metabolic rate-mass scaling relationships both within and across species. This includes those offering explanations for $\frac{3}{4}$ – power scaling, curvilinear scaling and observed variation in metabolic rate that deviates from the surface area ($b = \frac{2}{3}$) or Kleiber's law ($b = \frac{3}{4}$) (Banavar *et al.*, 2010; Clarke, Rothery and Isaac, 2010; Glazier, 2010; Glazier, Hirst and Atkinson, 2015; Hirst, Glazier and Atkinson, 2014; Kooijman, 1986, 2000; Speakman and Król, 2010a,b; West, Brown and Enquist, 1997). However, it is apparent that no single model or mechanism can explain the wide range of metabolic scaling relationships present both within and across species (Glazier, 2005). Instead, some argue that multiple models or theories must be considered to create a truly comprehensive theory of metabolic scaling (Glazier, 2014a,b). Creating a single

unified framework of metabolic scaling is beyond the scope of this thesis, but instead I aim to consider multiple known correlates of metabolic rate and a range of theories and mechanisms when examining the metabolic scaling relationships of animals both within and across species. When examining relationships across species (or broader taxonomic groups) it is important to control for phylogenetic relatedness because species are not truly independent, but instead share characteristics from common ancestors (Symonds and Elgar, 2002). In this thesis, comparative analysis is performed across: species and broader taxonomic groups of aquatic invertebrates, species of oligochaetes and mammals. Phylogenetically controlled comparative methods require a fully known phylogeny with no error (Symonds and Elgar, 2002). Known phylogenies are widely available for mammals and were applied in this thesis (Smaers *et al*., 2018). However, phylogenies for aquatic invertebrate species are scarce in the literature and thus phylogenetically controlled comparative analysis could not be performed for these organisms in this thesis.

Generally, most models or theories of metabolic scaling fall into one (or more if they are multi-mechanistic) of four categories of theory, which are elegantly described by Glazier (2018): surface area, resource transport network, resource demand and system composition. The main scope of this thesis is to explore surface area models and theories, but because theories and models can often be multi-mechanistic, and many metabolic scaling models are taxon-specific, it is relevant to acknowledge and understand them all for a comprehensive view of the field of metabolic scaling.

1.2.1. Surface area models

Under Euclidean geometry, the body surface area of an isomorphically (shape-invariant) growing organism is predicted to scale in proportion with body volume (and hence body mass) to the $\frac{2}{3}$ exponent. However, some organisms display changes in body shape over ontogeny (Figure 2a), as indicated by the body mass-body length exponent, b_L (Figure 2c), on a double logarithmic plot. Changes in body shape over ontogeny can result in steeper mass-scaling of body surface area (b_A) over ontogeny (Figure 2b), for example, by increasing convolutions of the body or of key organs for material and energy exchange (see Figure 2 for a schematic diagram on the

relationship between body shape change, b_L and b_A). Surface area theory predicts that because changes in body shape over ontogeny can induce changes in the mass-scaling of body surface area (b_A), body shape changes can correlate with the mass-scaling of metabolic rate (b_R). Hence, surface area models can predict that body shape changes that increase the mass-scaling of surface areas responsible for resource uptake (oxygen and food) and waste removal (e.g. nitrogen, carbon dioxide), such as the integument of pelagic invertebrate species or the gills of numerous aquatic invertebrate and vertebrate species, will display a 1:1 relationship with the mass-scaling of metabolic rate (Glazier, Hirst and Atkinson, 2015; Hirst, Glazier and Atkinson, 2014). Such prediction is based on the assumption that oxygen, uptake, and not food uptake, is limiting across the integument of pelagic invertebrates or gills of aquatic organisms. Furthermore, aquatic invertebrates can consume oxygen through a variety of structures including a permeable integument, gills and other ventilatory structures. In addition, some aquatic invertebrate species have functions that can also contribute to the rate of oxygen consumption, for example, the beating activity of the thoracic limbs to pump water through the carapace chamber in *Daphnia magna* (Seidl, Pirow and Paul, 2002) and the undulation of the posterior region in *Tubifex tubifex* (Kaster and Wolff, 1982).

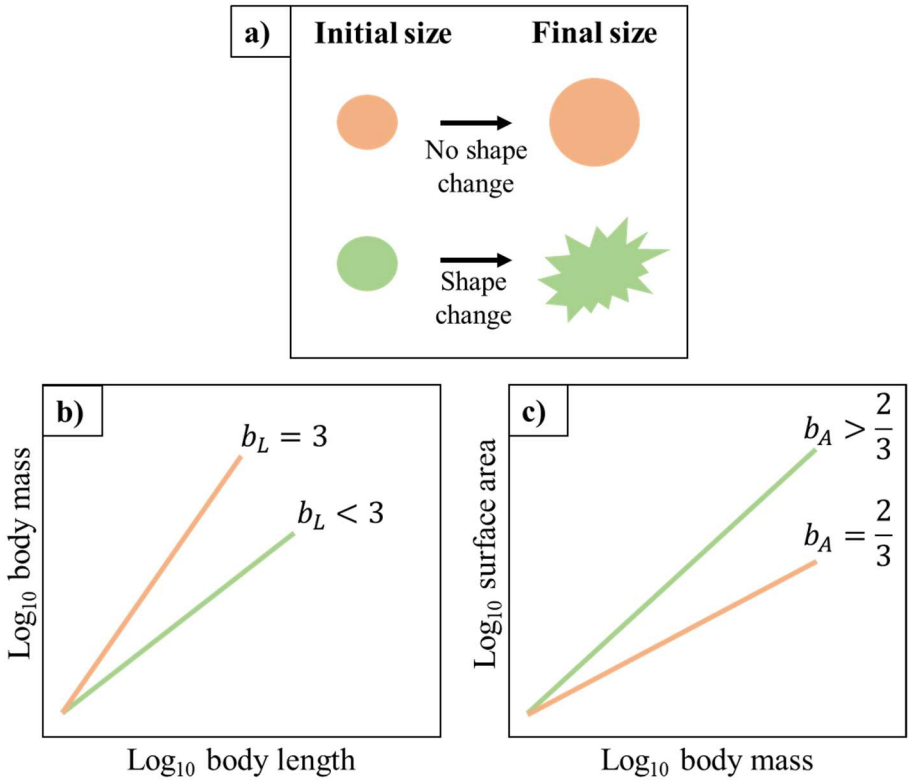

Figure 2. A schematic diagram of the Euclidean relationship between body size, body shape change (mass-length exponent b_L on a log-log plot) and the mass-scaling of body surface area (b_A, the surface area-mass exponent on a log-log plot) for the ontogenetic growth of a shape-invariant (isomorphic) and a shape changing organism, which displays increasing body convolutions over ontogeny. For isomorphically growing organisms, no changes in body shape will occur and hence b_L = 3, and body surface area is predicted to scale in proportion to volume and hence body mass which predicts a b_A value of $\frac{2}{3}$ (orange shapes and line). For organisms that display changes in body shape over ontogeny, such as an increase in body convolutions where b_L will tend towards one, body surface area is predicted to scale with body volume (and hence mass) with an exponent greater than $\frac{2}{3}$ (green shapes and line). The exact b_A and b_L values will be dependent on the specific degree or type of body shape change.

Resource uptake surface area models

Applying surface area theory (Rubner, 1883), resource uptake surface area models assume that metabolic rate is determined by resource uptake (food and oxygen) and metabolic waste excretion (e.g. nitrogen and carbon dioxide) across body surface areas. These models mainly consider the exchange of materials across external body surface areas (Glazier, Hirst and Atkinson, 2015; Hirst *et al*., 2014, 2017), and are generally applicable to ectotherms with permeable exoskeletons or integuments and hence are likely to be less applicable to those with impervious exoskeletons, such as arthropods. Resource uptake and waste excretion can also occur across internal body surface areas, for example the gut surface area of mammals (Karasov and Diamond, 1985), and thus changes in both external and internal surface areas (Okie, 2013) may influence the scaling of metabolic rate over ontogeny.

Resource uptake surface area models have been applied in recent studies on the ontogenetic development of pelagic invertebrate species, which represent an ideal taxonomic group to explore external body surface-area related effects because they often have permeable integuments that enable exchange of respiratory gas, uptake of nutrients and excretion of wastes (Hirst, Glazier and Atkinson, 2014). It has been

shown that the scaling of both oxygen consumption (required for respiration) (Glazier, Hirst and Atkinson, 2015; Hirst, Glazier and Atkinson, 2014) and nitrogen excretion (metabolic waste) (Hirst *et al.*, 2017) correlate with the degree of body shape change over ontogeny as predicted from surface area theory. Interestingly, however, upward deviation from a predicted one-to-one relationship (between b_A and the mass-scaling of resource uptake, and b_A and the mass-scaling of waste excretion) made from Euclidean surface area theory occurred for the scaling of both oxygen consumption (b_R) and nitrogen excretion was observed in these studies. Upward deviation in b_R can occur if the efficiency of respiratory exchange across body surface areas becomes enhanced over ontogeny, or if body surface area (responsible for uptake) becomes proportionately larger over ontogeny (Glazier, Hirst and Atkinson, 2015). As discussed by Glazier, Hirst and Atkinson (2015), the first may occur if the boundary layer between the integument and external resources becomes smaller with organism size, and the latter may occur if there is an organism becomes increasingly convoluted or increases in fractal dimension over ontogeny.

Thermoregulatory surface area models and theory

Based on Rubner's 'surface area law' that body surface area should scale with body mass to the $\frac{2}{3}$ exponent in animals that do not change shape (isomorphic), thermoregulatory surface area models assume that endotherms must balance heat production (resulting from maintenance) with heat loss, in order to prevent overheating, and as such heat loss may also scale with body mass to the $\frac{2}{3}$ exponent. Generally, thermoregulatory surface area models are applied to endotherms but not ectotherms, because the latter do not actively maintain a constant body temperature or produce a continuous net outflow of heat to the environment (Atkinson, 1994).

Metabolic heat production and its balance with surface-area related heat loss is a feature of the heat dissipation limit (HDL) theory of Speakman and Król (2010a,b). HDL theory argues that the maximal capacity for dissipating body heat generated from metabolism is the key process that constrains the expenditure of energy within an endotherm. Heat loss is a surface-related processes, and thus surface area theory predicts heat loss, and hence total energy expenditure, to scale with body mass to the

$\frac{2}{3}$ exponent. As body size increases, body surface area-to-volume ratio declines, and so larger-sized species will have reduced capacity to dissipate body heat generated from metabolism, and hence shallower mass-scaling of daily energy expenditure, in comparison to smaller-sized species (Speakman and Król, 2010a,b). Specifically, HDL models predict for terrestrial mammals that surface area, and hence daily energy expenditure, scales with body mass to the 0.63 exponent (Speakman and Król, 2010a), hence differing from the $\frac{2}{3}$ exponent predicted by surface area theory. Data on field metabolic rates (FMR, the metabolic rate of a free-living animal, Speakman and Król, 2010a,b) support this prediction with an average FMR exponent for terrestrial mammals between 0.576-0.679, but not significantly different to 0.63 (Speakman and Król, 2010a). The lower exponent for FMR compared to BMR (estimated around 0.68 – 0.76 (Speakman and Król, 2010a,b) implies that the sustainable theoretical maximum scope for increasing metabolic rate decreases with body size, where theoretical maximum scope is define as the maximum capacity to dissipate heat divided by BMR (Speakman and Król, 2010a,b). Therefore, if larger-sized species are more limited by their capacity to dissipate heat they are more constrained in their ability to elevate metabolism, they may display shallower scaling of metabolic rate than smaller-sized species.

For a theoretical representation of the body-mass scaling of FMR and BMR see Figure 3. It is important to note that the body-mass scaling of FMR may exhibit a shallower slope (b_R) than BMR (Speakman (Speakman and Król, 2010a), but FMR will generally exhibit a higher intercept (or elevation) (a) than BMR (Figure 3). This results in a phenomenon where FMR is generally higher than BMR (Figure 3). Exceptions to this phenomenon can occur, for example, for small-sized mammals undergoing torpor where FMR is smaller than BMR (Geiser, 2004).

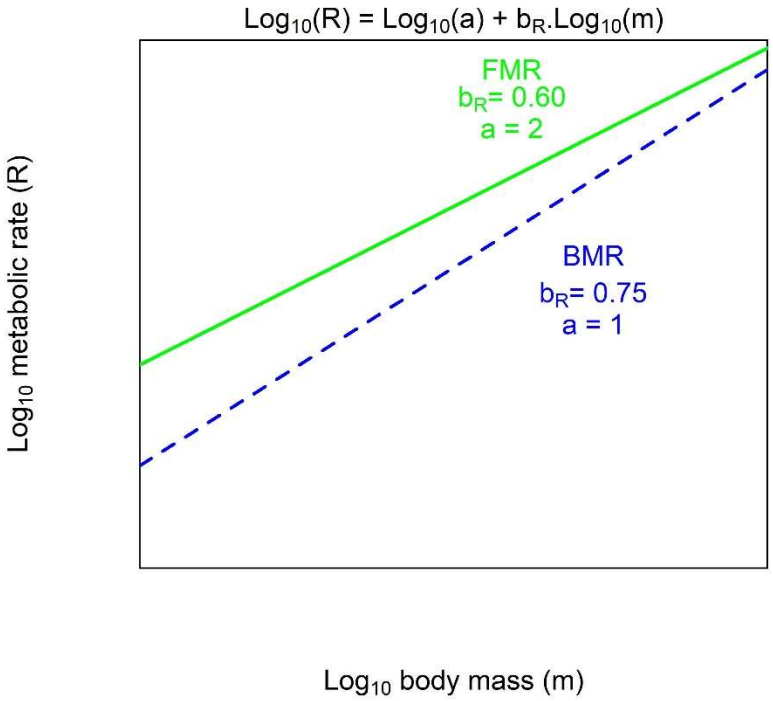

Figure 3. A schematic illustration of theoretical body mass-scaling relationships of Field Metabolic Rate (FMR) (green solid line) and Basal Metabolic Rate (BMR) (blue dashed line) on a double logarithmic plot. These relationships are based on the equation: $\log(R) = \log(a) + b_R \log(m)$, where a represents the intercept (or elevation) and b_R represents the slope of the given metabolic scaling relationship.

The thermodynamic surface area model of metabolic scaling by Ballesteros *et al.* (2018) has been proposed as a unified framework of metabolic scaling that can be used to explain variation in inter-specific metabolic scaling slopes of both endothermic and ectothermic species. Applying principles of HDL theory, this thermodynamic model predicts that variation in b_R across species can be explained by differences in the trade-off between energy efficiency and energy inefficiency. Specifically, it assumes that organisms face the issue of limitations to heat dissipation generated from metabolism (energy inefficiency) and maintaining metabolism to stay alive (energy efficiency) (Ballesteros *et al.*, 2018). Ballesteros *et al*. (2018) applied this model to BMR data of insects and plants, and to mammal species to account for variation in BMR responsible for apparent upward curvature. They utilise BMR data for polar and

desert mammalian species to argue that adaptation to different climates, or ambient temperatures, results in variation in energy inefficiency across mammal species that is responsible for variation in BMR scaling responsible for the curvature of the relationship. The performance of this model is superior to that of some other previous thermodynamic models of metabolic scaling (e.g. Kolokotrones *et al.*, 2010). However, it has yet to be compared to other competing models or theories (which are not necessarily surface area-related models) that also claim to explain upward curvature of mammalian metabolic scaling, such as the model proposed by Müller *et al.* (2012) which posits that mammalian curvature is a resulting artefact from the presence of two metabolic scaling relationships for each axis of reproductive strategy – uniparity (a single offspring per litter) and multiparity (multiple offspring per litter). Therefore, this thesis aims to apply a multi-mechanistic approach to determining the predictors of variation in BMR responsible for curvature across mammal species by distinguishing between these two contrasting models (Ballesteros *et al.*, 2018; Müller *et al.*, 2012) that are reported to account for curvature.

1.2.2. Resource transport network models

Whilst both resource transport network (RTN) and surface area models posit that metabolic rate is determined by geometrical influences of resource and/or waste transport, RTN models assume that the size dependence of metabolic rate is constrained by internal transport networks. This appears to contrast with SA models that assume metabolic rate is dependent on resource transport across body surface areas. One well-known RTN model is the West, Brown & Enquist (WBE) model, and was the first influential explanation for Kleiber's law ($\frac{3}{4}$ – power scaling of metabolic rate) (West, Brown and Enquist, 1997). Specifically, the WBE model assumes organisms have hierarchical fractal-like internal distribution networks, such as the blood vessels of vertebrates, in which nutrients are transported to supply all cells in the body (West, Brown and Enquist, 1997, 1999). The WBE theory proposes that individual cells of different-sized organisms require the same quantity of energy to function *in vitro*, but *in vivo*, as body size increases, the full demand of cells is not reached owing to the geometrical scaling of the supply network. Thus, as animals increase in size there is an apparent supply issue. West, Brown and Enquist (1997,

1999) propose that this supply issue is overcome by maximising metabolic capacity through maintaining supply networks at a fixed percentage of the body volume (6-7% for mammals (Glazier, 2014b)). The internal volume of the fractal-like network is proposed to act as an additional body dimension which scales as the fourth power of internal length, i.e. metabolic rate should scale with body mass to the $\frac{3}{4}$ power.

Subsequently, the WBE has formed a central tenet of the later developed Metabolic Theory of Ecology (MTE) (Brown *et al.*, 2004) – a more general theory that combines the effects of both body size and temperature on metabolic rate to explain ecological patterns more generally. Specifically, the MTE aims to explain how metabolic rate relates to a range of ecological processes at all levels of organisation, and including life history attributes, population interactions and ecosystem processes (Brown *et al.*, 2004). Generally, models developed from the MTE describe the effect of temperature on the metabolic rates within organisms by incorporating the Boltzmann-Arrhenius term $e^{-E/kT}$ together with the $\frac{3}{4}$ exponent of body mass scaling of metabolic rates (Brown *et al.*, 2004; Gillooly *et al.*, 2001). Where E represents is the activation energy (the minimum energy required for a metabolic reaction to occur), k is Boltzmann's constant (Arrhenius, 1889; Bolztmann, 1872) and T is temperature in Kelvin (Brown *et al*., 2004; Gillooly *et al*., 2001). This Boltzmann-Arrhenius term describes the exponential effect of temperature on biological rates (e.g. chemical or metabolic) and has received support in the literature for its application in modelling metabolic scaling relationships (Gillooly *et al.*, 2006; Kolokotrones *et al.*, 2010).

Application of the WBE model and theory has been extensive (Brown *et al.*, 2004; Kearney and White, 2012; Price *et al.*, 2012; van der Meer, 2006), and as a result has received plenty of critique for its unrealistic assumptions (e.g. see Banavar *et al*., 2002; Ricklefs, 2003; van der Meer, 2006a) and criticism for its inconsistent mathematics (Kozlowski and Konarzewski, 2004) and lack of fit to empirical data, for example to marine invertebrate species (Hirst and Forster, 2013). For example, the WBE model assumes the supply systems of organisms conform to closed branching circulatory systems with fractal-like geometry, which is not true for some organisms such as some molluscs which do not have branching structures (Kooijman, 2000; van der Meer, 2006a). As a result, the WBE model may be applicable to a specific subset of taxa that conform to the assumptions laid out by WBE theory, and less applicable

382 to taxa that violate these assumptions, such as those that lack fractal-like supply
383 systems. Moreover, the mathematics of the WBE model has been demonstrated as
384 inconsistent, for example, Kozlowski and Konarzewski (2004) show that $\frac{3}{4}$ – power
385 scaling of metabolic rate can only occur if the assumption of size-invariance of
386 terminal supply vessels is violated. Furthermore, the $\frac{3}{4}$ – power scaling of the WBE
387 does not capture diversity in metabolic scaling exponents, observed among organisms,
388 with the exponent generally ranging between $\frac{2}{3}$ and 1 (Glazier, 2005).

389 In light of the limitations to the WBE model, there has since been a
390 development of numerous proponents that modify the WBE and other similar RTN
391 models, that allow for a broader range of metabolic scaling exponents (e.g. Banavar *et*
392 *al.*, 2010; Delong *et al.*, 2010; Dodds, 2010; Enquist *et al.*, 2007). For example,
393 Banavar *et al.* (2010) proposed two RTN models based on modifications to WBE
394 theory that describe two different design systems of organism distribution networks –
395 radial explosion and hierarchically branched networks. Rather than assuming fractal-
396 like geometry of organism supply systems, these models suggest that $\frac{3}{4}$ – power scaling
397 arises because of $\frac{1}{12}$ power scaling of blood velocity, and also allow for deviations in
398 metabolic scaling exponent towards $\frac{2}{3}$ if velocity does not significantly vary with mass.

399

400 **1.2.3. Combined approaches to metabolic scaling**

401 The metabolic-level boundaries hypothesis (MLBH) proposed by Glazier (2005) is a
402 conceptual framework that invokes resource demand and surface area theory, and also
403 resource transport theory to a lesser-extent, and aims to explain extensive variation in
404 metabolic scaling observed both within and across species. Resource demand models
405 and theories often assume that whole organism metabolic rate is influenced by demand
406 of resources to fuel biological and physiological processes such as growth,
407 reproduction and locomotion (Glazier, 2018). The MLBH incorportates resource
408 demand theory as well as surface area theory because it considers how resource
409 demand from various physiological, developmental and ecological characteristics
410 influence the metabolic level (defined as the vertical elevation of the scaling
411 relationship between metabolic rate and body size on a log-log plot) of an organism

and hence the scaling of metabolic rate (Glazier, 2014). Resource transport theory can be incorportated into the MLBH for vertebrate animals with closed circulatory systems, which predicts a b_R value that tends towards $\frac{3}{4}$ for an isomoprhic organism with high levels of resting metabolism (Glazier, 2005, 2018).

Rather than proposing a single universal or fixed metabolic scaling exponent (b_R) for organism, the MLBH predicts that b_R can vary between $\frac{2}{3}$ and 1, depending on the degree of surface area related constraints to heat loss for endotherms (or flux of resources or wastes for some ectotherms) and body mass constraints to energy use (Glazier, 2008). Hence, the MLBH can be applied as both a thermoregulatory surface area model for resource uptake or waste removal in endotherms and a surface area model to ectotherms. Furthermore, MLBH argues that these surface area and body mass constraints of an organism are mediated by metabolic level, which in turn can induce variation in b_R. For example, active animals should have a metabolic level (L) that positively correlates with b_R due to enhanced metabolic demand of metabolising muscle tissue, which scales in direct proportion to muscle mass. By contrasts, inactive animals are predicted to display a negative relationship between L and b_R, when maintenance costs are high because metabolic scaling is mainly governed by limitations to surface area fluxes of resources, wastes and or heat across surfaces (Glazier, 2010a. 2014b). Evidence supporting the MLBH exists for a range of taxa including birds and mammals (Glazier, 2008), insects and plants (Glazier, 2010a), teleost fish (Killen, Atkinson and Glazier, 2010a) and cephalopods (Tan *et al.*, 2019) that qualitatively account for variation in b_R through differences in metabolic level.

System composition models consider how metabolic rate is influenced by changes in the relative proportions of system components within an organism (e.g. tissue). Some metabolic scaling frameworks aim to explain variation in metabolic rate by applying theory from both resource demand and system composition, for example the multi-mechanistic Dynamic Energy Budget (DEB) theory (Kooijman, 1986, 2000, 2010), which also invokes further principles from surface area theory. DEB theory assumes that energetic processes of organisms (e.g. assimilation or maintenance) are dependent either on surface area or body volume. Thus, rates of assimilation and consumption of resources are predicted to scale with body mass to the $\frac{2}{3}$ exponent under surface area theory for an isomorphically growing organism, as predicted from

surface area scaling. Moreover, DEB theory also invokes resource demand theory to explain variation in the intraspecific (ontogenetic) metabolic scaling slopes, which are argued to be a result of ontogenetic changes in the resource demand of growth (Kooijman, 1986, 2000, 2010). Furthermore, system composition theory can be applied to DEB theory to explain the hypoallometric scaling of metabolic rate slopes, where larger sized species have lower mass-specific metabolic rates than small-size ones. Specifically, DEB argues that hypoallometric metabolic scaling can result if there is a disproportionately increase in the relative proportion of non-metabolising tissue (e.g. lipid tissue) with body size (Kooijman, 1986, 2000, 2010).

Offering a competing mechanistic explanation to WBE theory for metabolic scaling, DEB that predicts a metabolic scaling exponent between $\frac{2}{3}$ and 1, rather than a fixed $\frac{3}{4}$ exponent as predicted by WBE theory (West, Brown and Enquist, 1997). DEB models can be applied to understand metabolic scaling relationships, but can also be applied to ontogenetic and interspecific scaling relationships of consumption and assimilation (Maino and Kearney, 2015a), and also to other related biological processes including ontogenetic growth and reproduction (Maino *et al*., 2014; Maino and Kearney, 2015b). Importantly, DEB theory categorises organisms as having two compartments: structural body and reserves (although more categories are possible (Kooijman, 2010)) and assumes that assimilated resources initially enter a reserve pool before they are allocated to biological processes such as growth or reproduction. Specifically, DEB theory states a fixed fraction of reserves, $'\kappa'$ is available for maintenance and growth and the remaining $(1 - \kappa)$ to other processes such as reproduction – known as the kappa-rule (Kooijman, 1986, 2000, 2010). Consequently, processes other than maintenance and somatic growth will occur if there is surplus energy reserve within an organism.

Another example of a metabolic scaling model that invokes system composition theory is that of Harrison (2017) which has been proposed as an explanation for hypoallometric metabolic scaling in animals. This study (Harrison, 2017) also provided extensive evidence against existing resource transport theory that hypoallometric (aerobic) metabolic scaling results from increased constraints to oxygen supply with body size (Banavar *et al.*, 2014; Price *et al.*, 2012). Harrison (2017) postulates that hypoallometric metabolic scaling may be, at least partially, due

476 to a declining proportion of neurosensory tissue, and hence ATP energy demand, with
477 body size. Declining ATP demand with body size was linked to differences in
478 performance-safety tradeoffs between small and large sized species (Harrison, 2017).
479 For example, compared to large-sized species, small-sized species generally have
480 shorter lifespan, reproduce at a young age and are often subjected to predator-prey
481 interactions. Thus, they may have evolved enhanced neurolocomotory performance to
482 increase vision, locomotory performance and agility, to detect and escape from
483 predators. In contrast, larger species are generally longer lived and reproduce later in
484 life and so invest into 'safety' strategies that protect against ageing, disease and
485 damage (Harrison, 2017). Harrison's (2017) model of metabolic scaling can also be
486 considered to invoke resource demand theory, as well as system composition theory,
487 if demand change within an organism is (at least partly) due to mitochondrial structural
488 or denisty changes within the same tissue (relative to the metabolic change) that arise
489 from changes in proportion of different tissues or bodily structures (Harrison, 2017).

490

491 **1.3. Introduction to growth scaling**

492 All living organisms accumulate new biomass over time – a process known as growth.
493 Life history theory predicts that because organisms are a product of multiple
494 generations of natural selection, they have evolved fitness maximising rates of growth
495 (Dmitriew, 2011). Hence, gaining a deeper understanding and description of the
496 observed variation in growth and metabolic rates that exists both within and across
497 species is imperative to understanding the ecology and evolution of organisms. There
498 are advantages generally associated with large adult body size, for example increased
499 fecundity (Charnov, Turner and Winemiller, 2001; Quesnel *et al.*, 2004), which can
500 be achieved by either a prolonged growth period or rapid growth rate during the
501 juvenile stage. For example, rapid juvenile growth rate may be selected when food
502 availability and/or nutrition is high, foraging risks are low (Kozlowski, Konarzewski
503 and Czarnoleski, 2020). Therefore, it can be predicted that organisms may exhibit
504 rapid growth rates to reach large body sizes, but in addition the rates of organism
505 growth are also likely to reflect adaptations to different environmental conditions.
506 Thus, observed rates of organism growth, or realised growth rates, are likely to reflect

optimal rates that result from a trade-off between the costs and benefits of growing at maximal rates in given environmental conditions.

Growth rate can be influenced by, or correlate with, many physiological and ecological factors including environmental temperature (Maranhão and Marques, 2003; Tripathi and Bhardwaj, 2004), food intake and availability (Connor *et al.*, 2009; Speakman and McQueenie, 1996), predation risk (McPeek, Grace and Richardson, 2001), immunity (van der Most *et al.*, 2011) and lifespan (Metcalfe and Monaghan, 2003). For example, ambient temperature significantly positively correlates with the intrinsic growth rates of amphipod *Echinogammarus marinus* (Maranhão and Marques, 2003), and the feeding rates and specific growth rate (proportional mass increase per unit time) of juvenile common carp, *Cyprinus caprio* (Oyugi *et al.*, 2011). Moreover, because resources are finite, investment into rapid growth can be predicted to negatively correlate with immune function. This is supported by a meta-analysis of growth and immune function data for farmed poultry species (van der Most *et al.,* 2011) which revealed a significantly reduced immune response when selecting for accelerated growth.

Furthermore, growth rate can be constrained directly by the food intake of an organism. For many species, foraging is often associated with a high risk of mortality because it exposes individuals to predators, and thus organisms face a challenge between gaining resources to maintain growth and avoiding predators. When experimentally exposed to a fish predator species, larval damselfly *Enallagma* sp. and *Ishnura* sp. display reduced food ingestion rates and growth rates (McPeek, Grace and Richardson, 2001). Interestingly, this study (McPeek, Grace and Richardson, 2001) also revealed differences in the growth efficiency between *Enallagma* sp. and *Ishnura* sp. in the presence of a predator: *Ishnura* sp. grew faster than *Enallagma* sp. due to higher conversion efficiency of ingested food into new biomass, suggesting differences in physiological stress response to predators that result in different growth rates and growth efficiency.

1.3.1. The relationship between growth and metabolic rates

All biological processes are fuelled by metabolism – the conversion of acquired energy and resources from the environment. For example, the generation of energy-rich ATP from respiration fuels the assembly of organic macromolecules and elements from monomers to create new biomass required for growth (Clarke, 2019). Thus, the metabolic rates of organisms, such as oxygen consumption rates, provide an indicator of available resources to fuel various biological processes including growth. Resources are finite and thus it is expected that after basic maintenance costs (e.g. tissue or cell repair) are met, organisms must optimally allocate remaining resources to fuel other processes such as growth, reproduction, locomotion and immune activation (Kozłowski, Konarzewski and Czarnoleski, 2020). Therefore, it can be predicted under life history theory that organisms will exhibit trade-offs between the allocation of resources to various biological processes in order to maximise fitness (see Figure 4 for a schematic diagram on the flow of energy within an organism).

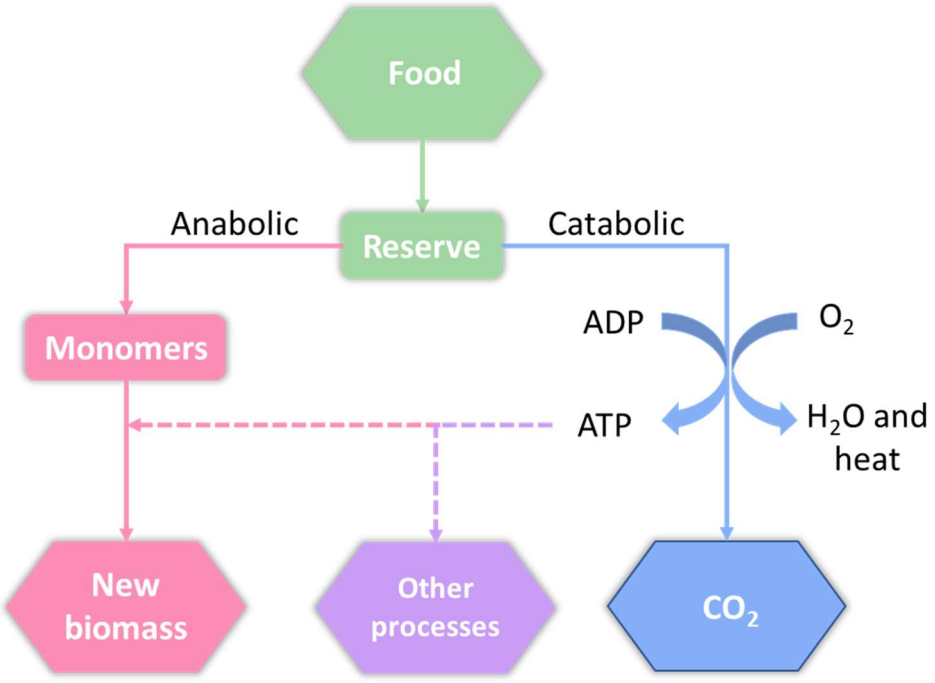

Figure 4. A flow diagram of the simplified relationship between growth (accumulation of new biomass) and metabolism (maintenance or catabolism). Resources (food) may firstly enter a reserve pool, which is allocated to either the anabolic or catabolic pathway. The catabolic pathway is responsible for generating

energy (ATP, adenosine triphosphate) from the metabolic conversion (oxidative phosphorylation) of ADP (adenosine diphosphate) for essential maintenance (to keep the body alive) and fuelling other processes. The anabolic pathway is responsible for the construction of new biomass (growth) from monomers obtained from food and is fuelled by ATP generated by metabolism. ATP is directed towards essential maintenance (e.g. tissue or cell repair) before being allocated to processes other than growth, such as locomotion, immune function or reproduction.

Furthermore, an understanding of both the body-mass scaling of growth and metabolic rate over development can provide insight into the growth efficiency of organisms. For example, if an individual sustains a high, or constant, relative growth rate (RGR, the rate of body mass increase per unit mass per unit time) but with a decline in mass-specific basal metabolic rate over ontogeny, this suggests that growth can be maintained despite a decrease in resources required for growth (e.g. oxygen), and hence implying high scaling of growth efficiency. High scaling of growth efficiency may occur, for example, if most resources are diverted towards growth (and thus away from other processes such as reproduction), or if conversion efficiency of food increases over ontogeny. Conversely, an individual that displays a reduction in RGR and an increase in metabolic rate (e.g. oxygen consumption rate) over ontogeny, suggests that growth rate is not being sustained despite having increased resources (e.g. oxygen) over ontogeny. This suggests that over ontogeny resources are increasingly allocated to processes other than growth, for example to reproduction or locomotion, hence implying low growth efficiency. For example, Anger (1996) revealed a decline in net growth efficiency (defined as growth rate / (growth rate + metabolic rate)) over ontogeny for northern stone crab, *Lithodes maja*, due to reduced rates of instantaneous growth rate despite an approximately constant mass-specific metabolic rate over development.

In addition, because metabolism fuels growth and can correlate with the growth efficiency of an organism, it becomes relevant to explore correlates of metabolic rate in relation to growth rate. Hirst, Glazier and Atkinson (2014) and Glazier, Hirst and Atkinson (2015) demonstrated a positive correlation between the scaling of aerobic metabolic rate (oxygen consumption), b_R, and the likely scaling of body surface area,

as indicated by the index of body shape change, $^{1}/_{b_L}$, for diverse integument-breathing pelagic invertebrate species. Surface area theory predicts that an increase in degree of body shape change towards body elongation (where growth occurs in one axis of length) or body flattening (where growth occurs in two axes of length) can reduce the decline in surface area to mass ratio as body size increases. Hence, a sustained surface area-to-mass ratio can sustain levels of uptake of resources, such as oxygen, across body exchange surfaces such as the integument of many pelagic invertebrate species. Therefore, because metabolism fuels growth it is relevant to address to what extent body shape change correlates with the scaling of growth for pelagic invertebrate species. The scope of this thesis will focus on exploring the relationship between the scaling of growth and metabolic rate in relation to growth efficiency, and whether changes in body shape correlate with the scaling of growth over ontogeny for diverse taxonomic groups including pelagic invertebrates.

1.3.2. Growth models and theory

Growth rate correlates with many key life-history traits, making it a relevant rate to explore in studies concerning organism fitness (Pardo *et al*., 2013), and thus research concerning the ecology or evolution of organisms would benefit from an understanding of the variation displayed in growth rates. Therefore, successfully predicting and understanding variation in growth and metabolic rates both within and between species has widespread relevance and importance in ecology and evolution. For example, individual variation in growth rates may ultimately correlate with variation in metabolic rates, since growth is fuelled by metabolism (Vincenzi *et al*., 2016). In turn, variation in metabolic rates can lead to differences in ecologically important features between individuals, such as access to resources or foraging dynamics.

Individual body mass versus time trajectories of animals are often proposed to be similar or nearly identical when scaled with body size (Karkach, 2006). Consequently, this has led to the search for a universally applicable model of ontogenetic growth (Moses *et al.*, 2008; West, Brown and Enquist, 2001). Developing such a model would aid our current understanding of animal growth and hence the implications to such work are extensive. Growth models often face trade-offs between model complexity,

accuracy, ease of estimation and the biological interpretability of parameters (Karkach, 2006). Numerous growth models have been proposed over time and vary in these trade-offs but many models fail to account for substantial variation in growth rate over ontogeny (Hirst and Forster, 2013; Marshall and White, 2019). Furthermore, growth models can often lack flexibility in parameterisation and have limited applicability to specific taxonomic groups (Marshall and White, 2019) such as fish (Lester, Shuter and Abrams, 2004; Quince *et al.*, 2008).

Arguably, the most well-known growth models are the von Bertalanffy growth function (VBGF), logistic, Gompertz, Schnute, MTE-based ontogenetic growth model (OGM) and those based on DEB theory. Although many more have been proposed and developed over time, a complete description of these is beyond the scope of this thesis (see Panik, 2014 for a review on growth curve modelling). Instead, the most commonly applied growth models will be evaluated in this thesis. Indeed, many growth models are nested, or related, because they share the same mathematical structure, for example, the VBGF, OGM and DEB models are based on the following function that describes the change in body mass (m) over time (t):

$$\frac{dm}{dt} = Hm^A - Km^B \tag{1.3}$$

For the VBGF this equation is often interpreted as the resource availability for growth in an organism (or anabolism) (Hm^A), minus non-growth metabolism (or catabolism) (Km^B) which is predicted to scale in relation to body volume (Bertalanffy, 1938, 1957). In comparison, the OGM predicts growth to prevail if the rate of assimilation of metabolic energy (Hm^A) is greater than the rate of energy allocation to maintenance (Km^B). Furthermore, the scaling exponent within the Hm^A term often varies between models, with the OGM predicting $\frac{3}{4}$ exponent scaling for the rate of assimilation and the VBGF commonly predicting $\frac{2}{3}$ exponent scaling for the rate of anabolism, although other values can be taken.

Importantly, growth models often assume, or have imposed restrictions to, fixed values for the scaling exponent of anabolism or assimilation (A) which are unlikely to hold universally across taxa. For example, the OGM is an extension of the authors' previously proposed WBE model (West, Brown and Enquist, 1997b, 2001) and

assumes a fixed value of $\frac{3}{4}$ for the scaling of assimilation, which is based on the view that the $\frac{3}{4}$ – power scaling law of metabolic rate can also apply to the scaling of ontogenetic growth. Furthermore, although the VBGF can be parameterised to hold a range of values for scaling exponent A (Bertalanffy, 1938, 1957; Ohnishi, Yamakawa and Akamine, 2014), authors commonly apply a parameterisation that fixes scaling exponent A at $\frac{2}{3}$ on the basis that resource availability for growth scales in relation body surface area, but crucially implies that growth occurs without any change in body shape – termed isomorphic growth. The assumption of isomorphic growth is unlikely to hold for certain taxonomic groups that are likely to display changes in body shape over development such as insects or aquatic invertebrates (Glazier, Hirst and Atkinson, 2015; Hirst, Glazier and Atkinson, 2014). In addition, because a large amount of evidence in the literature suggests that the body size scaling of metabolic rate does not hold universally (Bokma, 2004; Glazier, 2006; White, Cassey and Blackburn, 2007), it is likely that organisms also display variation in the body size scaling of growth because the production and accumulation of new biomass is fuelled by metabolism. This thesis will further explore potential diversity in the scaling exponent of anabolism (A) that may be present for certain taxonomic groups including aquatic invertebrates, by developing an improved framework for fitting growth curves to empirical growth data.

The applications of individual growth models are extensive; growth models can be applied to understand how growth rate and size-at-age change over time in given environmental conditions, and infer life-history strategies through trade-offs between growth and other biological processes such as reproduction (Karkach, 2006). In addition, growth models can be used to predict lifetime growth trajectories for farmed populations in aquaculture and fisheries industries, and hence are imperative to gaining reliable and accurate estimates of yield and profit (Ansah and Frimpong, 2015; González-Wangüemert, Valente and Aydin, 2014; Olaya-Restrepo, Erzini and González-Wangüemert, 2018). Thus, gaining improved predictions of animal growth rates will be beneficial for aiding biological, ecological and physiological research but also to those working in production industries such as aquaculture or fisheries.

1.4. Major research aims and objectives

The overall aim of this thesis is to improve current understanding and predictions of animal growth and metabolism. Specifically, the major themes of this thesis focus on the following research aims:

Chapter 2 – Improving current predictions of animal growth rates by developing a new framework for growth curve fitting.

Chapter 3 – Exploring the relationship between mass-scaling of growth and metabolic rate in relation to body shape change during ontogeny in pelagic invertebrate species.

Chapter 4 – Empirically examining the growth, metabolism and body shape change of two commonly cultured oligochaete species.

Chapter 5 – Evaluating and testing mechanistic theories and models that aim to account for variation in mammalian metabolic scaling that is responsible for apparent upward curvature.

Chapter 2. A new framework for growth curve fitting

2.1. Abstract

All organisms grow. Numerous growth functions have been applied to a wide taxonomic range of organisms, yet some of these models have poor fits to empirical data and lack of flexibility in capturing variation in growth rate. The von Bertalanffy Growth Function (VBGF) has prevailed for modelling animal growth trajectories, but authors often impose restrictions in the parameterisation which limits the range of possible growth curves. Here, I propose a new VBGF framework that broadens the applicability and increases flexibility of fitting growth curves. This framework offers a curve-fitting procedure for five parameterisations of the VBGF: these allow for different body-size scaling exponents for anabolism (biosynthesis), besides the commonly assumed $\frac{2}{3}$ power scaling, and allow for supra-exponential growth, which is at times observed. This procedure is applied to twelve species of diverse aquatic invertebrates, including both pelagic and benthic organisms. Widespread variation in the body-size scaling of biosynthesis and consequently growth rate is observed, ranging from isomorphic to supra-exponential growth. This curve-fitting methodology offers improved growth predictions and applies the VBGF to a wider range of taxa that exhibit variation in the scaling of biosynthesis. Applying this framework results in reliable growth predictions that are important for assessing individual growth, population production and ecosystem functioning, including in the assessment of sustainability of fisheries and aquaculture.

2.3. Introduction

2.3.1. Current growth models

Body size is a fundamental characteristic of all organisms. Body size has received much attention from biologists owing to its widespread covariation with a plethora of ecological and evolutionary functions and physiological traits (Davies, 1966; Green, 2015; Gutowsky *et al*., 2015; Holm *et al*., 2006; Illius and Gordon, 1992; Kwapich *et*

al., 2018; Mayer *et al*., 2016; Mirth *et al*., 2016; Woodward *et al*., 2005). Understanding growth (i.e. the changes in body size over time) is fundamental to many areas of biology, as well as being crucial for industries based on animal and plant production. Accurate growth predictions are fundamental to aquaculture and production industries, for example, over- or underestimating species growth will result in unreliable predictions of production and hence revenue and profit for producers (González-Wangüemert *et al*., 2015). For example, modelling the growth rates of farmed tiger prawns, *Penaeus monodon*, under varying environmental conditions including temperature and pond age, allows for predictions of production rates, and hence profitability, in new farming locations (Jackson and Wang, 1998). Moreover, gaining knowledge of growth parameters can help to inform management plans, which are required for effective conservation management of target species in aquaculture or reducing pressure on natural populations (Anash and Frimprong, 2015). For example, growth models have predicted parameter values associated with slow growth and long lifespan in the sea cucumuber *Stichopus vastus* (Echinodermata: Stichopodidae) which has helped inform restrictions on catch quotas to allow natural populations to recover (Sulardiono *et al*., 2012). In addition, understanding growth dynamics has been shown to be important for bivalve species in aquaculture and their use in mitigating eutrophication in coastal areas, for example, gaining accurate growth predictions of soft tissue can help the efficiency of mussel production that is required for eutrophic coastal waters (Petersen *et al*., 2014).

Methods for fitting growth curves to empirical data are applied extensively (Bridges *et al*., 1986; Chang *et al*., 2012; Fuentes-Santos *et al*., 2017; Higgins *et al*., 2015; Huchard *et al*., 2014; Jager and Ravagnan, 2016; Kirkwood, 1983; Panik, 2014; Potthoff and Roy, 1964; Richards, 1959; Strenio *et al*., 1983), but many of these approaches can be taxon-specific and lack flexibility to capture variation in growth over ontogeny or between conditions (Marshall and White, 2018). Here, I propose a new framework for fitting growth curves which applies a set of re-parameterisations of the von Bertalanffy Growth Function (VBGF). This new framework improves on existing methods by allowing for growth-curve fitting to a wide range of taxa which may exhibit variation in rates of growth, including exponential and supra-exponential growers.

The VBGF has been used extensively to model growth for numerous taxa such as fish (Quince *et al*., 2008), mammals (Derocher and Wiig. 2002), birds (Tjørve and Tjørve, 2010), invertebrates (Ernsting *et al*., 1993; Siegel, 1987) and dinosaurs (Leham and Woodward, 2008). It is a special case of the Richards model (Richards, 1959) and is based on biological principles originally developed by Pütter (Pütter, 1920). The mechanistic interpretation of the VBGF has varied over time, but most commonly growth is argued to occur if the building up of materials prevails over the breakdown of materials (Bertalanffy, 1938, 1949) as denoted by the differential equation:

$$\frac{dm}{dt} = Hm^A - Km^B, \tag{2.1}$$

where m denotes mass, t is time from birth or hatch, A, B are the mass-scaling exponents of anabolism (synthesis of component materials) and catabolism (breakdown of component materials) respectively, and H and K are the coefficients of anabolism and catabolism, respectively (Bertalanffy, 1938). The Hm^A term in equation (2.1) can represent the resource availability for growth in an organism, with the mass-scaling exponent A often assumed to relate to the body-mass scaling of surface area available for resource uptake, from which non-growth basal metabolism (referred to as catabolism by Bertalanffy (1938)) is then subtracted to obtain growth. Therefore, I hereafter refer to 'anabolism' as 'biosynthesis'. The Km^B term on the right-hand side of equation (2.1) represents resource consumption by tissues and is often proposed to scale in proportion to body mass (Bertalanffy, 1938), i.e. $B = 1$, though potential causes of deviation from this value will be discussed later.

A common assumption imposed on the VBGF is isomorphic scaling of biosynthesis, corresponding to growth without change in body shape, represented by the commonly chosen Euclidean value of $\frac{2}{3}$ for the mass-scaling exponent, A. This assumption is widely imposed despite recognition from von Bertalanffy of the potential range of values for A, for example, rod-like bacteria that grow in one-dimension of length ($A = 1$), with volume increasing proportionally to length and to surface area for resource uptake (Bertalanffy, 1938).

The Schnute model is a four-parameter growth model developed by Schnute (1981) often applied in aquaculture research (Góngora-Gómez *et al*., 2018; Reynaga-

Franco, 2019). The Schnute model has been proposed as superior to the VBGF for modelling growth of aquaculture species including the spotted rose snapper (Castillo-Vargasmachuca *et al*., 2018), *Lutjanus guttatus*, and turbot (Lugert *et al*., 2017), *Scophthalmus maximus*. However, comparisons made between the Schnute model and the VBGF often apply the common parameterisation of $\frac{2}{3}$ scaling of parameter A (equation (2.1)) (Lugert *et al*., 2017), which limits the range of growth curves that can be captured. Additionally, Yuancai *et al*. (1997) show through analytical transformation, that the Schnute model and the generalised VBGF (equation (2.1)) can be formally equivalent despite having different function forms and parameters: the two models gave the same growth predictions for stand density of *Eucalyptus grandis*. Therefore, by considering the flexibility of the VBGF a wide range of growth types can be captured and accurate predictions of growth can be achieved.

Restriction in the parameterisation of the mass-scaling of biosynthesis is also present in the Gompertz model (Gompertz, 1825) which has been used to model growth of plants, birds, fish, mammals, tumour cells and bacteria (Tjørve and Tjørve, 2017). Like the VBGF, the Gompertz model is also part of the Richards growth model family (Richards, 1959) where it is a special case of both the VBGF and Richards model where a complementary limit arises when $A \to 1^-$ (i.e. when parameter A approaches 1 from the left hand side of the plotted function), where $K(A - 1)$ is fixed (Richards, 1959). As the Gompertz model is achieved by calculating the body-size scaling of biosynthesis as a limit ($A \to 1^-$) it assumes an exponential decline in absolute growth rate with body size, making it inappropriate for taxa displaying other growth types that range from isomorphic to supra-exponential. For example, during ontogeny thaliacean organisms, such as salps and doliolids (Alldredge and Madin, 1982), exhibit increasing relative growth rate (RGR), the rate of body mass increase per unit mass per unit time, and thus have potential for supra-exponential growth.

Other well-known models with the same mathematical structure as the VBGF include the Dynamic Energy Budget (DEB) and the ontogenetic growth model (OGM), an extension of the 'West, Brown and Enquist' (WBE) model for metabolic scaling (West et al., 1997), which has been developed and improved over time (Barneche and Allen, 2018; Moses *et al*., 2008; West *et al*., 2001). The OGM predicts the rate of energy devoted to growth is equal to the rate of assimilation of metabolic

energy (the 'anabolic' term) minus the rate of energy allocated to maintenance (the 'catabolic' term). Although the mathematical structure is the same as the VBGF (equation (2.1)) the mechanism of growth varies. The OGM assumes a mass-scaling exponent of biosynthesis (Moses *et al*., 2008) (assimilation) of $\frac{3}{4}$. As a result, application of the OGM to taxa with differing mass-scaling of resource supply is likely to result in poor-fitting growth curves and inappropriate predictions. Further, Hirst & Forster (2013) found poor fit of the WBE to marine invertebrate growth data due to overestimating body size early in ontogeny and underestimating later in ontogeny.

2.3.2. Improving current methods of growth curve fitting

More parsimonious versions of the VBGF may provide better fits, and incorporate more biologically meaningful parameters, than some other simple equations, such as the logistic model. The logistic model (Verhulst, 1839) is regarded as the simplest of sigmoidal growth models with its symmetry about the point of inflection as given by the parameterisation (Katsanevakis, 2006):

$$L_t = \frac{L_\infty}{1 + e^{-c(t-t_1)}} \tag{2.2}$$

Where $L_t$and L_∞ represent body length at a given time, t, and asymptotic body length, respectively; and c and t_1 represent the relative growth rate parameter and time at inflexion of the sigmoid growth curve, respectively (Katsanevakis, 2006). Shi *et al*. (2014) compared the performance of the OGM with the logistic model and a generalised VBGF given by:

$$L_t = L_\infty[1 - \exp\big(-KD(t - t_0)\big)]^{1/D} \tag{2.3}$$

Where L_t, L_∞ and t have the same interpretation as the logistic model (equation (2.2)), and K and t_0 represent the growth rate constant and theoretical time at length zero, respectively. Parameter D in equation (2.3) represents $\lambda(1 - A)$,where A is the mass-scaling exponent of biosynthesis and is allowed to vary between 0.5 and 1 (Shi *et al*., 2014). Based on Akaike Information Criterion (AIC) scores, the logistic model was found to be best fit for late-larval stage empirical growth data for three fish species. However, for all cases the value for A for the VBGF (equation (2.3) was 1.0, suggesting that more parsimonious models such as the Gompertz or Exponential

model may better fit the data where $A \rightarrow 1^{-}$ and $A = 1$, respectively. Shi *et al*. (2014) argue that using a generalised version of the VBGF results in poor predictions of parameters, K and t_0, but this may be resolved by applying the Gompertz or Exponential parameterisation of the VBGF. Additionally, it is unknown what a "good" prediction of t_0 in the generalised VBGF is, considering that t_0 is a mathematical artefact representing time at zero body mass and the biological interpretation of K is debatable (Schnute and Fournier, 1980). Furthermore, the authors determine goodness of fit of these models through use of both AIC and R-squared. However, R-squared is an inappropriate method for assessing non-linear models (Kvålseth, 1985; Spiess and Neumeyer, 2010; Willet and Singer, 1988), for example, because the total sum of squares (SS) does not equal the regression SS plus the residual SS as is the case with linear regression (Spiess and Nemeyer, 2010). For example, Shi *et al*. (2014) inappropriately used R-squared to determine the goodness of fit of various fitted values of parameter A in the VBGF (equation (2.3)). R-squared contrasts AIC, which is based on likelihood and the number of model parameters and is a widely accepted and adopted method of determining goodness of fit for both linear and non-linear models (Spiess and Neumeyer, 2010).

Despite the numerous debated biological mechanisms underpinning growth models, discussed above, the VBGF (equation (2.1)) often prevails as a mathematical growth function, which can be parameterised in many ways to capture variation in RGR. Recent studies have highlighted growth curve diversity through the variation in the mass-scaling exponent of biosynthesis, A. Insects, for example, seldom grow isomorphically; instead, mass often scales almost in proportion to surface area, and the growth curve is near-exponential (Maino and Kearney, 2015a). Thus it can be predicted that $\frac{2}{3} < A < 1$ for insect growth. Maino and Kearney (2015b) found support for this hypothesis, with reported values of A between $\frac{3}{4}$ and 1 for the mass-scaling exponent of consumption and assimilation in 41 insect species. In addition, if oxygen uptake at rest is considered to be proportional to biosynthesis, as oxygen fuels both growth and non-growth, even at rest (Rosenfield *et al*., 2015), estimates of values of A may be derived from the mass-scaling of resting or routine metabolic rates. Thus, Killen *et al*. (2010) report values between $\frac{2}{3}$ and 1 for the body size scaling of resting metabolic rate for 89 species of teleost fish. The lack of universality in the mass-

882 scaling of biosynthesis, if assumed to be proportional to routine metabolic rate, has
883 also been highlighted within invertebrate species; including a littoral crustacean
884 (Ellenby, 1951) and diverse pelagic and benthic invertebrate species, which display a
885 diverse range in the mass-scaling of oxygen consumption (Glazier, Hirst and
886 Atkinson, 2015; Hirst, Glazier and Atkinson, 2014). If the mass-scaling of metabolic
887 rate does not hold universally it is suggestive that neither does the mass-scaling of
888 growth, since growth is fuelled by metabolism (albeit only a component of the total
889 respiration rate may relate to the costs of biosynthesis).

890 The above arguments highlight that when fitting growth curves to empirical
891 data, a single fixed value or limit, for the body mass-scaling exponent of biosynthesis
892 is unlikely to hold universally. Therefore, it is proposed that growth-curve fitting
893 methods should not pre-determine this exponent, but instead allow for and test for all
894 plausible possibilities. The importance of applying a multimodel approach to fitting
895 growth curves has been shown by Reynaga-Franco *et al*. (2019) where different
896 growth models were favoured by AIC for *Crassostrea gigas* raised under identical
897 conditions. Evidence (Hirst, 2012; Hirst, Glazier and Atkinson, 2014) suggests most
898 variation among diverse aquatic taxa relates to scaling of surface area, and hence to
899 the scaling of biosynthesis (Hm). By contrast, I argue that the scaling of non-growth
900 metabolism or catabolism (Km) varies less among organisms, and as assumed by von
901 Bertalanffy (1938) and Kooijman (1993, 2000), scales approximately linearly with
902 body mass where $B = 1$. I recognise that this assumption is contentious and may
903 require modification for certain taxa, where catabolism (or maintenance) does not
904 necessarily scale in proportion to body volume, such as when the proportion of body
905 composition taken up by non-metabolising fat reserve increases during ontogeny, as
906 reported in some insects (Maino and Kearney, 2015b).

907 Previous work by Ohnishi *et al.* (2014) addressed the need to allow mass-
908 scaling exponents to vary when applying the VBGF to organisms. These authors
909 developed a standardised form of the VBGF which allowed variation in both
910 exponents A and B. However, the derivation of their solution effectively ensures that
911 the value of exponent A cannot exceed exponent B. Consequently, if $B = 1$ is fixed,
912 values of A greater than 1 cannot be estimated. This becomes problematic when
913 organisms have supra-exponential growth ($A > 1$) such as in thaliaceans, as discussed
914 above. In addition, Ohnishi *et al.* do not give methods for calculating confidence

intervals or comparing estimates of exponent A to obtain a best-fit value for an organism.

2.4. Aims

Growth rate has been shown to correlate with many life-history traits, such as fecundity and lifespan for numerous taxa including fish (Charnov, 2008; Lester *et al*., 2004), reptiles (Armstrong *et al*., 2017), arthropods (Moore and Farrar, 1996; Bouchard and Winkler, 2018), mammals (Quesnel *et al*., 2018; Rollo, 2002) and tetrapods (Bruce, 2016), making it a key determinant of organism fitness (Pardo *et al*., 2013). Therefore, the aim of this study is:

1. To improve the flexibility and applicability of current growth-curve fitting methods by developing a new framework, based on the widely known VBGF (equation 1), that allows for diverse growth types (including both isomorphic and non-isomorphic) by applying a set of re-parameterisations that allow variation in the mass-scaling of biosynthesis.

Marine invertebrates display diverse variation in the mass-scaling of growth and metabolic rate (Glazier, Hirst and Atkinson, 2015; Hirst, Glazier and Atkinson, 2014; Glazier, 2006) and thus provide an ideal group to test the applicability of this framework. Further, it has been shown by Glazier (2006) that pelagic and benthic invertebrates display marked variation in their metabolic mass-scaling relationships, with pelagic species having significantly greater metabolic mass-scaling exponents than benthic species. By exploring both open-water and bottom-dwelling invertebrate species, the potential diversity in growth rate that may be attributed by differences in lifestyle and environmental conditions can be captured.

2.5. Methods

2.5.1. Theoretical background of growth models

The solution (Richards, 1959) to the original VBGF (equation (2.1)) when $B = 1$ is:

$$m = m_0 \left\{ \frac{1 - (1 - Z)\exp\big(K(A-1)(t - t_0)\big)}{Z} \right\}^{-\frac{1}{A-1}} \tag{2.4}$$

where m_0 represents mass m at time t_0 (time at birth or hatch). The mass-scaling exponent for biosynthesis is given by A and the rate at which final mass is reached is represented by parameter K. Parameter

$$Z = \left(\frac{m_\infty}{m_0}\right)^{A-1} \tag{2.5}$$

Where

$$m_\infty = \left(\frac{H}{K}\right)^{1/(1-A)} \tag{2.6}$$

has no simple biological interpretation. Parameter H is the coefficient of biosynthesis, i.e. it has the same meaning as the original VBGF (equation (2.1)). While equation (2.4) represents a valid solution for all $A > 0$, it is not the most suitable form for fitting to data because of collinearity of parameters, and because the expression is singular when $A = 1$. Different parameterisations are appropriate for the parameter A, corresponding to the Pure Isomorphy model (VBGF) and four nested non-isomorphic growth models: Exponential, Gompertz, Generalised-VBGF and Supra-exponential. These five parameterisations represent different categories of relative growth rate (RGR) (i.e. the body mass increase per unit mass per unit time) (Bhowmick *et al*., 2006), including constant RGR over time (Exponential model), decreasing RGR over time (Gompertz, Generalised-VBGF and Pure Isomorphy models) and increasing RGR over time (Supra-exponential model). For full derivation of equation (2.4) and further detail of the five parameterisations see Lee *et al*. (2020) Supplementary Information.

(i) Parameterisation of the Exponential model

When $A = 1$ relative growth rate is constant and growth is purely exponential, which yields the solution

971 $$m = m_0 \exp\big(k(t - t_0)\big) \quad (2.7)$$

972 Where $k = H - K$. Firstly, this model is fitted by setting m_0 as the mass at the first
973 time point. This solution involves fitting just one parameter, k. Parameter k is
974 estimated iteratively, after inputting the reasonable start value of 0.1. This estimate is
975 subsequently used as a starting value, along with m_0 as the mass at the first time point,
976 for the subsequent model run where I fit parameter m_0.
977

978 *(ii) Parameterisation of the Gompertz model*

979 The Gompertz model is a generalisation of the exponential model and a special case
980 of the General-VBGM where RGR decreases over time as the exponent of
981 biosynthesis, A, approaches limit a, represented by a second parameterisation (b, k)
982 (see Lee *et al*. (2020) Supplementary Information for derivation):

983 $$\lim_{A \to 1^-} m = m_0 \exp\left[-b\left(\exp(-k(t - t_0) - 1)\right)\right] \quad (2.8)$$

984 When parameter m_0 is initially fixed and t_0 is known, this involves estimating two
985 parameters: b and k. Starting values for k are taken from the estimates of the
986 exponential model, and the starting value for b is chosen so that the asymptotic mass
987 predicted by the model is twice the largest mass in the data. The justification is that
988 the starting value must be larger than the largest mass in the data set for the fitting to
989 work. If this value is too much larger, then the fit will be indistinguishable from an
990 exponential solution and so the fitting will struggle to identify the asymptote, which
991 makes a factor of two a good compromise to ensure the inflection in the model is tested
992 against the data.

993

994 *(iii) Parameterisation of the Generalised-VBGF*

995 The Generalised-VBGF allows for non-isomorphic growth where RGR decreases over
996 time where the mass-scaling exponent A can hold a value between 0 and 1. Problems
997 were encountered problems when fitting the model by varying the parameters A, Z,
998 and K, because of strong collinearity between A and K, and because of numerical
999 roundoff errors when Z was close to 1. Therefore, the model was fitted by varying the
1000 parameters (A, f, k) where

$$k = (A-1)K \tag{2.9}$$

and

$$f = 1 - Z \tag{2.91}$$

In terms of these parameters, equation (2.4) can be written as:

$$m = m_0 \left\{ \frac{1 - f\exp\left(-k(t-t_0)\right)}{1-f} \right\}^{-\frac{1}{A-1}} \tag{2.92}$$

The parameter range that represents biological growth is $0 < f < 1$, $0 < A < 1$, $k > 0$.

When A is close to 1, it is expected that k is similar to its value in the Gompertz model and so I apply the estimates from the Gompertz model as starting values for the Generalised-VBGF. The initial values for the other parameters are given by:

$$(1-A) = \min\left(a_{max}, \frac{f_{max}}{max(b)}\right) \tag{2.93}$$

$$f = (1-A)\max(b) \tag{2.94}$$

where a_{max}, f_{max} are chosen numbers between 0 and 1, and $\max(b)$ is the largest fitted value of b (amongst all individuals of the species under consideration) from the Gompertz model. This ensures that the initial values of f and A are in the biologically relevant range.

(iv) Parameterisation of the Pure Isomorphy model

Under three-dimensional Euclidean geometry, growth that is purely isomorphic is represented by the fixed value of $\frac{2}{3}$ for the mass-scaling exponent, A, and hence is a reduced version of the Generalised-VBGF where $A = \frac{2}{3}$. This means only two parameters are estimated: f and K from starting values obtained from the estimates given by the Generalised-VBGF.

(v) Parameterisation of the Supra-exponential model

The case $A > 1$ occurs when RGR increases over time and corresponds to supra-exponential growth, but the model exhibits biologically unrealistic behaviour, such as infinite mass, unless the parameter values are chosen with care. To avoid this, the optimiser varied parameters Z, α, and s, where $\alpha = \frac{1}{A}$, $s = -(t_{max} - t_0)\frac{K(A-1)}{\log(1-Z)}$ and t_{max} is the largest value of t in the data set for the individual in question. The full biologically relevant parameter space corresponds to each of Z, α, and s being constrained to lie between 0 and 1. To give the original biological parameters the estimates are inverted by the transformations:

$$m_\infty = m_0 Z^{\frac{1}{A-1}} \tag{2.95}$$

$$A = \frac{1}{\alpha} \tag{2.96}$$

$$K = -\frac{s\log(1-Z)}{(A-1)(t_{max} - t_0)} \tag{2.97}$$

Candidate starting values for these parameters are chosen so that the solution is close to the fitted exponential model. To achieve this, Z was chosen to be small, A to be just greater than 1, and $K = kZ$ (where k is taken from the exponential model fit). The above formulae were then used to compute the corresponding values of α, and s.

2.5.2. Fitting and assessing candidate growth models

The five candidate models were fitted to empirical mass-time data of a single individual for each species with log least-squares method of optimisation by using the general-purpose optimisation function *optim()* in R (v3.5.0) (R code is available at github.com/lauraleemoore). For a user guide for this growth curve fitting framework, including how to use the R code, please see Lee *et al*. (2020) Supplementary Information. This function was chosen for its robust method of applying Nelder-Mead algorithms (Nelder and Mead, 1965). The Nelder-Mead algorithm is a simple direct search algorithm for multidimensional unconstrained minimisation (Nelder and Mead, 2965). Nelder-Mead algorithms attempt to minimise a scalar-valued nonlinear

function of given variables without requiring any derivative information, and hence Nelder-Mead algorithms are widely used for nonlinear unconstrained optimisation (Lagarias *et al*., 1998). Since *optim()* does not allow constrained Nelder-Mead optimisation, biological parameters were transformed (using a log or logit transform) so the biologically meaningful range corresponded to $(-\infty, \infty)$ in the space explored by optim().

Optimisation initially fitted the models with the m_0 parameter fixed at the first empirical mass value. Parameter estimates gained from this optimisation were consequently used as starting parameters for optimisation where the m_0 parameter was estimated. It is often unrealistic that the first recorded mass value is the precise mass at time zero (at birth or hatch) and so only the optimised parameter estimates for model fitting where m_0 was estimated were used in subsequent analysis. Hence, the purpose of carrying out optimisation where m_0 is fixed at the first empirical mass value was to produce reasonable starting values for *optim()*.

Log least-squares fitting was chosen over least-squares because it allows for more weighting of error at smaller mass values. This comes from the reasoning that it is biologically realistic to assume fluctuations in growth rate between individuals are proportional to body size, i.e. individuals will grow similarly initially but display more variation in size (mass) later in life. To determine the best fitting value for the mass-scaling exponent of biosynthesis, A, the model with the most negative log likelihood value was taken as the best fit model. Confidence intervals for parameter A were constructed using profile likelihood in R (v3.5.0). A purely likelihood-based approach was used, rather than the Akaike Information Criterion, because this framework aims to provide a confidence interval for the parameter A rather than in selecting which single model (i.e. value of A) to use for forecasting. The 95% confidence intervals show the range of values of A that would not be rejected as a null model, and hence are consistent with the data.

For the purpose of providing a statistical comparison of the five VBGF parameterisations and to provide methods for hypothesis testing, the Likelihood Ratio Test (LRT) was also conducted to determine the best fitting model overall, rather than selecting the best model fit for parameter A as outlined above. The four non-isomorphic VBGF parameterisations (Exponential, Gompertz, Generalised-

VBGF and Supra-Exponential) are directly nested, and the Pure Isomorphy and Generalised-VBGF are directly nested. The LLRT was carried out between nested VBGF parameterisations, i.e. for general (the model with the most free number of parameters) and reduced (the least free parameters) VBGF parameterisations. The LRT was calculated as:

$$D = 2(LL_{general} - LL_{reduced}) \quad (2.98)$$

Where D represents the LRT statistic and the negative log likelihood (LL) is calculated by:

$$LL = \frac{\left(n\left(\log(2\pi) + \log\frac{S}{n} + 1\right)\right)}{2} \quad (2.99)$$

where S represents the sum of squares and n the number of datapoints. The reduced model was rejected in favour of the general model if $D > \chi 2$ where $\chi 2$ is a one-tailed chi-squared statistic whose degrees of freedom is the extra number of parameters the general model has in comparison to the reduced. Firstly, the Exponential model (reduced) was tested against Gompertz (general). If $D < \chi 2$ the model testing stops here and the reduced model (Exponential) was taken as the best fitting model. However, if $D > \chi 2$ the following proceeded: the Gompertz was tested against Generalised-VBGF (general) and separately against the Supra-exponential model (general). It was not possible to test the Generalised-VBGF against the Supra-exponential because the models are not nested. Therefore, in the case where the Gompertz model is consecutively rejected in favour of both the Generalised-VBGF and Supra-exponential model, the general model with the most significant statistic (D) value was taken as the best fitting model. To test the common assumption of pure isomorphic growth I applied the LRT to the two nested VBGF parametrisations: Pure Isomorphy VBGM and Generalised-VBGM. In the case where two models were determined as the best fitting model by LLRT, the model with the lowest sum of squared residuals was taken as the best fitting growth model.

2.5.3. The dataset

Aquatic invertebrates assimilate resources through different body surfaces, for example, integument and/or gills for oxygen uptake. Differences in environmental conditions (e.g. predation) that exist between benthic and pelagic habitats of aquatic invertebrates may affect the mass-scaling of an organism's uptake of resources. For example, high predation risk throughout ontogeny in the sunlit epipelagic zone, which lacks refuges from predators, may lead to the evolution of steeper mass-scaling of resource uptake, compared with more benthic conditions where invertebrates can reduce predation risk by finding refuge (L'Abée-Lund *et al*., 1993; Seibel, 1997; Tan *et al*., 2019). The diversity in the mass-scaling of biosynthesis (A) makes benthic and pelagic invertebrate species two ideal groups to explore variation in A when fitting the VBGF.

Published ontogenetic mass-at-age data were collected for seven pelagic and five benthic invertebrate species using Web of Knowledge. Search terms included "growth AND pelagic AND (lab* OR cultur* OR ontogen* OR development*)" for pelagic species and "growth AND benthic AND (lab* OR cultur* OR ontogen* OR development*)" for benthic species. Species were chosen based on availability of growth data that conforms to the specific requirements described below. To provide a diverse sample of growth curve fits to empirical data, species comprising both gelatinous and non-gelatinous zooplankton across four phyla were chosen: Arthropoda, Cnidaria, Chordata and Mollusca. Species were considered pelagic or benthic based on the zone inhabited by the developmental stage in which growth data was obtained from. For example, for many adult benthic invertebrates the larval stage occurs in the pelagic zone, e.g. many decapod species that occur in the pelagic zone during their zoeal stage before migrating to their benthic habitat. The species used in analysis were as follows. Pelagic: *Daphnia magna* (Branchiopoda) (Mitchell *et al*., 1992), *Pelagia noctiluca* (Scyphozoa) (Lilley *et al*., 2014), *Euphausia pacifica* (Euphausiacea) (Ross, 1982), *Oikopleura dioica* (Appendicularia) (Lombard *et al*., 2009), *Aurelia aurita* (Scyphozoa) (Båmstedt *et al*., 2001), *Cyanea capillata* (Scyphozoa) (Båmstedt *et al*., 1997) and *Crassostrea gigas* (Bivalvia) (Kheder *et al*., 2010). Benthic: *Mytilus edulis* (Bivalvia) (Thomsen *et al*., 2013), *Sepia officinalis* (Cephalopoda) (Domingues *et al*., 2002), *Echinogammarus marinus* (Amphipoda) (Maranhão & Marques, 2003), *Cherax quadricarinatus* (Decapoda) (Stumpf & Greco,

2014) and *Petrarctus demani* (Decapoda) (Ito and Lucas, 1990). Species identities were checked using the World Register of Marine Species (WoRMS) to ensure accepted names were used.

When required, data were extracted from graphs using the software WebPlotDigitizer (Rohatgi, 2017). Data were accepted if collected under controlled and constant environments; field data were therefore excluded. Mass data selected were from time at hatch up until but excluding reproductive maturity, where reproductive maturity was defined as the development of sexual organs.. The time of reproductive maturity reported by the authors themselves was used, or, when this was unavailable, an approximate age at maturity at the given temperature was obtained from the scientific literature. Data for *C.gigas*, *A.aurita* were from pelagic larvae or juveniles and *M.edulis* data were from benthic juveniles, and did not include growth data up to maturity (incomplete juvenile development) due to lack of available data that conform to the data requirements. Therefore, I recognise that for these three species utilising data across larger parts of life history may result in different model fits. The data requirements were as follows. Growth data were not collected when conditions included starvation, predation or toxin treatments, or temperatures/salinities beyond the normal range encountered by the species in its natural setting. Mass type (either dry, ash-free or wet), treatments, culture conditions, developmental stages, sex and site of origin were also recorded. If only length data were available, published length-mass conversion equations for a given species were applied. I justify the use of mass-length conversions based on the scarcity of available mass versus time data for certain species, for example, length measurements would often be collected instead of mass on the basis that length measurements are less destructive to some study organisms. Mass-length conversion equations were applied to the following five species: *Daphnia magna* (Burns, 1969), *Pelagia noctiluca* (Rosa *et al*., 2013), *Cyanea capillata* (Lesniowski *et al*., 2015), *Echinogammarus marinus* (Marques and Nogueira, 1991) and *Mytilus edulis* (Jespersen and Olsen, 1982). Therefore, I acknowledge that for these five species, applying mass-length conversion equations obtained from the literature means that theoretical, rather than actual (raw), mass versus time trajectories were applied to the VBGF parameterisations. Hence, the model fits obtained for these five species may differ to that obtained from actual (raw)

mass data, and thus this must be considered as a caution when drawing any conclusions from these fits.

The analysis in this Chapter was carried out for a single individual per species. For species where growth data for multiple individuals was available, the individual with the most natural (i.e. similar to that of the natural habitat range) temperature and salinity conditions was selected.

2.6. Results

2.6.1. A note on the comparison of model performances within species

For some species, growth data (mass versus time) was available for more than one individual. The results reported in this Chapter are for a single individual per species (criteria for selection are stated in the Methods section), but observations of the performance of this growth curve fitting framework revealed that individuals within a species did not differ in the best fitting model (as determined by the most negative log likelihood). For example, seven *Daphnia magna* individuals had growth data recorded in this study, and all seven showed the Gompertz model to be the best fitting model. However, this was not the case when comparing complete and incomplete developmental data within a species, for example, growth data for 11 individual *Sepia officinalis* was obtained but only two represented complete development and the other nine incomplete development. The two individual *S.officinalis* undergoing complete development had the same best fitting model (Gompertz), but the nine individuals with incomplete development had either the Generalised-VBGF or Supra-Exponential as the best fitting model.

2.6.2. Comparison of models across species

The negative log likelihood values for the five candidate re-parameterisations of the von Bertalanffy Growth Function (VBGF) showed that there was no universal agreement in best-fitting VBGF model across the twelve pelagic and benthic invertebrate species with a range of best-fitting values for the mass-scaling exponent

of biosynthesis, A, between 0.72 and 1.22 (Table 1) (see Supplementary Appendix 1 Table S1 for negative log likelihood values). Both pelagic and benthic species displayed the same mixture of best-fitting models including the Generalised-VBGF, Gompertz and the Supra-exponential model (Figures 4 and 5). The Generalised-VBGF was found to be the best fit for 58% (7 out of 12) of species, followed by the Gompertz (25%) and Supra-exponential (17%) model (Table 1). The two models where parameter A remains fixed, the Exponential and Pure Isomorphy model, were not found to be the best fit for any species.

2.6.3. Comparison of models across taxa

Across the arthropods the Generalised-VBGF was the best fit for all four malacostracan species (Table 1), whereas the branchiopod *Daphnia magna* had a growth trajectory best fit by the Gompertz model (Figure 5). Cnidarian species *Pelagia noctiluca* (Figure 5) and *Cyanea capillata* (Figure 5) both displayed decreasing RGR with the Generalised-VBGF model (where A = 0.76 and 0.92, respectively), whereas, during an incomplete juvenile development, the cnidarian *Aurelia aurita* (Figure 5) displayed increasing RGR with the Supra-exponential model as the best fit (A = 1.22) (Table 1). The appendicularian, *Oikopleura dioica*, also displayed supra-exponential growth where A = 1.12 (Figure 5). Across the molluscs, there was no universal agreement in best-fitting model for the incomplete developmental growth of the two bivalve species, *Mytilus edulis* and *Crassostrea gigas* agreeing with the Generalised-VBGF and the Gompertz model, respectively and the benthic cephalopod *Sepia officinalis* agreeing with the Gompertz model (Table 1).

2.6.4. Likelihood Ratio Test

In comparison to determining and reporting the best fitting A value via the most negative log likelihood (Table 1), the Likelihood Ratio Test (LRT) was conducted to statistically determine the overall best fitting VBGF model (hereon termed the best fitting LRT model). The results of the LRT are reported in Supplementary Appendix 1 Table S2. The best fitting LRT model differed to the model reported for the best fitting A value (see Table 1) for the following six species only: *Oikopleura dioica*

(Exponential, $A = 1$), *Aurelia aurita* (Exponential, $A = 1$), *Cyanea capillata* (Gompertz, $A = 1$), *Echinogammarus marinus* (Gompertz, $A = 1$), *Cherax quadricarinatus* (Gompertz, $A = 1$) and *Petrarctus demani* (Gompertz, $A = 1$). For the remaining six species (*Daphnia magna*, *Euphausia pacifica*, *Pelagic noctiluca* *Crassostrea gigas*, *Mytilus edulis* and *Sepia officinalis* the best fitting LRT model (Supplementary appendix 1 Table S2) did not differ to the best fitting model as determined by the most negative log likelihood (as reported in Table 1).

Table 1. The best-fitting values for the mass-scaling exponent for biosynthesis, A, as determined by the most negative log-likelihood between the five parameterisations of the VBGF: Exponential, Gompertz, Generalised-VBGF, Pure Isomorphy and Supra-exponential for empirical mass versus time data for twelve individuals of pelagic and benthic invertebrate species. The zone (pelagic or benthic) represents the zone inhabited during the development phase in which growth data was obtained for. The number of datapoints for each individual is represented by N. The 95% confidence intervals for parameter A were calculated using profile likelihood.

Habitat	Zone	Phylum	Class	Species	N	Best fit model	*d.f.*	***A*** estimate	95% confidence intervals
Freshwater	Pelagic	Arthropoda	Branchiopoda	*Daphnia magna*	11	VBGF-Gompertz	7	1.0	0.58 – 1
Marine	Pelagic	Arthropoda	Malacostraca	*Euphausia pacifica*	7	Generalised-VBGF	2	0.79	0.68 – 0.91
Marine	Pelagic	Cnidaria	Scyphozoa	*Pelagia noctiluca*	39	Generalised-VBGF	34	0.76	0.73 – 0.78
Marine	Pelagic	Chordata	Appendicularia	*Oikopleura dioica*	7	VBGF-Supra-exponential	2	1.12	1.06 – 1.16
Marine	Pelagic	Cnidaria	Scyphozoa	*Aurelia aurita*	10	VBGF-Supra-exponential	5	1.22	1.21 – 1.32
Marine	Pelagic	Cnidaria	Scyphozoa	*Cyanea capillata*	14	Generalised-VBGF	9	0.92	0.88 – 0.96
Marine	Pelagic	Mollusca	Bivalvia	*Crassostrea gigas*	7	VBGF-Gompertz	3	1	0.80 – 1
Marine	Benthic	Arthropoda	Malacostraca	*Echinogammarus marinus*	11	Generalised-VBGF	7	0.79	0.64 – 0.93
Freshwater	Benthic	Arthropoda	Malacostraca	*Cherax quadricarinatus*	9	Generalised-VBGF	4	0.89	0.81 – 0.95
Marine	Benthic	Arthropoda	Malacostraca	*Petrarctus demani*	8	Generalised-VBGF	3	0.79	0.76 – 0.93
Marine	Benthic	Mollusca	Bivalvia	*Mytilus edulis*	8	Generalised-VBGF	3	0.87	0.79 – 0.95
Marine	Benthic	Mollusca	Cephalopoda	*Sepia officinalis*	23	VBGF-Gompertz	19	1.0	0.80 – 1

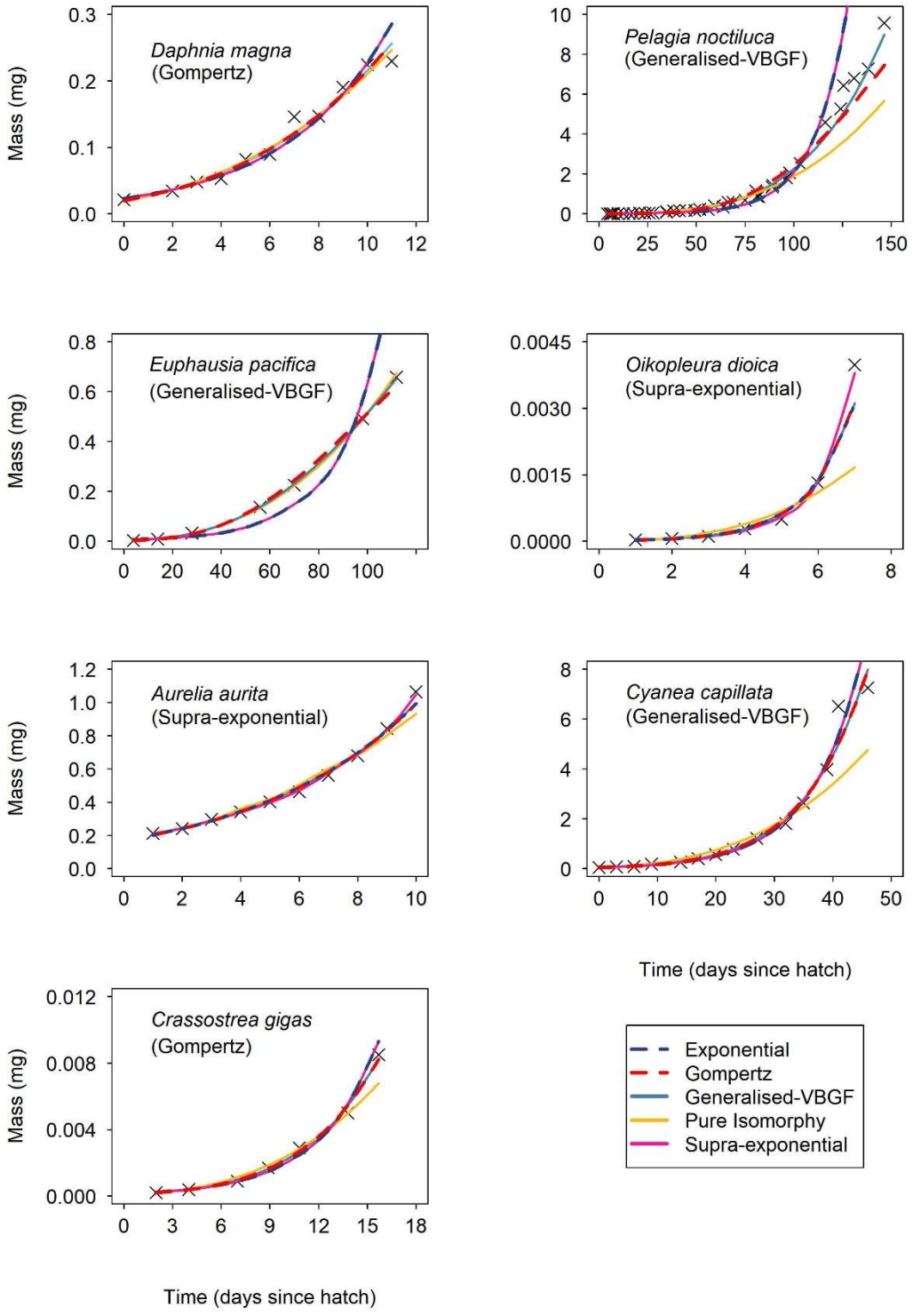

1255

1256 **Figure 5.** Model fits for the five von Bertalanffy growth function (VBGF) (equation
1257 1) parameterisations (equation 1) for empirical mass versus time data for six species
1258 of pelagic invertebrates. From top left: *Daphnia magna* (Gompertz), *Pelagia noctiluca*
1259 (Generalised-VBGF), *Euphausia pacifica* (Generalised-VBGF), *Oikopleura dioica*
1260 (Supra-exponential), Aurelia aurita (Supra-exponential), Cyanea capillata
1261 (Generalised-VBGF) and *Crassostrea gigas* (Gompertz).

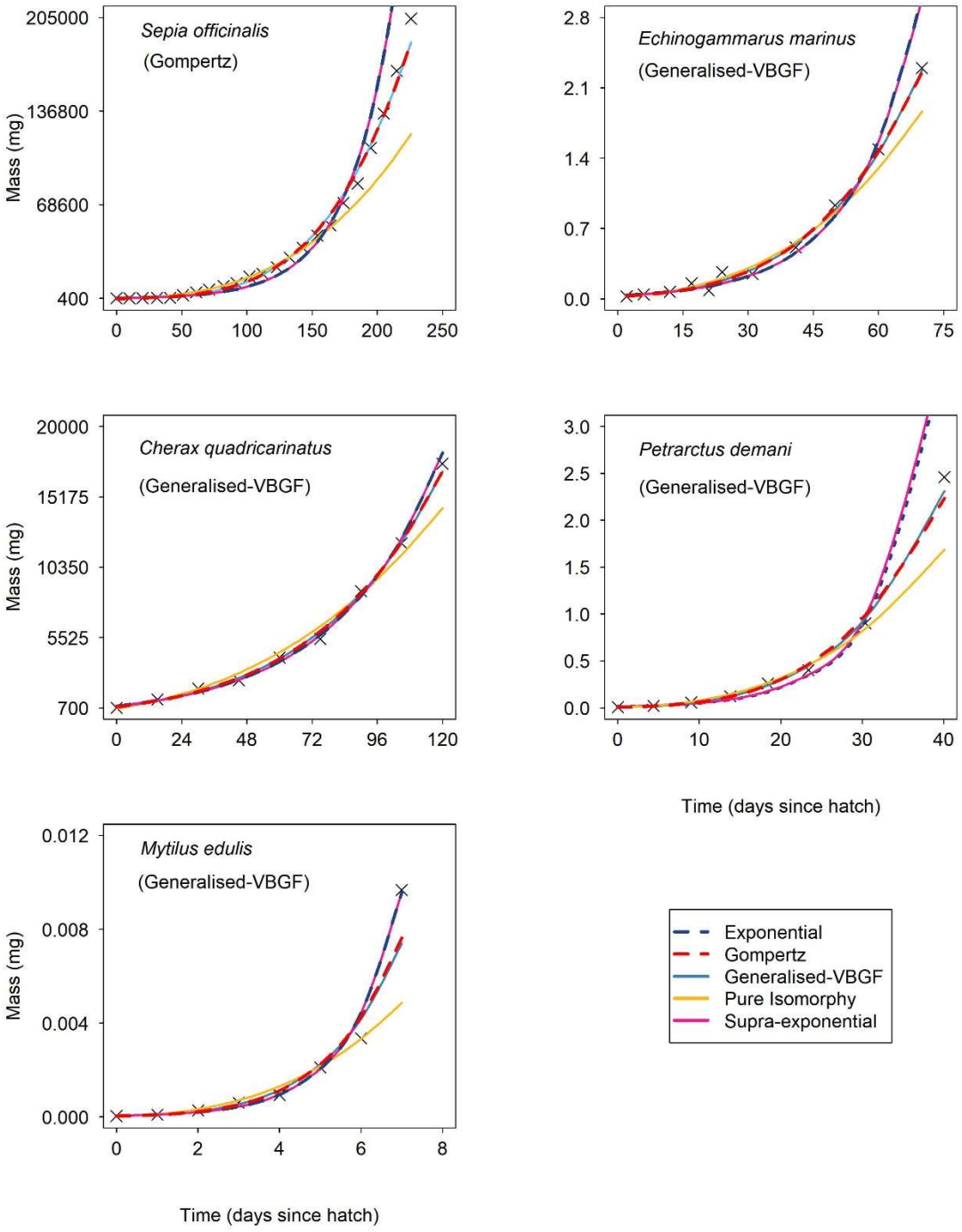

1262

1263 **Figure 6.** Model fits for the five von Bertalanffy growth function (VBGF) (equation
1264 1) parameterisations for empirical mass versus time data for six species of benthic
1265 invertebrate. From top left: *Sepia officinalis* (Gompertz), *Echinogammarus marinus*
1266 (Gompertz), *Cherax quadricarinatus* (Exponential), *Petrarctus demani* (Generalised-
1267 VBGF)and *Mytilus edulis* (Generalised-VBGF).

2.7. Discussion

A range of values for the mass-scaling exponent of biosynthesis, A, ($0.72 < A \leq 1.22$) (Table 1) highlights the diversity of growth curves amongst species (Figures 5 and 6). The proposed new framework for fitting growth curves provides improved predictions of growth and increased model validity for species displaying growth curves that differ from commonly fixed values of the mass-scaling of biosynthesis such as $\frac{2}{3}$ (isomorphic growth) or 1 (pure exponential growth). This includes two cases of supra-exponential growth (where $A > 1$) found in the appendicularian *Oikopleura dioica* (Figure 5) and during part of juvenile development of the scyphozoan *Aurelia aurita* (Figure 5) (Table 1). Widespread diversity in the mass-scaling of biosynthesis highlights the range of growth curves present amongst organisms. This brings into question current methods of growth curve-fitting which impose a fixed value, limit or range for exponent A that are unable to capture variation in the mass-scaling of biosynthesis, and consequently growth rate.

However, it is important to note that the fitted values (estimates) of the VBGF parameters, including A, for the five VBGF parameterisations can be influenced by errors in the empirical growth data and hence caution should be taken when drawing conclusions from the reported best fitting values of A in this Chapter. For example, growth data for some species (see Methods) in this Chapter comprised length versus time data, which was converted to mass through mass-length conversion equations. Hence, for these species mass represents predicted mass and not actual mass, which is likely to result in different growth curves and hence fitted parameter values. Furthermore, errors may have occurred during the measuring of body mass by the researchers themselves. If this error varied over development then this could change the shape of the growth curve. For example, if the degree of measurement error is largest at younger stages of development then body mass will be overestimated during this stage and hence the point of inflection (if growth does plateau) and/or the shape of the growth curve will be impacted. Therefore, if measurement error results in an alteration of the shape of the growth curve (e.g. via changing initial mass, final mass or the point of inflection) then this will result in different fitted parameter values and potentially a different best fitting model compared to the case where there is no error in the data. Thus, caution should be taken when drawing conclusions for the reported

fitted parameter values and best fit model, and where possible, future studies should outline known or potential error in growth data and the implications this may have on the model fitting and results. Both pelagic and benthic species displayed variation in the best-fitting model, suggesting that there is no general difference in pattern of growth between pelagic and benthic species or ontogenetic phases, although a larger sample would be required to test this more definitively. Generally, there was no trend between best-fitting model and taxonomic group, except for the malacostracan crustacean growth curves, which all agreed with the Generalised-VBGF (Table 1). The Generalised-VBGF is a flexible model, allowing A to vary between 0 and 1, so even though all malacostracan species display the same best-fitting model they show diversity in exponent A. This lack of consensus in the best-fitting growth model within taxonomic groups in this study indicates a potentially problematic issue with applying a single growth model when studying specific taxonomic groups.

Gaining accurate predictions of exponent A can aid biological understanding and open up new hypotheses. For example, the steep mass-scaling ($A = 1.12$) of *O.dioica* during ontogenetic growth prompts suggestions about the selective effects on growth of mortality risk in an open-water environment. With no refuges from predators, rapid sustained uptake of resources may be required to reach maturity fast before being consumed (Siebel *et al*., 1997; Tan *et al*., 2019). The scyphozoan *Pelagia noctiluca* also exists within a high-mortality pelagic environment but instead exhibits a shallower mass-scaling of biosynthesis ($A = 0.76$). This difference in exponent can prompt hypotheses about selective differences in mortality risks, including whether mortality reduces as size increases, or whether energy is invested into functions other than growth such as locomotion and/or buoyancy mechanisms. Furthermore, variation in the mass-scaling of biosynthesis was also present amongst benthic species (Table 1). For example, the common cuttlefish, *Sepia officinalis,* exhibits rapid exponential growth where relative growth rate (RGR) is constant ($A = 1$) (Figure 6), whereas the amphipod *Echinogammarus marinus* displays decreasing RGR where $A = 0.79$ (Figure 6). Despite partial covering of sand/seaweed, the predation risk for *S.officinalis* may be high considering the lack of parental care of eggs and high rates of cannibalism (Ibánez and Keyl, 2010). The relatively short lifespan of one to two years for *S.officinalis* (Pérez-Losada *et al*., 2007) supports the idea that sustained rapid growth is required to reach maturity before dying. In contrast, *E.marinus* lives

sheltered under algae, mud and/or rocks and exhibits egg development fully within the brood pouch (Maranhão and Marques, 2003). These features are indicative of low mortality risk throughout development, suggesting that gains in survival may accrue from investing in survival at the expense of sustained rapid feeding and exponential growth. Thus, fitting growth curves under this proposed framework helps formulate specific testable hypotheses about the selective effects of an organism's ecology on their growth.

The lack of universal agreement in the best-fitting growth model suggests applying a single parameterisation is not necessarily the best method of fitting growth curves to data. Instead, using a framework based on a set of parameterisations of a prevailing mathematical function increases flexibility (by allowing for variation in A). Flexibility enables us to find the best-fitting model with reliable predictions of growth and capture variation in growth rate, i.e. isomorphic and non-isomorphic growth. Ultimately, this framework enhances model applicability to a wider range of taxa. To further test and explore this framework, future work should focus on testing the validity of the $B = 1$ assumption for the mass-scaling of maintenance often made in the VBGF. It was assumed by von Bertalanffy (1938) that $B = 1$ on the basis that maintenance costs are approximately proportional to body mass. However, for some organisms, body mass composition can change throughout ontogeny, for example, insects have been shown to have increasing energy reserves (non-metabolising body mass) with age, which results in reduced mass-specific maintenance costs (Maino and Kearney, 2015b). Therefore, I recognise the need for flexibility in parameter B for certain animal groups where maintenance does not scale in proportion to body mass.

To achieve accurate predictions of growth rates, the pattern of growth must be accurately captured by the growth model. The common $\frac{2}{3}$ parameterisation (Pure Isomorphy model) of the VBGF captures sigmoidal growth patterns whereby growth rate declines over time (Bertalanffy, 1938). For organisms where mass-specific growth rate is maintained (exponential growth) or increased (supra-exponential growth) a sigmoidal growth function will predict lower than expected mass-specific rates of growth over time – resulting in poor predictions of growth. The results reported here show that while the five VBGF models can produce almost indistinguishable growth predictions in some cases, for example the Gompertz and Generalised-VBGF model

for larval *Crassostrea gigas* (Figure 1), over the twelve species (Figures 4 and 5) the five models can show great differences in growth predictions for given data. For example, applying the Pure Isomorphy model to *S.officinalis* (Figure 5) would underestimate late juvenile growth whereas the Supra-exponential and Exponential models would overestimate this growth.

Instead, the proposed growth curve fitting procedure for the five parameterisations of the VBGF allows the optimal value for exponent A to be found which results in the most accurate predictions of growth obtained by the VBGF. Hence, this procedure offers application of the VBGF to a wider range of taxa such as marine invertebrates which have previously poorly fitted the VBGF (Hirst and Forster, 2013). Modelling growth of marine invertebrates has proved difficult, for example, in sea cucumbers owing to their naturally flaccid bodies and ability to shrink in size (degrow) (Olaya-Restrepo *et al*., 2018), but accurate growth predictions are key to understanding how well species may survive in specific environmental conditions.

Extensive and successful use of the VBGF occurs for numerous fish species to aid the understanding of growth in relation to reproduction (Lester *et al*., 2004), fishing mortality (Taylor *et al*., 2005) and environmental temperature (Pauly, 1980), all of which are relevant to the sustainability of aquaculture. By applying this growth curve-fitting framework, I extend the range of taxa to which the VBGF (equation (2.1)) can be applied and hence to a wider range of ecological issues, such as the sustainability of marine invertebrate aquaculture. To further test and explore this framework, future work should focus on testing the validity of the $B = 1$ assumption for the scaling of maintenance often made in the VBGF. For some organisms, body mass composition, and hence mass-specific maintenance costs, can change throughout ontogeny, for example, insects (Maino and Kearney, 2015b).

Chapter 3. Growth and size-dependence of metabolic rates and body shape in pelagic invertebrates

3.1. Abstract

Rates of growth and metabolism are fundamental biological processes. Organism growth is fuelled by metabolic conversion of energy and resources from the environment, and so factors influencing the body mass-scaling of metabolic rate are predicted to also influence the growth rate trajectory over ontogeny. Current evidence indicates that ontogenetic changes in body shape, which induce changes in the area of surface responsible for resource uptake, correlate with changes in the body size scaling exponent of metabolic rate, b_R, across diverse species of pelagic invertebrates. Explicit predictions can also be made for the relationship between body shape change, expressed as the body length scaling exponent of body mass (b_L), and the body mass scaling exponent of anabolism (biosynthesis) (A), under Euclidean surface area theory. On this basis, if shape change influences, or is evolutionarily influenced by both growth and metabolism I predict that the body mass-scaling of growth will positively correlate with the scaling of metabolic rate across species of pelagic invertebrates. To test this, I collated data for diverse species of pelagic invertebrates to explore whether degree of body shape change correlates with scaling exponent A, and whether b_R correlates with A. No significant relationship between A and b_L, and A and b_R was found across either species or higher taxonomic groups. Instead, an overwhelming proportion of species displayed approximately exponential growth rate (constant relative growth rate, the body mass increase per unit mass per unit time, over ontogeny) with time despite variation in the degree of shape change or in the metabolic scaling exponent. The widespread presence of exponential growth may be explained by multiple intrinsic and extrinsic factors including variation in reproductive investment, lipid reserves and the energetic investment into locomotion and/or maintaining buoyancy across species.

3.2. Introduction

3.2.1. Variation in growth rates

Growth is a universal feature of all organisms. Individual growth rates correlate with a plethora of physiological and ecological variables (Karkach, 2006; Sibly *et al*., 2015). Thus, determining and understanding variation in growth rates is a fundamental biological research area. Organism growth is commonly defined as the acquisition and transformation of resources from the environment that results in the accumulation of new organic biomass (Karkach, 2006). The process of growth is fuelled by metabolism, whereby ATP energy generated from carbon compounds is used to fuel the synthesis of new biomass (Clarke, 2019; Sibly *et al.*, 2015). Although growth rate can be simply defined as the rate of increase of new biomass, the specific detail that this includes can be diverse: examples include the addition of segments in annelids (Balavoine, 2014), regeneration of body parts in echinoderms (Carnevali, 2006) and the rapid growth burst at moulting in arthropods (Karkach, 2006). Ontogenetic growth is typically described as determinate or indeterminate. Individuals displaying determinate growth, including many birds and mammals, will cease somatic growth when a certain body size is reached, usually at sexual maturation, but may continue to produce gametes and offspring. By contrast, indeterminate growers, such as several aquatic invertebrate taxa and fish, continue with somatic growth after maturation (Karkach, 2006). Ultimately, organism growth rates will be adapted to given environmental conditions and are often linked to fertility, mating success and survival rates (Bouchard and Winkler, 2018; Marshall, Bolton and Keough, 2003; Pardo, Cooper and Dulvy, 2013). Consequently, because growth correlates with traits governing fitness, the rate of organism growth is likely to be subject to selection, Therefore, the determinants of variation in growth rate are fundamental to understanding organismal ecology and evolution.

Numerous models and theories have been proposed to understand and predict variation in growth rates (e.g. Bertalanffy, 1938, 1957; Charnov, Turner and Winemiller, 2001; Kozlowski, Czarnoleski and Danko, 2004; West, Brown and Enquist, 2001, and see Chapter 2 for further information on growth modelling). Despite this, there is lack of agreement and understanding of the major drivers and

limitations of organism growth. Two theories which have been used to explain rates of supply of material over ontogeny and which in turn underpin growth rates, are surface area (SA) (e.g. Bertalanffy, 1938; Hirst, Glazier and Atkinson, 2014) and resource transport network (RTN) models (e.g. Banavar *et al.*, 2010, 2014; Moses *et al.*, 2008). For example, a well-known RTN model is the ontogenetic growth model (OGM), an extension of the West, Brown & Enquist (WBE) model for metabolic scaling (West, Brown and Enquist, 2001). The OGM posits that organism growth rate is constrained by the capacity of an organism's supply network to distribute resources required for the accumulation of new biomass (growth). In contrast, SA models, such as those based on Dynamic Energy Budget (DEB) theory (Kooijman, 2010) argue that growth rate is dependent on the assimilation of resources through body surface areas and the density of stored resources within an individual (van Der Meer, 2006b). Similarly, the extensively applied von Bertalanffy growth function (VBGF) (Bertalanffy, 1938, 1957) also assumes the assimilation of resources (required for growth) to scale in relation to body surface area available for uptake (Bertalanffy, 1938). For isomorphic organisms, whose body shape does not change with enlargement of body size, this theory predicts assimilation of resources to scale in proportion to relevant surface area and hence commonly with mass to the $\frac{2}{3}$ power (Bertalanffy, 1938; Kooijman, 2010). The VBGF is given by the equation:

$$\frac{dm}{dt} = Hm^A - Km^B, \tag{3.1}$$

where m and t denote body mass and time from birth or hatch, respectively, and A, B are the mass-scaling exponents of anabolism (synthesis of component materials) and catabolism (breakdown of component materials) respectively, and H and K are the coefficients of anabolism and catabolism, respectively (Bertalanffy, 1938). The Hm^A term in equation (3.1) represents resource availability for growth in an organism, with the mass-scaling exponent A often assumed to relate to the body-mass scaling of relevant surface area available for resource uptake (and hence commonly with mass to the $\frac{2}{3}$ power), from which non-growth metabolism (or catabolism as referred to by Bertalanffy, 1938) is then subtracted to obtain growth. Therefore, 'anabolism' is hereon referred to as 'biosynthesis'. The Km^B term represents resource consumption by tissues and is often proposed to scale in proportion to body mass (Bertalanffy,

1938), i.e. $B = 1$. Evidence (Hirst, 2012; Hirst *et al.*, 2014) suggests that most variation in the mass-scaling of metabolic rate during ontogeny among diverse aquatic taxa relates to scaling of surface area, and hence to the scaling of biosynthesis. Hence, I argue that the scaling of non-growth metabolism or catabolism (Km) varies less among organisms, and as assumed by von Bertalanffy (1938) and Kooijman (1993, 2000), scales approximately linearly with body mass where $B = 1$. This assumption may require modification for certain taxa where maintenance costs do not scale in direct proportion to body mass, such as when there is an increasing proportion of non-metabolising lipid reserves over ontogeny, for example, in holometabolous insect species (Maino and Kearney, 2015b).

3.2.2. The relationship between the mass-scaling of growth and metabolic rate

Application of existing growth models such as the VBGF, often imposes the assumption that growth of organs for resource uptake is proportional to growth of total body mass, so that the uptake surface area is proportional to body mass to the power $\frac{2}{3}$. For organisms that take up resources through body surfaces, the equivalent assumption is isomorphic (shape-invariant) growth, whereby all linear dimensions of body grow in equal proportion to one another and thus body mass is proportional to body length to the $\frac{2}{3}$ power. Variation in body geometry of organisms that change shape during ontogeny could offer insight into why some current growth models are poor in predicting growth trajectories over ontogeny in animals such as marine invertebrates (Hirst and Forster, 2013). At the extremes, non- isomorphic growth can occur along a single axis of length, i.e. body elongation, as occurs in rod-like bacteria (Bertalanffy, 1938), or along two axes of length in organisms exhibiting body 'flattening', such as in some pelagic medusae (Hirst, Glazier and Atkinson, 2014). Many other geometrical permutations are possible and include the boundary between body flattening (two-dimensional growth) and body elongation (one-dimensional growth), the boundary between elongation and isomorphy (three-dimensional growth) and the boundary between flattening and isomorphic growth. Furthermore, non-isomorphic growth can also occur as an organism becomes more squat (where diameter increases proportionately more than body length) over ontogeny.

Understanding changes in body shape, such as elongation or flattening, is important for understanding both growth and metabolic rates of integumentary breathers. Body shape governs the relationship between body surface areas, which relate to resource availability (for growth), and body volume, which relates to maintenance (where maintenance is often considered proportional to body volume, or volume of metabolising tissue) (Kooijman, 2000; see Chapter 2). In contrast, this assumption may be less applicable for species that respire through localised respiratory organs whose surface areas are not proportional to Euclidean body surface area. For example, some pelagic invertebrate taxa have gills, such as some crustacean species (e.g. *Euphausia* spp.) and hence may be less likely to satisfy this assumption. However, evidence from Bertalanffy (1957) suggests gill-breathers appear to follow the surface rule (that metabolic rate is proportional to the $\frac{2}{3}$ power of body mass) and hence are also included in this study. In addition to the presence of gills, there may also be other structures or functions that are important for determining the rate of oxygen uptake in aquatic organisms. For example, oxygen consumption rate has shown to be influenced by both gill surface area and ventilation frequency in carp and goldfish species (Luo *et al*., 2020), and rate of posterior tail undulations in freshwater oligochaete *Tubifex tubifex* (Kaster and Wolff, 1982).

Predictions for the relationship between the scaling of growth (specifically, the scaling of biosynthesis) and the body mass-scaling exponent of metabolic rate ($\log_{10}$ rate of oxygen consumption versus $\log_{10}$ body mass), hereafter called b_R, can be made based on the three metabolic and growth 'types' deduced by Bertalanffy (1951) which differ in their relationship between metabolic rate and body size. The three 'types' assume that the scaling of maintenance (or 'catabolism' by Bertalanffy) in equation (3.1) is proportional to body mass ($B = 1$) and are described as follows. (i) Type 1 organisms have metabolic rates that are surface-proportional, where the metabolic scaling slope $b_R = \frac{2}{3}$. This predicts an isomorphic growth type with a scaling exponent of biosynthesis of $A = \frac{2}{3}$, as is true for some fish and mammals and results in a sigmoidal pattern of mass-growth over time. (ii) Type 2 organisms have metabolic rates that scale in proportion to body mass ($b_R = 1$) and hence an exponential growth type over time (where relative growth rate – body mass increase per unit mass per unit time – is constant) is predicted ($A = 1$), as is the case for some insects (Bertalanffy,

1951; Maino and Kearney, 2015b) and aquatic invertebrates that elongate or flatten during ontogeny. (iii) Type 3 organisms exhibit an intermediate metabolic type – where metabolism scales in between surface- (type 1) and body mass- (type 2) proportionality, which results in a predicted range of $\frac{2}{3} < A < 1$ where mass- growth trajectories can display a range of sigmoidal patterns. Therefore, a positive 1:1 relationship between b_R and A can be predicted under these metabolic and growth 'types'.

For some organisms, such as arthropods, the process of growth can also involve growth spurts and the moulting of exoskeletons at specific stages over ontogeny, and thus it is important to consider developmental stages when examining growth curves. For example, copepods have several moults during the Nauplius (larval) and Copepodite (juvenile) stages. In the literature, growth measurements (mass or length) are generally recorded at each moult at the same time to reduce any bias in mass (or length) pre- or post- moult, which hence results in a smooth growth curve. From a personal examination of copepod growth data (mass or length versus time) in the literature, the Nauplius growth curve can differ to the copepodite growth curve. For example, the Nauplius stage often exhibits approximate exponential growth curve with no plateau, whereas the Copepodite stage often exhibits a sigmoidal growth curve where growth reaches a plateau. Therefore, the decision to either combine or separate Nauplius and Copepodite stage growth data when fitting growth curves will impact the outcome and results of the growth curve fitting; caution must be taken when making this decision and drawing conclusions from the growth curve fitting output. A major aim of this Chapter is to explore the growth trajectories (mass versus time) over the complete ontogenetic development of pelagic invertebrate species, and thus this Chapter will combine stages (such as Nauplius and Copepodite) when fitting growth curves to data. I acknowledge that this is likely to result in different growth curves to that of using specific stages of ontogeny only.

3.2.3. Does ontogenetic body shape change predict growth rate?

Previous work by Hirst, Glazier and Atkinson (2014) and Glazier, Hirst and Atkinson (2015) highlighted the potential for changes in body shape (e.g. elongation or flattening) during ontogeny to predict metabolic scaling in pelagic invertebrates. Body

shape was quantified as the mass-body length scaling exponent, $\frac{1}{b_L}$, which displayed a significant positive correlation with the body-mass scaling of metabolic rate, b_R, across diverse species and broader taxonomic groups of pelagic invertebrates. As growth is fuelled by metabolism, does body shape shifting also predict the intra-specific scaling of ontogenetic growth rates in pelagic invertebrates? Specifically, because changes in body shape cause alterations in external body surface areas, shape shifting is predicted to play a role in mediating the uptake of resources required for metabolism and growth in taxa that assimilate resources through external body surface areas, e.g. in some pelagic invertebrate groups with respect to oxygen. Hence, ontogenetic shifts in body shape are predicted to correlate with shifts in growth rates, in the same way that body shape-metabolic scaling relationships have already been demonstrated in pelagic invertebrates (Glazier, Hirst and Atkinson, 2015; Hirst, Glazier and Atkinson, 2014). Pelagic invertebrates include relatively isomorphic animals (e.g. euphausiids) as well as strong shape-shifters that display a plethora of body shapes that change throughout development (e.g. salps, ctenophores and many medusae) (Glazier, Hirst and Atkinson, 2015; Hirst, Glazier and Atkinson, 2014), and hence provide an ideal group to test the relationships between metabolism, growth and body shape.

Assuming that body mass is proportional to volume or body density is constant, the exponent b_L represents the relationship between body mass (m) and body length (L) by the equation: $m = aL^{bL}$. Thus, b_L is obtained as the slope of a least-squares regression between $\log_{10}$ mass and $\log_{10}$ length. Under Euclidean geometry, an organism growing isomorphically will have a b_L value of 3, because $m \propto L^3$. Thus, organisms that do not conform to this geometry are expected to deviate from $b_L = 3$. One extreme is pure body elongation, as discussed previously, which predicts $b_L = 1$, because $m \propto L$. In contrast, organisms that 'flatten' in body shape grow in length and width only, hence giving $b_L = 2$ because $m \propto L^2$. The diversity of body shapes observed in highly variable taxa, such as pelagic invertebrates, produces a range of b_L values (as shown by Glazier, Hirst and Atkinson, 2015; Hirst, Glazier and Atkinson, 2012, 2014). Inverse b_L values $(\frac{1}{b_L})$ have log(mass) as the x-variate which allows prediction of a linear relationship with b_R or mass-scaling exponent of biosynthesis, A, instead of a non-linear relationship (see Figure 7 for a visual representation).

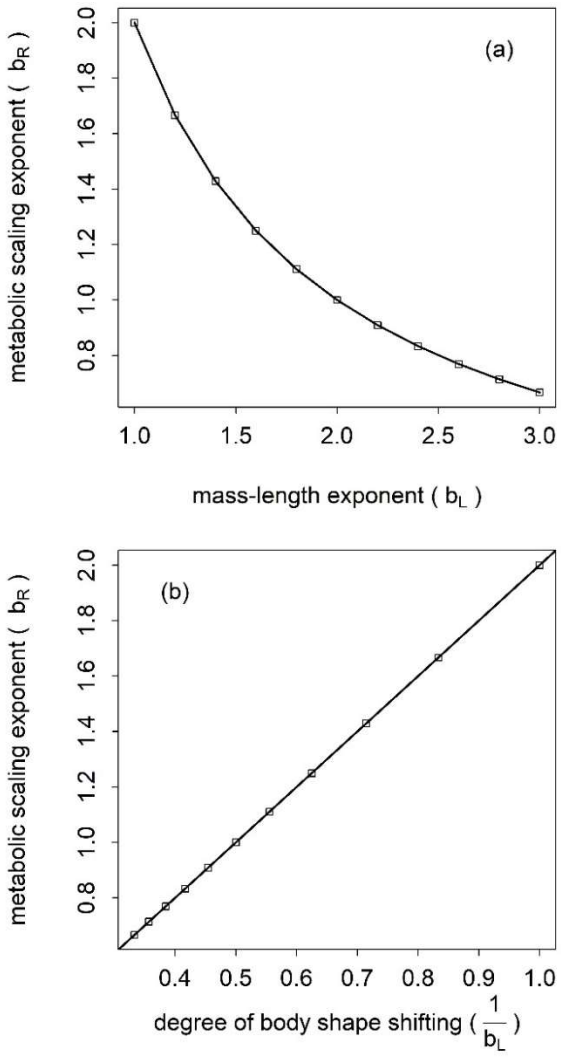

1610

1611 **Figure 7**. A representation of the nonlinear relationship between the metabolic
1612 scaling exponent, b_R, and the mass-length scaling exponent, b_L (a) and the linear
1613 relationship between b_R and the inverse mass-length scaling exponent, $\frac{1}{b_L}$ (b). Note
1614 the data shown is hypothetical and produced solely for the purpose of this plot.

1615

1616 **3.2.4. Explicit predictions based on Euclidean surface theory: growth and body**
1617 **shape change**

1618 Specific predictions can be made for the relationship between the scaling of growth
1619 and body shape change over ontogeny by applying a Euclidean surface area model,
1620 previously described in Hirst, Glazier and Atkinson (2014) and Glazier, Hirst and
1621 Atkinson (2015). As described above, or an isomorphic (shape-invariant) organism,

the body mass-length exponent (b_L) will equal 3. Applying Rubner's (1883) surface area law predicts for isomorphic organisms that body surface area scales in proportion to $M^{\frac{2}{3}}$ and thus the body mass scaling exponent of biosynthesis (A) is predicted to be $\frac{2}{3}$ (for further interpretation and mathematical properties of exponent A see Chapter 2). For organisms that change shape, (i.e. deviate from $b_L = 3$), such as pure body elongation ($b_L = 1$). surface area theory predicts that body surface area scales in proportion to body mass, and hence it is predicted that $A = 1$ because uptake of resources (required for growth) is expected to increase with surface area under Euclidean theory. Growth in just two axes of length, for example body flattening ($b_L = 2$), predicts body surface area to scale in proportion to mass and hence $A = 1$ (Hirst, Glazier and Atkinson, 2014). Euclidean surface area theory also predicts $b_L > 3$ when an organism becomes more squat in shape during ontogeny, i.e. when the shorter length axes grow disproportionately faster than a longer length axis and A is predicted to be less than $\frac{2}{3}$ (Hirst, Glazier and Atkinson, 2014).

3.3. Aims and hypotheses

The aim of this study is to explore to what extent changes in body shape change correlate with the mass-scaling exponent of biosynthesis, A, and whether A correlates with the mass-scaling exponent of oxygen consumption, b_R, across diverse species and broader taxonomic groups of pelagic invertebrates. Specifically, I hypothesise that across species and broader taxonomic groups of pelagic invertebrates:

1. If changes in body shape ($^1/_{b_L}$) result in changes in body surface areas responsible for resource uptake then $^1/_{b_L}$ will positively correlate with changes in the body mass scaling of biosynthesis, A, over ontogeny.
2. Because metabolism fuels the process of growth, the scaling of metabolic rate, b_R, will display a positive 1:1 correlation with the scaling of biosynthesis, A over ontogeny as proposed by the metabolic and growth types of Bertalanffy (1951).

3.4. Methods

3.4.1. The dataset

Pelagic invertebrates are an ideal group to explore the effects of body shape change on growth and metabolic rate because they often exchange oxygen and wastes across external body surface areas (Glazier, Hirst and Atkinson, 2015; Hirst, Glazier and Atkinson, 2014). Published ontogenetic mass-at-age data for pelagic invertebrate species were collected from the literature using Web of Knowledge. Search terms included "growth AND pelagic AND (lab* OR culture* OR ontogen* OR development*)" under the data requirements and collection methods described in Chapter 2.4.3 (The dataset). Ontogenetic growth data were obtained from time at hatch or birth, up until, but excluding, sexual maturity for species where possible. When only incomplete juvenile development data were available this was used and recorded in the dataset (see Supplementary Appendix 2 Table S3 for detail on each species). In total, growth data were collected for 76 species from the major taxonomic groups: Anostraca (2), Amphipoda (2), Cladocera (5), Appendicularia (1), Cephalopoda (1), Chaetognatha (1), Copepoda (26), Ctenophora (5), Decapoda (15), Mysida (1), Thaliacea (2), Euphausiacea (5), Bivalva (2), Polychaeta (4), Scyphozoa (4) and Hydrozoa (1), where the number in brackets denote the number of species included per taxonomic group. All analysis in this Chapter was performed for a single individual per species. For species where growth data for more than one individual was available, the individual with the most natural (i.e. most similar to that of the natural habitat range) temperature and salinity conditions was selected.

3.4.2. The body mass-scaling of biosynthesis

Candidate growth models and fitting

To explore the allometric growth-scaling relationships of diverse pelagic invertebrate species, I applied the growth curve fitting procedure described in Chapter 2. This procedure involves fitting a set of candidate growth models based on the von Bertalanffy growth function (VBGF) (Bertalanffy 1938, 1949) (equation (3.1)) to empirical growth data. As discussed in the Introduction, I assume a fixed value for the

body mass-scaling exponent of maintenance, $B = 1$. This assumption allows equation (3.1) to be solved to allow variation in parameterisation of the mass-scaling exponent of biosynthesis, A. Importantly, allowing for variation in A allows a range of growth rate types to be captured including isomorphic, intermediate ($0 < A < 1$), exponential growth and supra-exponential growth. This is represented by five different parameterisations of the VBGF (see Chapter 2.5 Methods for information on the development and fitting of these candidate models).

These candidate models capture diverse variation in relative growth rate (RGR, the body mass increase per unit mass per unit time) by allowing variation in the body mass scaling exponent of biosynthesis, A, and hence are useful for determining the growth patterns of marine invertebrates. These models are: Pure Isomorphy model ($A = \frac{2}{3}$) and four nested non-isomorphic growth models: Exponential ($A = 1$), Gompertz ($A \to 1^{-}$), Generalised-VBGF ($0 < A < 1$) and Supra-exponential ($A > 1$). These five parameterisations represent different categories of RGR (Bhowmick *et al*., 2006), including constant RGR over time (Exponential model), decreasing RGR over time (Gompertz, Generalised-VBGF and Pure Isomorphy models) and increasing RGR over time (Supra-exponential model) and hence are useful for capturing the potential diversity in RGR for diverse pelagic invertebrate species. These models represent five different parameterisations of the original VBGF expressed as a standardised solution (Richards, 1959), where the scaling exponent of catabolism is fixed at $B = 1$, given as:

$$m = m_0 \left\{ \frac{1-(1-Z)\exp\left(K(A-1)(t-t_0)\right)}{Z} \right\}^{-\frac{1}{A-1}} \quad (3.2)$$

where m_0 represents mass m at time t_0 (time at birth / hatch). The mass-scaling exponent for biosynthesis is given by A and the rate at which final mass is reached is represented by parameter K. Parameter $= \left(\frac{m_\infty}{m_0}\right)^{A-1}$, where $m_\infty = \left(\frac{H}{K}\right)^{1/(1-A)}$, has no simple biological interpretation. For further description of these candidate models see Chapter 2.5 (Methods) and for full derivation of these candidate growth models and equation (3.2) see Supplementary Appendix 1.

The five candidate models were fitted to empirical mass-time data with log least squares method of optimisation by using the general-purpose optimisation

function *optim()* in R (v3.5.0) as described in Chapter 2.5.2 (Fitting and assessing candidate growth models). The models were fitted to individuals, or to cohorts of individuals if individuals did not differ in treatment or condition, for all species.

The best fitting growth model was determined by calculating the negative log-likelihood (NLL) for each model fit:

$$NLL = \frac{1}{2}\left(n\left(\log(2\pi) + \log\frac{S}{n} + 1\right)\right) \quad (3.3)$$

Where S represents the sum of squared residuals and n the number of datapoints (Patefield, 1985). The model with the most negative NLL (i.e. closest to negative infinity) was taken as the best fitting model. For the purpose of providing a statistical comparison of the five VBGF models in this Chapter, I also applied Likelihood Ratio Testing (LRT) to determine the best fitting model overall and the associated value for exponent A. This was performed following the LRT methods described in Chapter 2 (2.5.2 Fitting and assessing candidate growth models).

In the case where species had data from multiple individuals or cohorts, the best fitting A value from the most complete developmental data (from hatch/birth up to, but excluding, sexual maturity) was chosen and when no complete juvenile data was available the growth data which contained the highest rate of survival was chosen. If no survival rate data was reported, individuals raised under salinity and temperature conditions most similar to that experienced in nature were chosen. The justification of this method is because in some cases individuals of a given species would have a best fit $A = \frac{2}{3}$ and others $A = 1$ and so averaging these would give an A value that is not necessarily representative of either individual.

When performing comparative analysis, it is often necessary to consider evolutionary relatedness because species are not independent, but share characteristics through descent of common ancestors (Symonds and Elgar, 2002). Controlling for phylogeny in comparative analysis requires an evolutionary tree that is fully known and without error (Symonds and Elgar, 2002). However, the paucity of information or data on the phylogeny of diverse pelagic invertebrate species in the literature meant that phylogenetic comparative methods could not be applied in this Chapter. Consequently, because phylogenetic comparative methods were not feasible, I averaged species data

to provide taxonomic averages for exponent A, the degree of body shape change, $\frac{1}{b_L}$ and the metabolic scaling exponent b_R. I acknowledge the limitations of this method of averaging that will likely result in different values and scaling relationships compared to that of phylogenetic comparative methods, and hence caution should be used when drawing conclusions from these taxonomic averages.

3.4.3. Variation in specific growth rates across exponential growers

Species may not only exhibit variation in the body mass scaling of biosynthesis (A) over ontogeny but may also differ in their specific growth rate at a given point in ontogeny. Variation in growth rate can be compared most easily across pelagic invertebrate species with exponential growth. In these species, $A = 1$, RGR is maintained, and specific growth rate is calculated as the slope of ln(body mass) versus time regression. For species not growing exponentially, RGR is not constant but either decreases ($A < 1$) or increases ($A > 1$) over ontogeny, and thus specific growth rate cannot be accurately described by the above regression equation. Hence, for the purpose of providing a simple analysis to explore variation in growth rate across species, specific growth rate (SGR) was calculated for exponential growers only. Data for SGR was corrected for temperature using a Q_{10} value of 2.16 obtained from Seebacher, White and Franklin (2015). This Q_{10} value represents the mean Q_{10} value for diverse marine ectotherm species data obtained from a literature search (Seebacher, White and Franklin, 2015). These species were exposed to a minimum of two temperatures for at least one week, and included a range of temperatures from -1.7 to 29°C (Seebacher, White and Franklin, 2015).

3.4.4. The influence of body shape change on the mass-scaling of growth and metabolic rate

To explore the potential influence of degree of body shape change during ontogeny on the mass-scaling of biosynthesis (A) and metabolic rate (b_R) the inverse body mass-body length scaling exponent, $\frac{1}{b_L}$ was plotted against both A and b_R. Ontogenetic species data for b_L were obtained from the dataset compiled by Hirst, Glazier and

Atkinson (2014) which contains body shape and metabolic scaling data for both immature and mature species (however, the stage is not defined). This dataset (Hirst, Glazier and Atkinson, 2014) was used in this study because time did not allow collection of immature body shape and metabolic scaling data for immature species only. Therefore, I acknowledge this caveat and future work should consider obtaining a body shape and metabolic scaling dataset for immature stages of pelagic invertebrate species, or at least distinguish between stages. Only b_L values where the $R^2 \geq 0.80$ were used in my analysis.

To explore the relationship between growth and body shape change over ontogeny in relation to surface area theory, the plots of A versus $\frac{1}{b_L}$ will also contain an envelope of predictions from the Euclidean surface area model of Hirst, Glazier and Atkinson (2014). The model predictions of Hirst, Glazier and Atkinson (2014) are based on the relationship between $\frac{1}{b_L}$ and the mass-scaling of body surface area (b_A) and were applied to plots of both b_R versus $\frac{1}{b_L}$ and b_A versus $\frac{1}{b_L}$ (Hirst, Glazier and Atkinson, 2014). This model explores the changes from shape-invariant (isomorphic) growth ($\frac{1}{b_L} = \frac{1}{3}$) to different degrees of body shape change including pure elongation (where $\frac{1}{b_L} = 1$), pure body flattening (where $\frac{1}{b_L} = 0.5$) and increasing body thickness (or increasing squatness) (where $\frac{1}{b_L} < \frac{1}{3}$).

Therefore, this chapter will extend these predictions to plots of A versus $\frac{1}{b_L}$ to explore whether the relationship between the scaling of biosynthesis and the degree of body shape change agrees with Euclidean surface area theory. The Euclidean model assumes that body mass is proportional to body volume over ontogeny, and a minimum of three length scales: l_1, l_2 and l_3 are present (Hirst, Glazier and Atkinson, 2014). Detailed derivations of the model predictions are presented in the Supplementary Information of Hirst, Glazier and Atkinson (2014). By extending these predictions to the scaling exponent of biosynthesis, A, the explicit model predictions for different types of body shape change include:

Isomorphic to body flattening $$A = 2\left(\frac{1}{b_L}\right) \quad (3.4)$$

Isomorphic to body elongation	$A = 0.5(1 + \frac{1}{b_L})$	(3.5)
Between pure elongation and flattening	$A = 1$	(3.6)
Thickening (in length dimension l_3)	$A = 2\left(\frac{1}{b_L}\right)$	(3.7)
Thickening (in length dimension l_2)	$A = 1 - \left(\frac{1}{b_L}\right)$	(3.8)

These model predictions (equations 3.4 to 3.8) will be applied to plots of A versus $\frac{1}{b_L}$ for diverse pelagic invertebrate species and wider taxonomic groups.

3.4.5. The body mass-scaling of growth and metabolic rate

To explore the relationship between ontogenetic changes in growth (biosynthesis) and metabolic rate, b_R was plotted against A. These b_R values were obtained from the same source as the empirical growth data if available, or the dataset compiled from Hirst, Glazier and Atkinson (2014) and only b_R values where $R^2 \geq 0.80$ were used. Relationships were explored using Reduced Major Axis (RMA) regression when the correlation was significant ($p < 0.05$) and Ordinary Least Squares (OLS) regression was applied when the correlation was not significant, as described by the *lmodel2* package in R. All analyses were performed in R (v3.6.2).

3.5. Results

3.5.1. Growth rate and body shape change over ontogeny

The best-fitting value for the scaling exponent of biosynthesis, A, as determined by the most negative log likelihood was ≥0.99 for 62 out of the 76 studied species of pelagic invertebrates. Within these 62 species, 53 species exhibited approximately exponential growth ($0.99 \leq A \leq 1$) and nine species displayed supra-exponential growth (where $A > 1$). For the remaining 14 species, A varied between 0.54 and 0.99 (see Figure 8 for range of A values and Supplementary Appendix 2 Table S3 for the

complete dataset). The best-fitting mean values of A for 13 wider taxonomic groups ranged between 0.86 and 1.17 (see Table 2 for best-fitting mean values for A and the 95% confidence intervals for each wider taxonomic group). Six taxonomic groups displayed decreasing average relative growth rate (RGR) over time with A values between $0.86 - 0.97$ (Euphausiacea, Bivalvia, Decapoda, Ctenophora, Copepoda, Scyphozoa). Four taxonomic groups (Amphipoda, Chaetognatha, Cladocera, Hydrozoa) exhibited constant RGR (exponential growth) over time where $A = 1$. The remaining three taxonomic groups (Thaliacea, Appendicularia, Cephalopoda) averaged supra-exponential growth where RGR increases over time ($A > 1$).

The best fitting model as determined by the most negative log likelihood is presented alongside the best fitting model overall as determined by Likelihood Ratio Testing (LRT) for 76 studied species of pelagic invertebrates in Supplementary Appendix 2 Table S4.

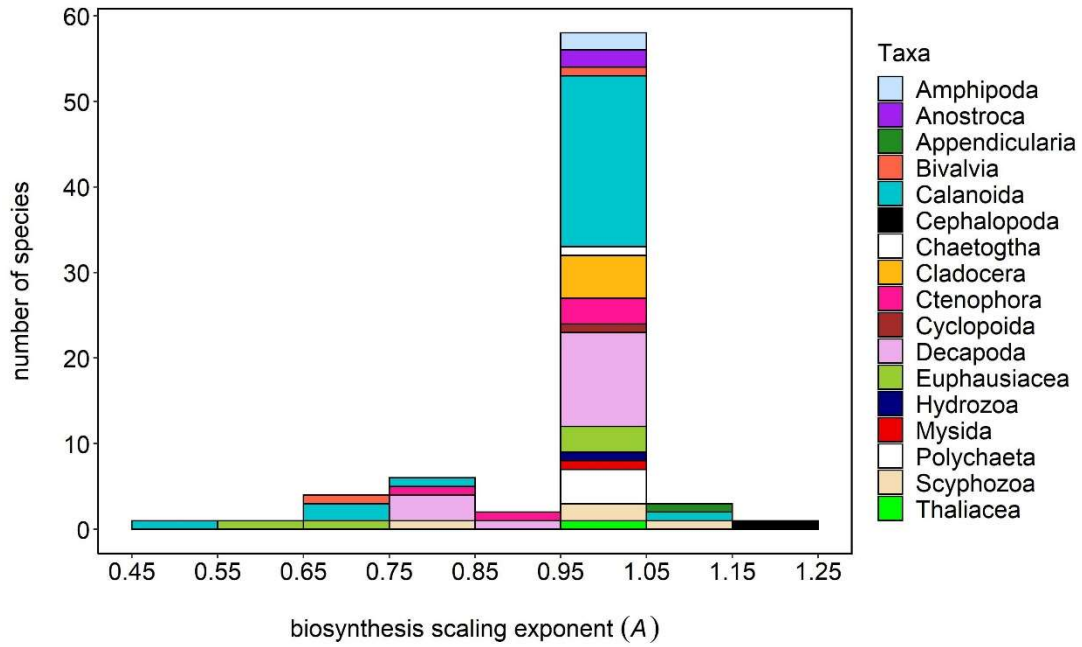

Figure 8. The best-fitting biosynthesis scaling exponent, A, values for 76 species of pelagic invertebrates (see Supplementary Appendix 2 Table S3 for complete dataset). The best-fitting value was determined using negative log-likelihood for a set of von Bertalanffy-based growth models (see section 3.4.2. for further information).

Table 2. The average exponent A value and 95% confidence intervals (denoted by lower CI and upper CI) for each wider taxonomic group, where n denotes the number of species within each wider taxonomic group.

Taxa	n	Average A	Lower CI	Upper CI
Amphipoda	2	1	1	1
Anostraca	2	1.00	1.00	1.00
Appendicularia	1	1.08	1.08	1.08
Bivalva	2	0.87	0.70	1.05
Cephalopoda	1	1.17	1.17	1.17
Chaetognatha	1	1	1	1
Cladocera	5	1.00	1.00	1.00
Copepoda	26	0.96	0.91	1.00
Ctenophora	5	0.95	0.90	1.01
Decapoda	15	0.95	0.91	0.99
Euphausiacea	5	0.86	0.71	1.01
Hydrozoa	1	1	1	1
Nematoda	1	1	1	1
Polychaeta	4	1	1	1
Scyphozoa	4	0.97	0.84	1.09
Thaliacea	1	1	1	1

Out of the 76 species of pelagic invertebrates in this study, 49 had corresponding b_L data available. The values for the best-fitting scaling exponent of biosynthesis, A, are plotted against the degree of body shape shifting ($\frac{1}{b_L}$) for these 49 species of pelagic invertebrates in Figure 9, for data averaged both within species (Figure 9a) and within broader taxonomic groups (Figure 9b). There was no significant relationship between exponent A and $\frac{1}{b_L}$ for data averaged either within species (OLS regression: $p > 0.05, R^2 = 0.05, n = 49$) or within broader taxa (OLS regression: $p > 0.05, R^2 = 0.04, n = 12$).

Predictions made by Euclidean surface area theory (equations 3.43 to 3.8), as indicated in Figure 9 by the area contained within the dashed lines, are therefore not supported by the data on the pelagic invertebrate species in this study. This is true for all species except the euphausiid *Euphausia pacifica* ($A = 0.67$, $\frac{1}{b_L} = 0.32$) and the copepod *Oithona similis* ($A = 1$, $\frac{1}{b_L} = 0.69$), which have A and b_L values that fulfil Euclidean surface area predictions (Figure 7a). No taxon-specific averages of A and b_L supported predictions made by Euclidean surface area (Figure 9b). Taxon-specific

averages of exponent A were calculated from a varied range of species-specific A values for different wider taxonomic groups, and the sample size (number of species) for each wider taxonomic group also varied (see Table 2).

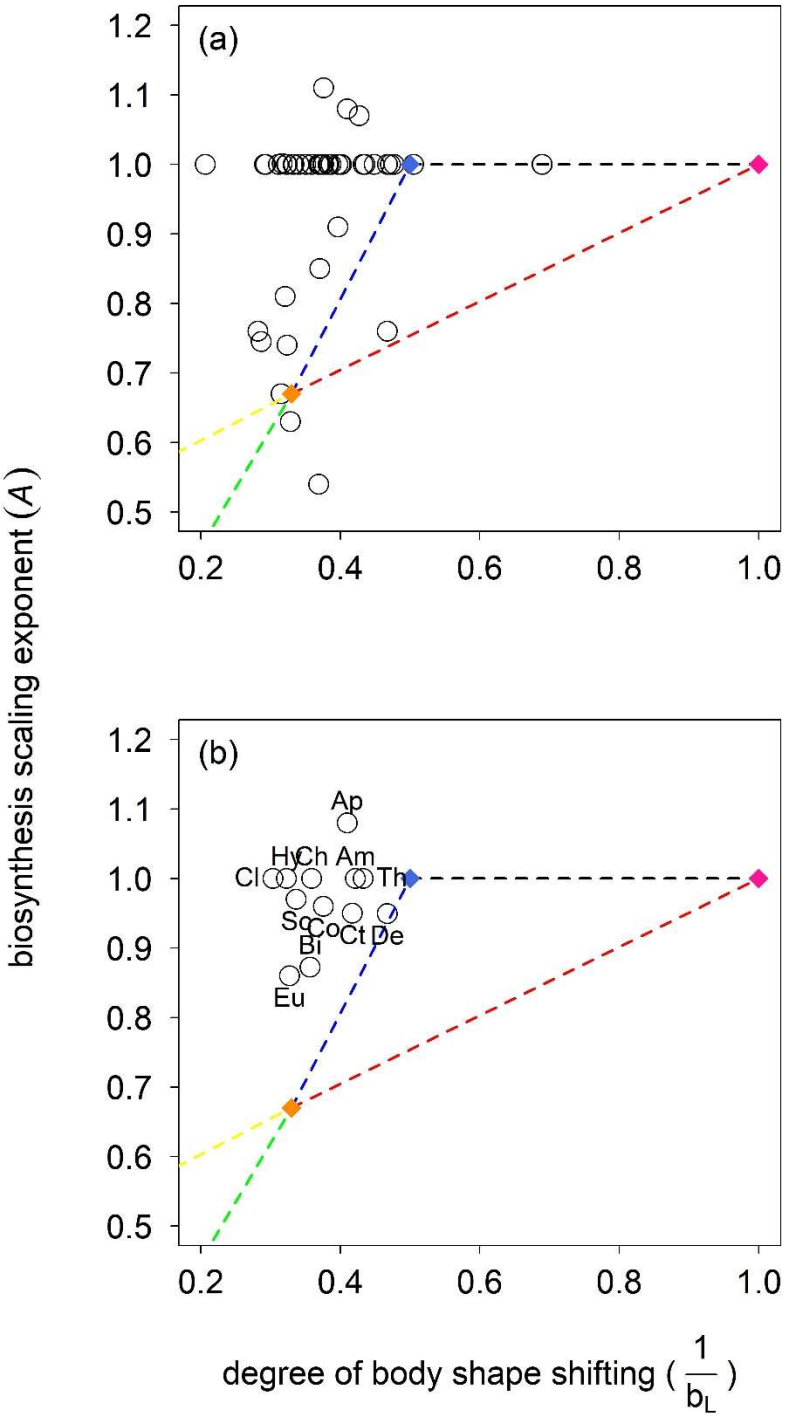

Figure 9. Mass-scaling exponent of biosynthesis, A (as obtained from the best-fitting growth model to empirical mass versus time data) versus the degree of body shape

shifting ($\frac{1}{b_L}$) for pelagic invertebrate species. (a) Species-specific averages for 49 species. (b) Averages for 12 broader taxonomic groups: Eu (Euphausiacea), Bi (Bivalvia), De (Decapoda), Ct (Ctenophora), Co (Copepoda), Sc (Scyphozoa), Am (Amphipoda), Ch (Chaetognath), Hy (Hydrozoa), Cl (Cladocera), Th (Thaliacea) and Ap (Appencidularia). The dashed lines represent an envelope of predictions (diamonds) made from a Euclidean surface area model based on: isomorphic growth (yellow diamond), exponential growth of flattening organisms (blue diamond) and exponential growth of elongating organisms (pink diamond). The Euclidean surface area model is described by Hirst *et al*. (2014) and predicts the following relationships between $\frac{1}{b_L}$ and b_A as indicated by the dashed lines. Black line: $A = 1$; red line: $A = 0.5(1 + \frac{1}{b_L})$; blue line: $A = 2(\frac{1}{b_L})$; yellow line: $A = 1 - (\frac{1}{b_L})$; green line: $A = 2(\frac{1}{b_L})$ (see Methods 3.4.4. for description of these predictions). Two species fit within the area of the Euclidean surface area model range (within the dashed lines): *Euphausia pacifica* ($A = 0.67,\ \frac{1}{b_L} = 0.32$) and *Oithona similis* ($A = 1,\ \frac{1}{b_L} = 0.69$).

3.5.2. Variation in specific growth rate across exponential growers

The distribution of specific growth rate (SGR) values for species exhibiting exponential growth (biosynthesis) (52 out of 76 species) is shown in Figure 10. SGRs varied between 0.01 and 0.39 d^{-1} (see Supplementary Appendix 2 Table S3 for standard error of SGR estimates and complete dataset). Most exponential growers (where mass scaling exponent of biosynthesis, $A = 1$ at a fixed value for the mass scaling exponent of catabolism at $B = 1$) displayed specific growth rates within the range of 0.01 to 0.20 d^{-1} (38 out of 52 species), with the remaining 14 species displaying more rapid growth rates within the range of 0.2 to 0.39 d^{-1}. Specific growth rate varied within broader taxonomic groups (Figure 10); for example, that for calanoid copepods ranged from 0.06 to 0.39 d^{-1}. For a detailed representation of the frequency distribution of SGRs within broader taxonomic groups see Supplementary Appendix 2 Figure S1.

There was no significant relationship between: degree of body shape change, $\frac{1}{b_L}$, and SGR (OLS regression: $p > 0.05, R^2 = 0.0003, n = 33$), or between the

metabolic scaling exponent, b_R, and SGR (OLS regression: $p > 0.05, R^2 = 0.007, n = 11$).

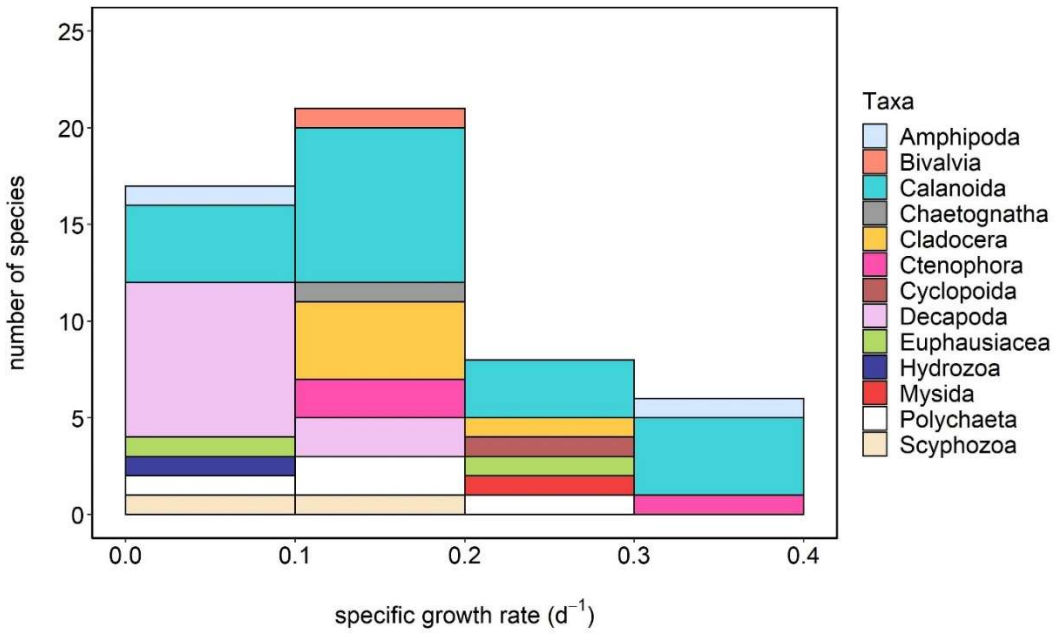

Figure 10. Temperature-corrected specific growth rates (d^{-1}) for the 52 species of pelagic invertebrates displaying exponential growth ($A = 1$) (see Supplementary Appendix 2 Table S3 for complete dataset). Specific growth rate was determined from the slope of the regression between the natural logarithm of body mass against time.

3.5.3. The relationship between body mass-scaling of growth and metabolic rates

Out of the 76 species of pelagic invertebrates in this study, 23 had corresponding b_R data available. Across these 23 species, b_R varied between 0.50 and 1.09 (see Supplementary Appendix 2 Table S3 for all b_R data). The mean body mass scaling exponents for metabolic rate, b_R, are plotted against mean mass-scaling exponent of biosynthesis (as determined from the best-fitting growth model), A, for pelagic invertebrate species in Figure 11a, and for broader taxonomic groups in Figure 11b. There was no significant relationship between b_R and A for either species-specific averages (OLS regression: $p > 0.05, R^2 = 0.06, n = 23$) or averages for broader taxonomic groups (OLS regression: $p > 0.05, R^2 = 0.006, n = 11$).

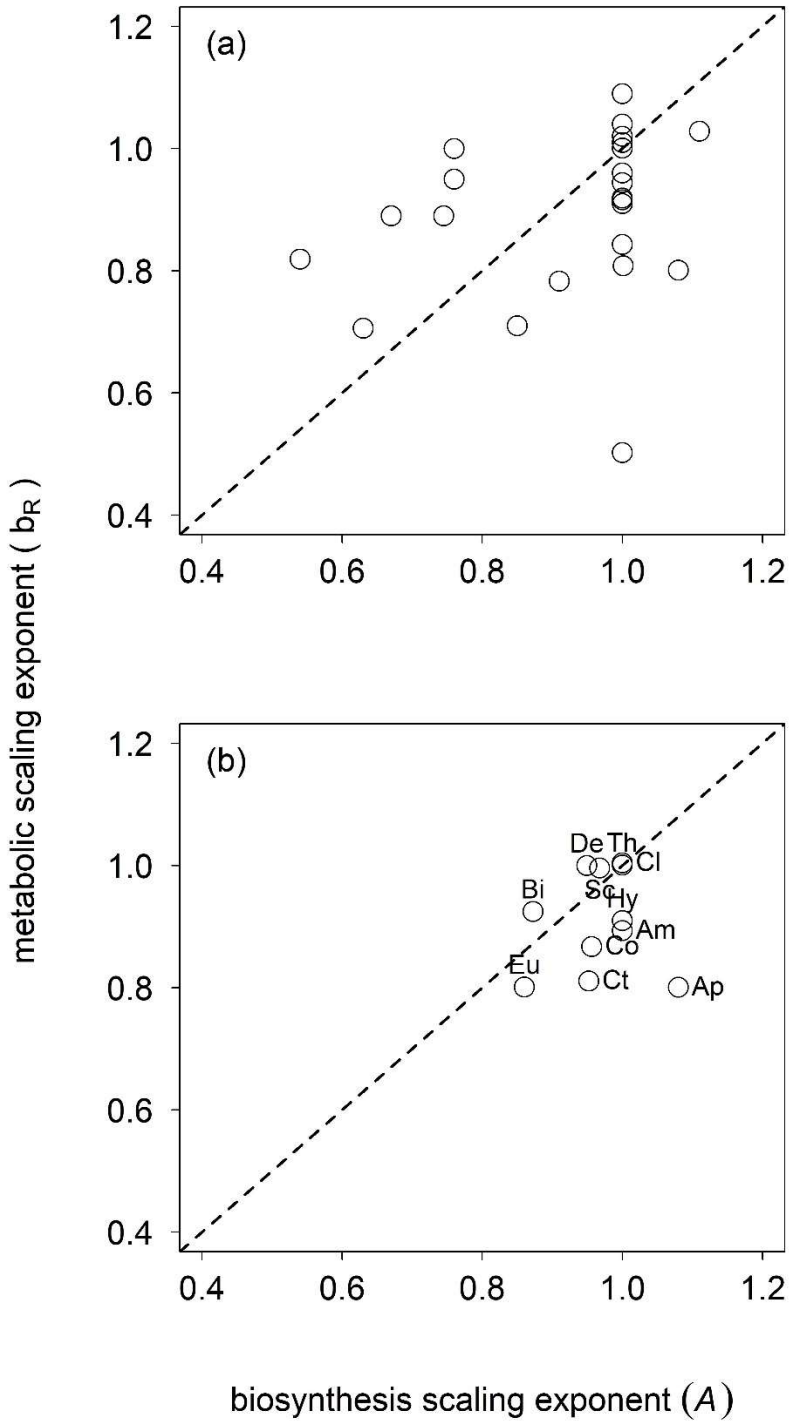

1922

1923 **Figure 11.** Metabolic rate-body mass scaling exponent, b_R versus mass scaling of
1924 biosynthesis, A (as obtained from the best-fitting growth model to empirical mass
1925 versus time data) for pelagic invertebrate species. (a) Species-specific averages for 23
1926 species. (b) Taxon-specific averages for 11 taxa: Eu (Euphausiacea), Bi (Bivalvia), De
1927 (Decapoda), Ct (Ctenophora), Co (Copepoda), Sc (Scyphozoa), Am (Amphipoda), Hy

(Hydrozoa), Cl (Cladocera), Th (Thaliacea) and Ap (Appendicularia). Dashed lines represent a theoretical one-to-one relationship between A and b_R.

3.6. Discussion

3.6.1. The relationship between the body mass-scaling of growth and body shape change over ontogeny

Considering that growth is fuelled by metabolism, it can be hypothesised that changes in body shape over ontogeny could also correlate with changes in growth rate. Such hypothesis is based on the assumption that an organism's metabolic rate is limited by the relationship between body surface area and volume, i.e. body shape rather than being limited by body mass. The scaling exponent of biosynthesis, A, shows no relationship with the degree of body shape change, $\frac{1}{b_L}$, across species or across broader taxonomic groups of diverse pelagic invertebrates. Changes in body shape over ontogeny are likely to result in deviations in the body-mass scaling of body surface area from the exponent of $\frac{2}{3}$, and so organisms that exchange oxygen and wastes through external body areas whose sizes are limiting to resource uptake that is needed for growth (such as many species of pelagic invertebrates; Hirst, Glazier and Atkinson, 2014) are likely to display marked shifts in the scaling of resource uptake and consequently growth rate. Thus, if the assumptions made throughout this Chapter are true (that mass is proportional to volume or that body density stays constant over ontogeny, and that metabolic rate is limited by body shape), the lack of relationship between A and $\frac{1}{b_L}$ is thus somewhat unexpected.

A lack of correlation between the scaling of biosynthesis and body shape change over ontogeny could potentially be described by the large proportion of pelagic invertebrate species displaying exponential growth (biosynthesis), where $A = 1$ (Figure 8), despite wide variation in the degree of body shape change (Figure 9a). The presence of exponential growth despite degree of body shape change suggests that relative growth rate (RGR, the body mass increase per unit mass per unit time) can be maintained over ontogeny despite likely limitations to resource exchange across the

body surface. For example, isomorphic organisms do not change shape over ontogeny and hence do not exhibit enhanced scaling of body surface area responsible for resource uptake over ontogeny. Therefore, for organisms that exhibit little or no body shape change over ontogeny, exponential growth may occur if resources taken up from body surface areas (such as oxygen uptake across the integument) are increasingly diverted away from other biological processes, such as immune function, locomotion or reproduction, and allocated towards growth over ontogeny. Conversely, resources (such as oxygen) may be less limited for organisms exhibiting shape change over ontogeny due to enhanced scaling of body surface area responsible for resource uptake. Thus, for shape shifting organisms that increase scaling of body surface area responsible for uptake over ontogeny, exponential growth may occur without diverting resources, or diverting relatively less resources, away from biological processes other than growth in comparison to isomorphic organisms. Alternatively, the widespread presence of exponential growth despite variation in the degree of body shape change could also suggest that the assumption that resource exchange is limiting over ontogeny is incorrect. Thus, if there are no limitations to resource exchange then it is possible that both isomorphic (shape-invariant) and strong shape shifting organisms (for example displaying body elongation) could maintain a constant supply of resources to fuel a constant relative growth rate (exponential growth) over ontogeny.

Unlike their benthic counterparts, pelagic organisms generally lack cover or refuge from predators in open water, which leaves them visually exposed to predators, especially in well-lit epipelagic waters. The high mortality risk of a pelagic environment may select for faster development to maturity (to reduce time spent at high mortality risk before reproduction), and may also select for exponential growth, where RGR is constant over ontogeny, if high mortality is sustained throughout ontogeny. Furthermore, it is also plausible that high mortality risk selects for exponential growth over time, if it is associated with truncation of the 'traditional' sigmoidal VBGF growth curve at the point of inflexion so that the growth curve assumes an exponential shape and does not plateau. Therefore, the high mortality risk associated in an open water pelagic environment may account for the widespread presence of exponential growth in this study. However, the growth data in this Chapter were collected from laboratory studies with low mortality risk (for example predation treatments were excluded). Therefore, the presence of exponential growth (sustained

RGR) in this Chapter is not due to direct exposure to sustained mortality risks (e.g. predation risks) but instead may be an adaption that has evolved in response to living in a pelagic environment that is associated with sustained mortality risk. Exponential growth implies that species are maintaining the same relative growth rate (the rate of body mass increase per unit mass per unit time) over ontogeny, however, the specific growth rates (SGR, absolute mass increase per unit time) of the 53 exponentially growing species in this study varied between 0.01 and 0.39 d^{-1} (Figure 10). Variation in SGR across the pelagic invertebrate species in this Chapter implies that mortality risk may be influencing SGR as well as the shape of the growth curve, which can occur if specific growth rate to reach a larger and safer (lower risk of predation) size trades off with metabolic scope, for example. In addition, if there is metabolic scope for activities other than growth over ontogeny then this implies that resource exchange, for example across the integument or gills in pelagic invertebrate species, are not limiting growth over ontogeny.

The widespread presence of approximately exponential growth in somatic mass over time across diverse species of pelagic invertebrates (Figure 8) can also be explained by the optimal allocation of resources to somatic growth and reproduction, which can be considered key to maximising fitness (Kozlowski, 1992). Exponential growth may occur if organisms avoid early diversion of resources to reproduction, for example building reproductive organs and secondary sexual characteristics in the lead up to maturation. Sustained allocation of resources or surplus energy to growth can result in an exponential growth curve (where RGR is constant) and may occur, for example, if reproductive rate is size-dependent or is associated with a high mortality risk (Loman, 2003). For some species of pelagic invertebrates, reproductive events are high risk, and in some cases sexual reproduction is a terminal life history event where death shortly follows reproduction (e.g. cephalopods and appendicularians). Thus, it may be beneficial to avoid early diversion of reproduction, which is likely to result in a larger adult body size and hence a larger capacity to produce more offspring compared to reaching a smaller size (Olive, 1985; Loman, 2003). This is supported by the many pelagic invertebrate species whose reproduction results in large numbers of small eggs that develop planktotrophic larvae (Olive, 1985). Moreover, this is supported by the cephalopod *Amphioctopus aegina* and the appendicularian *Oikopleura dioica* that both exhibit terminal reproductive strategies (Promboon *et al*.,

2011; Troedsson *et al*., 2002) and displayed supra-exponential growth in this Chapter (Supplementary Appendix 2 Table S3). In addition, reproduction can be associated with high mortality risk in an open-water environment, because migration (to find a mate) or swarming can increase exposure to predators. In this case, allocating surplus energy to growth, or to reserves for future reproduction, may be an optimal life history strategy.

It is also possible that noise in the data, or other issues with data, account for the lack of relationship between the scaling of biosynthesis and body shape change in this study. Potential issues include the measure of body shape change itself, which is based on the relationship between body mass and length and will not be accurate for organisms who display changes in the fractal-dimensions of exchange surfaces. For example, the magnitude of error or uncertainty in b_L values will increase with the degree of convolutions, invaginations and/or appendages on the body surface area In addition, growth data for complete ontogenetic development was not available for some species (see Supplementary Appendix 2 Table S3) and so growth exponent values for incomplete developmental data may differ from complete developmental data. For example, if the incomplete growth data excludes a final stage of development in which relative growth rate declines, the biosynthesis scaling exponent A will be overestimated. However, utilising only complete developmental data in this study also results in no significant relationship between A and b_R (OLS regression: $p > 0.05$, R^2 = 0.16, n = 14) and A and $\frac{1}{b_L}$ (OLS regression: $p > 0.05$, R^2 = 0.07, n = 32), but a larger sample size would be beneficial for future studies to confirm this. Furthermore, whereas empirical growth data collection to calculate values for A excluded all mature data, the empirical body shape scaling (b_L) and metabolic (b_R) scaling dataset from Hirst, Glazier and Atkinson (2014) included data from treatments including mature stages. Therefore, it is possible a lack of relationship between A and b_L is due to a mismatch between the growth and body shape data collected over different stages of development, and future work would benefit from exploring matching growth and body shape data from the same individuals within a species.

3.6.2. The relationship between body-mass scaling of growth and metabolic rates

Organism growth is fuelled by the metabolic conversion of energy and resources; hence, if it is assumed that the entirety of metabolism is always devoted to growth, growth and metabolic rate are predicted to positively correlate. The results reported in this study do not support this because there was no significant relationship between biosynthesis scaling exponent A and metabolic scaling exponent, b_R, across diverse species (Figure 11a) or broader taxonomic groups (Figure 11b) of pelagic invertebrates. Therefore, the lack of relationship between A and b_R could also be due to noise or issues with the growth data (e.g. when development is incomplete or discontinuous) and also if there is a mismatch between growth and metabolic data, for example, if the nutritional value of food differed or if growth and metabolic data were collected at different developmental stages and/or the metabolic data from Hirst, Glazier and Atkinson (2014) contains mature animals. The growth data utilised in this Chapter were collected from laboratory studies where food is unlimited (*ad libitum*) only, but it is possible that the nutritional value of food differed across species. Limitations to other resources such as oxygen availability or concentration was seldom reported in these studies. Therefore, future next steps could involve an investigation of potential variation in nutritional value of food and oxygen availability to explore whether these resources could have been limited in these studies and hence be shaping the relationship between A and b_R in this study.

A mismatch in the scaling of metabolic rate and growth (biosynthesis) can also arise if species differ in the mass-scaling or rate of accumulation of non-metabolising tissue or energy reserves. Pelagic organisms must optimally allocate and store energy reserves to survive changing environmental conditions including periods of starvation; balancing investment into acquiring resources with the energetic benefits gained through consuming resources is key to survival (Koop *et al.*, 2011). Two 'strategies' of reproduction are: (i) capital breeding, whereby an organism uses energy stores for reproduction, and (ii) income breeding, whereby an organism relies on resources acquired during a reproductive period (Kuklinski *et al.*, 2013). Investment into capital breeding strategy can result in an increase in energy reserves over ontogeny (growth) as well as the production of somatic tissue or 'structure', thus giving potential for a change in body composition over ontogeny. This implies that the scaling exponent of

biosynthesis (A) not only captures the growth of somatic tissue but also the accumulation and storage of lipids from food. Lipid reserves have a lower metabolic demand than structural tissue (Kearney and White, 2012), and hence the scaling of metabolism will be lower than that of an organism with no (or a lesser amount of) lipid reserves and hence a mismatch may occur with the scaling of biosynthesis. Thus, variation in body composition over ontogeny, such as an increase in lipid reserves in capital breeders, may account for lack of relationship between A and b_R.

Gammarid amphipods are often capital breeders that use lipid reserves to fuel future reproductive events (Wilhelm, 2002), which may be occurring in the gammarid *Cyphocaris challengeri* analysed in this study. *C.challengeri* displayed exponential growth ($A = 1$) with a relatively lower b_R value of 0.84 than expected from exponential growth. It is possible that gammarids such as *C.challengeri* accumulate lipid reserves over ontogeny to fuel future development of reproductive organs and reproductive events. Such changes in body composition throughout development will result in an increase of the proportion of low metabolising tissue (lipid reserves) and hence metabolic demand is lower than expected and scaling of metabolism (b_R) declines. However, body composition can also change over ontogeny if there is an increasing proportion of (non-metabolising) water or ash content. Yamada and Ikeda (2000) reported a lower lipid content and higher content of water, ash and carbon-to-nitrogen ratio in *C.challengeri* compared to three other pelagic amphipod species. Furthermore, the daily metabolic loss of body carbon and body nitrogen in *C.challengeri* was lower compared to other species studied. Locomotory (swimming) activity and metabolic rate was also lower for *C.challengeri*, perhaps because of the lower locomotory demand in a mesopelagic environment compared to epipelagic. Together, this is suggestive that because *C.challengeri* has low locomotory energetic demand, there is little need for accumulating lipid reserves and instead *C.challengeri* comprises a high proportion of non-metabolising water and ash content. It is possible that the low locomotory demand and changes in body composition contributed to the shallower scaling of metabolic rate than expected from exponential growth in this study. Future studies will benefit from determining changes in body composition (e.g. lipid, water and ash) over ontogeny to confirm this, which was not explored by Yamada and Ikeda (2000).

Many pelagic invertebrate species, such as copepods, undergo several moult cycles over ontogeny (Carlotti and Nival, 1992) and hence such discontinuous growth could influence the shape of the growth curve and hence estimation of the biosynthesis scaling exponent, A. Thus, discontinuous growth could also consequently influence the relationship between A and b_R in this Chapter. However, the laboratory studies in which the growth data utilised in this Chapter were collected from collected body size (mass or length) measurements at the same time post-moult to avoid any size bias across the moult stages. For example, if growth was collected immediately after a moult cycle then it was subsequently always collected immediately after moult cycles. From my observation, the growth data utilised in this Chapter displayed smooth growth curves (mass versus time trajectories) and thus I did not observe any issues of periods of degrowth. Therefore, it is unlikely that discontinuous growth strongly contributed to the estimation of A values and consequently the relationship between A and b_R in this Chapter

Most species displayed approximately exponential growth (Figure 8) despite differences in the scaling of metabolic rate (Figure 11a), which is suggestive that energetic costs other than somatic growth are shaping the rate of metabolism in this study. For example, the appendicularian *Oikopleura dioica* and the scyphozoan *Aurelia aurita* both display supra-exponential biosynthesis ($A = 1.08$ and $A = 1.11$, respectively) over parts of ontogeny, but differ in the scaling of metabolic rate ($b_R = 0.80$ and $b_R = 1.03$, respectively). Arguably a major energetic cost to *O.dioica* is the continuous production of mucous 'houses' in which the animal resides, and provides an efficient structure for passively filtering food amongst other benefits such as protection from predators (Troedsson *et al.*, 2002) and may be a means of maintaining buoyancy. The lifespan of *O.dioica* is extremely short (around 3-6 days) (Sato, Tanaka and Ishimaru, 2001) and individuals undergo a single spawning event before dying shortly afterwards. In contrast, *A.aurita* has a comparatively longer lifespan of up to two years (Miyake, Iwao and Kakinuma, 1997), and may have higher locomotory costs of maintaining buoyancy. Specifically, pulse frequency and swimming speed have shown to be highest during the early life stages of *A.aurita* (McHenry and Jed, 2003), such as the ephyrae stage data used in this study, suggesting that mass-specific locomotory costs are higher in younger *A.aurita* stages. Therefore, differences in life history strategies may result in differences in the scaling of metabolic rate across the

diverse pelagic invertebrate species in this study. Perhaps the production of mucous 'houses' by *O.dioica* is a more efficient strategy for feeding, providing protection and perhaps maintaining buoyancy over a short lifespan in comparison to the energetic investment into active swimming of *A.aurita* over a longer lifespan. A detailed account of the life histories of diverse species of pelagic invertebrates would further shed light on the relationship between growth and metabolic rate.

3.6.3. Ontogenetic growth modelling: implications within a pelagic invertebrate system

Growth rates often correlate with traits governing fitness (Pardo *et al*., 2013), and hence understanding and accurately predicting ontogenetic growth trajectories of pelagic invertebrates is fundamental to understanding their metabolism, life history and ecology. Current growth models often display poor fits to the ontogenetic growth trajectories of invertebrates such as pelagic species. Hirst and Forster (2013) compared the performance of growth models on empirical ontogenetic growth data of diverse marine invertebrate species. The exponential model provided the best fit for 53 out of 76 datasets, which comprised nine out of 15 taxonomic groups used in the study. In comparison, the West, Brown and Enquist (WBE) growth model proved best fit for ten datasets and a power model for nine datasets, implying that whilst there is no single universal growth function suitable for marine invertebrates the exponential function has the most support. In this study (Chapter 3) most species (53 out of 76) agreed with the exponential solution of the von Bertalanffy growth Function (VBGF) (where $A = 1$ and $B = 1$), which is in agreement with Hirst & Forster (2013) that exponential growth is a common feature across pelagic invertebrate species. However, the remaining 23 species in this study exhibited a range of growth scaling exponents (A) from 0.54 to 1.17 (see Supplementary Appendix 2 Table S4 for likelihood ratio test results and confidence intervals), as captured by a set of flexible parameterisations of the VBGF that allow for a range of A values. Therefore, this study advances on the findings of Hirst and Forster (2013) by revealing further diversity in the scaling of growth across species of pelagic invertebrates, that deviates from the exponential function (where $A = 1$) and the WBE model (where $A = \frac{3}{4}$), which supports the idea

2183 that there is no single universal growth function for modelling the ontogenetic growth
2184 of pelagic invertebrates.

Chapter 4. Comparison of growth, metabolic rate and body shape in a terrestrial and aquatic oligochaete system

4.1. Abstract

Growth is a universal feature of all organisms and is fuelled by metabolic conversion of energy and resources. Consequently, predictors of the body mass-scaling of metabolic rate, b_R, are predicted to also correlate with the scaling of growth, or biosynthesis (A). However, studies on pelagic invertebrate species suggests that metrics that quantitively assess changes in body shape over ontogeny (which induce changes in body surface area responsible for uptake) correlate with b_R but not with A as reported in Chapter 3. Temperature is another known predictor of metabolic rate, b_R and body size and hence may also contribute to variation in A. This study aims to investigate the relationships among temperature, body shape, body surface area, growth and metabolism across two temperature treatments (18°C and 26°C) within an aquatic (*Tubifex tubifex*) and terrestrial (*Eisenia fetida*) oligochaete species. Specifically, I examine the relationship between A and b_R, which can provide an indicator of the scaling of growth efficiency across individuals. Furthermore, I explore the mass-scaling of surface area (b_A) and degree of body shape change (body mass – body length exponent, b_L and body diameter – body length exponent, b_{DL}) across individuals and potential correlations with A and b_R. Both *T.tubifex* and *E.fetida* displayed significant negative relationships between body mass at maturity and temperature, supporting the temperature-size rule for ectotherms. There was no significant correlation between A and b_R for either *T.tubifex* or *E.fetida*, which is suggestive of individual variation in the scaling of growth efficiency. In addition, no significant relationship between b_A and b_R, or between b_A and A was found for *E.fetida*. For *T.tubifex*, b_A significantly positively correlated with b_R, but not with A, and was influenced by temperature. Temperature had no significant effect on either A or b_L, but did significantly positively correlate with b_{DL} and negatively correlate with b_R and b_A in *T.tubifex* (but not in *E.fetida*). An inverse relationship between temperature and b_R may be explained by reduced locomotion costs, or reduced mass-specific oxygen availability in warm water over ontogeny in *T.tubifex*. A significant negative relationship between b_{DL} and b_R was present for *T.tubifex* (but not for

E.fetida), suggesting that an increase in body thickness may indiciate an increased proportion of water or lipid content over ontogeny that is associated with a decreased metabolic demand over ontogeny. Overall, this study reveals presence of body shape shifting over ontogeny for both *E.fetida* and *T.tubifex*, with *T.tubifex* displaying strong shape shifting towards body elongation. Furthermore, this study highlights differences in the relative importance of temperature between *E.fetida* and *T.tubifex* on the mass-scaling of: growth efficiency, metabolic rate, surface area and the degree of body shape change.

4.2. Introduction

All living organisms metabolise energy and materials to fuel biological processes such as growth. It can be predicted that those organisms that have evolved high metabolic rates have done so in part to fuel faster rates of biological processes (e.g. growth and reproduction). Thus, gaining a deeper understanding of observed variation in the rates of growth and metabolism is an important topic in biology. Many models and theories have been developed to predict the rates of growth and metabolism, which describe both intrinsic (physiological) and extrinsic (environmental) predictors of metabolic rate (e.g. Banavar *et al.*, 2010; Bertalanffy, 1938; Charnov, Turner and Winemiller, 2001; Glazier, 2010; Glazier, Hirst and Atkinson, 2015; Hirst, Glazier and Atkinson, 2014; West, Brown and Enquist, 1997, 2001). Typically, variation in metabolic rate with body mass is described by the power function:

$$R = am^{b_R} \tag{4.1}$$

Where R represents metabolic rate, m is body mass, and a and b_R are the scaling co-efficient and scaling exponent of metabolism, respectively. On a double logarithmic plot, the a and b_R terms become the elevation and the slope of a linear relationship, respectively. Equation (4.1) is also used to relate other biological processes, such as organism biosynthesis (of component materials required for growth) and reproductive rates (Sibly and Brown, 2007).

Much variation in metabolic rate can be accounted for by body size, but other factors such as temperature have been shown to be important in influencing metabolic rates in both vertebrate and invertebrate species (Ballesteros *et al.*, 2018; Brown *et al.*,

2004; Clarke, Rothery and Isaac, 2010; Ehnes, Rall and Brose, 2011; Gillooly *et al.*, 2001; Kolokotrones *et al.*, 2010; Meehan, 2006). The metabolic rate of ectothermic organisms, in particular, is strongly dependent on environmental temperature as well as body size (Clarke and Johnston, 1999). For example, b_R has been found to decrease with increased temperature for ectotherm species including teleost fish (Killen, Atkinson and Glazier, 2010) and crustaceans (Ivleva, 1980).

4.2.1. The influence of temperature on body size, metabolic rate and the body mass-scaling of metabolic rate

Temperature can influence metabolic rate through its direct effect on the rates of biochemical reactions. The effects of temperature on whole organism metabolism are often incorporated into multivariate equations to account for variation in metabolic rate (Brown *et al.*, 2004; Gillooly *et al.*, 2001; Kolokotrones, Savage *et al.*, 2010). Furthermore, temperature forms a key component of the influential Metabolic Theory of Ecology (MTE) (Brown *et al.*, 2004), which proposes a $\frac{3}{4}$ – power relationship for the dependence of metabolic rate on body mass ($b_R = \frac{3}{4}$). Specifically, the MTE incorporates a Boltzmann-Arrhenius term ($e^{-E/kT}$) to describe the exponential effect of temperature on the biological rates, such as the $\frac{3}{4}$ power body mass (m) scaling of metabolic rate (R):

$$R = r_0 \cdot m^{3/4} \cdot e^{-E/kT} \qquad 4.2$$

Where r_0 represents the normalisation constant (which is independent of body size and temperature), E denotes the activation energy (for a metabolic reaction to occur), and k and T represent Boltzmann's constant (Arrhenius, 1889; Bolztmann, 1872) and temperature (in Kelvin), respectively (Brown *et al.*, 2004; Gillooly *et al.*, 2001). The MTE argues that because metabolic rate reflects the energetic costs of energy and matter transformation involved in taking up resources, growing, reproducing and maintaining tissues, it can influence some ecological processes, but equally ecological processes can also affect metabolic rate (Brown *et al.*, 2004). However, the body size scaling exponent of metabolic rate (b_R) can display marked variation over ontogeny in some species (Clarke, Rothery and Isaac, 2010; Glazier, 2005; Painter, 2005;

Streicher, 2012) and among broader taxonomic groups (Glazier, 2005; Glazier, Hirst and Atkinson, 2015; Hirst, Glazier and Atkinson, 2014), thus deviating from $\frac{3}{4}$ – power scaling law which forms the basis of the MTE (Brown *et al.*, 2004). Generally, the range of values of b_R have been reported as between $\frac{2}{3}$ and 1 for diverse taxa (Glazier, 2005, 2014a,b; Glazier, Hirst and Atkinson, 2015; Hirst, Glazier and Atkinson, 2014; Hayssen and Lacy, 1985; Killen, Atkinson and Glazier, 2010; Kozlowski and Konarzewski, 2005; Meehan, 2006 and see Glazier, 2018 for a review), and has been linked to ambient temperature in crustaceans (Ivleva, 1980), teleost fish (Killen, Atkinson and Glazier, 2010) and diverse animal and plant species (Glazier, 2020).

The metabolic-level boundaries hypothesis (MLBH) aims to explain the effects of ambient temperature on b_R, through the relative importance of surface-area-related (e.g. resource uptake and heat dissipation) versus volume-related (e.g. tissue maintenance or muscle power production) metabolic processes (Glazier, 2005, 2010, 2020). The MLBH predicts for a resting organism, that surface-area-related processes will dominate when level of metabolism (as indicated by the elevation of the metabolic scaling relationship) is low, because surface area related fluxes of resources and wastes will dominate, and hence b_R will tend towards $\frac{2}{3}$, for isomorphic (shape-invariant) organisms. In contrast, volume-related processes are predicted to dominate when metabolic level (the vertical elevation of a metabolic scaling relationship) is high, because the capacity for resource supply and waste removal dominates, causing b_R to scale in proportion to body volume (which is assumed to be proportional to body mass) and hence tend towards 1 (Glazier, 2005, 2010, 2020).

Therefore, the MLBH can predict b_R to inversely correlate with metabolic level, which in turn positively correlates with temperature in relatively sedentary resting, non-growing organisms. In contrast, for active animals, the MLBH predicts that b_R will positively correlate temperature if increased temperature increases locomotory activity, and hence metabolic level, because volume-related processes (such as muscle energetic demand) dominate and hence b_R tends toward 1. Thus, for active animals the relationship between temperature and b_R is malleable and is predicted to depend on specific level of activity and size-specific responses to temperature (Glazier, 2005, 2010, 2020). For example, Glazier (2020) reported negative correlations between ambient temperature and b_R for inactive ectotherm animal and plant species, but varied

(positive and negative) relationships between b_R and temperature for active ectotherms. Therefore, the MLBH highlights the potential for both intrinsic (activity) and extrinsic (ambient temperature) factors to influence variation in b_R in ectothermic animal and plant species.

Furthermore, temperature commonly displays an inverse relationship with body size at maturity. Bergmann (1847) revealed an increase in body size with increasing latitude (or decreasing temperature) in intraspecific comparisons of endotherms species, which led to the proposition of a general rule for temperature and organism body size. A negative correlation between temperature and size at maturity and offspring size has since been reported for ectotherm species and was coined as the temperature-size rule (Atkinson, 1994; Atkinson *et al.*, 2001). The temperature-size rule has been observed in over 80% of investigated ectotherm species including plants, protists, bacteria and animals (Atkinson, 1994; Atkinson, Ciotti and Montagnes, 2003; Atkinson and Sibly, 1997; Sibly and Atkinson, 1994). Most physiological processes are temperature dependent and so it can be predicted that individuals will reach a larger size at maturity in warmer temperatures than colder ones, hence the fact that many ectotherm species conform to the temperature-size rule is a puzzling topic that has received much attention in the literature. Furthermore, because size at maturity is often linked to reproductive success (Roff, 2002) it can be considered as a key life history trait. Therefore, understanding observed variation in size at maturity in response to environmental change, as is highlighted by the temperature-size rule, is thus crucial to understanding the adaptive evolution of organisms. Whilst temperature can correlate with body size at maturity, metabolic rate, the mass-scaling of metabolic rate, it is perhaps unlikely that temperature will strongly correlate with the scaling of biosynthesis. The rate of biosynthesis (the building of component materials required for growth) over ontogeny will depend on factors including resource (e.g. food) availability and quality (e.g. food nutrition), which are unlikely to be strongly influenced by temperature.

4.2.2. Body shape changes and the mass-scaling of metabolic rate and growth rate

Considering that growth is fuelled by metabolism, understanding the scaling of growth, or the scaling of biosynthesis of component materials, from which non-growth metabolism, or catabolism (the breakdown of materials) is subtracted from to obtain growth, is relevant to exploring to what extent growth efficiency scales with body mass. In Chapter 3, a predicted one-to-one relationship between the scaling of biosynthesis, A, and the scaling of metabolic rate, b_R, was made based on the three metabolic and growth types proposed by Bertalanffy (1951), which relate to the relative influence of body surface area and body mass on the scaling of metabolic rate (for complete description see Chapter 3. Introduction). Deviations from a one-to-one relationship between A and b_R can represent variation in the body mass-scaling of growth efficiency. Specifically, in the case where an organism exhibits $A > b_R$ over ontogeny, this suggests increased growth efficiency over ontogeny because an increase in growth rate is not met with a relative increase in oxygen utilisation over ontogeny. Conversely, if $A < b_R$ over ontogeny this will imply decreased growth efficiency over ontogeny because the relative increase in oxygen utilisation that is not met with an increase in growth rate.

A correlation between ontogenetic body shape change (that relates to the mass-scaling of body surface area, b_A, and hence resource uptake capacity) and the body size scaling of metabolic rates (b_R) was reported across species and wider taxonomic groups of pelagic invertebrates (Glazier, Hirst and Atkinson, 2015; Hirst, Glazier and Atkinson, 2014). Specifically, pelagic invertebrates display variation in b_R, which correlates with the degree of body shape change over ontogeny, as defined by the inverse of the body mass-length scaling exponent $\frac{1}{b_L}$ (Glazier, Hirst and Atkinson, 2015; Hirst, Glazier and Atkinson, 2014). Body shape change governs the relationship between body surface areas and body volume. Hence, changes in body shape, such as body elongation or flattening, can induce changes in the mass-scaling of body surface areas b_A, responsible for resource uptake (hence potentially for growth) and changes in body mass (for maintenance of metabolising tissue) (Kooijman, 2000; see Chapter 2). Thus, assuming a broad correlation between routine metabolic rate (where an individual is in a resting, post-absorptive state and normal random activity can occur) and maximum metabolic rate (the maximum achievable metabolic rate of an

individual), it may also be predicted that body shape changes correlate with the mass-scaling of biosynthesis in pelagic invertebrate species.

However, I previously found no support for a relationship between the scaling of biosynthesis (A) and b_R, or correlation between A and degree of body shape change ($\frac{1}{b_L}$) or b_R and $\frac{1}{b_L}$ over ontogeny among diverse species of pelagic invertebrates (see Chapter 3). The growth (body mass versus time), metabolic scaling and body shape (body mass versus length exponent, b_L) data utilised in that work (Chapter 3) were extracted from different sources: b_R and b_L data were obtained from the dataset compiled from a literature search by Hirst, Glazier and Atkinson (2014), whereas empirical growth data was collected through a separate literature search (see Supplementary Appendix 2 Table S3 for data sources). Therefore, the lack of relationship between A and b_R, and between A and b_L in Chapter 3 may be a result of utilising mismatched growth and body shape data. Consequently, an empirical evaluation of the changes in growth, routine metabolic rate and body shape over ontogeny would be beneficial to further shed light on the relationship between the mass-scaling of biosynthesis, the mass-scaling of metabolic rate and degree of body shape change over ontogeny.

Furthermore, whilst the reported b_R values for diverse pelagic invertebrate species positively correlates with degree of body shape shifting ($\frac{1}{b_L}$), the b_R values were greater than predicted from a Euclidean surface area model used by Hirst, Glazier and Atkinson (2014). Thus, species exhibit steeper metabolic scaling than predicted from their degree of body shape change, which can relate to area of exchange surfaces, and may be explained by the following hypotheses: (i) the boundary layer (between an organism's uptake surface and external resources) decreases with organism body size, which results in increased efficiency of oxygen uptake in a moving viscous fluid and hence a higher metabolic rate potential at larger body sizes (Glazier, Hirst and Atkinson, 2015; Hirst, Glazier and Atkinson, 2014). For example, consider two aquatic species with the same initial body size: the individual that reaches a larger adult body size will have a relatively smaller boundary layer and consequently a more efficient uptake of oxygen over ontogeny, and hence a higher maximal achievable metabolic rate, than the species with a smaller adult body size. Or, (ii) there is an underestimation of body surface area if there is an increase in surface convolutions,

furrows or invaginations (i.e. fractal dimension), or an increase in body surface area of nutrient-absorptive or specialised respiratory appendages or structures, such as gills, as body mass increases which contributes to a larger body surface area and hence higher potential metabolic rate (Glazier, Hirst and Atkinson, 2015; Hirst, Glazier and Atkinson, 2014).

Hypothesis (i) relates to Reynold's number, which describes the relative importance of viscous and inertial forces to an object moving through fluid (Massel, 2012). Reynold's number (Re) is calculated by the equation:

$$Re = \frac{Ua}{v} \qquad 4.3$$

Where U and a denote the body length and speed (ms^{-1}) of the object (such as an organism) moving through fluid, respectively, and v the kinematic viscosity (m^2s^{-1}) of the fluid (Doostmohammadi, Stocker and Ardekani, 2012). Changes in body shape and mode of locomotion can be associated with a change in Reynold's number over ontogeny, for example, squid can exhibit changes in Reynold's number from one to 1 000 000 associated with changes in body shape and locomotory mode over ontogeny (O'Dor *et al*., 2010). When viscous forces dominate inertial forces, Reynolds number is low and body shapes that minimise surface area (e.g. spheroid forms) will move more efficiently (in terms of energy) than body shapes that maximise surface area (e.g. elongate forms). Conversely, when inertial forces dominate a 'streamlined' or elongate body shape form that displaces a minimum amount of water will move most efficiently (O'Dor *et al*., 2010).

Thus, an empirical evaluation of species that fulfil the requirements to explore hypotheses (i) and (ii) would be beneficial to determine the causes of upward deviations in b_R. These hypotheses can be tested by comparing an aquatic study system, where importance of viscous and inertial forces in moving water are likely to be important, against a system where boundary layer is less of an issue. Earthworms are terrestrial species that easily move through wet soil (Li *et al.*, 2010) and hence are likely to be less affected by boundary layer issues in comparison to aquatic species. In addition, because air is less viscous than water and oxygen concentration is higher in air than it is in water, oxygen diffusion is relatively faster for air-breathers, such as earthworms, compared to water-breathers (Hoefnagel and Verberk, 2015). To move efficiently through soil, earthworms use electro-osmotic flow near the body surface,

2436 that plays a role in both body surface lubrication and creating vortices, which both
2437 reduce adhesion of soil and hence friction when moving through soil (Yan *et al.*,
2438 2007). In addition, movement through soil is further aided by minute hairs which cover
2439 the body surfaces of earthworms and increase grip of soil (they do not contribute to
2440 respiration) (Yan *et al.*, 2007). In addition, studying relatively smooth-bodied
2441 organisms, or organisms that generally lack external body appendages and external
2442 respiratory structures such as gills, will exclude the contribution of substantial body
2443 surface areas (that cannot be easily captured by simple body mass, length and diameter
2444 measurements) or convolutions that may contributing to uptake and therefore controls
2445 for the mechanism in hypothesis (ii).

2446 Oligochaetes provide an ideal study group that fulfils these requirements because
2447 they comprise both aquatic and terrestrial species and lack substantial 'frills' or
2448 appendages and gills, i.e. they are relatively smooth-bodied. For example, the
2449 earthworm *Eisenia fetida* lacks appendages and gills and is relatively smooth-bodied
2450 (Yan *et al.*, 2007). Whilst the posterior region of freshwater sludge worm *Tubifex*
2451 *tubifex* contains surface convolutions and furrows (Kaster and Wolff, 1982), it does
2452 not contain any appendages or gills. In addition, there is potential for organisms,
2453 including oligochaete species, to change shape over ontogeny if they become
2454 increasingly elongate (growing in one dimension of length), flattened (growing in two
2455 dimensions of length), squat (growing proportionately more in the shorter length axes
2456 than the long) or any intermediate of these extreme forms (Okie, 2013). Furthermore,
2457 exploring variation in body thickness (the relationship between body diameter and
2458 body length) over ontogeny can provide another useful measure of body shape change.
2459 Degree of body thickness can be linked to body condition if increasing thickness is a
2460 result of increased lipid reserves, body musculature, or water content, but also to other
2461 factors such as gut thickness or a limitation to the number of segments that can be
2462 added to the body. Oligochaetes exchange respiratory gases through a permeable
2463 integument (Kaster and Wolff, 1982), and so changes in body shape that result in
2464 alterations in these exchange surface areas may correlate with changes in the mass-
2465 scaling of oxygen consumption over ontogeny.

2466 The efficiency of respiratory exchange surfaces has been explored in the
2467 freshwater oligochaete *Tubifex tubifex* (Kaster and Wolff, 1982), which is a deposit
2468 feeder that burrows its anterior end within sediment and protrudes its posterior end

into the adjacent water where gas exchange occurs. Efficiency of gas exchange in *T.tubifex* is increased by adaptations to the posterior region as described by Kaster and Wolff (1982). Firstly, *T.tubifex* displays ventilatory movements of the posterior end which enhance the convective transport of respiratory gases (Kaster and Wolff, 1982). These ventilatory movements, or posterior tail undulations, are a result of alternating and unilateral contractions of longitudinal body muscles that enable mixing of water – drawing in aerated surface water and returning non-aerated water to the surface – allowing them to gain oxygen from as large a volume as possible (Drewes and Zoran, 1989). Secondly, the posterior region is convoluted and comprises a structure of furrows and ridges that enhance surface area and hence exchange of respiratory gases (Kaster and Wolff, 1982). Thirdly, the body wall of the posterior region is thinner than the anterior region, which enables a short pathway for diffusion of respiratory gases (Kaster and Wolff, 1982). Consequently, if changes in body shape induce changes in the efficiency of gas exchange, for example by increasing the mass-scaling of body surface area, this gives potential for changes in body shape to correlate with changes in the rate of metabolism over ontogeny.

An empirical comparison of growth and metabolism in a terrestrial versus aquatic system also offers an opportunity to explore the effects of temperature, a known predictor of metabolic rate, on the mass-scaling of growth (biosynthesis) and metabolic rate and degree of body shape change. Warmer temperatures can increase metabolic rate which results in enhanced toxicity of heavy metals in freshwater *T.tubifex* (Rathore and Khangarot, 2002). Furthermore, rates of carbon dioxide production for cocoon, juvenile and mature stages of terrestrial oligochaete *Lumbricus rubellus* were shown to increase with temperature (Uvarov and Scheu, 2004). Temperature also correlates with growth and cocoon production in some oligochaete species including *E.fetida*, which has reported optimum temperature of 25°C for growth and reproduction (Tripathi and Bhardwaj, 2004).

Oligochaetes are widely used in studies concerning toxicity, disease, environmental pollutants, and disposal of hazardous wastes. Gaining a deeper understanding of the factors influencing or predicting variation in growth or metabolism over ontogeny in oligochaetes is therefore important to numerous areas of environmental impact and is economically relevant. For example, *T.tubifex* and *E.fetida* are widely used as bioindicators of heavy metals and pollutants to help advise

on the risks and impacts of contaminated soil to human and animal health (Kaonga, Kumwenda and Mapoma, 2010; Tang *et al.*, 2016). Additionally, because *E.fetida* is an efficient composting worm it has been used to aid the disposal of hazardous wastes (industrial, urban and agricultural) and hence is of high economic and environmental value (Li *et al.*, 2016).

4.3. Aims and hypotheses

This study aims to examine the ontogenetic scaling of biosynthesis (of component materials required for growth) (A) and routine metabolic rate (b_R) in relation to: ambient temperature (a known predictor of whole organism metabolic rate), the mass-scaling of body surface area (b_A) and degree of body shape change (the body mass-body length exponent $\frac{1}{b_L}$, and scaling of body diameter relative to body length, b_{DL}) for a terrestrial and an aquatic oligochaete species: *Eisenia fetida* and *Tubifex tubifex*. Specifically, I hypothesise that:

1. Temperature will display an inverse relationship with body size at maturity as predicted from the temperature-size rule for ectotherms (Atkinson, 1994).
2. Because metabolism fuels whole organism growth, A will display a positive correlation with b_R over ontogeny.
3. The exponent b_R will negatively correlate with temperature if warming is linked to decreased locomotory demand, and hence demand of metabolising muscle tissue, over ontogeny. Conversely, if warming results in increased locomotory demand then b_R will positively correlate with temperature as predicted by the MLBH (Glazier, 2010, 2020). While A will not strongly correlate with temperature because it is expected that resource supply for growth and metabolism may have lower thermal sensitivity than metabolic demand.
4. Additionally, the mass-scaling of body surface area (b_A) will display a positive 1:1 correlation with b_R and A due to enhanced surface area for resource uptake as predicted from a Euclidean surface area model.

5. The scaling of body diameter relative to body length (b_{DL}) will positively correlate with b_R and A across individuals due to enhanced scaling of body surface area and hence respiratory exchange over ontogeny.

4.4. Methods

4.4.1. Culture of study species

Adult *Eisenia fetida* individuals were obtained from Yorkshire Worms Ltd and maintained in a 42 L opaque box with a transparent lid at 26°C. An opaque plastic box was chosen because *E.fetida* is photophobic (Venter and Reinecke, 1988). All sides of the box and lid contained 2 mm diameter holes to allow ventilation and drainage of excess moisture. The culture box was monitored daily for the presence of cocoons, which were transferred to individual 50 ml glass vials. Individual cocoons were monitored three times a week for hatching events and hatchlings were placed in 280 ml glass jars covered with 1.5 mm hole diameter insect netting. Multiple individuals from a single cocoon were separated so only a single individual remained in a culture beaker. All worms were cultured on coconut coir substrate which was manually monitored using an ExoTerra Hygrometer © and maintained at 80-85% moisture content by spraying dechlorinated water every two days if needed. All worms were fed weekly. Food comprised a ground mixture of plant matter including melon, banana skins, potato peelings, coffee grounds, tea bags, mixed leafy greens, broccoli, newspaper and cardboard. The composition of food changed throughout the experiment, but all individuals received the same composition of food at a given feed to maintain the same level of nutritional quality amongst individuals. Individuals were subjected to one of two temperature treatments throughout development: 18°C or 26°C. Individuals raised under the 18°C treatment were maintained under a constant laboratory room temperature of 18°C, and individuals raised in 26°C were maintained through use of Elixir Gardens © soil warming cables. The temperature (18°C and 26°C,) and moisture (80-85%) conditions used in this study are within the range of reported optimal growing conditions for *E.fetida* (Gunadi and Edwards, 2002; Haukka, 1987)

Adult *Tubifex tubifex* were obtained from Northampton Reptile Centre and cultured in a 29 L aquarium tank containing dechlorinated freshwater and a 5 cm deep layer of inorganic mineral clay sand (commercial chinchilla sand) at 26°C. *T.tubifex* is photophobic (Marian and Pandian, 1984) so all four sides of the tank were blacked out apart from the top eight centimeters to allow some penetration of light. The tank was kept clean by an internal filter, which itself was cleaned once a week, and through manual use of an algal scraper once a week. The tank was monitored daily for the presence of cocoons, which were placed individually in 50 ml test tubes filled with dechlorinated water. Vials were monitored daily for hatchlings. All individuals were fed one ground down Tetramin © fish flake every other day. Fish flakes were grounded down because preliminary culture trials revealed that whole fish flakes settled on top of the sediment and became moldy, causing a decrease in water quality which led to a high mortality rate. Individual hatchlings were cultured in 50 ml test tubes under either 18°C, as maintained by a constant laboratory room temperature, or 26°C as maintained by an aquarium heater. Individual vials and test tubes were manually aerated every other day by inserting and squeezing a pasteur pipette into the top three centimeters of the water, and the water (dechlorinated) replaced once a week. Due to the highly delicate and small bodies of *T.tubifex* hatchlings, data collection for growth, body shape and metabolic rate commenced after allowing hatchlings to develop for one week, as handling before this period resulting in high injury and fatality to hatchlings.

Both *E.fetida* and *T.tubifex* were subjected to a 15 hour light photoperiod via use of timed fluorescent strip lights. Data for growth and metabolic rate were collected once a week until individuals reached sexual maturity as identified by the presence of the clitellum.

4.4.2. Growth and body shape data

Individual *E.fetida* were gently washed to remove soil and blotted onto blue roll to remove excess water and placed on balancing scales to measure wet mass (mg). Body length (mm) and average body diameter (mm) (the average of the widest anterior and posterior diameters) were measured using callipers.

It was not possible to collect wet mass data for *T.tubifex* because handling caused injury or destruction of individuals due to the high delicacy of their bodies. Instead, the relationship between dry mass (mg) and body length (mm) was calculated to allow conversion of body length into dry mass. Body length and diameter data were collected by taking photographs of individuals (placed on a micrometre) through a microscope. Dry mass data was collected for 34 individuals of various sizes (immature and mature) by placing them in a drying oven at 80°C for five hours and weighing them on balancing scales. Both immature and mature stages were included due to time limitations required to identify and exclude mature stages. To reduce the number of sacrificed individuals, this was performed for a single temperature treatment only (26°C). This resulted in the following relationship:

$$ln\ dry\ body\ mass = (1.82 \times ln\ body\ length) - 7.06 \qquad (R^2 = 0.96) \quad (4.4)$$

Thus, body length was determined from photographs taken of individual *T.tubifex*, which was converted to dry body mass using equation 4.4.

In addition, the scaling of growth efficiency, $\frac{A}{b_R}$, was calculated for each individual and averaged across individuals for both *T.tubifex* and *E.fetida*. Body mass, body shape measurements (body length, body diameter and body length / body diameter) and metabolic rate were collected at sexual maturity as determined by the presence of the clitellum.

4.4.3. Oxygen consumption rate data

Oxygen consumption rates were computed as a measure on metabolic rate in this Chapter. Oxygen levels were measured for *T.tubifex* and *E.fetida* individuals using optical fluorescence-based oxygen respirometry with the PreSens 1700 µL 24-glass well microplate Sensor Dish Reader (SDR) which records oxygen levels (mg O_2/L) over time. The SDR allows non-invasive measurements of oxygen consumption through planar oxygen sensor spots glued on the bottom of each 1700 µL glass well. Before use, the SDR was manually calibrated using the pre-defined calibration data from the manufacturer as outlined in the PreSens SDR manual. This calibration data included the following data for both aquatic and dry systems: Cal0 (first calibration point at 0% oxygen), t_0 (temperature at which the first calibration point was measured),

Cal2nd (second calibration point), t2nd (temperature at which the second calibration point was measured), O_2-2nd (oxygen concentration of the second calibration point) and pATM (atmospheric pressure at which the calibration was performed).

The SDR was placed inside a dark (no light) incubator (because *T.tubifex* and *E.fetida* are photophobic) and connected to a computer to record data on oxygen consumptionover time. The incubator was used to maintain temperature treatments (18°C and 26°C). A flashing red light was emitted through each of the 24 glass wells every time the SDR recorded oxygen data. Both *T.tubifex* and *E.fetida* are photophobic, but the exact tolerance to red light is not reported in the literature. This flashing red light could not be avoided because it was a requirement for the SDR to read oxygen levels. The SDR was set up to alert the user if oxygen levels reached or subceeded a critical oygen level, which was defined by oxygen saturation in the SDR at a minimum of 50%, which was not reached or subceeded at any point in the study. The critical oxygen saturation for *E.fetida* or *T.tubifex* is not reported in the literature, so the critical oxygen value of 50% was chosen arbitrarily.

For *T.tubifex* oxygen consumption data collection, dechlorinated freshwater was placed in each well and individual *T.tubifex* placed in 22 wells of the SDR. For *T.tubifex*, self-adhesive PCR film was used to cover the glass microplate to make the microplate airtight, i.e. to prevent air from mixing with the water in the wells. Two wells contained dechlorinated water (but no *T.tubifex* individuals) to provide control wells. The purpose of having two blank control wells was to check for any large spikes or drops in oxygen levels during the period of data collection, which would indicate issues with equipment error (e.g. if the PCR film was placed incorrectly or vials were not sealed properly) or malfunction (e.g. if the SDR software malfunctioned). Oxygen consumption data for *T.tubifex* were recorded by the SDR every 30 seconds over two hours for both 18°C and 26°C temperature treatments, which were maintained by the the incubator in which the SDR system was placed in.

For *E.fetida*, 24 individual airtight sealed PreSens SV-PSt5 4 ml glass SensorVials were used in addition to the 24-well glass microplate. These vials were calibrated by using the pre-determined calibration data from the manufacturer (PreSens), which contained the same calibration variables as described above for the SDR. The SensorVials were slotted into each of the 24 wells of the SDR microplate.

Two vials were left empty (containing air only) as controls. SensorVials were used for *E.fetida* because of the bigger size of *E.fetida* individuals in comparison to *T.tubifex*, requiring a larger volume of container space to measure individual metabolic rate. Data were collected every 30 seconds over three hours for both 18°C and 26°C temperature treatments. A longer data collection duration for *E.fetida* in comparison to *T.tubifex* was required to obtained significant declines in oxygen consumption over time.

Oxygen consumption rates (OCR) were calculated as the change in oxygen concentration (mg O_2) (O) divided by the volume (v) of the glass well (0.0017 L) or vial (0.004 L) over the recorded time period (t) in seconds (two hours for *T.tubifex* and three hours for *E.fetida*) for each individual (i.e. each glass well or vial):

$$OCR\ (mg\ O_2 L^{-1} s^{-1}) = \frac{(O_{initial} - O_{final})/v}{t} \quad 4.5$$

4.4.4. Quantifying changes in body shape and surface area over ontogeny

For *E.fetida*, the degree of body shape change over ontogeny was calculated as the body mass-body length scaling exponent, b_L, for each individual. This was not performed for *T.tubifex* because body mass was determined through mass-length equation (see Methods 4.4.1). Inverse b_L values were used in analyses ($\frac{1}{b_L}$) to create a linear rather than a non-linear relationship (with surface area scaling, hence predicted A and b_R) by having log(mass) as the x-variate (see Chapter 3, Figure 6 for a visual representation).

In addition, individual changes in the scaling of body diameter relative to length, b_{DL}, were explored as another measure of body shape change over ontogeny by computing the slope of a least squares regression of log body diameter against log body length. For individuals with b_{DL} values greater than 1, body diameter is growing faster than body length, i.e. the individual's shape becomes proportionately thicker relative to length, i.e. more squat in form. When $b_{DL} < 1$, body length grows faster than body diameter over ontogeny, and the organism shape becomes proportionately thinner relative to length, i.e. more elongate in form. For *T.tubifex*, b_{DL} was calculated using posterior region diameter data only, because respiratory exchange occurs in the

posterior region and the anterior region remains buried in sediment for feeding (Kaster and Wolff, 1982). For *E.fetida*, b_{DL} was calculated using average diameter values (the average of anterior and posterior diameter) because the whole body is exposed to soil and hence both the anterior and posterior region are likely to be involved in respiratory exchange.

Furthermore, individual changes in the mass-scaling of body surface area, b_A, were calculated from body diameter and body length data using the equation: $b_A = (b_{DL} + 1)/(2b_{DL} + 1)$ which was determined from Euclidean surface area theory and was proposed by Hirst, Glazier and Atkinson (2014) and Glazier, Hirst and Atkinson (2015).

Ordinary Least Squares regression was applied to examine relationships between scaling exponents when the correlation was not significant and Reduced Major Axis (RMA) regression using the *lmodel2* package in R was applied when the correlation was significant ($p < 0.05$). When correlations between scaling exponents were significant, RMA regression was chosen over Ordinary Least Squares regression because it assumes equal weighing of error for the x- and y-axis rather than only the x-axis. To test for significant differences between temperature treatments an unpaired Two-sample t-test was used. All analysis was performed in R (v3.6.2).

4.5. Results

4.5.1. *Eisenia fetida*: growth, metabolic rate and body shape

Body size, shape and metabolic rate at maturity

The average body size at maturity (mass, length and diameter), shape (length-to-diameter ratio) and metabolic rate (oxygen consumption rate) at maturity for *E.fetida* is reported in Table 3 for both temperature treatments (18 and 26°C). Average body mass at maturity was significantly larger for the 18°C treatment than the 26°C treatment (Two sample t-test: $P < 0.01$, $t = 3.14$, $df = 42$). Average body diameter at maturity did not statistically differ between temperature treatments (Two sample t-

test: $P > 0.05$, $t = 2.00$, $df = 42$). Furthermore, both average body length (Two sample t-test: $P > 0.05$, $t = 1.01$, $df = 42$) and body length-to-diameter ratio (Two sample t-test: $P > 0.05$, $t = 1.46$, $df = 42$) at maturity was not significantly different between temperature treatments. Average metabolic rate at maturity was larger in the 18°C treatment but was not statistically different to the 26°C (Two sample t-test*:* $P > 0.05$, $t = 1.12$, $df = 24$).

Table 3. Average adult values, body mass (grams), length (mm), diameter (average diameter for *E.fetida* and posterior diameter for *T.tubifex*), body shape (body length (mm)/body diameter (mm) and body length/body mass) and oxygen consumption rate (mg O2 L^{-1} s^{-1}) for *n Eisenia fetida* and *Tubifex tubifex* individuals for two different temperature treatments: 18 and 26°C and combined data for both treatments. Note that body mass was collected as wet mass for *E.fetida* and dry mass obtained from dry mass – body length conversion equations for *T.tubifex*. The 95% confidence intervals (±) are given for each value. Bold values indicate a significant difference between temperature treatments.

Treatment (°C)	Average measurements at maturity				
	Body mass	Body length (L)	Body diameter (D)	L / D	Oxygen consumption rate
Eisenia fetida					
18	**153.12** ±12.55	28.24 ±1.67	2.69 ±0.154	9.58 ±0.587	0.63 ±0.178
26	**126.46** ±10.78	26.52 ±2.83	2.94 ±0.175	10.25 ±0.608	0.48 ±0.189
Combined	137.37 ±9.05	27.21 ±1.84	2.84 ±0.126	9.99 ±0.446	0.57 ±0.133
Tubifex tubifex					
18	**0.26** ±0.019	**22.61** ±0.904	**0.30** ±0.00952	**76.75** ±3.87	**0.35** ±0.0280
26	**0.19** ±0.016	**18.89** ±0.799	**0.27** ±0.0148	**70.93** ±3.57	**0.08** ±0.0178
Combined	0.22±0.013	20.59 ±0.673	0.289 ±0.00715	73.59 ±2.67	0.20 ±0.0331

During the experiment, some individual hatchlings and young juveniles (i.e. the smallest stages) escaped from culture pots, resulting in a small sample size of 44 individuals. In addition, the data for individual metabolic rate became further reduced (to 26 individuals) due to uncertainty in some datasets that displayed biologically unrealistic spikes in oxygen levels, likely due to the curling up of individuals directly on the oxygen sensor spot. For raw body mass versus oxygen consumption rate data for both temperature treatments for *E.fetida* and *T.tubifex* please see https://github.com/lauraleemoore/LLM_Thesis_datasets.

There was no significant difference between the two temperature treatments in the mass-scaling of biosynthesis (Two sample t-test: t = 0.356, df = 39.5, $P > 0.05$) or the mass-scaling of metabolic rate (Two sample t-test: t = 0.294, df = 20.7, $P > 0.05$). The average value for the scaling of biosynthesis, A, across both temperature treatments was 0.93 (n = 44), which was significantly different from pure exponential growth where $A = 1$ (One-sample T-test: t = -3.33, df = 43, $P < 0.001$). The average value for the scaling of metabolic rate (b_R) was 1.05 (n = 26) (Table 4) (see Supplementary Appendix 3 Table S6 for individual *E.fetida* data).

In addition, temperature treatment did not significantly affect the two measures of body shape change: the scaling of body diameter relative to length (b_{DL}) (Two sample t-test: t = -0.807, df = 17.6, $P > 0.05$) or degree of body shape change ($\frac{1}{b_L}$) over ontogeny (Two sample t-test: t = -0.898, df = 37.4, $P > 0.05$). The average b_{DL} and $\frac{1}{b_L}$ across both temperature treatments was 0.71 and 0.37, respectively (Table 4). The average $\frac{1}{b_L} = 0.37$ was near that of pure isomorphy (where $\frac{1}{b_L} = \frac{1}{3}$), but the alternative hypothesis that the true mean contains $\frac{1}{b_L} < 0.34$ is not significant (One sample t-test: t = 4.11, df = 40, $P > 0.05$). Further, temperature had no significant effect on the body mass-scaling exponent of surface area, b_A (Two sample t-test: t = 0.762, df = 36.9, $P > 0.05$), with an average b_A of 0.71, or the scaling of growth efficiency ($\frac{A}{b_R}$) (Two sample t-test: t = 0.0382, df = 23.4, $P > 0.05$) with an average $\frac{A}{b_R}$ value of 1.13 (Table 4).

Table 4. Average values for the body mass-scaling exponent of: biosynthesis (A), metabolic rate (b_R), surface area (b_A), growth efficiency ($\frac{A}{b_R}$), and average values for the degree of body shape change ($\frac{1}{b_L}$ and b_{DL}) for *Eisenia fetida* and *Tubifex tubifex* individuals for two different temperature treatments: 18 and 26°C and combined data for both treatments. Note that for *T.tubifex* body thickness (b_{DL}) averages represent data from the posterior region where the majority of respiratory exchange is likely to occur (Kaster and Wolff, 1982). (*For *T.tubifex* average $\frac{1}{b_L}$ was computed by an empirically determined relationship between dry mass and body length for 34 individuals). The 95% confidence intervals ($\pm$) are given for each value. Bold values indicate a significant difference between temperature treatments.

Treatment (°C)	Averaged scaling exponent values										
	A	N	b_R	n	$\frac{1}{b_L}$	N	b_{DL}	n	b_A	n	$\frac{A}{b_R}$
Eisenia fetida											
18	0.94 ±0.06	18	1.07 ±0.24	11	0.39 ±0.02	18	0.68 ±0.09	18	0.72 ±0.01	18	1.14 ±0.46
26	0.93 ±0.05	26	1.03 ±0.19	15	0.35 ±0.02	26	0.74 ±0.09	26	0.71 ±0.01	26	1.13 ±0.46
Combined	0.93 ±0.05	44	1.05 ±0.15	26	0.37 ±0.01	44	0.71 ±0.06	44	0.71 ±0.01	44	1.13 ±0.33
Tubifex tubifex											
18	0.95 ±0.03	64	**0.84** ±0.05	44	-	-	**0.30** ±0.02	64	**0.82** ±0.01	64	**1.19** ±0.10
26	0.96 ±0.02	78	**0.7** ±0.06	45	0.55 ±0.04 *	34	**0.45** ±0.03	78	**0.77** ±0.01	78	**1.50** ±0.15
Combined	0.95 ±0.02	142	-	-	-	-	-	-	-	-	-

Eisenia fetida: Relationships between the scaling of growth, metabolic rate and body shape

The body size scaling exponent of metabolic, b_R, is plotted against the body size scaling exponent of biosynthesis, A, for *E. fetida* in Figure 12. There was no significant correlation between A and b_R (OLS regression: n = 26, R^2 = 0.04, $P > 0.05$). In addition, the body mass-scaling of surface area, b_A, did not significantly affect either the scaling of metabolic rate (OLS regression: n = 26, R^2 = 0.02, $P > 0.05$) or the

scaling of biosynthesis (OLS regression: n = 44, $R^2 = 0.002$, $P > 0.05$) (Figure 13). The scaling of body diameter relative to length did not significantly correlate with b_R (OLS regression: n = 26, $R^2 = 0.01$, $P > 0.05$).

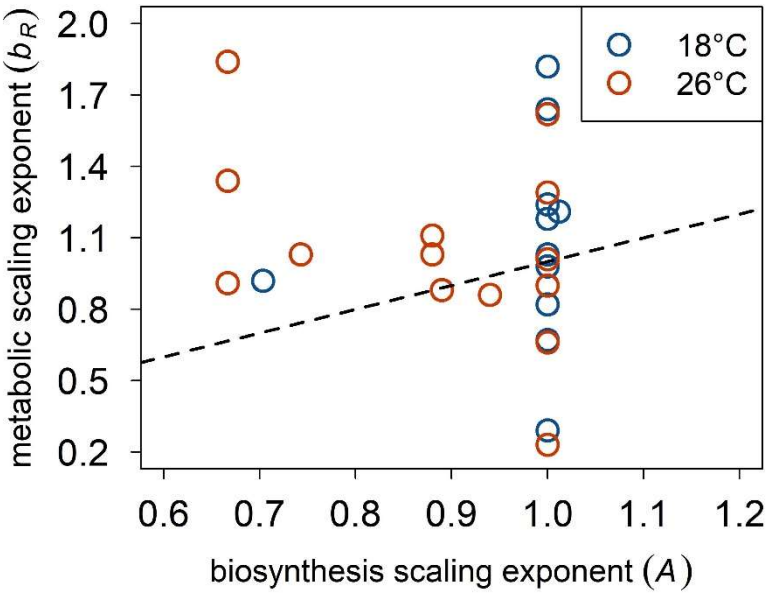

Figure 12. The relationship between biosynthesis scaling exponent, A, and metabolic scaling exponent, b_R for 26 *Eisenia fetida* individuals. Blue points and orange points represent individuals cultured under 18°C and 26°C, respectively. Dashed lines represent a theoretical one-to-one relationship between A and b_R.

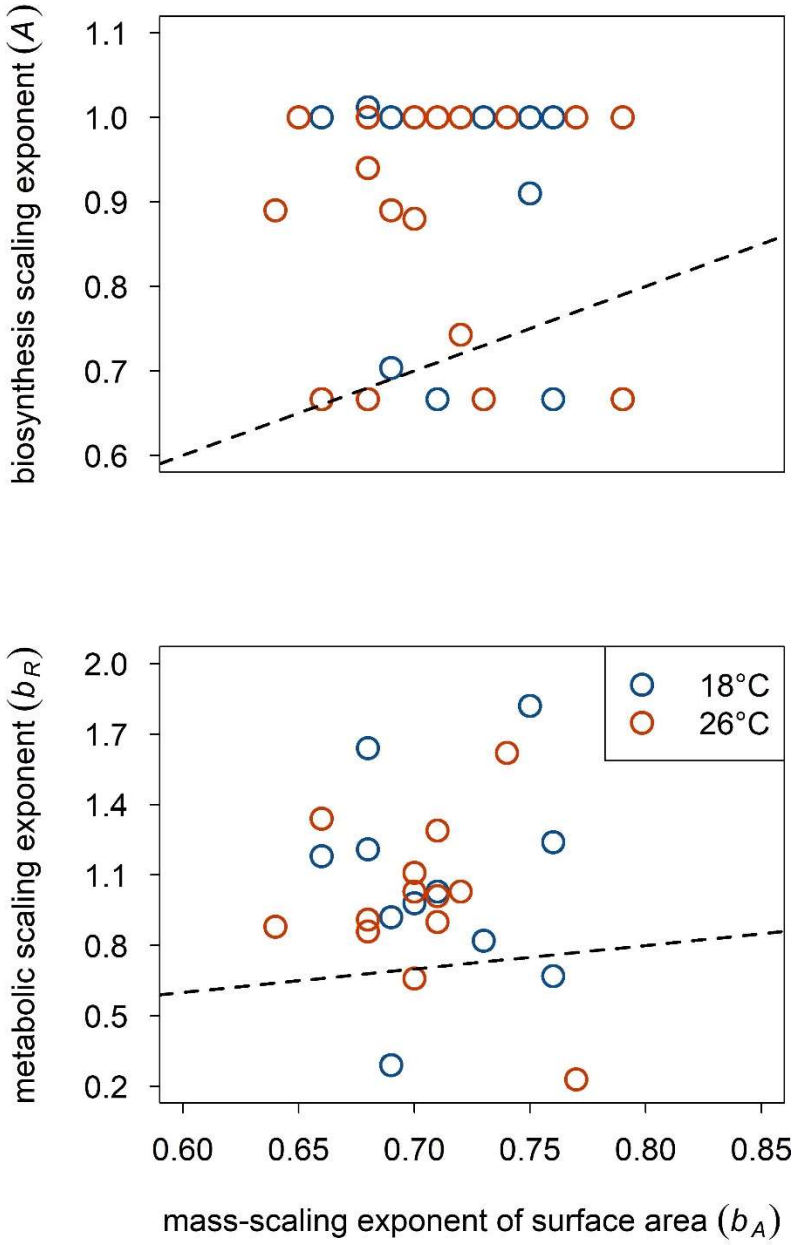

Figure 13. The relationship between biosynthesis scaling exponent, A, and the mass-scaling exponent of Euclidean surface area (b_A) for 44 *Eisenia fetida* individuals (top) and the relationship between metabolic scaling exponent, b_R, and b_A for 26 *E.fetida* individuals (bottom). Blue points and orange points represent individuals cultured under 18°C and 26°C, respectively. The dashed black lines represent a Euclidean surface area prediction of a one-to-one relationship between A and b_A, and b_R and b_A.

4.5.2. *Tubifex tubifex*: growth, metabolic rate and body shape

Tubifex tubifex: Body size, shape and metabolic rate at maturity

Table 3 show the average final body size (mass, length and diameter), shape (length-to-diameter ratio) and metabolic rate (oxygen consumption rate) at maturity for *T.tubifex* for both temperature treatments (18 and 26°C). Average body mass at maturity was significantly larger for the 18°C treatment compared to the 26°C treatment (Two sample t-test: $P < 0.001$, $t = 5.64$, $df = 140$). In addition, average body length was significant longer (Two sample t-test: $P < 0.001$, $t = 6.07$, $df = 140$) and average body diameter significantly wider (Two sample t-test: $P < 0.05$, $t = 2.56$, $df = 140$) in for the 18°C treatment compared to the 26°C treatment. Further, metabolic rate was significantly higher at the 18°C treatment than the 26°C treatment (Two sample t-test: $P < 0.001$, $t = 16.26$, $df = 87$). Average body length-to-diameter ratio at maturity was significantly higher for the 18°C treatment than the 26°C treatment (Two sample t-test: $P < 0.03$, $t = 2.17$, $df = 140$). The scaling of growth efficiency ($\frac{A}{b_R}$) was significantly different between the 18°C and 26°C treatments (Two sample t-test: $t = -3.33$, df = 74.3, $P < 0.01$) with average $\frac{A}{b_R}$ values of 1.19 and 1.50 for 18°C and 26°C, respectively (Table 4).

Tubifex tubifex: Temperature and the scaling of growth, metabolic rate and body shape

There was no significant difference between the two temperature treatments in exponent A (Two sample t-test: $t = -0.757$, df = 128.77, $P > 0.05$). The average value for the A across both temperature treatments was 0.95 (n = 142) (Table 4) which was significantly different from an average of $A = 1$ (pure exponential growth) (One-sample T-test: $t = -5.17$, df = 141, $P < 0.001$). Temperature treatment significantly affected b_R (Two sample t-test: $t = 3.13$, df = 85.56, $P < 0.01$), with average values of 0.83 (n =44) and 0.70 (n = 45) for temperature treatments 18°C and 26°C, respectively (Table 4). Furthermore, differences in temperature treatment had a significant effect on the scaling of body diameter relative to length (b_{DL}) (Two sample t-test: $t = -7.61$,

df = 126.45, p < 0.001), and the average b_{DL} value for temperature treatments 18°C and 26°C were 0.30 and 0.45, respectively (Table 4). Further, there was a significant effect of temperature on the body mass-scaling of surface area, b_A (Two sample t-test: t = 7.14, df = 139.6, p < 0.001), with average b_A values of 0.82 and 0.77 for temperature treatments 18°C and 26°C, respectively (Table 4) (see Supplementary Appendix 3 Table S5 for individual *T.tubifex* data).

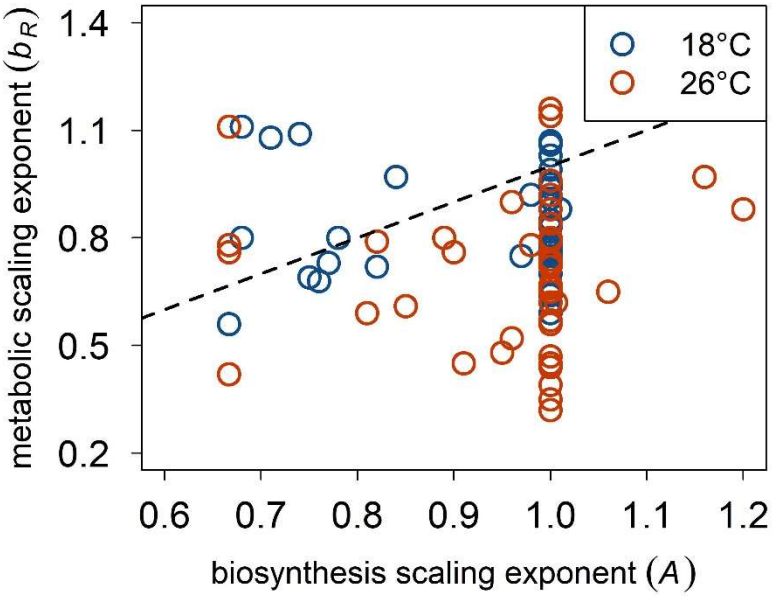

Figure 14. The relationship between biosynthesis scaling exponent, A, and metabolic scaling exponent, b_R for 89 *Tubifex tubifex* individuals. Blue points and orange points represent individuals cultured under 18°C and 26°C, respectively. Dashed lines represent a theoretical one-to-one relationship between A and b_R.

Tubifex tubifex: Relationships between the scaling of growth, metabolic rate and body shape

The average b_R for *T.tubifex* (0.77) was significantly less than the average b_R for *E.fetida* (0.71) (Two sample t-test: t = 3.48, df = 28.70, P < 0.01), but not for A (Two sample t-test: t = -0.904, df = 61.6, P > 0.05). Furthermore, the average b_A was significantly greater for *T.tubifex* (0.79) than *E.fetida* (0.71) (Two sample t-test: t = -11.3, df = 81.1, P < 0.001). Figure 14 shows the relationship between b_R and A. There

was no significant correlation between A and b_R (OLS regression: n = 89, R^2 = 0.002, P > 0.05). In addition, the body mass-scaling of surface area (b_A) did not significantly correlate with A (OLS regression: n = 142, R^2 = 0.06, P > 0.05) (Figure 15). There was a significant positive correlation between b_A and b_R for both temperature treatments: 18°C (RMA regression: n = 44, R^2 = 0.13, P < 0.01) and 26°C (RMA regression: n = 45, R^2 = 0.10, P < 0.05) (Figure 15). Further, a significant positive correlation between b_{DL} and b_R was present for both temperature treatments: 18°C (RMA regression: n = 44, R^2 = 0.15, P < 0.01) and 26°C (RMA regression: n = 45, R^2 = 0.12, P < 0.05).

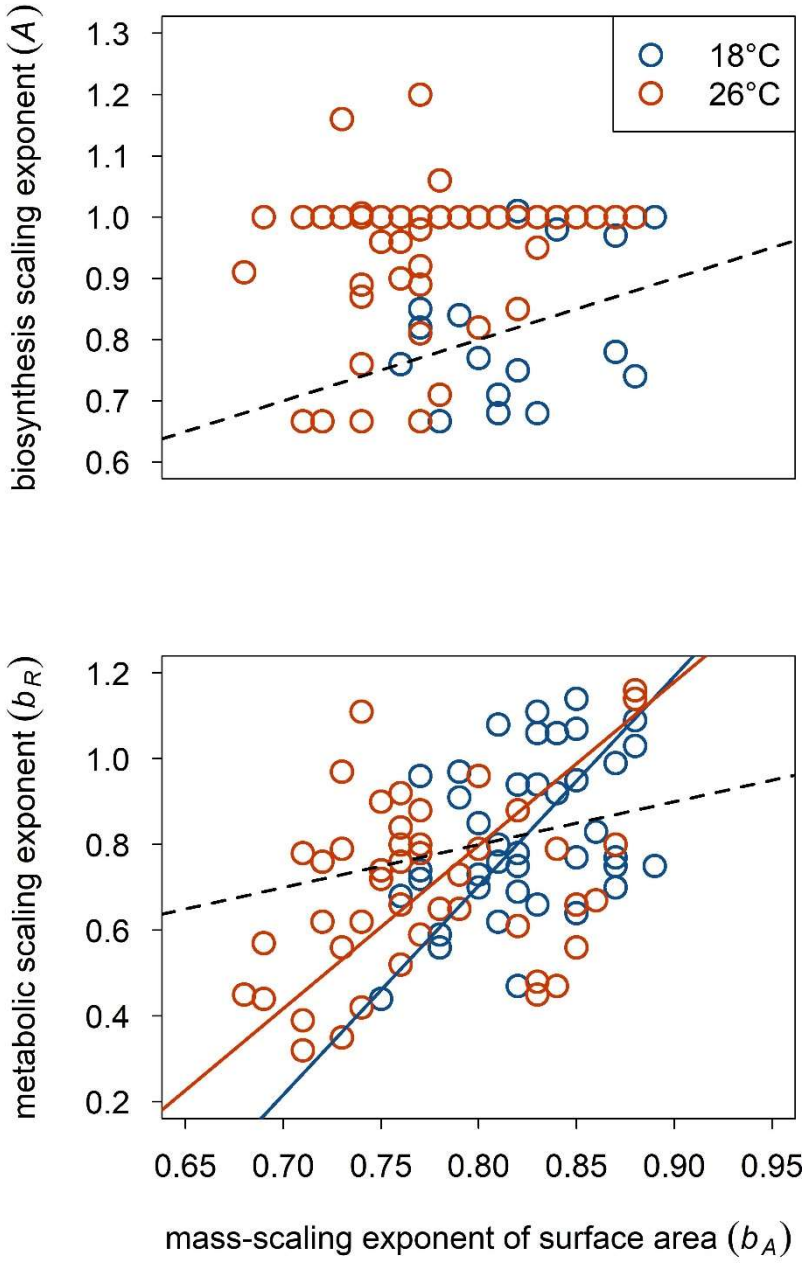

Figure 15. The relationship between biosynthesis scaling exponent, A, and the mass-scaling exponent of surface area (b_A) for 142 *Tubifex tubifex* individuals (top) and the relationship between metabolic scaling exponent, b_R, and b_A for 89 *T.tubifex* individuals (bottom). Blue points and orange points represent individuals cultured under 18°C and 26°C, respectively. The solid lines represent the Reduced Major Axis (RMA) regression between b_R and b_A for 18°C (blue line) and 26°C (orange line) treatments (**18°C:** slope = 4.88, intercept = -3.20, n = 44, R^2 = 0.13, $P < 0.01$; **26°C:** slope = 3.81, intercept = -2.25, n = 45, R^2 = 0.10, $P < 0.05$). The dashed black lines

represent a Euclidean surface area prediction of a one-to-one relationship between A and b_A, and b_R and b_A.

4.6. Discussion

4.6.1. The mass-scaling of growth and metabolic rate in *Eisenia fetida* and *Tubifex tubifex*

Metabolism fuels all biological processes, including growth, and thus it can be predicted that the scaling of biosynthesis (synthesis of component materials required for growth) (A) will correlate with the scaling of metabolism (b_R) over ontogeny. The results reported in this study do not support this prediction because there was no significant correlation between A and b_R for the ontogenetic development of oligochaete species *T.tubifex* and *E.fetida* (Figures 12 and 14). This finding agrees with the results reported in Chapter 3 for diverse pelagic invertebrate species, but instead this study explores A and b_R across individuals within a species and is based on matching growth and metabolic data rather than utilising data from different sources.

Both *E.fetida* and *T.tubifex* display clustering at $A = 1$ for the scaling of biosynthesis (Figures 12 and 14), which is representative of exponential growth where relative growth rate (the body mass increase per unit mass per unit time) is maintained over ontogeny. The lack of relationship between A and b_R for *E.fetida* and *T.tubifex* can, at least partly, be described by this large proportion/cluster of exponentially growing individuals. Widespread presence of exponential growth was also reported for diverse species of pelagic invertebrates in Chapter 3, that also showed variation in b_R. Thus, this is suggestive that energetic costs other than somatic growth are influencing metabolic rate across pelagic invertebrate species (Chapter 3) and within the two oligochaete species in this study. In Chapter 3 this was explained by multiple potential factors including variation in energy (lipid) reserves, reproductive strategy, locomotion and average lifespan. Considering that individuals within a species are likely to have similar lifespans and undergo the same reproductive strategy, the lack

of relationship between A and b_R within *E.fetida* and *T.tubifex* may be more likely explained by individual variation in locomotion and/or energy reserves.

A mismatch between A and b_R may be due to changes in body composition over ontogeny, for example, if there is an accumulation of energy (lipid) reserves over ontogeny. The body diameter – body length scaling exponent, b_{DL} indicates the scaling of body diameter relative to length and hence may provide a useful indication of changes in body composition. In this study, the average b_{DL} for *E.fetida* and *T.tubifex* was 0.71 and 0.39 (Table 3), respectively, whereby $b_{DL} < 1$ indicates length is increasing proportionately faster than diameter (body thinning) over ontogeny and $b_{DL} > 1$ the reverse (body thickening). Thus, both *E.fetida* and *T.tubifex* show decreased scaling of body thickness relative to length over ontogeny in this study, which may be due to decreasing proportion of lipid reserves, or other low-metabolising mass such as water, over ontogeny. The scaling exponent of biosynthesis (A), however, captures both somatic (metabolising) and low- or non- metabolising tissue (e.g. lipids), and hence A can mismatch with the scaling of metabolism (b_R) if changes in body composition (or proportion of metabolising structure) occur over ontogeny. The accumulation of energy reserves may represent a 'capital breeding' strategy for investment into future reproduction and/or building sexual organs, such as the clitellum in oligochaetes, although it is unclear in the literature whether oligochaetes adopt a capital or income breeding strategy. Capital breeding contrasts with income breeding (fuelling reproduction via simultaneous feeding), and is a common feature of ectotherm organisms because they have lower energetic costs associated with storage, maintenance and utilisation of energy reserves in comparison to endotherms (Bonnet, Bradshaw and Shine, 1998). Both *E.fetida* and *T.tubifex* individuals displayed variation in b_{DL}, ranging from approximately 0.3 to 1.3 and 0.1 to 0.9, respectively. Therefore, individual variation in body composition, perhaps due to individual differences in investment into building the clitellum, may account for the lack of relationship between A and b_R within *E.fetida* and *T.tubifex* in this study.

Metabolism fuels growth and so the relationship between A and b_R can indicate the proportion of metabolised energy allocated towards the process of growth over ontogeny, which can represent the scaling of growth efficiency over ontogeny. Thus, the lack of relationship between A and b_R across individuals indicates individual variability in the scaling of growth efficiency for both *E.fetida* and *T.tubifex*. For example, in this study across the two temperature treatments *T.tubifex* displayed almost-constant (but slightly declining) relative growth rate (RGR, the body mass increase per unit mass per unit time) over ontogeny ($A = 0.95 \pm 0.02$) but a larger decline in mass-specific metabolic rate over ontogeny ($b_R = 0.77 \pm 0.04$), suggesting an increase in growth efficiency over ontogeny. When considering temperature, the average A did not vary across treatments for *T.tubifex* but the average $\frac{A}{b_R}$ value (average scaling of growth efficiency) was higher in the warmer temperature (26°C) treatment compared to the cooler treatment (18°C) (Table 4). This suggests that *T.tubifex* has enhanced scaling of growth efficiency at 26°C because the same relative rate of growth is fuelled by proportionately less metabolised resources over ontogeny compared to 18°C.

In contrast, for *E.fetida*, mass-specific metabolic rate increased over ontogeny ($b_R = 1.05 \pm 0.15$) despite an almost-constant (but slightly declining) RGR over ontogeny ($A = 0.93 \pm 0.05$), which implies decreased growth efficiency over ontogeny because proportionately more metabolised resources are available to fuel to the almost-constant relative growth rate over ontogeny. However, the 95% confidence intervals for the average b_R value overlap with the average A value for *E.fetida*, suggesting that constant scaling of growth efficiency over ontogeny cannot be ruled out. In contrast to *T.tubifex*, temperature had no significant effect on $\frac{A}{b_R}$ for *E.fetida* (Table 4), suggesting that temperature may be a relatively more important influencer of the scaling of growth efficiency for water-breathers than terrestrial organisms. Further examination of the scaling of growth efficiency of terrestrial versus aquatic species would be required to confirm this. The importance of temperature on the scaling of metabolic rate and growth efficiency for *T.tubifex* but not for *E.fetida* can be expected when considering that increasing temperature decreases the availability

of oxygen in an aquatic environment (Hoefnagel and Verbeck, 2015) but not in a terrestrial environment. The effects of temperature on *T.tubifex* will be further discussed below.

Individual variation in the scaling of growth efficiency (deviations from the line of best fit in Figures 12 and 14) can be explained by variation in the energetic investment into biological processes other than somatic growth, such as locomotion. For *E.fetida*, locomotion involves the use of circular and longitudinal muscles to burrow through soil to search for food, access moisture and to create pores through which exchange of respiratory gases can occur (Barnett, Bengough and Mckenzie, 2009; Lee and Foster, 1991). For *T.tubifex,* locomotion is restricted mainly to the ventilatory movements of the posterior region whilst the anterior region remains burrowed within sediment to filter food (Kaster and Wolff, 1982). It is possible that individual variability in these methods of locomotion caused variability in metabolic demand and hence the scaling of growth efficiency in this study. However, because locomotory activity is linked to searching for food and enhancing respiratory exchange (Graham, 1990), significant variation in locomotion across *E.fetida* and *T.tubifex* individuals is unlikely because they were cultured in the same sized containers, received the same food quantity and nutrition, and the same degree of aeration (manual aeration for *T.tubifex*) and soil substrate in this study.

It is, however, plausible that issues with respiratory data collected may account for some noise in b_R and hence $\frac{A}{b_R}$ across individuals of *E.fetida* and *T.tubifex*. For example, oxygen levels reported from the respirometry device used may be inaccurate if *E.fetida* individuals curled onto the oxygen sensor spots (which detect oxygen levels) within the respirometry vials. Observations throughout the experiment suggested that the incidence of curling onto sensor spots did not increase with body size (i.e. the incidence was not size-biased) and hence may have contributed to noise in metabolic rate data, but is less likely to affect the overall scaling slope (b_R) of individuals. Furthermore, the ventilatory movements of the posterior region of *T.tubifex* individuals may have been impaired because of a lack of sediment (and hence lack of anchoring) within the respirometry microplate, which was a requirement to enable the sensor spots to remain exposed in water to read oxygen levels within respirometry wells.

4.6.2. Body shape changes and the mass-scaling of growth and metabolic rate

The average $\frac{1}{b_L}$ value (0.55 ± 0.04) indicates that *T.tubifex* is a strong shape shifter that tends towards body elongation in form (growth occurs in a single axis of body length). Shape shifting also occurred for *E.fetida* in this study, albeit to a lesser extent as represented by the species average $\frac{1}{b_L}$ value of 0.37 ± 0.01, which is near, but significantly greater than, pure isomorphy ($\frac{1}{b_L} = \frac{1}{3}$) where no shape change occurs, and tends toward elongation form. Body shape change towards an elongate form is also indicated by the average b_{DL} values for *E.fetida* (0.71) and *T.tubifex* (0.39) in this study (Table 4), which indicates proportionately more growth in body length relative to body diameter over ontogeny, and is most profound in *T.tubifex*.

Potential for body shape changes, as quantified by the body mass – body length exponent ($\frac{1}{b_L}$), to influence the ontogenetic scaling of metabolic rate of pelagic invertebrate species was reported by Hirst, Glazier and Atkinson (2014) and Glazier, Hirst and Atkinson (2015). Under Euclidean surface area theory, changes in body shape over ontogeny will result in changes to the body mass-scaling of body surface area (b_A). Thus, it can be predicted for organisms where respiratory exchange of gases occurs across external body surface areas, such as the integument of oligochaete species (Graham, 1990), b_A will display a positive one-to-one correlation with b_R (dashed lines in Figures 13 and 15) and consequently the mass-scaling of growth or biosynthesis, A. Hence, the average b_A values for *E.fetida* (0.71 ± 0.01) and *T.tubifex* (0.79 ± 0.01) should correlate with b_R values of around 0.71 (*E.fetida*) and 0.79 (*T.tubifex*). The average b_R value reported for *E.fetida* in this study is significantly higher than this prediction ($b_R = 1.05 \pm 0.15$), but in agreement with Euclidean surface area theory for *T.tubifex* ($b_R = 0.77 \pm 0.04$) (Table 4), suggesting a higher rate of resource (oxygen) uptake over ontogeny than expected from surface area theory for *E.fetida*. A higher rate of oxygen uptake could occur, perhaps, if there is enhanced respiratory exchange efficiency over ontogeny. For example, if diffusion pathways across the integument become increasingly shorter over ontogeny. Extending this surface area theory to the scaling of biosynthesis, A, the average A values for *E.fetida*

(0.93) and *T.tubifex* (0.95) should match the average b_A values, but actual b_A values are less for both *E.fetida* (0.71) and *T.tubifex* (0.79). Lower than predicted b_A values suggests a higher rate of biosynthesis over ontogeny than expected from surface area theory for both *E.fetida* and *T.tubifex*, which may occur if an increased proportion of available resources and/or energy are allocated towards biosynthesis over ontogeny.

When looking across individuals, a significant positive correlation between b_R and b_A occurred for *T.tubifex* (Figure 15) (but not *E.fetida* as shown in Figure 13) in this study, but with a larger slope of 4.88 at 18°C and 3.81 for 26°C than predicted from surface area theory (Figure 15), suggesting a higher rate of resource uptake than expected from body surface area. Upward deviation in b_R from Euclidean surface area predictions was also reported by Hirst, Glazier and Atkinson (2014) and Glazier, Hirst and Atkinson (2015) for diverse species of pelagic invertebrates. Another aim of conducting this study was to explore hypotheses that can account for this upward deviation in b_R from Euclidean surface area predictions. Hypothesis (i) stated that the boundary layer (between an organism's uptake surface and external resources) and hence relative importance of friction forces decreases with organism body size, which results in more efficient uptake of oxygen and hence a higher metabolic rate at larger body sizes. This study reports an average b_R value less than one (0.77 ± 0.04) for *T.tubifex*, an aquatic oligochaete, suggesting that mass-specific oxygen consumption rate declines with size. Conversely, terrestrial *E.fetida* displays an average $b_R = 1.05$, and may be less constrained by friction forces due to presence of electro-osmotic flow near the body surface that lubricates the body surface and creates vortices to reduce adhesion and hence friction when moving through soil (Yan *et al*., 2007). This suggests slight increase in mass-specific oxygen uptake with body size, although the confidence intervals for *E.fetida* (0.90 to 1.20) suggest that a constant rate or declining rate of mass-specific oxygen uptake with size cannot be ruled out. Nonetheless, b_R is significantly higher for *E.fetida* than *T.tubifex*, thus this study does not support hypothesis (i) and instead implies that relatively small effects of a boundary layer (or small effects of friction in soil) may result in higher metabolic rate at larger body sizes.

Hypothesis (ii) posits upward deviation in b_R in relation to b_A is due to an increase in body frilliness, or fractal dimension, as body mass increases which contributes to a larger body surface area and hence higher rate of metabolism. Both *T.tubifex* and *E.fetida* lack appendages and frills, but both displayed individual

variation in b_R, including higher b_R values than predicted from b_A (Figures 13 and 15), thus providing no support for hypothesis (ii). It is possible that upward deviation in b_R for *T.tubifex* is due to increased relative size of body surface convolutions over ontogeny, which are present on the posterior region of the body and are linked to enhanced respiratory uptake (Kaster and Wolff, 1982). Further examination of potential changes in the surface area of body convolutions over ontogeny warrants investigation in order to further explore hypothesis (ii). For *E.fetida*, upward deviation in b_R in relation to bA, despite being relatively smooth-bodied, suggests that reasons other than degree of fractal dimensions are shaping the relationship between b_A and b_R. For example, it is plausible that *E.fetida* exhibits changes in body composition over ontogeny such as decreased proportion of moisture or lipid reserves, and hence have a higher proportion of metabolising tissue and hence metabolic demand, which is supported by the average b_{DL} value of 0.71, that indicates decreasing body thickness relative to length over ontogeny. Decreasing relative body thickness could also occur if energy reserves are replaced by more compact muscle, or increased musculature, which would result in increased metabolic demand over ontogeny. The body size scaling of circular and longitudinal muscle area in earthworm *Lumbricus terrestris* has shown to increase over ontogeny – scaling at an exponent of 0.86 to 0.99 – at a faster rate than expected from isometry, and the body size scaling of burrowing forces scaled lower than expected from isometry (0.43 to 0.47) (where muscle properties are constant as a function of body size) (Quillin, 2000). Burrowing through soil requires the use of both circular and longitudinal muscles in *E.fetida* (Barnett, Bengough and Mckenzie, 2009) and thus it is possible that energy stores decrease and musculature increases over ontogeny. Anatomic examination of the body composition (ratio of lipid reserves to muscle tissue) of *E.fetida* over ontogenetic development would be required to confirm this hypothesis.

4.6.3. The influence of temperature on body shape changes and the mass-scaling of growth and metabolic rate

Both *E.fetida* and *T.tubifex* displayed inverse relationships between body mass at maturity and ambient temperature (Table 3), and hence support the temperature-size rule for ectotherms (Atkinson, 1994). Furthermore, temperature also negatively

influenced a measure of body shape at maturity (length-to-diameter ratio) for *T.tubifex*, with a proportionately thicker diameter relative to length (relatively squat in form) for the warmer temperature treatment compared to the cooler treatment. Increased squatness at the warmer temperature may explain why oxygen consumption rate at maturity was significantly lower in the warmer temperature than the cooler, if increased squatness also increased the length of diffusion pathways for respiratory exchange. However, oxygen consumption rate may have been lower in the warmer temperature if metabolic demand, for example from locomotory activity, was lower than the cooler temperature for *T.tubifex*. *T.tubifex* exhibits ventilatory movements in the posterior region that can enhance exchange of respiratory gases (Kaster and Wolff, 1982). Thus, it is plausible that decreased ventilatory movement in the warmer temperature could have result in a lower metabolic demand and hence oxygen consumption rate for *T.tubifex*. This could have occurred if the individuals at the warmer temperature were not well, for example, if they obtained any injuries during handling. No visible injuries were observed for these individuals, but because of the small size and delicacy of *T.tubifex* individuals, this idea cannot be ruled out. An increase in environmental temperature is often expected to result in an initial increase in organism metabolic rate, including oxygen consumption rate, until it reaches an thermal optimum where metabolic rate subsequently declines. Therefore, the negative correlation between temperature and oxygen consumption rate for *T.tubifex* warrants further investigation to understand this phenomenon. For example, reproducing this experiment and using a higher magnification microscope to check for injuries that were not visible in this study, and also conducting experiments that explorie the frequency and rate of locomotory activity in relation to oxygen consumption rate under several temperatures.

In contrast, temperature had no significant influence on length-to-diameter ratio or oxygen consumption rate at maturity for *E.fetida* (Table 3), suggesting that the body shape and metabolic rate (or oxygen consumption rate) of an air-breather may be less influenced by ambient temperature than a water-breather. Future work would benefit from further comparisons of terrestrial versus aquatic species to confirm this.

Temperature did not affect the ontogenetic scaling of biosynthesis (A) for *E.fetida* or *T.tubifex* in this study, suggesting that scaling of the synthesis of new component materials (required for growth) over ontogenetic development has low

thermal sensitivity. The building of new component materials over ontogeny is a requirement for organisms to grow to maturity and build sexual organs for reproduction. Hence, the scaling of biosynthesis may be independent of environmental temperature if it is pre-determined and influenced only by factors directly impacting biosynthesis such as the availability of resources (food) to build new body mass, which was constant in this study. Oligochaetes often have wide tolerances to a range of environmental conditions including temperature (Oplinger and Wagner, 2011), as evidenced by their prevalence around the world. For example, it has been shown that *T.tubifex* total mass recovered and mass production (daily growth per stocked mass) is not significantly affected by temperature treatment, which ranged between 12 and 27°C (Oplinger and Wagner, 2010). Whereas, growth was limited when food was restricted or of poor nutrition (Oplinger and Wagner, 2010). Thus, the adaptation to wide environmental tolerances may enable individuals to grow optimally over ontogeny, for example by sustaining RGR or delaying declines in RGR when mortality risk is constant over ontogeny, which may account for the lack of relationship between the scaling of growth (biosynthesis) and temperature in this study.

The significant negative effect of temperature on b_R in *T.tubifex* in this study (Table 4) suggests that individuals reared at 18°C displayed comparatively lower declines in oxygen consumption rates over ontogeny than those raised at 26 °C. An increase in temperature could result in decreased locomotory activity, or ventilatory movements in *T.tubifex*, resulting in lower energetic costs and hence oxygen demand as predicted by the metabolic-level boundaries hypothesis (MLBH). However, it has been shown in *T.tubifex* that a decline in oxygen availability results in enhanced frequency and amplitude of posterior ventilatory movements (tail undulation) and consequently increased respiratory uptake (Guerin and Giani, 1996). Since oxygen availability decreases with temperature in an aquatic environment (Hoefnagel and Verberk, 2015) it can be predicted that ventilatory movements of *T.tubifex* increase with temperature. Over ontogeny, if this enhanced oxygen demand (from increased locomotory activity) is not met, then the metabolic scaling slope will become shallower and hence mass-specific metabolic rate decline with size. However, the oxygen consumption rate at maturity was significantly higher at 18°C than 26°, and given that temperature did not influence the scaling of biosynthesis, this suggests the difference in oxygen consumption rate at maturity is not due to differences in the

allocation of energy towards growth. Instead, these results suggest that energetic demand for processes other than growth, such as locomotory demand, was higher at 18°C compared to 26°C. Thus, agreeing with the MLBH that because locomotory activity likely decreases with temperature, b_R will negatively correlate with temperature in active organisms. Moreover, the inverse relationship between ambient temperature and b_R for *T.tubifex* in this study is in agreement with previously studies on crustacean species (Ivleva, 1980), teleost fish (Killen, Atkinson and Glazier, 2010), animals and plants (Glazier, 2020). Temperature did not influence b_R in *E.fetida* in this study, which may be due to temperature having less influence on the oxygen availability in air compared to water, but owing to the small sample size of b_R measurements (n = 26) further studies are required to confirm this.

Furthermore, temperature significantly positively correlated with the scaling of body diameter relative to length, b_{DL}, over ontogeny and the body length-to-diameter ratio ($\frac{L}{D}$) at maturity in *T.tubifex*, suggesting that individuals reared under warmer temperatures were proportionately thicker in diameter relative to length, or more squat in shape, than those in cooler temperatures. Respiratory exchange occurs across the protruding posterior region of *T.tubifex*, whilst the anterior region remains burrowed in sediment (Kaster and Wolff, 1982), and thus under Euclidean surface area theory a decline in body thickness relative to length over ontogeny could indicate a shift towards a more 'squat' body shape form, which implies decreased relative body surface area, and hence respiratory exchange, in comparison to more 'elongate' forms where body length increases faster than body thickness (Hirst, Glazier and Atkinson, 2014). The reported b_R values in this study agree with this hypothesis. Individual *T.tubifex* reared under the cooler temperature treatment displaying significantly steeper scaling of oxygen consumption rate, and hence increased respiratory efficiency, than those in the warmer treatment (Table 4). Therefore, it is possible that an increase in temperature results in shallower metabolic scaling slopes in *T.tubifex* due to a shift towards a more 'squat' body shape, and hence decreased respiratory exchange over ontogeny.

4.6.4. Wider implications

Furthering current understanding of the prevailing factors influencing growth and metabolic rate in oligochaetes is crucial to research concerning metabolic response to toxicity or pollution, nutrient recycling and production that has direct application to environmental, economic and societal issues. For example, the use of earthworms in composting of hazardous wastes (Li *et al.*, 2016) and the use of freshwater *T.tubifex* as a bioindicator of heavy metal toxicity to aid the protection of human and animal health (Rathore and Khangarot, 2002). Furthermore, because temperature is an important environmental factor for ectothermic animals, predicting the relationship between the scaling of metabolic rate and ambient temperature is crucial to predict how organisms will respond to thermal change. Temperature affected the mass-scaling of metabolic rate in freshwater *T.tubifex*, but not terrestrial earthworm *E.fetida* in this study, thus shedding light on potential variation in the response to thermal conditions between aquatic and terrestrial environments. Future work would benefit from gaining further data on the metabolic rate of *E.fetida* to improve on the small sample size that was achievable in this study.

Chapter 5. Exploring the drivers of metabolic rate across mammals

5.1. Abstract

All biological activities are fuelled by metabolism, and so understanding the drivers and limitations of metabolic rate is fundamental to biology. The allometric scaling of basal metabolic rate (BMR, the metabolic rate of non-reproducing individuals in a post-absorptive state under thermo-neutral conditions) has long been debated, with evidence for both linear and curvilinear scaling patterns. Apparent curvature of mammalian BMR scaling has been explained by variation in reproductive parity (litter size), and also through differences in ambient temperature that relate to limits to heat dissipation and energy efficiency. I propose that animals with larger litter sizes will have high costs of gestation and lactation, which will also correlate with high BMRs, and that differences in parity will therefore correlate with BMR and potentially its allometry. To test two competing theories, I apply phylogenetically controlled path analysis to BMR data of eutherian mammalian species to determine whether reproductive parity or ambient temperature better predicts variation in BMR. I reveal differences in the scaling of maternal production rates between uniparous and multiparous species that is suggestive of differences in the energetic costs of lactation and gestation. However, path analysis revealed ambient temperature and body size, but not parity or maternal production, to be significant predictors of the variation in BMR, thus providing support for variation in energy efficiency driving BMR scaling across mammals. By providing a better understanding of the major drivers of apparent curvature in BMR scaling this study further contributes to a more comprehensive framework for mammalian interspecific metabolic scaling.

5.2. Introduction

5.2.1. Variation in metabolic scaling

Metabolic rate (R) is commonly related to body size (m) using a power function of the form: $R = am^b$ where a is a normalisation constant. Linear regression is typically

used to examine metabolic allometry – the relationship between metabolic rate (R) and body size (m) on a log-log scale. Based on intraspecific comparisons of dogs, the allometric scaling exponent, b, was originally argued to hold a value of $\frac{2}{3}$ on the basis that maintenance costs, or metabolic costs, scaled in proportion to body surface area (Sarrus and Rameaux, 1839; Rubner, 1883). This 'surface area law' (Kleiber, 1932) was challenged by evidence from interspecific comparisons of mammal and bird species, which predicted a metabolic scaling slope of approximately $\frac{3}{4}$ (Brody and Procter, 1932; Kleiber, 1932). The first influential theoretical explanation for this observed quarter-power scaling was offered by West *et al*. (1997) who proposed the West Brown and Enquist (WBE) model of metabolic scaling. The WBE model is based on the optimisation of resource transport through networks that have fractal-like geometries and has since formed a mechanistic basis for the Metabolic Theory of Ecology (MTE). WBE theory posits that because metabolic rate determines the rates of resource uptake and allocation (to growth, survival and reproduction), it is a driver of ecological processes at all levels of organisation from individuals to the biosphere (Brown *et al.*, 2004). Following the publication of the WBE model, the values of metabolic scaling exponents and the theoretical explanations for them have been vigorously debated. Numerous other metabolic scaling theories and models have been proposed (Banavar *et al*., 2010; Gillooly *et al*., 2001; Glazier, 2010; Hirst, Glazier and Atkinson; Kolokotrones *et al*., 2010; Kooijman, 1986; Speakman and Król, 2010a) and see Glazier (2018) for a review). However, there remains a lack of consensus on the numerical value of the metabolic scaling slope, with reported values generally varying between approximately $\frac{2}{3}$ and 1 for basal metaolic rate for diverse taxa (Clarke, Rothery and Issac, 2010; Glazier, 2005, 2014; Hayssen and Lacy, 1985; Kozlowski and Konarzewski, 2005; Müller *et al*., 2012).

In general, variation in the inter-specific scaling of mammalian metabolic rate has been linked to numerous factors based on physiology (Clarke, Rothery and Isaac, 2010; Speakman and Krol, 2010a; Streicher, Cox and Birchard, 2012), geography (Lovegrove, 2000), taxonomy (Capellini, Venditti and Barton, 2010; Hayssen and Lacy, 1985) and ecology (Glazier *et al.*, 2011; Müller *et al.*, 2012). Recently, musculature of mammal species has been linked with the scaling of BMR (McNab, 2019), with higher values of mass-independent BMR reported for mammal species

with >40% muscle mass than expected at a given total body mass. Conversely, mammals with <30% muscle mass have lower than expected BMRs at a given body size. In addition, incorporating differences in mammalian body temperature predicts different BMR scaling relationships than the 'traditional' $\frac{3}{4}$ exponent across mammals (Clarke, Rothery and Isaac, 2010). By accounting for body temperature, it was shown that the metabolic scaling exponents decrease in magnitude with body size. Furthermore, deviations from a single universal relationship between BMR and body size have been explained by diet and temperature differences between herbivorous and carnivorous mammals (Clarke and O'Connor, 2014). Specifically, it was shown that because herbivory requires a warmer body than carnivory, herbivores generally have higher BMRs than carnivores owing to the positive relationship between body temperature and BMR and a higher maintenance costs of digesting plant matter.

5.2.2. Does curvature exist?

In addition, the linearity of the mass-scaling of mammalian BMR has been challenged with evidence of curvilinear scaling – steepening as species body sizes increase - from numerous authors (Bueno and López-Urrutia, 2014; Capellini, Venditti and Barton, 2010; Clarke, Rothery and Isaac, 2010; Hayssen and Lacy, 1985; Kolokotrones *et al.*, 2010; Kozlowski and Konarzewski, 2005; Painter, 2005; Savage, Deeds and Fontana, 2008). Curvilinearity indicates steeper scaling across larger mammal species, and shallower scaling across smaller species, which differs from a constant value of $\frac{3}{4}$ power scaling across species, and hence the exponent which forms the basis of the MTE (Brown *et al.*, 2004). Yet the existence of curvature, and type of curvature, in metabolic scaling across mammal species continues to be debated (Griebeler and Werner, 2016; MacKay, 2011; Müller *et al*., 2012; Packard, 2012, 2015; White, 2011), for example based on the size range of species included in the dataset and use of inappropriate statistical methods such as the use of R-squared to compare linear and non-linear models in Kolokotrones *et al.* (2010). In addition, in contrast to the claimed steepening curvature, two influential theories for explaining metabolic scaling relationships do not explain the steeping of mammalian BMR curvature. Instead, Dynamic Energy Budget theory (Maino *et al*., 2014) and WBE theory (Savage, Deeds and Fontana, 2008) have both predicted downward curvature of mammalian metabolic

rate – mass-scaling becoming shallower as species size increases (Maino *et al*., 2014). Hence, there remains a lack of consensus to both the existence of and a mechanistic explanation for mammalian BMR curvature. Despite this lack of consensus, there is undoubtably an overwhelming amount of evidence for curvilinear mammalian metabolic body-mass scaling in the literature that highlights the need for further mechanistic exploration, and importantly, incorporation of potential mechanisms may benefit allometric models of mammalian metabolic scaling.

5.2.3. Potential causes of curvature and variation in metabolic rate

Upward curvature of the mass-scaling of mammalian basal metabolic rate has been related to surface area theory on the basis that BMR of small mammal species scales with an exponent of approximately $\frac{2}{3}$ due to the effects of body surface area related heat loss owing to their relatively high surface area-to-volume ratio (Degen *et al.*, 1998; Glazier, 2005; Speakman, 1999). In comparison, for large mammal species heat loss is not as problematic due to their relatively small surface area-to-volume ratio, and in some cases the opposite is true – limits to heat dissipation arise at large body sizes and are compensated by factors such as thinning insulation and the evolution of large surface area structures such as the ears of elephants (Glazier, 2014). Instead of body surface area effects, large sized mammals are likely to be more influenced by volume related tissue demand or resource supply limits of internal transport networks (for a review of this see Glazier, 2014), as suggested by their metabolic scaling exponents that generally tend to $\frac{3}{4}$, or even 1 for very large species (Glazier, 2014; Makarievaw, Gorshkovw and Li, 2003; Painter, 2005b). Furthermore, upward curvature of mammalian metabolic rate can also be linked to differences between aquatic and terrestrial species at large body sizes. For example, Speakman and Król (2010a) propose that large aquatic mammals have the ability to achieve higher metabolic rates than terrestrial species, at a given size, due to the comparatively lower ambient temperature of an aquatic environment enabling a larger capacity to dissipate body heat.

Furthermore, Clarke, Rothery and Isaac (2010) also linked the effects of heat flow to the apparent curvature of mammalian BMR scaling, specifically through

ambient and body temperature. Whilst the majority of variation in the scaling of BMR is explained by body size, both body temperature (T_b) and ambient temperature (T_a) displayed significant relationships with BMR, which was complicated by an interaction between T_b and T_a (Clarke, Rothery and Isaac, 2010). A generalised linear model revealed that T_a but had a small but significant effect on BMR, and T_a also had a significant negative effect on T_b , suggesting that ambient temperature is a driver of the variation in both BMR and body temperature across mammals (Clarke, Rothery and Isaac, 2010) . Low ambient temperatures are associated with high energy demands and mechanisms to maintain high body temperature, hence high BMR and body temperature. Overall, across mammals a general linear model found that the scaling coefficient of BMR increases with both T_a and T_b, with the effect of T_b decreasing with the inclusion of T_a (Clarke, Rothery and Isaac, 2010). Additionally, the inclusion of phylogenetic correction also reduced dependence of BMR on T_b. Thus, it is plausible that T_b is a not a predictor of metabolic rate but rather a product if an organism's T_b is a result of metabolic activity and/or maintaining constant T_b in the face of ambient temperature. This idea is acknowledged by Clarke, Rothery and Isaac (2010), who argue that T_b forms a feedback loop with resting metabolism, whereby heat generated from metabolism generates T_b, which subsequently influences the level of resting metabolism. Therefore, if T_b is viewed as a product of BMR, the results reported by Clarke, Rothery and Isaac (2010) suggest that ambient temperature partly governs the relationship between BMR and body mass, and BMR and body temperature. This is supported by previous studies that have reported significant effects of biogeographical zones (Lovegrove, 2003) and climate (McNab, 2008) on the variation of BMR across mammals.

In addition, a thermodynamic model has recently been proposed to explain how ambient temperature influences variation in mammal BMR responsible for apparent curvature (Ballesteros *et al.*, 2018). This model predicts the dependence of metabolic rate with body size to emerge through a trade-off between the capacity for an organism to dissipate body heat and the energy efficiency of maintaining metabolism (to stay alive). Ballesteros *et al*. (2018) present this model as a unified framework capable of recovering various effective scaling exponents of metabolic rate, as highlighted by its applicability to empirical data of diverse taxa including mammals, birds, insects and plants. This thermodynamic model builds on the work by

Swan (1974), which states that mammals require more than essential energy to keep warm, and the Heat Dissipation Limit (HDL) theory proposed by Speakman and Król (2010a,b). Ballesteros *et al*. (2018) show this thermodynamic model to be equally as good as the quadratic model of Kolokotrones *et al.* (2010) at predicting curvature for mammalian BMR, but instead has the benefit of only two free parameters rather than three.

Specifically, this thermodynamic model produces upward curvature on a double logarithmic plot through a linear combination of two power laws: one based on the fraction of energy used efficiently to maintain metabolism, and the other representing heat loss of an organism. These two power laws represent isometric (proportional to mass, m) and allometric (proportional to $m^{\frac{2}{3}}$) terms, respectively, and are balanced by biologically meaningful Meeh factors k and k' that are considered as constants that are independent of mass, m (Ballesteros *et al.*, 2018). Meeh factors were developed by Meeh (1879) as constants that relate an organism's surface area to weight, and depend on the shape of the organism. Ballesteros *et al*. (2018) posit that the metabolic and physiological processes of organisms (e.g. ATP synthesis) are neither purely thermodynamically efficient nor inefficient because some energy is lost as heat, and thus variation in the energy efficiency of species can account for different metabolic scaling relationships. For example, Ballesteros *et al*. (2018) propose that differences in climatic adaptations in mitochondrial energy efficiency between polar and desert species can account for their differences in metabolic scaling – with polar species having higher BMRs than desert species in general. Specifically, polar species have proportionately larger levels of thermogenin inside their mitochondria, an uncoupling protein that generates heat by uncoupling oxidative phosphorylation from ATP synthesis, hence warming the animal. This is achieved without creating ATP and so decreases energy efficiency of the mitochondria. Furthermore, the larger size, and hence smaller surface area-to-volume ratio of polar species than desert species highlights their adaptation for reducing the effects of heat dissipation in a cool climate. Therefore, differences in energy (in)efficiency that relate to adaptations to different ambient temperatures (climate) can account for variation in mammalian BMR responsible for apparent curvature.

In contrast, curvature of mammalian metabolic scaling has also been accounted for by differences in life history traits across species. Müller *et al.* (2012) argued that the presence of curvilinear scaling is not necessarily the result of a universal non-linear metabolic scaling law, but instead a resulting artefact from the presence of two reproductive axes: uniparity (one offspring per litter) and multiparity (more than one offspring per litter). Specifically, Müller *et al.* (2012) reported that uniparous species, that tend to be larger in body size, exhibit steeper metabolic scaling relationships than multiparous species, which tend to be restricted to small body sizes. These axes exhibit different metabolic scaling patterns and hence can account for upward curvature observed for the interspecific mass-scaling of BMR of eutherian mammals. Despite the link between metabolic scaling and reproductive strategy reported by Müller *et al.* (2012) a mechanistic explanation as to why degree of parity influences BMR is lacking, especially because, by definition, BMR data are collected when individuals are not reproducing (Speakman, Krol and Johnson, 2004).

Life history rates (e.g. growth, reproduction) can be considered to either be fuelled by, or pose a limit to, the rate of metabolism and hence may account for variation in metabolic rate responsible for curvature. The Heat Dissipation Limit (HDL) theory of Speakman & Król (2010a,b) postulates that an organism's total energy expenditure is constrained by its maximal capacity to dissipate heat, with daily energy expenditure predicted to scale with body mass with an exponent of 0.63. HDL theory predicts that the low surface area-to-volume ratio of large-sized endothermic mammals limits the dissipation of body heat generated by reproductive effort, suggesting that the maximal rate at which mammals can produce (and wean) offspring may be limited by turnover of invested maternal energy. Arguably, pre-natal (gestation) and post-natal (lactation) energy investment are the major costs of production, with Speakman & Król (2010b) suggesting lactation as the main energetic cost. Therefore, according to HDL theory, variation in production, and in turn metabolic rate, which cannot be explained by body size alone may be accounted for by differences in maternal investment of energy into lactation and/or gestation.

Thus, if it is assumed that generally across mammal species there is an approximately constant conversion of maternal energy into each gram of offspring produced, it can be hypothesised that the variation in litter size will correlate with variation in maternal energy investment (into lactation and/or gestation) if litter size

relates to the capacity of species to dissipate heat generated by lactation and/or gestation. It is plausible that degree of parity relates to the rate of maternal energy investment because, at a given neonate body size, pre-natal and post-natal development of multiple offspring is likely to be larger than that of a single offspring.. Consequently, this implies that differences in maternal energy investment will correlate with differences in basal metabolic scaling between uni- and multi-parous species as reported by Müller *et al.* (2012). Because uniparous species are generally larger than multiparous species, potential increased mass-scaling of maternal energy investment for uniparous species at larger body sizes could account for curvature in mammalian BMR scaling. For example, increased (steeper) scaling of maternal energy investment could occur for uniparous species at a large size if the capacity to dissipate heat generated from reproductive effort becomes more limited as size increases, which can occur because larger sized bodies have comparatively smaller surface area-to-volume ratios than small sized bodies, as predicted by HDL theory. A correlation between maternal energy investment and BMR may arise if species with high reproductive demands (for lactation and/or gestation) have capacity for high basal metabolic costs during non-reproducing periods of adult life (because BMR data are collected from individuals that are not reproducing, lactating or gestating). Therefore, I propose the reported upward curvature of interspecific scaling of mammalian BMR that was accounted for by the presence of two reproductive axes (uniparity and multiparity) (Müller *et al.*, 2012) could be due to differences in maternal energy investment into lactation and/or gestation between uni- and multi- parous species.

5.3. Aims and hypotheses

Apparent curvature of the allometric scaling of mammalian BMR has been explained by disparity in the scaling of BMR between uniparous and multiparous mammal species, which exist at different size ranges, by Müller *et al.* (2012). However, variation in BMR responsible for curvature has also been explained by variation in ambient temperature (Clarke, Rothery and Isaac, 2010) which can be described by a thermodynamic model based on a trade-off between the energy dissipated as heat and the energy efficiency of an organism in different ambient temperatures (Ballesteros *et al.*, 2018). Therefore, the aim of this study is to explore whether differences in life

history factors (relating to parity) or differences in ambient temperature better explain variation in BMR.

There lacks a theoretical explanation for the presence of this dichotomy in metabolic scaling between the two reproductive axes as reported by Müller *et al.* (2012). Thus, I propose that the contributions of different degrees of parity to the variation in BMR in mammals comes from: (i) a correlate of different maternal production costs between uni- and multi- parous species, and ii) that this correlation would arise if species with high maternal reproductive demands have capacity for high metabolic rate at other times during adult life (when not reproducing), which will be reflected by high basal metabolic costs. Specifically, I make the following hypotheses:

1. Uniparous and multiparous species will exhibit differences in the body mass-scaling of maternal production rates that correlate with the body mass-scaling of BMR as reported by Müller *et al.* (2012).
2. Differences in life history factors (maternal production rates and parity) explains variation in BMR responsible for curvature if BMR correlates with the costs of maternal production, thus providing a mechanistic explanation for the findings of Müller *et al.* (2012).
3. Variation in ambient temperature accounts for variation in BMR responsible for curvature, agreeing with the findings of Clarke, Rothery and Isaac (2010) and Ballesteros *et al*. (2018).

Therefore, this study explores whether variation in BMR responsible for curvature is explained by either or both: (i) the costs of maternal production (supporting the findings of Müller *et al.* (2012)), or (ii) variation in ambient temperature, which relates to differences in the energy efficiency of species (supporting the results of Clarke, Rothery and Isaac (2010) and the framework of Ballesteros *et al.* (2018)).

5.4. Methods

5.4.1. The dataset

The online ecological database PanTHERIA (Jones *et al.*, 2009) was utilised to collect life-history data for eutherian mammal species. Analyses carried out by Müller *et al.* (2012) utilised the metabolic rate database compiled by McNab (2008), which lacks important life history data such as weaning age or gestation duration. Despite the difference in dataset, I justify the use of a different database to Müller *et al*. (2012) by showing that the marked difference in metabolic scaling relationships with body size between uniparous and multiparous species still holds for the PanTHERIA database (see Supplementary Appendix 4 Information SI2). Data on the following life history variables were collected: basal metabolic rate (mg O_2 h^{-1}), litter size, litters per year, weaning mass (grams), weaning age (days), gestation duration (days), neonate mass (grams) and adult mass (grams). To explore the effect of ambient temperature (T_a) on basal metabolic rate the PanTHERIA database was utilised. For the complete database for this Chapter please see https://github.com/lauraleemoore/LLM_Thesis_datasets.

Species were classified into to parity categories: 'uniparous' if average litter size < 1.5 and 'multiparous' if average litter size ≥ 1.5. This division between uniparity and multiparity is the same as applied by Müller *et al*. (2012), and can be justified on the basis that some mammal species can produce both a single offspring per litter and two offspring per litter during a lifetime, such as humans. In this case, the average litter size should be less than 1.5 if the litter size is more often one offspring than two offspring during a lifetime. Comparing metatherians to eutherian (placental) mammals may be inappropriate because they exhibit differences in body temperature and the mass-scaling of body temperature, which may influence (or correlate with) the mass-scaling of metabolic rate if body temperature (at least partly) determines metabolic rate (Clarke and Rothery, 2008)). In addition, non-placental metatherian mammal groups (monotremes and marsupials) are long-divergent lineages that have very different reproductive biologies that undergo egg laying or pouch rearing. Therefore, analysis included eutherian mammal species only.

5.4.2. Parity, maternal production rates and the mass-scaling of BMR

Measuring maternal production rates

To explore potential differences in the body size scaling of maternal production between uniparous and multiparous species (hypothesis 1), I applied measures that reflect the maternal energetic investment into the production of offspring mass both prenatally (gestation) and/or postnatally (weaning). The measure of weaning production rate can be used as an indicator of investment into lactation, since juveniles with rapid weaning growth rates are likely to require more nutrition (milk) per unit time than juveniles that are more slowly weaned. The measure of gestation production rate reflects the rate at which neonates are produced pre-natally from the zygote, which I assume is of negligible mass. By applying these measures, I assume that generally over species there is a constant conversion factor of maternal energy (into gestation and lactation) to the production of offspring per gram. To explore rates of total maternal production (weaning and gestation costs) the rates of weaning and gestation production were combined. Thus, the three maternal production rates were calculated as:

$$\text{Weaning production rates (grams per day)} = \frac{(weaning\ mass - neonate\ mass)}{weaning\ age} \times litter\ size \quad (5.1)$$

$$\text{Gestation production rate (grams per day)} = \frac{neonate\ mass}{gestation\ duration} \times litter\ size \quad (5.2)$$

$$\text{Total maternal production rate (grams per day)} = \frac{(weaning\ mass * litter\ size)}{(weaning\ age + gestati\quad duration)} \quad (5.3)$$

This applied measure of weaning production rate assumes that all neonates survive to weaning and thus does not incorporate mortality risk or mortality rate. Therefore, I acknowledge this measure will overestimate weaning production rate. Mortality risk or rates could not be incorporated into this equation because data on pre-weaning mortality risk were scarce in the literature, which is likely due to the practical difficulties obtaining pre-weaning mortality data in free-living wild mammals (e.g. see Sibly *et al*., 1997; Sibly and Brown, 2009).

Maternal production rates and BMR

To explore hypothesis (2) on whether the disparity in the body mass-scaling of maternal production rates correlates with the body mass-scaling of basal metabolic rate (BMR) between uni- and multi- parous species (as reported in Müller *et al.*, 2012) the effects of body size were removed, and the body mass residuals of total maternal

production rate were plotted against the body mass residuals of BMR for both uni- and multi- parous species combined. Reduced Major Axis (RMA) regression was applied instead of Ordinary Least Squares (OLS) because the error variation is likely to be present for both the y- and x-axis (RMA) and not just the x-axis (OLS) (Smith, 2009). It was not possible to apply phylogenetic correction to RMA regression because there were, to my knowledge, no accurate phylogenetically-controlled RMA techniques or methods reported in the literature or in statistical software (e.g. R) programs.

5.4.3. Exploring allometric scaling relationships

All analysis in this chapter used the BMR and adult body mass data obtained from the PanTHERIA database. When exploring the relationships between maternal production rates and body mass or BMR it would be beneficial to use maternal body mass and BMR. However, there was no maternal-specific BMR or body mass, or specification of sex for either BMR or body mass, in the PanTHERIA database. Therefore, the use of non-maternal (or unknown sex) BMR and body mass data could result in different relationships than maternal BMR and body mass data, and thus caution must be taken when drawing conclusions from the results.

To test hypothesis (1) I compared the allometric scaling relationships of maternal production rates (weaning, gestation and total) between uniparous and multiparous species by applying ordinary least squares (OLS) regressions on a log-log scale. I acknowledge that applying OLS regression assumes independence of species data, and for my dataset this assumption may be considered invalid because of the shared evolutionary history of species. To account for the evolutionary relatedness amongst species, I also applied phylogenetic general least squares (PGLS) regression. To test whether the maternal production rate scaling relationships significantly differ between multiparous and uniparous species an interaction term (between body mass and parity) was incorporated into the PGLS regression, which is the same statistical method applied in Müller *et al*. (2012).

In order to examine ambient temperature in relation to the upward curvature of BMR scaling (hypothesis 3), as proposed by Ballesteros *et al.* (2018) and Clarke, Rothery and Isaac (2010), ambient temperature data was separated into two data bins of approximately equal temperature range: -11 to 10 °C and 10.0 to 26.1°C,

representing cool to temperate and temperate to warm climatic conditions. These two data bins were chosen on the basis that 10 °C likely represents a reasonable 'middle ground' ambient temperature for mammals. I acknowledge that this is arbitrary and by using other data bins would result in a different output. PGLS regression was applied to examine potential disparity in the body size scaling of BMR for each ambient temperature bin. To explore whether the two ambient temperature bins exhibited statistically different slopes and elevations (i.e. scaling relationships) an interaction term between ambient temperature bin and body mass was incorporated into the PGLS model, which is the same statistical method applied in Müller *et al*. (2012).

Applying phylogenetically informed statistics help to determine what variation was explained by relatedness. This methodology is becoming increasingly popular in the study of metabolic scaling with evidence of PGLS performing better than OLS (White, Blackburn and Seymour, 2009; Lemaître, Müller and Clauss, 2014). Furthermore, applying OLS techniques across species, including mammals. violates the assumption of independence required for OLS because species are not truly independent but instead share common ancestry. PGLS methods infer phylogenetic signal through parameter λ, which represents the rate of evolution of the residuals of the PGLS model (the tendency of species to resemble each other more than predicted at random from the same tree), with λ usually varying between 0 and 1 (White, Blackburn and Seymour, 2009). When $\lambda = 0$, variation in the data is modelled as a function of independent evolution, and when $\lambda = 1$, covariance is modelled using a model of pure Brownian motion. Thus, models where $\lambda > 0$ indicates that a phylogenetic method of comparison is needed. I applied maximum likelihood (ML) estimation to determine the best fitting value of λ for each PGLS model. To compare the performance of the OLS and PGLS models, I computed Akaike's Information Criterion (AIC) scores. All analyses were carried out in the open source software R (v3.5.3) with use of the following R packages for PGLS analysis: *Phylogenetics*, *ape*, *geiger*, *phytools* and *caper*. PGLS analyses were performed using a currently accepted mammalian phylogeny presented by Smaers *et al.* (2018). I present the results from both OLS and PGLS to allow comparison of methods that assume (OLS) and do not assume (PGLS) complete independence of species, thus shedding light on metabolic scaling studies that do not account for phylogeny. For PGLS models where λ was significantly different to zero. it was deemed that PGLS provided a better stasticial

model because data are not independent (thus violating the assumption of OLS regression).

5.4.4. Path analysis to infer relative weights of the predictors of BMR

Path analysis is a useful tool to quantify the relative effects of multiple predictor variables on an independent variable. Phylogenetic path analysis was performed to better explore the relative weightings of the potential predictors of basal metabolic rate (total maternal production rate, litter size, ambient temperature and adult body mass) and the directional pathways between them (hypothesis 4). The relative effects of variables are described by path coefficients, also known as standardised beta weightings. Generally, predictor variables with beta weightings of < 0.10 are viewed as having a "small" effect, <.30 a "medium effect" and > 0.50 "large" effect. Path analysis was constructed in R using a full model based on biologically plausible relationships (model A) and a set (models B-F) of reduced models deduced by successively dropping variables with "small" beta weightings of ≤ 0.10, starting with the lowest beta weighting. This formed a total of six candidate path models (see Figure 16). Candidate models were ranked using C-statistics Information Criterion with correction ($CICc$) scores, with the best fit model taken as the model with the lowest $CICc$ score. Models with $\Delta CIC \leq 2$ of the best fit model are also strongly statistically supported. Path analysis was performed in R using the package *phylopath* (van der Bijl, 2018). All analyses were performed in R (v3.6.2).

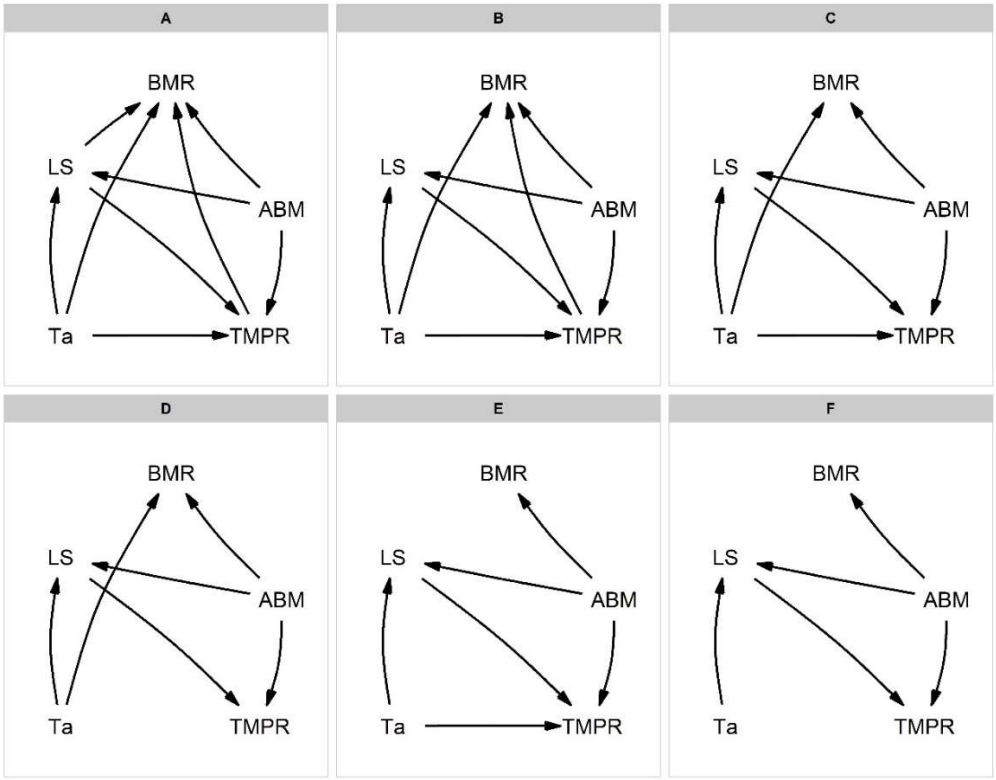

Figure 16. Candidate path models to explore the relative weightings of variables affecting basal metabolic rate (BMR), and the relationships between them. Predictors of BMR include total maternal production rate (TMPR), litter size (LS), ambient temperature (T_a) and adult body mass (ABM). All data are sourced from the PanTHERIA database (Jones *et al.*, 2009) apart from ambient temperature data which was sourced from (Clarke and O'Connor, 2014). A total dataset of 106 eutherian mammal species was obtained for this analysis.

5.5. Results

5.5.1. Do differences in life history explain variation in basal metabolic rate?

Three rates of maternal production: weaning, gestation and total are plotted against adult body mass on log-log scales for uniparous (< 1.5 offspring per litter) and multiparous (≥ 1.5 offspring per litter) eutherian mammal species across in Figure 17. It is apparent that all three measures of maternal production rate increase with adult

body mass, and the allometric scaling exponents (Table 4) exhibited significantly steeper scaling of all three maternal production rates for uniparous species in comparison to multiparous species ($P < 0.01$). These scaling patterns mirror the patterns reported for the mass scaling of basal metabolic rate (BMR) by Müller *et al.* (2012).

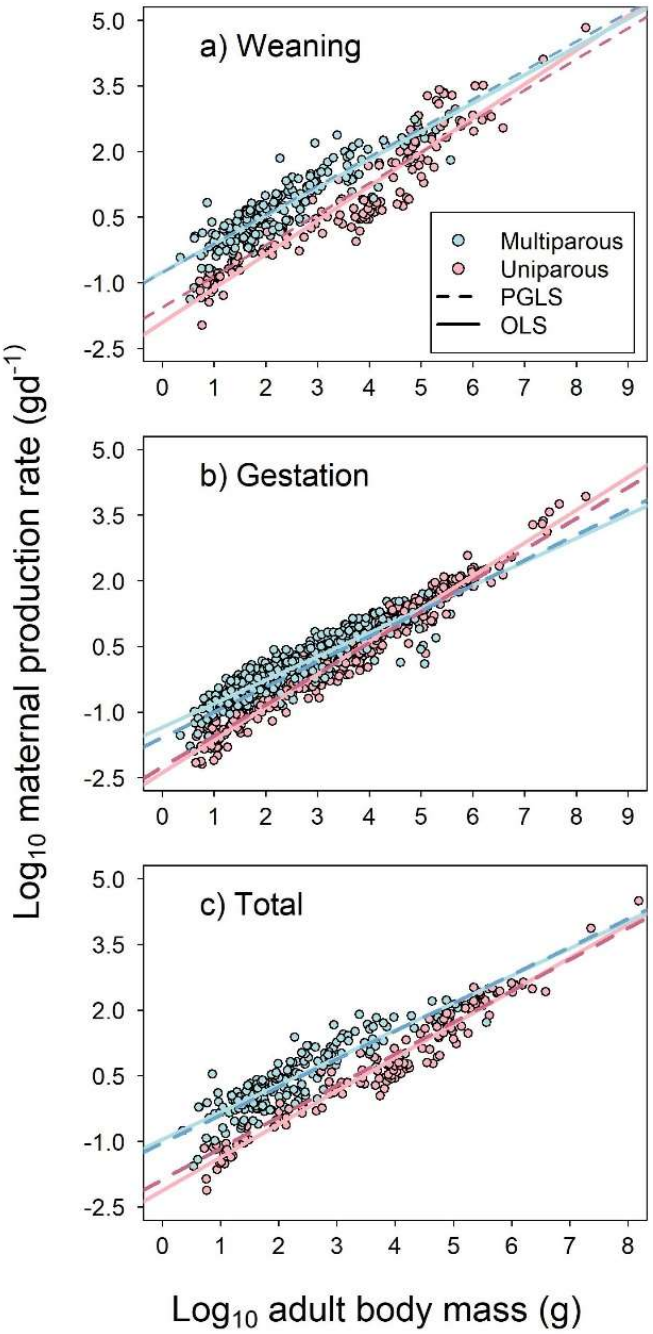

Figure 17. Maternal production rates (grams per day) of eutherian mammal species as a function of adult body mass (grams) on a log-log scale for: a) weaning production

rate, b) gestation production rate and c) total maternal production rate. Blue lines represent OLS regression (solid) and PGLS regression (dashed) for multiparous species. Pink lines represent OLS regression (solid) and PGLS regression (dashed) for uniparous species. Multiparous species are species with ≥ 1.5 offspring per litter) and uniparous species < 1.5 offspring per litter. Data were obtained from the ecological database PanTHERIA (Jones *et al*., 2009).

The apparent dichotomy in the scaling of maternal production rates with body size between uniparous and multiparous species was present for both Ordinary Least Squares (OLS) and Phylogenetic Generalised Least Squares (PGLS) regression methods (Figure 17, Table 5). Lambda statistic confidence intervals and significance testing (Table 5) revealed that all PGLS maternal production models (weaning, gestation and total maternal production rates as a function of adult body mass) had a lambda statistic significantly greater than zero, thus violating the assumption of data independence of OLS regression. Therefore, all PGLS were statistically supported over OLS models for both uniparous and multiparous species. Additionally, the shallower scaling of maternal production rate between uni- and multi- parous species still remains if multiparous species are further divided into smaller litter size bins (see Supplementary Appendix 4 Information S3).

After removing the effect of body size, total maternal production rate accounted for a small amount of variation ($R^2 = 0.08$) in basal metabolic rate (BMR) (Figure 18) for combined data on uni- and multi- parous mammal species.

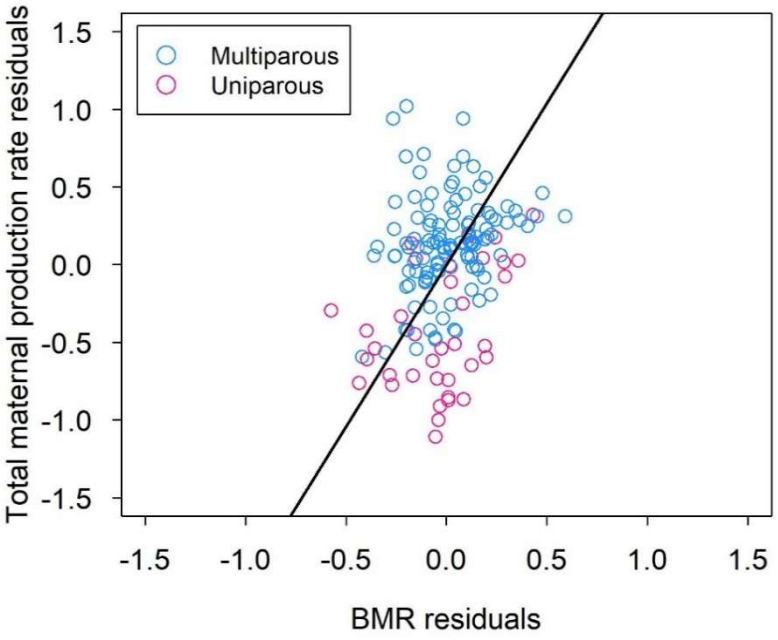

Figure 18. Scatterplot of the residuals from the allometry of total maternal production *versus* the residuals from the allometry of BMR. The solid black line represents Ranged Major Axes (RMA) regression from the *lmodel2()* R package for both uniparous and multiparous species (slope = 2.08, intercept = 0, $R^2 = 0.08$, $p < 0.01$). Note: RMA regression was chosen over OLS regression because error variation is likely to exist for both the y- and x- axis (RMA) rather than only for the y-axis (OLS).

Table 5. Log-log allometric relationships between adult body mass (grams) and life history measures: weaning production rate (g, d^{-1}), gestation production rate (g, d^{-1}) and total maternal production rate (g, d^{-1}) for n uniparous and multiparous eutherian species. The 95% confidence intervals for OLS regression slopes and intercepts are given in brackets. The 95% confidence intervals for the lambda statistic (λ) for PGLS regession are given in brackets. (* p (λ) indicates the p value determining whether the lambda statistic is significantly different from zero (independent evolution) as provided from the PGLS regression output). Relationships were determined through Ordinary Least Squares (OLS) and Phylogenetic Generalised Least Squares Regression (PGLS).

Life history measure ($g\ d^{-1}$)	**OLS regression**					**PGLS regression**						
	n	Slope	Intercept	R^2	p	n	Slope	Intercept	R^2	p	λ	p (λ) *
Uniparous:												
Weaning production rate	138	0.778(±0.048)	-1.91(±0.190)	0.88	<0.001	128	0.708	-1.57	0.73	<0.001	0.90(±0.09)	< 0.001
Gestation production rate	365	0.751(±0.014)	-2.39(±0.060)	0.97	<0.001	337	0.710	-2.26	0.83	<0.001	0.85(±0.08)	< 0.001
Total maternal production rate	138	0.761(±0.003)	-2.12(±0.13)	0.95	<0.001	130	0.716	-1.88	0.87	<0.001	0.89(±0.11)	< 0.001
Multiparous:												
Weaning production rate	210	0.645(±0.046)	-0.761(±0.112)	0.79	<0.001	201	0.660	-0.773	0.61	<0.001	0.85(±0.15)	< 0.001
Gestation production rate	497	0.540(±0.021)	-1.35(±0.06)	0.83	<0.001	457	0.579	-1.59	0.65	<0.001	0.91(±0.05)	< 0.001
Total maternal production rate	206	0.625(±0.043)	-0.960(±0.11)	0.80	<0.001	199	0.641	-1.04	0.63	<0.001	0.88(±0.11)	< 0.001

5.5.2. Does ambient temperature or life history better explain variation in BMR?

BMR is plotted against body mass with two data bins of ambient temperature (bin 1: -11 to 10°C and bin 2: 10.0 to 26.1°C) on a double logarithmic plot in Figure 19. PGLS regression revealed that species in 'bin 1' displayed elevated and shallower body size scaling of BMR in comparison to species in 'bin 2' (bin 1: slope = 0.64±0.04, intercept = 0.76±0.09, $R^2 = 0.8591$, $p < 0.001$; bin 2: slope = 0.72 ±0.02, intercept = 0.45±0.05, $R^2 = 0.89$, $p < 0.001$) (Figure 19). Inclusion of an interaction term between temperature bin and body mass revealed that the slopes and elevations of 'bin 1' and 'bin 2' were significantly different ($p < 0.001$).

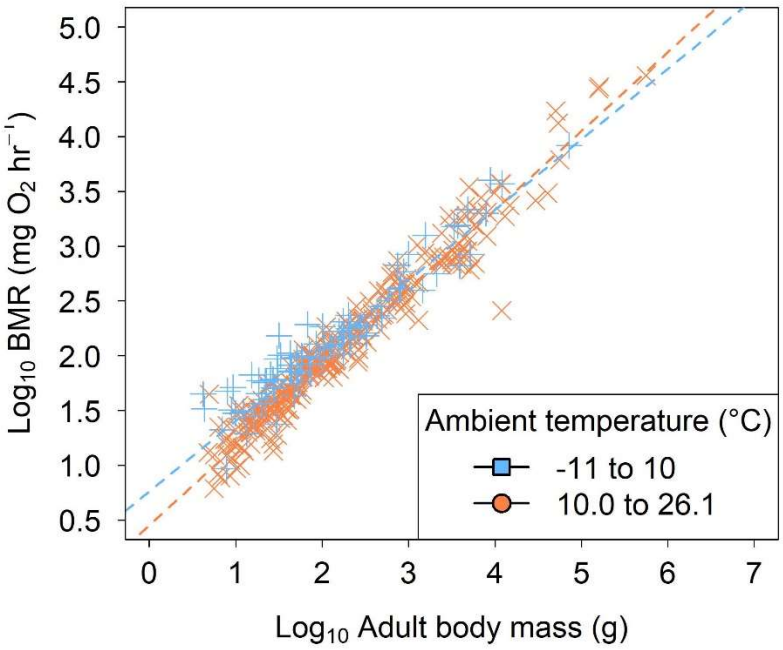

Figure 19. Basal metabolic rate (BMR) of eutherian mammal species as a function of adult body mass (grams) on a log-log scale for two bins of ambient temperature data: -11 to 10°C (blue squares) and 10.0 – 26.1°C (orange circles). Dashed lines represent PGLS regression. Data for BMR and body mass were obtained from the PanTHERIA database and ambient temperature was obtained from (Clarke and O'Connor, 2014).

Table 6 provides a comparison of the performance of the six candidate models (A-F) used in path analysis. Models E and F have significant p values ($p < 0.05$) and thus

are not statistically supported models in path analysis (van der Bijl, 2018) (Table 6). Models A-D are statistically supported with non-significant p values ($p > 0.05$) (Table 6). The lowest $CICc$ scoring model was model C, followed by model B which displayed $\Delta CICc \leq 2$ (Table 6). Hence, there is strong statistical support for both model B and model C.

Models B and C are directly nested, sharing all paths except from one – model B includes the effect of total maternal production rate (TMPR) on BMR (Figure 16). Model B predicts that a very small amount of variation in BMR is explained by TMPR, as described by the small beta weighting of -0.03 (see Figure 20) (where beta weightings of ≤ 0.10 are generally viewed as having a small effect), which overlaps with zero ($\beta = -0.03 \pm 0.05$ S.E.). The addition of an extra path, such as the effect of TMPR on BMR in model B, should lower the $CICc$ by approximately two (van der Bijl, 2018). This does not occur in this case (Table 6), thus the simpler model that has the lowest $CICc$ score, model C, is taken as the best fitting model (Figure 20).

Table 6. Candidate models A-F for path analysis with their respective p-values, C-statistic Information Criterion ($CICc$), the difference in $CICc$ ($\Delta CICc$), relative likelihoods (l) and CICc weights (w). Models are shown in increasing order of $CICc$ scores. Models with statistical support, at significance threshold $\alpha = 0.05$ (where a significant p-value does not provide statistical support for the model in path analysis), are shown in bold.

Model	p	$CICc$	$\Delta CICc$	l	w
C	**0.745**	**30.8**	**0.00**	**1.00**	**0.584**
B	**0.696**	**32.2**	**1.33**	**0.515**	**0.301**
A	**0.402**	**34.4**	**3.59**	**0.166**	**0.0969**
D	**0.114**	**37.7**	**6.89**	**0.0320**	**0.0187**
E	0.00467	46.9	16.10	0.000320	0.000187
F	0.000386	54.4	23.56	0.00000764	0.00000446

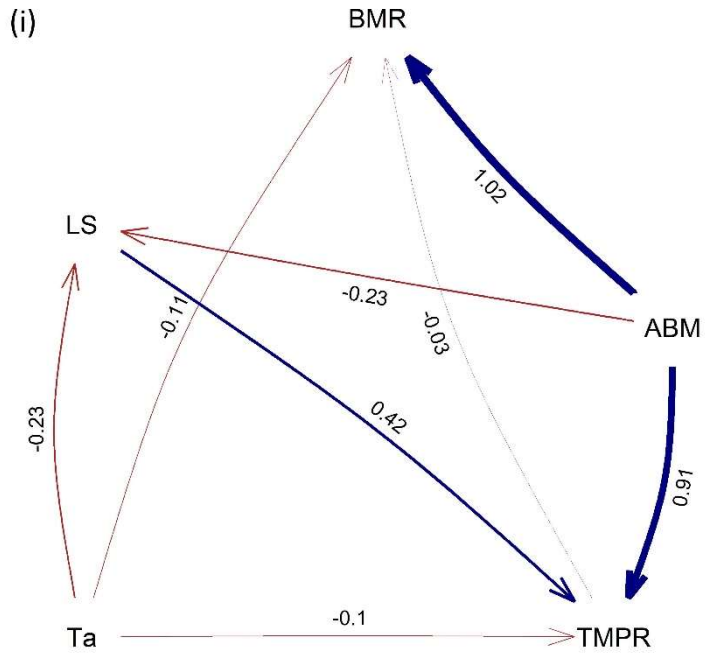

3727

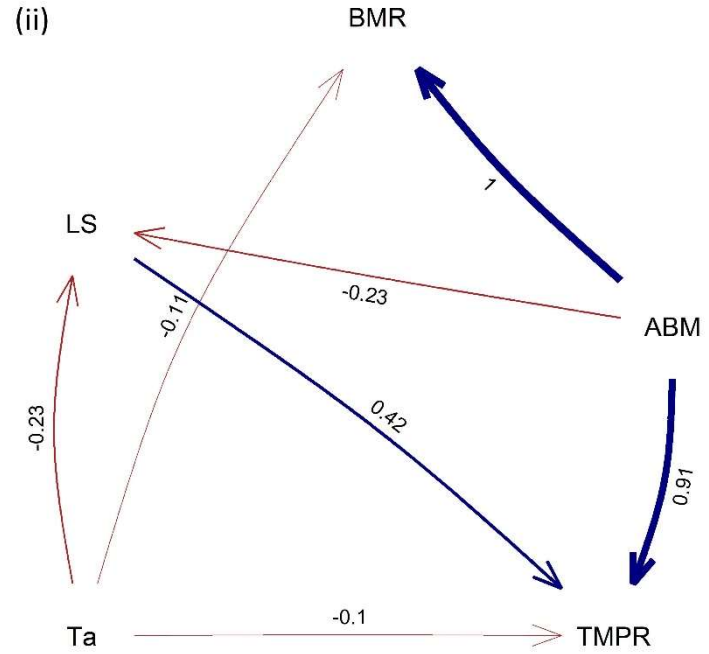

3728

3729 **Figure 20.** The best-supported causal models: model B (i) and model C (ii) C using
3730 path analysis in the R package *phylopath* for the variables: basal metabolic rate
3731 (BMR), total maternal production rate (TMPR), adult body mass (ABM), litter size
3732 (LS) and ambient temperature (Ta). Standardised path coefficients (beta weights) are

shown for each path (arrow). Red and blue arrows represent negative and positive relationships, respectively. Increasing arrow thickness indicates a higher relative standardised beta weighting.

The regression coefficients, or beta weightings, and their standard errors for model C are shown in Figure 21. Adult body mass has a large positive effect on the variation in BMR, with a beta weighting of 0.995, followed by a moderate negative effect of ambient temperature on the variation in BMR (-0.11) (Figure 20). Variation in TMPR is explained by a large positive effect of adult body mass (0.91), followed by a medium positive effect of litter size (0.42) and a moderate negative effect of ambient temperature (-0.10) (Figure 20). Variation in litter size is explained by negative relationships with adult body temperature (-0.23) and ambient temperature (-0.23) (Figure 20).

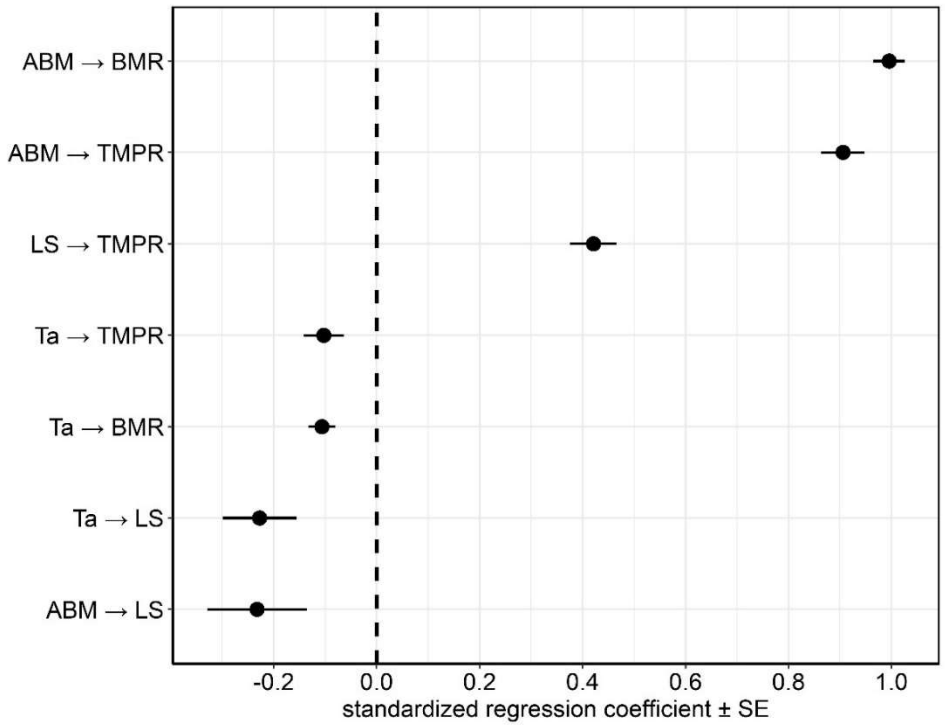

Figure 21. The regression coefficients (beta weights) and standard error (SE) for all paths in the best-fitting pathway model (model C) using the *phylopath* R package.

5.6. Discussion

5.6.1. Does life history influence variation in basal metabolic rate?

Biological processes, such as reproduction, are fuelled by metabolism and thus across species variation in (re)production can be predicted to correlate with variation in metabolic rate. Variation responsible for upward curvature of the body mass-scaling of basal metabolic rate across eutherian mammal species was accounted for by differences in litter size (uniparity and multiparity) by Müller *et al.* (2012). The results reported in this study show that differences in litter size, specifically comparing species with a single offspring per litter (uniparous) and multiple offspring per litter (multiparous), also account for variation in the body size scaling of three measures of maternal production rates: weaning, gestation and a combined measure of weaning and gestation for eutherian mammal species (Figure 17). These scaling patterns mirror the allometric BMR scaling relationships reported by Müller *et al.* (2012) whereby multiparous species exhibited shallower and elevated mass-scaling of BMR compared to uniparous species. This implies that, for eutherian mammals, uniparous species have higher production rates and higher BMR scaling at larger body sizes than multiparous species, and the opposite occurs at smaller body sizes (Figure 17), thus providing a potential mechanism for a link between parity and BMR as reported by Müller *et al.* (2012).

After accounting for the effects of body size, Reduced Major Axis (RMA) regression revealed total maternal production and BMR to be significantly positively correlated (Figure 18), which provides support for the idea of correlative costs of production (pre- and post- natal costs of gestation and lactation) to BMR, which could imply that BMR can be influenced by or constrained by the costs of production. However, it was not possible to control for phylogeny when using RMA methods and so this conclusion warrants caution; phylogenetically controlled methods may provide different results and hence conclusions about the relationship between BMR and total maternal production rate. Furthermore, the amount of variation in total maternal production rate explained by BMR is small (R^2 = 0.08), implying that maternal production rate is a poor predictor of variation in BMR. Thus, the disparity in the scaling of both metabolic rate (Müller *et al.*, 2012) and maternal production rate

between uniparous and multiparous species is unlikely to be directly linked, but perhaps is the result of a shared unknown correlate that directly influences both production and BMR. Litter size exhibits a strong relationship with total maternal production rate, which still remains when multiparity is divided into litter size 'data bins' (Supplementary Appendix 4 Figure S3). However, further examination of the disparity in BMR between uni- and multi-parous species (as reported by Müller *et al.*, 2012) reveals this to be fully dependent on data from intermediate litter sizes – multiparous species with small and large litters do not display significantly different BMR scaling slopes than uniparous species (see Supplementary Appendix 4 Figure S4), which offers another potential explanation for the lack of relationship between total maternal production rate and BMR.

5.6.2. Competing theories: does life history or ambient temperature better predict variation in basal metabolic rate?

In addition to life history factors, such as degree of parity (Müller *et al.*, 2012), ambient temperature has also been shown to predict variation in BMR responsible for curvature (Clarke, Rothery and Isaac, 2010) and can be explained by a thermodynamic framework that describes the dependence of BMR with body mass to emerge as a trade-off between heat dissipation (energy inefficiency) and energy to maintain metabolism (energy efficiency) (Ballesteros *et al.*, 2018). This study revealed significant disparity between two ambient temperature bins (-11 to 10°C and 10.0 to 26.1°C) in the body mass-scaling of BMR (Figure 19) – species in cold to temperate ambient temperatures (-11 to 10°C) exhibited elevated and shallower body mass-scaling of BMR than species in temperature to warm climates (10.0 to 26°C). This agrees with the findings of Clarke, Rothery and Isaac (2010) and Ballesteros *et al.* (2018) that ambient temperature influences variation in BMR responsible for curvature in mammals. Thus, the elevated BMR scaling of small-sized species in cold/temperate climates and the steeper scaling of large sized species in temperate/warm climates agrees with apparent upward curvature of BMR scaling across mammals. This phenomenon is similarly described Ballesteros *et al.* (2018) for a smaller subset of data on desert versus polar mammal species, whereby polar species exhibit elevated and shallower scaling of BMR than desert species of a given size.

Path analysis revealed the relative weightings for predictors of variation in mammalian BMR, including life history variables that represent energetic costs of production (total maternal production rate and litter size), ambient temperature and adult body mass (the major predictor of variation in BMR). Path analysis confirmed adult body mass as the major driver of BMR variation, but also revealed ambient temperature as a small but significant negative predictor of BMR. Therefore, path analysis further supports the theory and findings of Clarke, Rothery and Isaac (2010) and Ballesteros *et al.* (2018) – that low ambient temperature increases BMR especially in smaller species, thereby producing upward allometric curvature across mammals. This study did not find support for either parity (litter size) or maternal production rate significantly predicting variation in BMR, and thus does not support the findings of Müller *et al.* (2012) that disparity in the scaling of uni- and multi- parous species is responsible for BMR variation that causes apparent curvature. Ambient temperature displayed a small but significant negative effect on both BMR ($\beta = -0.11$) and total maternal production rate ($\beta = -0.10$) in this study (Figures 20 and 21). Therefore, incorporation of ambient temperature may explain why uni- and multi- parous species display the same scaling relationships with BMR and maternal production rate, despite maternal production rate and BMR not correlating well themselves (Figure 18).

The significant negative influence of ambient temperature on BMR reported in this study agrees with HDL theory (Speakman and Król, 2010a,b) that an organism's maximal capacity to dissipate heat constrains total energy expenditure. As ambient temperature increases, organisms face an increasing problem of dissipating body heat compared to cooler temperatures where dissipation capacities are higher. A decreased capacity to dissipate body heat in warmer ambient temperatures is observed in terrestrial *versus* aquatic mammal species, whereby aquatic mammals have on average higher BMRs than terrestrial mammals of a similar size owing to the cooler ambient temperature of an aquatic environment that allows a comparatively higher capacity for heat dissipation (Speakman and Król, 2010a). Similarly, under the thermodynamic framework proposed by Ballesteros *et al.* (2018) this will predict the higher BMRs of aquatic mammals to correlate with higher levels of heat dissipation/loss (energy inefficiency) than terrestrial counterparts. Furthermore, a link between limits to heat dissipation and body size is supported by aquatic mammals having, generally, larger body sizes than terrestrial mammals which allow for a smaller

body surface area-to-volume ratio required to overcome the issues faced with large amounts of heat dissipation. Such a phenomenon is also evidenced in desert *versus* polar mammal species as described by Ballesteros *et al.* (2018), whereby polar species exhibit higher BMRs and are more energetically inefficient than desert species of a given size.

5.6.3. Explaining disparity in the mass-scaling of maternal production rate

Multiparous species displayed shallower but elevated scaling of maternal production rates compared to uniparous species (Figure 17), suggesting they are more productive at smaller body sizes than uniparous species, but become comparatively less productive with increasing size than uniparous species. Conversely, uniparous species exhibit steeper scaling of weaning, gestation and total maternal production rates (Figure 17), implying that species investing in a single offspring per litter have higher production rates at a larger body size than multiparous species of the same body size. One possible explanation is that uni- and multi- parity represent different reproductive strategies to overcome differences in heat dissipation limits as predicted by HDL theory (Speakman and Król, 2010a,b). HDL theory states that the low surface area-to-volume ratio of large sized mammal species limits the dissipation of body heat generated by reproductive effort, such as lactation and gestation, which implies that the maximal rate of offspring production and/or weaning is limited by turnover of maternal energy investment. Consequently, it is plausible to view uniparity as a reproductive strategy favoured at large body sizes in response to overcoming imposed limits to heat dissipation. At smaller body sizes, by contrast, the body surface area-to-volume ratio is higher and consequently the limitations on heat dissipation may be small or negligible, and thus maternal energetic investment into gestation and lactation can extend to multiple offspring, making both uniparity and multiparity plausible reproductive strategies at small body size.

This idea is supported by the negative effect of adult body size on litter size and the negative effect of ambient temperature on both litter size and maternal production rate in this study (Figure 20). Hence, because litter size has a positive effect on maternal production rate (Figure 20), ambient temperature influences maternal production rate directly and also indirectly through litter size. Therefore, species

existing in warmer climates are likely to have smaller litter sizes and lower rates of maternal production than species in cooler climates. Agreeing with HDL theory (Speakman and Król, 2010a,b), this implies large species in warm climates will have a bigger problem of dissipating heat generated from reproductive effort due to their larger surface area-to-volume ratios, the added impact of a warm ambient temperature, and, especially for uniparous species, the inability to reduce litter size. Thus, the capacity to dissipate heat may effectively constrain maximal maternal energy expenditure and hence the rate of weaning and gestation production for a given litter size. In addition, although both uniparous and multiparous species exist across the range of body sizes used in this study (Figure 17), larger-bodied species are more likely to be uniparous than multiparous and smaller species are more likely to be multiparous (Figure 22). The tendency toward uniparity at large body size and toward multiparity at small size agrees with predictions made by HDL theory, hence the results reported in this study support the idea that body size-independent differences in production between uni- and multi- parous species may be accounted for by differences in the limits on the dissipation of heat.

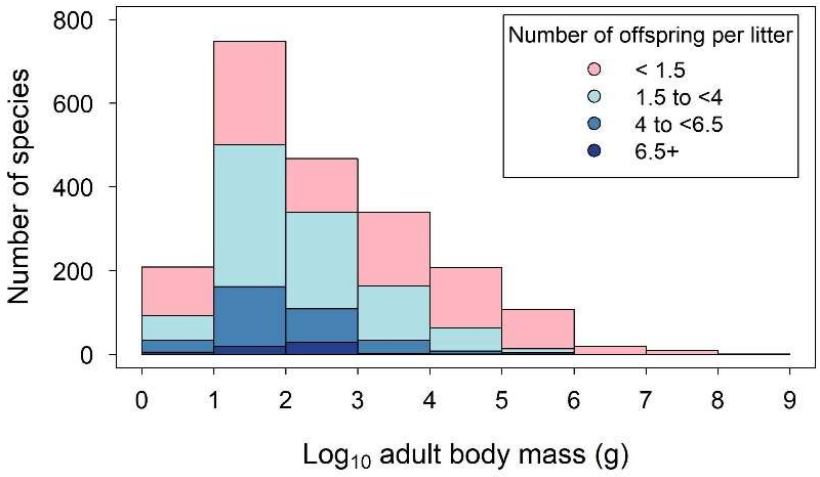

Figure 22. The number of uniparous (< 1.5 offspring per litter) and multiparous (> 1.5 offspring per litter) eutherian mammal species present at different log body mass ranges (grams) within the PanTHERIA database (Jones *et al*., 2009). Note there are no multiparous species present at adult body mass values ≥ 1000kg.

Although there is a bias towards uniparity at large sizes and multiparity at small sizes, both strategies exist across a wide range of body sizes used in this study (Figures 17 and 22), suggesting that differences in the heat dissipation limits cannot be the only explanation for the apparent differences in the scaling of maternal production rates between uni- and multi- parous species. Furthermore, small-sized species are predicted to have little or no limit to heat dissipation (Speakman and Król, 2010a,b), so it is unclear, based on just heat-loss arguments, why some invest in multiparity and some in uniparity when it can be expected that production of multiple offspring will increase production rate and hence fitness. Perhaps the survival benefits of parental care are greater in those small-sized species that invest in producing a single large and/or well-developed offspring (high energetic costs of gestation) and/or have long weaning periods and/or high energetic investment in lactation. By contrast, investment in increased parental care per offspring may yield smaller fitness benefits in other small-sized mammals, which invest in multiple offspring that are smaller or more under-developed (low energetic costs of gestation) and/or require a shorter weaning period and/or with low energetic costs of lactation.

In general, the results reported in this study do not provide support for a link between metabolic rate and production for eutherian mammal species as proposed by Müller *et al.* (2012), suggesting that metabolic rate is not significantly constrained by production costs that relate to lactation and gestation. Differences in the mass-scaling of maternal production rate between uni- and multi- parous species were revealed, with uniparous species exhibiting steeper scaling than multiparous species, which provides support for the Heat Dissipation Limit theory that production is constrained by limits to dissipation of heat generated from reproductive effort (lactation and gestation) (Speakman and Król, 2010a,b). Path analysis revealed ambient temperature to be a small but significant negative predictor of variation in BMR across mammals, in agreement with previous studies (Ballesteros *et al.*, 2018; Clarke, Rothery and Isaac, 2010). The negative influence of ambient temperature on BMR also provides support for HDL theory that an organism's total energy expenditure is limited by its maximal capacity to dissipate heat, which is directly constrained by ambient temperature. Importantly, the results reported in this study help to distinguish between two contrasting theories that aim to account for variation in BMR responsible for apparent curvature across mammal species. By providing a better understanding of the major

predictors of variation in BMR this study provides a step towards a more comprehensive framework for mammalian metabolic scaling. Future studies could benefit from considering differences in energy (in)efficiency when examining the interspecific scaling relationships of metabolic rate and/or maternal production rates. In addition, this study further supports the need to correct for phylogenetic relatedness amongst species when carrying out comparative analyses of life history variables across eutherian mammals.

Chapter 6. General discussion

Growth and metabolism are universal features of life. Understanding variation in the scaling of metabolic rate with body size is of fundamental importance because metabolism rate fuels many biological and physiological activities, such as growth, and correlates with numerous biological traits, such as body size. Furthermore, metabolic rate can represent a holistic measure of 'the pace of life' (Glazier, 2005). Thus, understanding changes in body size over time, growth, is relevant to understanding variation in metabolic rate, which is widely observed at various levels of biological organisation from cells to ecosystems (see Glazier, 2005 for a review). In addition, growth rate correlates with many traits governing fitness, such as mating success and survival (Marshall, Bolton and Keough, 2003; Pardo, Cooper and Dulvy, 2013) and hence explaining variation in the rates of organism growth is key to understanding the ecology and evolution of organisms. Thus, the overall aim of this thesis was to improve current understanding and predictions of growth and metabolism in the animal kingdom, including diverse species of pelagic invertebrates, mammals and two oligochaete species.

6.1. Exploring the relationship between growth and metabolism

Growth is fuelled by the metabolic conversion of resources and energy, and thus it can be predicted that organisms will display a positive relationship between growth and metabolic rate. Within this thesis, I explored the relationship between the ontogenetic scaling of growth, or biosynthesis potential (A), and the mass-scaling of metabolic rate (b_R) across diverse species and wider taxonomic groups of pelagic invertebrates (Chapter 3), and within two oligochaete species (*Tubifex tubifex* and *Eisenia fetida*) (Chapter 4). Both Chapter 3 and 4 found no support for a significant correlation between A and b_R, which implies variation in the scaling of growth efficiency both within and across species and broader taxonomic groups. The relationship between A and b_R provides an indicator for the scaling of growth efficiency because, over ontogeny, it can be predicted that after maintenance costs are met the remaining proportion of available metabolised energy will be optimally allocated amongst growth and other biological processes, such as immune function or locomotion (Figure

23). The proportion of available metabolised energy allocated towards growth, and hence away from other biological processes, may vary over ontogeny, which reflects the scaling of the proportion of available metabolised energy allocated towards growth over ontogeny, or the scaling of growth efficiency.

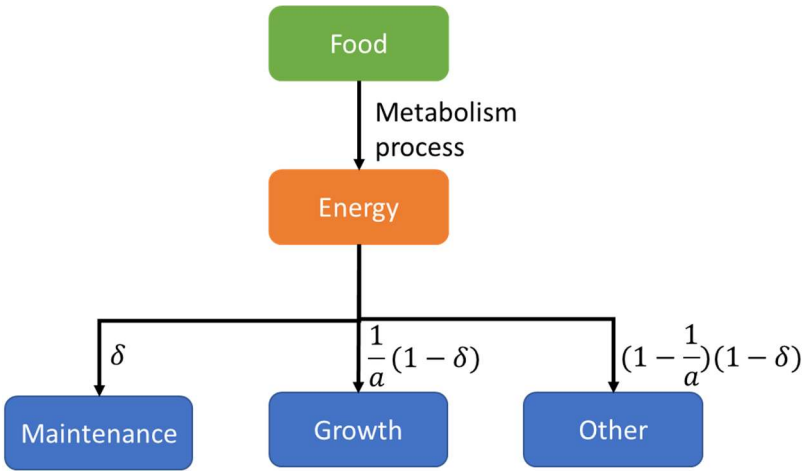

Figure 23. A schematic diagram of the metabolic conversion of food into energy which is allocated to various biological processes. A proportion of energy (δ) is firstly allocated to essential maintenance (e.g. tissue or cell repair) to keep the organism alive. The remaining proportion of metabolised energy is allocated towards somatic growth ($\frac{1}{a}(1-\delta)$) and to other biological processes ($(1-\frac{1}{a})(1-\delta)$), such as reproduction, immune activation or locomotory activity. Over ontogeny, the fraction of available energy allocated to growth ($\frac{1}{a}$) and to other biological processes ($1-\frac{1}{a}$) may change over ontogeny, which may be influenced by various intrinsic and extrinsic factors such as mortality risk (extrinsic) or reproductive state (intrinsic).

Thus, the fraction of available energy allocated to growth ($\frac{1}{a}$ in Figure 23) may increase or decrease over ontogeny in response to various intrinsic or extrinsic factors that may shape the allocation of energy towards growth or other biological processes in order to optimise fitness. For example, over ontogeny the allocation of resources toward growth may be shaped by mortality risks or the energetic demand of biological processes other than somatic growth including locomotion. Sustained mortality risks (e.g. in a high risk open-water environment) over ontogeny may select a constant

proportion of available energy allocated towards growth and hence a sustained relative growth rate (RGR, the rate of body mass increase per unit mass per unit time) to an optimal size, which results in an exponential growth curve, as was observed in the majority of pelagic invertebrate species studied in this thesis. Furthermore, changes in body composition over ontogeny, such as the accumulation on non-metabolising lipid reserves may result in a mismatch between A (which captures growth of metabolising and non-metabolising tissue) and b_R (which captures metabolising tissue only), which may occur in organisms that accumulate and store resources for future reproduction – so-called capital breeders (Stephens *et al.*, 2009). Hence, future work on empirically examining body composition changes in relation the A and b_R for pelagic invertebrate species, which may lie at difference positions along the continuum of energy sources used for reproduction – from capital to income breeding (where reproduction is fuelled by energy gained concurrently) strategies, and oligochaetes *Tubifex tubifex* and *Eisenia fetida* would be beneficial.

The reported relationships between A and b_R for pelagic invertebrate species and broader taxonomic groups (Chapter 3) and two oligochaete species (Chapter 4) were varied and diverse. Some pelagic invertebrate species and wider taxonomic groups (Chapter 3) and oligochaete individuals (Chapter 4) exhibited steeper scaling of growth (A) than metabolic rate (b_R), hence implying an increased proportion of metabolised energy allocated towards growth over ontogeny, or increased growth efficiency over ontogeny. Conversely, some species and wider taxonomic groups of pelagic invertebrates and oligochaete individuals had shallower scaling of A than b_R, implying decreased growth efficiency over ontogeny or a decreased proportion of energy allocated to growth over ontogeny. Allocation of energy to growth is predicted to trade off with the allocation of energy to other biological processes (see Figure 23), thus variation in the scaling of growth efficiency across individuals or species may reflect variation in the proportion of energy allocated to other biological processes, such as locomotion, over ontogeny (Figure 23). For example, locomotory activity may be a requirement for some pelagic invertebrate species to avoid sinking in an open-water environment. Thus, it is possible that the observed variation in the scaling of growth efficiency across pelagic invertebrate species in Chapter 3 relates to variation in energetic demand of locomotion over ontogeny. For example, nektonic squid larvae, *Loligo forbesi*, swim at relatively fast speed (33 to 120 cm min^{-1}) and can enhance

speed (900 to 1500 cm min^{-1}) for short intervals as an escape response to predators, which contrasts the comparatively slower swim speed (23.3 to 30 cm min^{-1}) of decapod *Panulirus japonicus* phyllosoma larvae during upward swimming (Mileikovsky and Shirshov, 1973). Furthermore, for oligochaetes *T.tubifex* and *E.fetida* variation in the scaling of growth efficiency observed across individuals (Chapter 4) may be a result of changes in body composition over ontogeny as suggested by observed variation in the scaling of body diameter relative to length over ontogeny, which may indicate variation in the relative proportion of muscle or non- or low- metabolising tissue (e.g. lipid) over ontogeny.

Thus, both Chapters 3 and 4 further shed light on the relationship between growth and metabolism amongst individuals, species and broader taxonomic groups by suggesting that the scaling of growth and metabolic rate of organisms, and hence the relationships between A and b_R, are diverse and may represent adaptive responses of organisms to numerous factors including intrinsic (e.g. body composition, locomotory activity, reproductive strategy) and extrinsic (e.g. mortality risk) factors. These adaptive responses of growth and metabolism to intrinsic and extrinsic factors may influence key life history traits, for example reproductive strategy (e.g. income or capital breeding) may correlate with fecundity and locomotory activity may correlate with survival (if it enhances change of escape from predators), and hence may shape the life history of an organism.

Therefore, future work on empirically exploring the predictors of variation in the scaling of growth efficiency between individuals, species and broader taxonomic groups would further enhance current understanding of the relationship between growth and metabolism. Specifically, I recommend that future research firstly prioritises exploring and quantifying potential variation in the energetic demand of locomotory activity for pelagic invertebrate species and broader taxonomic groups, which may be a key factor influencing the scaling of growth efficiency for organisms living in an open-water environment. In addition, because individuals within a species are likely to have similar locomotory demand, it is plausible that changes in the relative proportions of metabolising and non-metabolising tissue over ontogeny may be a more important factor influencing the scaling of growth efficiency within a species, such as oligochaetes *T.tubifex* and *E.fetida*. Hence, I advocate future work on anatomically exploring the body composition to quantify the relative proportions of metabolising

and non-metabolising tissues for *T.tubifex* and *E.fetida* in relation to growth and metabolic rate over ontogeny. Ultimately, determining why organisms differ in the scaling of growth efficiency is imperative to understanding how and why resources (energy) are allocated to biological processes (growth and non-growth processes – see Figure 23) over ontogeny. Variation in resource allocation over ontogeny may represent adaptive responses to various intrinsic and extrinsic factors, which could potentially vary amongst different species, taxonomic groups or lifestyles. These adaptive responses are important for understanding how organisms respond to environmental conditions and change, for example, introduction of non-native invasive species may induce an enhanced predation risk for native prey species, which may result in selection for increased relative growth rate (and hence allocation of energy to growth) over ontogeny to prey species to reach maturity rapidly before being consumed by a predator.

6.2. Exploring variation in the scaling of growth

Growth models are often applied to empirical growth data to predict and understand the growth trajectories of organisms. However, current models often fail to account for a substantial amount of variation in growth rates, and hence growth curves, that exist among organisms. This thesis aimed to improve applicability and flexibility of current growth models to empirical growth data for organisms, including marine invertebrates, whose growth curves have been previously poorly fitted by growth models (Hirst and Forster, 2013). By relaxing the common assumption of isomorphic (shape-invariant) scaling of biosynthesis potential in the well-known von Bertalanffy growth function, (VBGF) (Bertalanffy, 1938, 1957), I developed a new growth curve fitting framework capable of capturing diverse types of growth curves, from isomorphic to supra-exponential (Chapter 2). The proposed VBGF-based framework resulted in accurate predictions of growth rates for diverse aquatic invertebrate species, which displayed a range of growth curve types including isomorphic, exponential and supra-exponential (Chapters 2 and 3), and two oligochaete species that displayed near-exponential growth (Chapter 4). Therefore, this work highlights the diversity in growth curves that exists amongst organisms and implies that organisms do not conform to a single universal growth model or law; rather a diverse

range of growth curves are observed. Instead, this thesis supports the notion of a unified framework of multiple models or parameterisations, theories and mechanisms which would be beneficial for exploring the diversity in growth rate that exists amongst animals.

Future work would benefit from testing the performance of the growth curve fitting framework proposed in Chapter 2 against a wider range of empirical growth data from taxonomic groups other than aquatic invertebrates and oligochaetes to determine how widely applicable it is, for example to non-animals such as plants. Furthermore, important next steps would involve empirically testing the assumption made by my growth curve fitting framework that maintenance (or 'catabolism' by Bertalanffy, 1938, 1957) scales to the exponent one ($B = 1$) in order to further evaluate the validity of this framework for diverse taxonomic groups. For example, some holometabolous insect species change body composition over ontogeny by increasing the proportion of non-metabolising tissue (e.g. lipid reserves) to metabolising tissue over ontogeny and hence are likely to deviate from $B = 1$ (Maino *et al.*, 2015b). Specific taxonomic groups that deviate from $B = 1$ would benefit from a modified or extended version of my proposed growth curve fitting framework. Ultimately, gaining an improved growth curve fitting framework, such as the VBGF based framework proposed in this thesis, would benefit those in research and production industries, such as aquaculture, that rely on accurate predictions of growth rates in order to make reliable predictions of yield and hence profit (Ansah and Frimpong, 2015).

Furthermore, because metabolism fuels growth, correlates of metabolic rate may be used to explain observed variation in growth rate. Chapter 4 of this thesis explored two correlates of metabolic scaling slopes: body shape change and ambient temperature, in relation to growth scaling during the ontogenetic development oligochaete species *Tubifex tubifex* and *Eisenia fetida*. In addition, body shape change (but not ambient temperature) was explored in relation to the growth scaling of pelagic invertebrate species in Chapter 3. Surface area theory predicts changes in body shape that result in changes in the mass-scaling of body surface area responsible for resource uptake (e.g. oxygen) will correlate with changes in the capacity for oxygen uptake, hence the mass-scaling of metabolic rate over ontogeny and was supported by previous studies on pelagic invertebrate species (Glazier, Hirst and Atkinson, 2015; Hirst,

Glazier and Atkinson, 2014). In this thesis, it was predicted that body shape changes would also correlate with the scaling of biosynthesis of component materials required for growth (A) across species and wider taxonomic groups of pelagic invertebrates (Chapter 3) and within two oligochaete species *Tubifex tubifex* and *Eisenia fetida* (Chapter 4), but this was not supported in either case. Instead, A did not correlate with changes in surface area-mediated resource (oxygen) uptake. Considering that pelagic invertebrates and oligochaetes mainly exchange oxygen and wastes across the integument and little (or no) food (Graham, 1988), this suggests that other factors such as food nutrition and/or availability (which were constant in these experiments) may be more important for determining the relative rate of biosynthesis (of component materials) over ontogeny.

Therefore, the lack of relationship between A and the mass-scaling of surface area suggests that future studies that aim to understand variation in A (and the relationship between A and b_R) may benefit from examining the effect of varied food nutrition and availability rather than exploring surface-area resource uptake, which mainly involves the uptake of oxygen in pelagic invertebrates (Graham, 1988). Importantly, I do not imply that the rate of oxygen uptake is not important to the process of growth, because the conversion of food into new biomass relies on aerobic metabolism, but rather I argue that the scaling of growth may not correlate with surface area-mediated resource uptake if the minimum oxygen demand for metabolism is met throughout ontogeny, and instead may be more likely to depend on food quantity and quality after oxygen demand is met. However, the effects of additional respiratory structures or surface areas, such as gills or body convolutions, that are not captured by the applied measure of surface area may also account for the lack of relationship between A and the mass-scaling of surface area. Future work on improving methods for quantifying body surface area are required to address this issue, for example, development of digital software for three-dimensional imaging will enable additional surface area to be captured and hence quantified.

Furthermore, the scaling of biosynthesis (A) was explored in relation to ambient temperature, a reported predictor of both metabolic rate (Brown *et al*., 2004; Gillooly *et al*., 2001) and b_R (Glazier, 2020; Killen *et al*., 2010), for oligochaete species *T.tubifex* and *E.fetida* in Chapter 4. Chapter 4 revealed no significant effect of ambient temperature on A for either *T.tubifex* or *E.fetida*, suggesting that the scaling of growth

(biosynthesis) has low thermal sensitivity and instead may be shaped by food nutrition and/or quantity (as discussed above). The shape of von Bertalanffy growth curves can vary in relation to ambient temperature, for example, increasing temperature can increase the value of parameter K (commonly referred to as the growth coefficient) which consequently causes the growth curve to rise rapidly and sharply reaches final size, i.e. there is a strong plateau (Atkinson and Sibly, 1997). However, in Chapter 4, the scaling of biosynthesis (A) was near-exponential ($A \sim 1$, where RGR is near-constant over ontogeny) and hence did not plateau in either *T.tubifex* and *E.fetida* in both temperature treatments. It is possible that temperature influenced specific growth rate (SGR, proportional mass increase per unit time) over ontogeny in *T.tubifex* and *E.fetida*, which is supported by the difference in size at maturity between the two temperature treatments for *T.tubifex* and *E.fetida*. Assuming the same time to maturity across temperature treatments, the larger size at maturity in the cooler temperature treatment reported in Chapter 4 suggests that SGR may increase with temperature for both *T.tubifex* and *E.fetida*. Conversely, if time to maturity is temperature dependent then SGR could increase or decrease with temperature, depending on the exact differences in final size between temperature treatments. Further investigation into the relationship between ambient temperature, SGRs and age at maturity for *T.tubifex* and *E.fetida* would be required to confirm this.

Thus, it is apparent for pelagic invertebrate species, *T.tubifex* and *E.fetida* that the scaling of biosynthesis does not necessarily exhibit the same responses, or correlations, as metabolic scaling to intrinsic or extrinsic factors including changes in body shape over ontogeny and ambient temperature, respectively. Therefore, instead of being directly correlated or influenced by predictors of metabolic rate, growth rates (and hence their scaling) are likely to be the product of adaptive responses to food availability and/or nutrition. Future work on examining the effect of variation in food nutrition and availability on the scaling of biosynthesis would be required to test this idea.

6.3. Exploring variation in the mass-scaling of metabolic rate

Potential for the mass-scaling of metabolic rate, b_R to correlate with changes in body shape over ontogeny has previously been reported for pelagic invertebrate species

using metabolic and body shape data collected from literature searching (Glazier, Hirst and Atkinson, 2015; Hirst, Glazier and Atkinson, 2014). Within this thesis, I empirically examined the relationship between the mass-scaling of surface area, b_A (as determined from empirical data on body shape) and b_R for the ontogenetic development of oligochaete species *T.tubifex* and *E.fetida* in Chapter 4. Agreeing with surface area theory that surface area-mediated changes in resource uptake can correlate with metabolic scaling, Chapter 4 reported a significant positive relationship between b_A and b_R for freshwater *T.tubifex* but no such relationship was found for terrestrial *E.fetida*. Testing the possibility that aquatic and terrestrial systems may differ generally in the relative importance or influence of surface area-related effects on metabolic scaling will require investigation of more aquatic *versus* terrestrial systems.

Ambient temperature can directly influence the rates of biochemical reactions and processes within an organism, and has been shown to correlate with body size (Atkinson, 1994; Atkinson & Sibly, 1997), metabolic rate (Brown *et al.*, 2004; Gillooly *et al.*, 2001; Glazier, 2005), including metabolic level (the elevation of a metabolic scaling relationship), and the mass-scaling of metabolic rate (b_R) in varied ways for diverse animal and plant species (Glazier, 2020; Killen *et al*., 2010). Chapter 4 also revealed a negative effect of ambient temperature on b_R for *T.tubifex* but not for *E.fetida*. If larger bodies require adjustment of oxygen consumption later in ontogeny (to ensure that consumption matches their capacity for surface area-related oxygen uptake), it is possible that metabolic scaling relationships of aquatic organisms may have higher thermal sensitivities than terrestrial organisms because temperature is known to inversely correlate with oxygen availability in water, but not in air (Hoefnagel and Verberk, 2015). However, these conclusions are based on a comparison of only two species, which differ in many factors including body size, locomotory mode, physiology (e.g. *T.tubifex* individuals have many body surface furrows and convolutions on the posterior region that aid oxygen uptake; *E.fetida* does not), and thus the conclusions drawn from Chapter 4 are speculative; drawing any adaptive conclusions would require further investigation of metabolic rate, metabolic scaling and temperature over more aquatic and terrestrial invertebrate species.

Furthermore, temperature may have inversely correlated with b_R in *T.tubifex* by decreasing locomotory activity (and hence energetic demand) over ontogeny, as predicted by the Metabolic Level Boundaries Hypothesis, suggesting that activity and

temperature may shape metabolic scaling relationships (Glazier, 2005, 2010, 2020). However, locomotory activity was not explored for either T.tubifex or E.fetida in Chapter 4, and thus future work is required to explore this idea. For example, future experiments on exploring metabolic rate, metabolic scaling relationships and quantifying the rate and frequency of posterior ventilatory movement in *T.tubifex* under different ambient temperatures would aid interpretations of the results reported in Chapter 4. Warming not only reduced b_R for *T.tubifex*, but also reduced the mass-scaling of surface area (b_A) (Chapter 4). Because b_R and b_A exhibited a positive correlation for *T.tubifex*, the negative effect of temperature on b_R and b_A suggests that metabolic scaling may be influenced by temperature indirectly through its effect on the degree of body shape change in an aquatic organism. For example, *T.tubifex* individuals were generally more squat in form in the higher temperature treatment, which may result in longer pathways for diffusion of oxygen across the integument and hence shallower scaling of metabolic rate. However, body shape changes do not necessarily mean that integument thickness changes; instead the 'squat' body shape displayed by *T.tubifex* in the higher temperature treatment may be due to an increase in musculature or water or lipid content over ontogeny. Future work on determining the causal relationships between ambient temperature, b_R and b_A, particularly in aquatic organisms, may improve current understanding of variation in metabolic scaling relationships. For example, this can be achieved by exploring pelagic invertebrates species which comprise strong shape shifters, such as salps, and relatively isomorphic organisms, such as euphausiids (Chapter 3), have been shown to display diversity in metabolic scaling slopes (Glazier, Hirst and Atkinson, 2015; Hirst, Glazier and Atkinson, 2014), and exist in a wide range of climatic conditions from cold to tropical. Importantly, determining variation in the metabolic responses to thermal conditions is crucial for understanding how organisms will adapt to environmental change, such as global warming. For example, long-term experiments that increase ambient temperature could be conducted to examine the effects of warming on b_R and b_A, and their implications to growth rate, reproductive output and stability of populations of pelagic invertebrate species.

The relationship between ambient temperature and the mass-scaling of body surface area is also important for understanding variation in inter-specific metabolic scaling relationships for endothermic animals including mammals. Variation in the

trade-off between surface area-related constraints of heat loss and the energy efficiency of maintaining metabolism (to stay alive) is predicted to account for variation in the inter-specific mass-scaling of mammalian basal metabolic rate (BMR) that is responsible for reported upward curvature (Ballesteros *et al.*, 2018). At different ambient temperatures, variation in energy efficiency (the balance between heat loss constraints and essential maintenance processes) is predicted to exist as an adaptation to different climatic conditions (Ballesteros *et al.*, 2018). For example, polar mammal species have higher metabolic rates (on average) than dessert mammals due to an increased demand for heat production, i.e. they show decreased energy efficiency (Ballesteros *et al*., 2018). Thus, Chapter 5 investigates the relative importance of ambient temperature in explaining variation in mammalian BMR scaling responsible for upward curvature. However, an important focus of this thesis was to consider multiple hypotheses; hence multiple known correlates, mechanisms or models of metabolic rate that could explain variation in intra- or inter-specific metabolic scaling relationships. Therefore, Chapter 5 also investigated the relative importance of another proposed model of mammalian metabolic scaling that has been shown to account for curvature, which is based on reproductive parity, defined as the number of offspring per litter.

Chapter 5 revealed that ambient temperature, but not reproductive parity, to be a negative predictor of the variation in mammalian BMR, thus agreeing with the framework proposed by Ballesteros *et al*. (2018) that metabolic scaling relationships can vary as a result of differences in the relationship between heat dissipation capacity and energy efficiency which is observed under different climatic conditions. Chapter 5 also reported a negative correlation between ambient temperature and reproductive parity, which suggests that there is a decreased capacity for increasing litter size with temperature for mammals. Increasing litter size is likely to result in increased heat production as a resulting product from increased metabolic demand. Therefore, a reduced capacity for increasing litter size at warmer temperatures may occur as a result of decreased capacity to dissipate heat in a warmer environment, and hence supports theories and models of metabolic scaling that predict metabolic rate to be constrained by an organisms capacity to dissipate heat, such as the Heat Dissipation Limit theory (Speakman and Król, 2010a,b).

Therefore, by exploring multiple correlates of interspecific mammalian BMR scaling, and the relationships between them, Chapter 5 helps to distinguish between two competing theories that purport to explain curvature of BMR scaling. Specifically, it explains why reproductive parity correlated with BMR scaling in mammals but not with BMR itself – because both reproductive parity and BMR are negatively correlated with ambient temperature. Importantly, this emphasises the importance of a multi-mechanistic approach and highlights caution for future research reporting new correlates of metabolic scaling relationships because they may not necessarily directly predict, or be predicted by metabolic rate but instead may share a mutual correlate with metabolic rate.

6.4. Conclusion

The research conducted within this thesis reinforces growing evidence against simplistic single-cause metabolic scaling relationships (e.g. Banavar *et al*., 2010; Brown *et al*., 2004; Gillooly et al., 2001; West *et al*., 1997). Instead, it supports other research, frameworks and views that emphasise the influence of both intrinsic and extrinsic factors on metabolic scaling relationships and that the relative influences of these different factors are likely to differ for different levels of biological organisation. For example, within and across species and across broader taxonomic groups, hence resulting in a plethora of metabolic scaling relationships which are observed across organisms. Furthermore, this thesis helps to improve current predictions of growth rates for taxonomic groups that have previously poorly fitted growth models, including marine invertebrates. Importantly, this thesis revealed deviations in the scaling of growth (biosynthesis) from commonly assumed isomorphic growth, thus highlighting the potential range of growth rate types that are likely to present across organisms and hence opening new areas of research.

Ultimately, this research supports other views that future work within the field of metabolic scaling should not focus on searching for a universal scaling law or one-cause mechanistic explanation that applies to the mass-scaling of metabolic rate or growth rate (Glazier, 2014a,b, 2018; Kozlowski, Konarzewski and Czarnoleski, 2020). Instead, both growth and metabolic rates are likely to be malleable. Species and

broader taxonomic groups are likely to vary in their responses to an array of intrinsic and extrinsic factors in order to maximise fitness; metabolic rates and growth rates are not the mere result of universal physical constraints. Therefore, this thesis provides support for adopting a multi-mechanistic approach to the field of metabolic scaling – exploring multiple hypotheses, correlates, predictors, mechanisms or models of growth and metabolism is crucial for a more complete understanding of the variation in the rates of growth and metabolism within and across organisms, and hence their scaling. Specific models or frameworks may be applicable to a limited subset of taxa, but when possible, I recommend that combining multiple theories or models will likely result in a more truly comprehensive framework of metabolic scaling.

Supplementary Appendix 1. Supporting data for Chapter 2. A new framework for growth curve fitting based on the von Bertalanffy growth function.

Supplementary Information S1. Data format requirements and R user guide for the growth curve fitting framework in Chapter 2.

Data formatting

For these models, growth data must be in terms of body mass and time. Datasets must numerically (from 1) distinguish between individuals of a species and between species. This must be labelled for each data entry point. Where cohort growth data for a species is being used then this should be labelled as a single individual. Therefore, datasets must have columns: mass, time, individual, species. For excel datasets, a single sheet must be used and saved as a Comma Delimited file (.csv).

Running growth model R code

The R code for the growth curve fitting framework is available at www.github.com/lauraleemoore/Growth-curve-fitting. In R, the script "VBGFmodels_functions.R" must be completely run first to create all the five VBGF parameterisations and appropriate functions for model fitting in R. Next, the file "VBGFmodels.R" can be used to perform growth analysis on given growth data. For datasets with a single species use only the "unif.growth.mod" function. For datasets with multiple species run the "unif.growth.mod" function first and then the "unif.growth.mod.spec" function. After the function(s) have run, the growth analysis is carried out by simply inputting your data into the function(s):

yourgrowthresults < - unif.growth.mod(yourdata)

To save the model outputs use the save function in R:

save(yourgrowthresults, file="growthmodellingresults.Rdata")

This stored R file can then be reloaded into R using the load() function:

load("yourgrowthresults.Rdata")

Calculating profile likelihood confidence intervals in R

To compute the profile likelihood 95% confidence intervals for parameter A, the two files are used: "Profile_likelihood_confidence_intervals_Alt1model.R" (which explores parameter $A < 1$) and "Profile_likelihood_confidence_intervals_Agt1model.R" (which explores parameter $A > 1$).

The 95% confidence interval for A is defined as the range of values for which the profile log likelihood (i.e. maximised over all parameters except A) is within a particular threshold of the maximum log likelihood over all values of A. The threshold value is calculated as

0.5*qchisq(0.95, 1)=1.9207…

in the R profile likelihood scripts. The range of A-values that need to be explored is determined by which out of the best fitting Generalised VBGF ($A < 1$), Gompertz ($A = 1$), and supra-exponential ($A > 1$) models are within this threshold value of the best fitting model overall. When the best fitting model is Gompertz or Exponential the confidence interval contains the value A=1, and when Pure Isomorphy has highest (most negative) negative log likelihood (NLL) the confidence interval contains $\frac{2}{3}$. Here are some illustrative examples:

For *Euphasia pacifica*, from Table S1 the best fitting Gompertz ($NLL = -9.57$) and supra-exponential ($NLL = 4.84$) models are all more than 1.9207 away from the best fitting model overall ($A < 1, NLL = -13.32$). The entire confidence interval therefore lies in the range $A < 1$, and both confidence limits can be found using the code in the script "Profile_likelihood_confidence_intervals_Alt1model.R"

For *Daphnia magna,* the negative log likelihood of the best-fitting $A < 1$ model ($NLL = -10.934$) is within 1.9207 of the best fitting model overall (Gompertz, $NLL = -10.934$) so the lower confidence interval is found using the R script "Profile_likelihood_confidence_intervals_Alt1model.R". However, the best fitting $A > 1$ model has a NLL value (-8.093) that is more than 1.9207 above the best fitting model, so the upper confidence limit is A=1.

To run the profile likelihood code, the parameter estimates for the given model obtained from step **(ii)** must be loaded. The rest of the code can then run to obtain upper and lower confidence intervals.

Supplementary Table S1. The negative log likelihood values for the five von Bertalanffy growth function parameterisations: Exponential, Gompertz, Generalised-VBGF, Pure Isomorphy and Supra-exponential for twelve pelagic and benthic invertebrate species. The 'most negative' negative log likelihood values are shown in red for each species and were chosen as the best fitting model.

Species	Negative log likelihood				
	Exponential	**Gompertz**	**Generalised VBGF**	**Pure Isomorphy**	**Supra-exponential**
Daphnia magna	-8.0929	-10.934	-10.934	-9.996	-8.0929
Euphausia pacifica	4.84441	-9.5694	-13.332	-11.294	4.84441
Pelagia noctiluca	40.3285	6.45159	-1.3867	12.2505	40.3285
Oikopleura dioica	-3.2448	-3.5712	-3.2936	4.48466	-8.0544
Crassostrea gigas	-5.580309	-10.2303	-10.18726	-3.749798	-5.580358
Echinogammarus marinus	22.79021	2.503368	1.056863	1.112388	22.79021
Cherax quadricarinatus	-10.39	-12.284	-12.412	-7.0357	-10.39
Petrarctus demani	2.65892	-8.0612	-10.279	-1.9552	2.16543
Aurelia aurita	-18.807	-18.807	-18.808	-12.789	-27.88
Cyanea capillata	-7.6203	-11.253	-11.303	2.77648	-7.6968
Mytilus edulis	-0.7003123	-3.01859	-3.326951	1.972576	-0.700297

Sepia officinalis	12.4599	2.66006	2.66006	13.0807	12.4599

4404

4405

Supplementary Table S2. The best fitting model and its fitted value for parameter *A* as determined by the likelihood ratio test for the five parameterisations of the VBGF: Exponential, Gompertz, Generalised-VBGF, Pure Isomorphy and Supra-exponential for empirical mass versus time data for twelve pelagic and benthic invertebrate species. The zone (pelagic or benthic) represents the zone inhabited during the development phase in which growth data was obtained for. The number of datapoints is represented by N. The 95% confidence intervals for parameter *A* were calculated using profile likelihood.

Habitat	Zone	Phylum	Class	Species	N	LLRT preferred model	*d.f.*	***A*** estimate	95% confidence intervals
Freshwater	Pelagic	Arthropoda	Branchiopoda	*Daphnia magna*	11	VBGF-Gompertz	7	1	0.58 – 1
Marine	Pelagic	Arthropoda	Malacostraca	*Euphausia pacifica*	7	Generalised-VBGF	2	0.79	0.68 – 0.91
Marine	Pelagic	Cnidaria	Scyphozoa	*Pelagia noctiluca*	39	Generalised-VBGF	34	0.76	0.73 – 0.78
Marine	Pelagic	Chordata	Appendicularia	*Oikopleura dioica*	7	VBGF-Exponential	3	1	1.0 – 1
Marine	Pelagic	Cnidaria	Scyphozoa	*Aurelia aurita*	10	VBGF-Exponential	6	1	0.93 – 1.32
Marine	Pelagic	Cnidaria	Scyphozoa	*Cyanea capillata*	14	VBGF-Gompertz	10	1	0.88 – 1
Marine	Pelagic	Mollusca	Bivalvia	*Crassostrea gigas*	7	VBGF-Gompertz	3	1	0.80 – 1
Marine	Benthic	Arthropoda	Malacostraca	*Echinogammarus marinus*	11	VBGF-Gompertz	7	1	0.64 – 1
Freshwater	Benthic	Arthropoda	Malacostraca	*Cherax quadricarinatus*	9	VBGF-Gompertz	5	1	0.81 – 1
Marine	Benthic	Arthropoda	Malacostraca	*Petrarctus demani*	8	VBGF-Gompertz	4	1	0.76 – 1
Marine	Benthic	Mollusca	Bivalvia	*Mytilus edulis*	8	Generalised-VBGF	3	0.87	0.79 – 0.95
Marine	Benthic	Mollusca	Cephalopoda	*Sepia officinalis*	23	VBGF-Gompertz	19	1	0.80 - 1

Supplementary Appendix 2. Data tables to support the results presented in Chapter 3. Growth and size-dependence of metabolic rates and body shape in pelagic invertebrates.

Supplementary Table S3. Data for the best fitting biosynthesis scaling exponent A value (as determined by the most negative log likelihood), body mass – body length exponent b_L, and metabolic scaling exponent b_R for pelagic invertebrate species in Chapter 3. Values for b_L and b_R were obtained from Hirst *et al*. (2014) and values for A were obtained from empirical growth data collected from a literature search (see 'Growth data source' for references). T represents culture temperature from which growth data was obtained. Specific growth rate (SGR) data is temperature corrected to 15°C. SGR SE represents the standard error of the SGR estimate. Complete development (CD) refers to species growth data having complete (yes) or incomplete juvenile development (no).

Taxa	Binomial	A	b_L	b_R	T (°C)	SGR (t^{-1})	SGR SE	CD	Growth data source
Amphipoda	*Cycopharis challengeri*	1	2.13	0.84	5	0.0312	0.0013	yes	Yamade & Ikeda (2000)
Amphipoda	*Primno abyssalis*	1	2.61	0.94	2	0.334	0.000643	yes	Ikeda (1995)
Anostroca	*Artemia francisca*	1			25			yes	Olsen *et a*l. (2000)
Anostroca	*Artemia salina*	1			21			yes	Dagg & Littlepage (1972)
Appendicularia	*Oikopleura dioica*	1.08	2.44	0.80	13			yes	Paffenhöfer (1976)
Bivalvia	*Crassostrea gigas*	1	2.12	0.96	24	0.128	0.0134	no	Kheder et al. (2010)
Bivalvia	*Mytilus edulis*	0.87	3.49	0.89	12			no	Sprung (1984)
Calanoida	*Acartia Clausi*	1	2.94		10	0.394	0.00689	yes	Leandro et al. (2006)
Calanoida	*Acartia grani*	1	3.09		20	0.320	0.0426	yes	Saiz & Alcaraz (1991)
Calanoida	*Acartia hudsonica*	0.74	3.09		13.5			yes	Colin & Dam (2005)
Calanoida	*Acartia steuri*	1	1.45		19.1	0.116	0.00365	yes	Kang & Kang (1998)
Calanoida	*Acartia tonsa*	0.81	3.12		17			yes	Franco et al. (2017)
Calanoida	*Calanus chilensis*	1	2.71		15	0.102	0.0122	no	Escribano, Rodriguez & Irribarren (1998)

Calanoida	*Calanus euxinus*	1	2.71		18	0.151	0.0118	no	Svetlichny et al. (2010)
Calanoida	*Calanus finmarchicus*	1.0	3.43		12	0.327	0.0170	yes	Campbell et al. (2001)
Calanoida	*Calanus glacialis*	1	3.41		0	0.213	0.00222	no	Jung-Madsen & Nielsen (2015)
Calanoida	*Calanus helgolandicus*	1.0	2.71		15	0.315	0.0136	no	Rey et al. (2001)
Calanoida	*Calanus marshallae*	1	2.49		10	0.160	0.00886	yes	Peterson (1986)
Calanoida	*Calanus pacificus*	0.54	2.71	0.82	15			yes	Vidal (1980)
Calanoida	*Calanus sinicus*	1.0	2.61		20.2	0.295	0.0269	yes	Uye (1988)
Calanoida	*Centropages abdomilis*	1	3		7	0.0852	0.0105	yes	Slater & Hopcroft (2005)
Calanoida	*Centropages hamatus*	1.07	2.34		17			yes	Fryd, Haslund & Wohlgemuth (1991)
Calanoida	*Centropages typicus*	1	3.21	0.92	15	0.144	0.00832	yes	Fryd, Haslund & Wohlgemuth (1991)
Calanoida	*Notodiaptomus incompsitus*	1			20	0.0620	0.00716	no	Ortis, Muxagata & Bersano (2017)
Calanoida	*Paracalnus sp.*	1.0	2.23		15			yes	Uye (1991)
Calanoida	*Pseudocalanus elongatus*	1	2.50		12.5	0.106	0.0207	no	Paffenhöfer & Harris (1976)
Calanoida	*Pseudocalanus newmani*	1	2.30		10	0.173	0.00257	yes	Lee et al. (2003)
Calanoida	*Pseudodiaptomus dubia*	0.71			25			yes	Li et al. (2009)
Calanoida	*Pseudodiaptomus marinus*	1	2.59		20	0.0670	0.00382	yes	Uye, Iwai & Kasahara (1983)
Calanoida	*Rhincalanus nasutus*	1			15	0.267	0.0150	yes	Mullin & Brooks (1970)
Calanoida	*Sinocalanus tenellus*	1	2.52		20.3	0.121	0.0246	yes	Kimoto, Uye & Onbé (1986)
Calanoida	*Temora longicornis*	1	2.62		15	0.0718	0.00320	no	Bjærke, Andersen, & Titelman (2014)
Cephalopoda	*Amphioctopus aegina*	1.17			30			yes	Promboon, Nabhitabhata &

									Duengdee (2011)
Chaetognatha	*Sagitta hispida*	1	2.79		23	0.121	0.0182	yes	Reeve & Walter (1972)
Cladocera	*Bosmina longirostris*	1	4.85		20	0.103	0.00886	yes	Koivisto & Ketola (1995)
Cladocera	*Daphnia magna*	1	3.01	0.92	20	0.201	0.0581	yes	Baillieul, Smolders & Blust (2005)
Cladocera	*Daphnia pulex*	1	2.66	1.09	20	0.190	0.0621	yes	Koivisto & Ketola (1995)
Cladocera	*Leptodora kindtii*	1	2.67		17.5	0.123	0.0105	yes	Vijverberg & Koelewijn (2004)
Cladocera	*Simocephalus serrulatus*	1			15	0.135	0.00777	yes	Lemke & Benke (2003)
Ctenophora	*Beroa ovata*	1	2.69	1.04	20.5	0.156	0.0191	no	Annisky et al. (2007)
Ctenophora	*Bolinopsis infundibulum*	1	2.10	0.50	15	0.168	0.00770	no	Greve (1970)
Ctenophora	*Mnemiopsis leidyi*	1	1.98	1.02	21	0.323	0.0170	no	Baker & Reeve (1974)
Ctenophora	*Pleurobrachia bachei*	0.85	2.7	0.71	15			yes	Greve (1970)
Ctenophora	*Pleurobrachia pileus*	0.91	2.52	0.78	15			yes	Greve (1970)
Cyclopoida	*Oithona similis*	1	1.45		15	0.219	0.0128	yes	Sabatini & Kiørboe (1994)
Decapoda	*Armases miersii*	1			24	0.0540	0.0128	no	Annisky et al. (2407)
Decapoda	*Carcinus maenas*	1			12	0.131	0.00381	no	Dawirs (1985)
Decapoda	*Eusergestes similis*	0.78			14			no	Omori (1979)
Decapoda	*Geograpsus lividus*	1			24	0.0446	0.00462	no	Annisky et al. (2407)
Decapoda	*Hyas araneus*	0.83			12			yes	Schiffer et al. (2013)
Decapoda	*Hyas coarctatus*	1			12	0.0146	0.00513	no	Annisky et al. (1207)
Decapoda	*Menippe merceria*	0.87			27			no	Krimsky & Epifanio (2010)
Decapoda	*Mithrax spinosissimus*	1			26	0.00840	0.00113	yes	Tunberg & Creswell (1991)
Decapoda	*Pachygrapsus transversus*	1			25	0.0108	0.00148	no	Flores et al. (1998)
Decapoda	*Pandalus borealis*	1.0			4.2			no	Rasmussen & Tande (1995)

Decapoda	*Pandalus montagui*	1			18	0.0743	0.00418	yes	Anger & Schultze (1997)
Decapoda	*Panopeus margentus*	1			20	0.0793	0.0146	no	Rodríguez & Spivak (2001)
Decapoda	*Paralithodes camtschaticus*	1			7.5	0.0592	0.00434	no	Epelbaum & Kovatcheva (2005)
Decapoda	*Rhithropanopeus harrisii*	1			25	0.110	0.0123	no	Levin & sulkin (1979)
Decapoda	*Sagmariasus verreauxi*	0.76	2.14	1	22			no	Jenson et al. (2013)
Euphausiacea	*Euphausia pacifica*	0.79	3.17	0.89	12			yes	Ross (1982)
Euphausiacea	*Euphausia superba*	1.001	3.16	0.81	1.5			no	Marschall & Hirche (1984)
Euphausiacea	*Nyctiphanes australis*	0.63	3.04	0.71	16			yes	Haywood & Burns (2003)
Euphausiacea	*Nyctiphanes capensis*	1			12	0.0981	0.00632	no	Pillar (1985)
Euphausiacea	*Nyctiphanes simplex*	1	2.86		0.5	0.228	0.00280	no	Bertha (1992)
Hydrozoa	*Sarsia tubulosa*	1	3.1	0.91	12	0.0339	0.00460	yes	Daan (1986)
Mysida	*Metamysidopsis elongata*	1			17.5	0.202	0.0141	yes	Clutter & Theilacker (1971)
Polychaeta	*Alitta succinea*	1			22	0.0935	0.0233	no	Hansen (1999)
Polychaeta	*Arctonoe pulchra*	1			10	0.251	0.00637	no	Pernet (2000)
Polychaeta	*Polydora spp.*	1			22	0.171	0.0412	no	Hansen (1999)
Polychaeta	*Spio/Microspio spp.*	1			22	0.157	0.0434	no	Hansen (1999)
Scyphozoa	*Aurelia aurita*	1.11	2.66	1.03	18			no	Båmstedt, Lane & Martinussen (1999)
Scyphozoa	*Cotylorhiza tuberculata*	1	3.1		20	0.0381	0.00294	no	Astorga, Ruiz & Prieto (2012)
Scyphozoa	*Cyanea capillata*	1	2.7	1.01	15	0.112	0.00282	no	Båmstedt, Ishiib & Martlnussen (1997)
Scyphozoa	*Pelagia noctiluca*	0.76	3.55	0.95	18			yes	Lilley et al. (2014)
Thaliacea	*Dolioletta gegenbauri*	1.01	2.32	1.001	20			yes	Deibel (1982)

4426

Supplementary Table S4. The best fitting model and exponent *A* value as determined by the most negative log likelihood (LL) and through likelihood ratio testing (LRT) for pelagic invertebrate species in Chapter 3. The 95% confidence intervals are provided for each estimate of exponent *A*, and were determined using profile likelihood.

Taxa	Binomial	LL best fit model	*A*	95% CIs	LRT best fit model	LRT *A*	95% CIs
Amphipoda	*Cycopharis challengeri*	Gompertz	1	0.99 – 1	Gompertz	1	0.99 – 1
Amphipoda	*Primno abyssalis*	Gompertz	1	0.61 – 1.12	Exponential	1	0.61 – 1.12
Anostroca	*Artemia francisca*	Gompertz	1	0.93 – 1.16	Gompertz	1	0.93 – 1.16
Anostroca	*Artemia salina*	Supra-exponential	1.0	1 – 1.24	Exponential	1	0.99 – 1.24
Appendicularia	*Oikopleura dioica*	Supra-exponential	1.08	1 – 1.15	Exponential	1	1 – 1.15
Bivalvia	*Crassostrea gigas*	Gompertz	1	0.80 – 1	Gompertz	1	0.80 – 1
Bivalvia	*Mytilus edulis*	Generalised-VBGF	0.87	0.79 – 0.95	Gompertz	1	0.79 – 1
Calanoida	*Acartia Clausi*	Gompertz	1	0.84 – 1	Gompertz	1	0.84 – 1
Calanoida	*Acartia grani*	Exponential	1	0.93 – 1	Exponential	1	0.93 – 1
Calanoida	*Acartia hudsonica*	Generalised-VBGF	0.74	0.62 – 1	Gompertz	1	0.62 – 1
Calanoida	*Acartia steuri*	Gompertz	1	0.85 – 1	Gompertz	1	0.85 – 1
Calanoida	*Acartia tonsa*	Generalised-VBGF	0.81	0.74 – 1	Gompertz	1	0.74 – 1
Calanoida	*Calanus chilensis*	Generalised-VBGF	1	0.86 – 1	Exponential	1	0.86 – 1
Calanoida	*Calanus euxinus*	Gompertz	1	1 – 1.09	Gompertz	1	1 – 1.09
Calanoida	*Calanus finmarchicus*	Supra-exponential	1.0	1 – 1.29	Exponential	1	1 – 1.29
Calanoida	*Calanus glacialis*	Gompertz	1	0.94 – 1.10	Exponential	1	0.94 – 1.10
Calanoida	*Calanus helgolandicus*	Supra-exponential	1.0	1 – 1.43	Exponential	1	1 – 1.43
Calanoida	*Calanus marshallae*	Gompertz	1	0.82 – 1.05	Exponential	1	0.82 – 1.05
Calanoida	*Calanus pacificus*	Gompertz	1	0.64 – 1	Gompertz	1	0.64 – 1
Calanoida	*Calanus sinicus*	Supra-exponential	1.0	1 – 1.31	Exponential	1	1 – 1.31
Calanoida	*Centropages abdomilis*	Gompertz	1	0.51 – 1	Gompertz	1	0.51 – 1
Calanoida	*Centropages hamatus*	Supra-exponential	1.07	1 – 1.14	Exponential	1	1 – 1.14

Calanoida	*Centropages typicus*	Gompertz	1	1 – 1.15	Exponential	1	1 – 1.15
Calanoida	*Notodiaptomus incompsitus*	Gompertz	1	0.77 – 1.08	Exponential	1	0.77 – 1.08
Calanoida	*Paracalnus sp.*	Supra-exponential	1.0	1 – 1.10	Exponential	1	1 – 1.10
Calanoida	*Pseudocalanus elongatus*	Gompertz	1	0.82 – 1	Gompertz	1	0.82 – 1
Calanoida	*Pseudocalanus newmani*	Gompertz	1	0.91 – 1.05	Exponential	1	0.91 – 1.05
Calanoida	*Pseudodiaptomus dubia*	Generalised-VBGF	0.71	0.58 – 1	Pure Isomorphy	0.67	0.58 – 1
Calanoida	*Pseudodiaptomus marinus*	Gompertz	1	1 – 1.23	Exponential	1	1 – 1.23
Calanoida	*Rhincalanus nasutus*	Gompertz	1	1.0 – 1	Gompertz	1	1.0 – 1
Calanoida	*Sinocalanus tenellus*	Gompertz	1	0.99 – 1	Gompertz	1	0.99 – 1
Calanoida	*Temora longicornis*	Gompertz	1	0.93 – 1	Gompertz	1	0.93 – 1
Cephalopoda	*Amphioctopus aegina*	Supra-exponential	1.17	1.14 – 1.20	Exponential	1	1 – 1.20
Chaetognatha	*Sagitta hispida*	Gompertz	1	0.80 – 1	Gompertz	1	0.80 – 1
Cladocera	*Bosmina longirostris*	Gompertz	1	0.72 – 1	Gompertz	1	0.72 – 1
Cladocera	*Daphnia magna*	Gompertz	1	0.58 – 1	Gompertz	1	0.58 – 1
Cladocera	*Daphnia pulex*	Gompertz	1	0.56 – 1	Gompertz	1	0.56 – 1
Cladocera	*Leptodora kindtii*	Gompertz	1	0.79 – 1	Gompertz	1	0.79 – 1
Cladocera	*Simocephalus serrulatus*	Gompertz	1	0.54 – 1	Gompertz	1	0.54 – 1
Ctenophora	*Beroa ovata*	Gompertz	1	0.72 – 1	Gompertz	1	0.72 – 1
Ctenophora	*Bolinopsis infundibulum*	Gompertz	1	0.97 – 1	Gompertz	1	0.97 – 1
Ctenophora	*Mnemiopsis leidyi*	Gompertz	1	0.76 – 1	Gompertz	1	0.76 – 1
Ctenophora	*Pleurobrachia bachei*	Generalised-VBGF	0.85	0.85 – 1	Gompertz	1	0.85 – 1
Ctenophora	*Pleurobrachia pileus*	Generalised-VBGF	0.91	0.89 – 1	Gompertz	1	0.89 – 1
Cyclopoida	*Oithona similis*	Exponential	1	0.63 – 1	Exponential	1	0.63 – 1
Decapoda	*Armases miersii*	Gompertz	1	0.85 – 1.22	Gompertz	1	0.85 – 1.22
Decapoda	*Carcinus maenas*	Gompertz	1	0.99 – 1	Gompertz	1	0.99 – 1
Decapoda	*Eusergestes similis*	Generalised-VBGF	0.78	0.58 – 1	Generalised-VBGF	0.78	0.58 – 1

Decapoda	*Geograpsus lividus*	Gompertz	1	1.0 – 1.11	Exponential	1	1.0 – 1.11
Decapoda	*Hyas araneus*	Generalised-VBGF	0.83	0.66 – 1	Gompertz	1	0.66 – 1
Decapoda	*Hyas coarctatus*	Gompertz	1	0.67 – 1	Gompertz	1	0.67 – 1
Decapoda	*Menippe merceria*	Generalised-VBGF	0.87	0.73 – 1	Gompertz	1	0.73 – 1
Decapoda	*Mithrax spinosissimus*	Gompertz	1	1.0 – 1	Gompertz	1	1.0 – 1
Decapoda	*Pachygrapsus transversus*	Gompertz	1	1.0 – 1.22	Exponential	1	1.0 – 1.22
Decapoda	*Pandalus borealis*	Supra-exponential	1.0	1 – 1.18	Exponential	1	1.0 – 1
Decapoda	*Pandalus montagui*	Gompertz	1	0.73 – 1	Gompertz	1	0.73 – 1
Decapoda	*Panopeus margentus*	Gompertz	1	0.77 – 1	Gompertz	1	0.77 – 1
Decapoda	*Paralithodes camtschaticus*	Gompertz	1	0.79 – 1	Gompertz	1	0.79 – 1
Decapoda	*Rhithropanopeus harrisii*	Generalised-VBGF	1	1.0 – 1	Exponential	1	1 – 1.22
Decapoda	*Sagmariasus verreauxi*	Generalised-VBGF	0.76	0.56 – 1	Exponential	1	1 – 1.12
Euphausiacea	*Euphausia pacifica*	Generalised-VBGF	0.79	0.68 – 0.91	Generalised-VBGF	0.79	0.68 – 0.91
Euphausiacea	*Euphausia superba*	Supra-exponential	1.001	0.83 – 1.20	Exponential	1	0.83 – 1.20
Euphausiacea	*Nyctiphanes australis*	Generalised-VBGF	0.63	0. 51 – 0.92	Pure Isomorphy	0.67	0.51 – 0.92
Euphausiacea	*Nyctiphanes capensis*	Gompertz	1	1.0 – 1	Gompertz	1	1.0 – 1
Euphausiacea	*Nyctiphanes simplex*	Gompertz	1	0.75 – 1	Exponential	1	1 – 1.05
Hydrozoa	*Sarsia tubulosa*	Gompertz	1	0.95 – 1	Gompertz	1	0.95 – 1
Mysida	*Metamysidopsis elongata*	Gompertz	1	0.69 – 1.13	Gompertz	1	0.69 – 1.13
Polychaeta	*Alitta succinea*	Gompertz	1	0.74 – 1.17	Exponential	1	0.74 – 1.17
Polychaeta	*Arctonoe pulchra*	Gompertz	1	1.0 – 1.09	Exponential	1	1.0 – 1.09
Polychaeta	*Polydora spp.*	Exponential	1	0.83 – 1.15	Exponential	1	0.83 – 1.15
Polychaeta	*Spio/Microspio spp.*	Generalised-VBGF	1	0.63 – 1	Gompertz	1	0.63 – 1
Scyphozoa	*Aurelia aurita*	Supra-exponential	1.11	1 – 1.32	Exponential	1	0.93 – 1.32
Scyphozoa	*Cotylorhiza tuberculata*	Gompertz	1	0.57 – 1	Gompertz	1	0.57 – 1
Scyphozoa	*Cyanea capillata*	Generalised-VBGF	1	0.88 – 1	Gompertz	1	0.88 – 1
Scyphozoa	*Pelagia noctiluca*	Generalised-VBGF	0.76	0.73 – 0.78	Generalised-VBGF	0.76	0.73 – 0.78

	Thaliacea	*Dolioletta gegenbauri*	Supra-exponential	1.01	1 – 1.07	Exponential	1	0.71 – 1

4432

Supplementary Figure S1. The frequency distribution of specific growth rates (SGR) for 13 wider taxonomic groups of pelagic invertebrate species studied in Chapter 3.

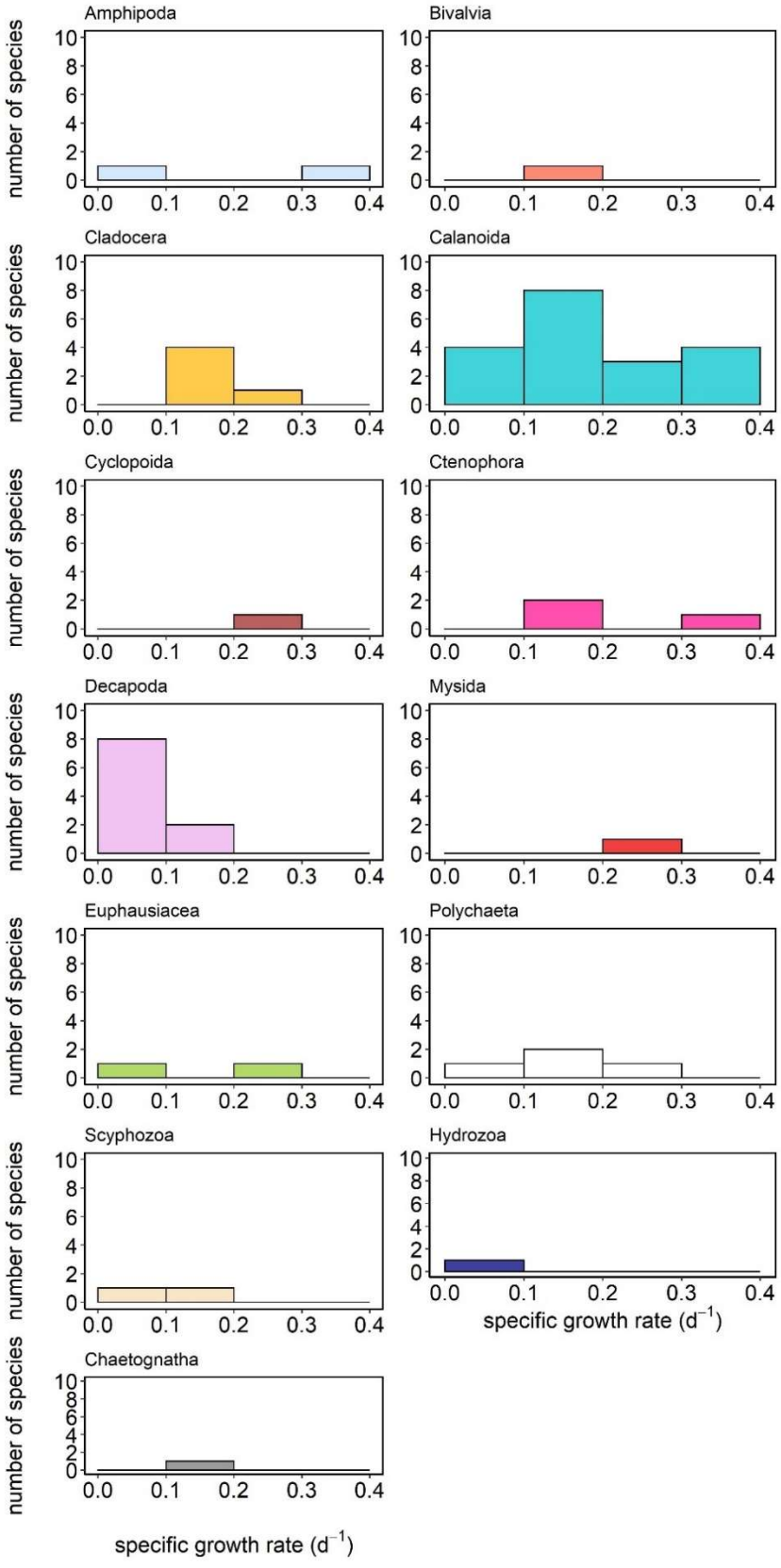

Supplementary Appendix 3. Data tables to support the results presented in Chapter 4. Comparison of growth, metabolism and body shape in a terrestrial and aquatic oligochaete system.

Supplementary Table 5. Data for the for the body mass-scaling exponent of: biosynthesis (A), metabolic rate (b_R), surface area (b_A), growth efficiency ($\frac{A}{b_R}$), and body diameter-body length exponent (b_{DL}) for *Tubifex tubifex* individuals for two different temperature treatments: 18°C (A) and 26°C (B). Note that for *T.tubifex* body thickness (b_{DL}) averages represent data from the posterior region where the majority of respiratory exchange is likely to occur (Kaster and Wolff, 1982).

Individual	Treatment	A	b_R	b_R R^2	b_{DL}	b_{DL} R^2	b_A	$\frac{A}{b_R}$
1	A	1			0.40	0.96	0.78	
2	A	1	0.59	0.90	0.38	0.95	0.78	1.71
3	A	1.00	0.44	0.95	0.50	0.95	0.75	2.29
4	A	1	0.79	0.96	0.34	0.95	0.80	1.26
5	A	1	0.74	1.00	0.44	0.92	0.77	1.35
6	A	1	0.70	0.95	0.35	0.95	0.80	1.42
7	A	1	0.96	0.95	0.41	0.91	0.77	1.04
8	A	1	0.91	0.95	0.37	0.96	0.79	1.10
9	A	0.68	0.80	0.99	0.30	0.99	0.81	0.85
10	A	0.67	0.56	0.98	0.39	0.97	0.78	1.20
11	A	1.00	0.85	0.97	0.34	0.85	0.80	1.18
12	A	1	1.07	0.97	0.22	0.96	0.85	0.93
13	A	1.00	0.99	0.98	0.17	0.88	0.87	1.01
14	A	1	0.94	0.94	0.29	0.81	0.82	1.07
15	A	1	0.66	0.99	0.25	0.97	0.83	1.51
16	A	1			0.24	0.94	0.84	
17	A	0.75	0.69	0.98	0.27	0.99	0.82	1.09
18	A	1	0.70	0.85	0.18	0.89	0.87	1.43
19	A	0.71	1.08	1.00	0.30	0.82	0.81	0.65
20	A	1	1.06	0.94	0.23	0.95	0.84	0.94
21	A	1	1.03	0.99	0.16	0.98	0.88	0.97
22	A	1	0.94	0.93	0.26	0.86	0.83	1.07
23	A	1	0.64	1.00	0.21	0.97	0.85	1.57
24	A	0.74	1.09	0.86	0.16	0.88	0.88	0.68
25	A	1	1.06	1.00	0.26	0.84	0.83	0.94
26	A	1	0.83	0.88	0.20	0.96	0.86	1.21
27	A	0.98	0.92	0.99	0.24	0.99	0.84	1.06
28	A	1	0.75	0.95	0.27	0.93	0.82	1.34
29	A	1	0.77	1.00	0.17	0.98	0.87	1.31
30	A	0.78	0.80	0.97	0.17	0.87	0.87	0.97
31	A	1	0.75	0.99	0.14	0.84	0.89	1.33

32	A	1	0.77	0.97	0.21	0.99	0.85	1.31
33	A	0.97	0.75	0.86	0.18	0.85	0.87	1.29
34	A	1	0.95	0.97	0.21	0.82	0.85	1.05
35	A	1			0.40	0.91	0.78	
36	A	0.53			0.33	0.94	0.80	
37	A	1.00			0.27	0.83	0.83	
38	A	1			0.33	0.95	0.80	
39	A	1			0.46	0.88	0.76	
40	A	1			0.28	0.96	0.82	
41	A	1			0.28	0.83	0.82	
42	A	1			0.35	0.97	0.79	
43	A	0.85			0.41	0.95	0.77	
44	A	1			0.26	0.84	0.83	
45	A	1			0.29	0.94	0.81	
46	A	1			0.39	0.92	0.78	
47	A	1			0.40	0.92	0.78	
48	A	1			0.41	0.94	0.77	
49	A	1			0.38	0.89	0.79	
50	A	1			0.29	0.88	0.82	
51	A	1			0.38	0.97	0.78	
52	A	1			0.37	0.85	0.79	
53	A	0.76	0.68	1.00	0.45	1.00	0.76	1.12
54	A	1	1.14	0.88	0.21	0.93	0.85	0.88
55	A	1	0.62	0.89	0.30	0.95	0.81	1.62
56	A	0.68	1.11	0.83	0.26	0.96	0.83	0.62
57	A	1	0.47	0.92	0.27	0.95	0.82	2.12
58	A	1	0.76	1.00	0.31	0.80	0.81	1.31
59	A	0.77	0.73	0.96	0.33	1.00	0.80	1.06
60	A	0.84	0.97	0.94	0.36	0.98	0.79	0.87
61	A	1.01	0.88	1.00	0.29	0.88	0.82	1.15
62	A	1	0.78	0.87	0.28	0.96	0.82	1.28
63	A	0.82	0.72	0.98	0.42	0.91	0.77	1.14
64	A	1	0.92	0.97	0.25	0.92	0.84	1.09
1	B	1	0.80	0.97	0.17	0.86	0.87	1.24
2	B	1	0.84	0.98	0.47	0.93	0.76	1.19
3	B	0.96	0.52	0.90	0.47	0.82	0.76	1.83
4	B	1	0.79	0.82	0.61	0.96	0.73	1.27
5	B	1	0.79	0.93	0.24	0.91	0.84	1.26
6	B	0.82	0.79	0.94	0.34	0.99	0.80	1.04
7	B	1	1.16	0.90	0.16	0.84	0.88	0.86
8	B	1	0.96	0.94	0.32	0.98	0.80	1.04
9	B	1	0.32	0.99	0.70	0.87	0.71	3.14
10	B	1.00	0.67	0.95	0.20	0.97	0.86	1.50
11	B	1	0.74	0.97	0.50	0.92	0.75	1.35
12	B	1	0.80	1.00	0.46	0.82	0.76	1.24
13	B	1	0.65	0.94	0.37	0.87	0.79	1.54
14	B	1	0.66	0.96	0.22	0.68	0.85	1.51
15	B	1	0.39	1.00	0.69	0.83	0.71	2.56
16	B	0.95	0.48	0.95	0.25	0.87	0.83	1.96

17	B	0.85	0.61	0.98	0.29	0.85	0.82	1.38
18	B	1	0.56	0.99	0.59	1.00	0.73	1.79
19	B	1	0.45	0.99	0.26	0.80	0.83	2.21
20	B	1	0.66	0.93	0.46	0.94	0.76	1.51
21	B	1	0.35	1.00	0.59	0.88	0.73	2.83
22	B	1	0.62	0.96	0.64	0.96	0.72	1.61
23	B	1	0.57	0.99	0.78	0.94	0.69	1.74
24	B	0.67	0.42	1.00	0.54	0.98	0.74	1.61
25	B	1	0.44	0.83	0.78	0.88	0.69	2.28
26	B	0.89	0.80	0.97	0.44	0.84	0.77	1.11
27	B	0.91	0.45	0.90	0.86	0.82	0.68	2.01
28	B	0.67	0.76	0.91	0.64	0.90	0.72	0.87
29	B	1.2	0.88	0.87	0.42	0.94	0.77	1.37
30	B	0.67	0.78	1.00	0.67	0.98	0.71	0.86
31	B	0.81	0.59	1.00	0.42	1.00	0.77	1.37
32	B	1	0.56	0.99	0.21	0.91	0.85	1.80
33	B	0.96	0.90	1.00	0.50	0.99	0.75	1.07
34	B	1.06	0.65	0.95	0.39	0.97	0.78	1.64
35	B	1	1.14	0.88	0.15	0.98	0.88	0.88
36	B	1.01	0.62	0.89	0.53	1.00	0.74	1.63
37	B	0.67	1.11	0.83	0.55	1.00	0.74	0.60
38	B	1	0.47	0.92	0.23	0.97	0.84	2.12
39	B	0.9	0.76	1.00	0.45	1.00	0.76	1.18
40	B	1	0.73	0.96	0.37	0.84	0.79	1.37
41	B	1.16	0.97	0.94	0.59	0.96	0.73	1.20
42	B	1	0.88	1.00	0.29	0.83	0.82	1.14
43	B	0.98	0.78	0.87	0.44	1.00	0.77	1.25
44	B	1	0.72	0.98	0.49	0.96	0.75	1.39
45	B	1	0.92	0.97	0.47	0.90	0.76	1.09
46	B	1.00			0.63	0.87	0.72	
47	B	1			0.51	0.86	0.75	
48	B	0.92			0.44	0.93	0.77	
49	B	1			0.59	0.99	0.73	
50	B	0.67			0.44	0.82	0.77	
51	B	0.87			0.56	0.99	0.74	
52	B	1			0.24	0.90	0.84	
53	B	1			0.52	0.99	0.75	
54	B	1			0.50	0.94	0.75	
55	B	1			0.42	0.98	0.77	
56	B	1			0.43	0.98	0.77	
57	B	0.76			0.54	0.98	0.74	
58	B	0.92			0.42	0.99	0.77	
59	B	1			0.46	0.95	0.76	
60	B	1			0.31	0.92	0.81	
61	B	1			0.51	0.99	0.75	
62	B	1			0.44	0.98	0.77	
63	B	1			0.69	0.99	0.71	
64	B	1			0.33	0.89	0.80	
65	B	1			0.38	1.00	0.78	

66	B	1	0.64	1.00	0.72	
67	B	1	0.48	0.98	0.75	
68	B	1	0.54	0.94	0.74	
69	B	1	0.32	0.94	0.80	
70	B	1	0.35	0.98	0.80	
71	B	1.00	0.47	0.96	0.76	
72	B	0.89	0.52	0.92	0.74	
73	B	1	0.47	0.88	0.76	
74	B	1	0.45	0.96	0.76	
75	B	1	0.48	0.99	0.76	
76	B	1	0.46	0.96	0.76	
77	B	0.71	0.41	0.88	0.78	
78	B	1	0.32	0.98	0.81	

Supplementary Table 6. Data for the for the body mass-scaling exponent of: biosynthesis (A), metabolic rate (b_R), surface area (b_A), growth efficiency ($\frac{A}{b_R}$), body diameter-body length exponent (b_{DL}) and body mass-body length exponent (b_L) for *Eisenia fetida* individuals for two different temperature treatments: 18°C (A) and 26°C (B).

Individual	Treatment	A	b_L	$b_L\ R^2$	b_R	$b_R\ R^2$	b_{DL}	$b_{DL}R^2$	b_A	$\frac{A}{b_R}$
1	A	1	2.79	0.97	1.82	0.91	0.51	0.82	0.75	0.55
2	A	1.01	3.05	0.98	1.21	0.96	0.92	0.81	0.68	0.84
3	A	0.91	2.52	0.98			0.52	0.98	0.75	
4	A	1.00	2.02	0.94	1.24	0.86	0.45	0.98	0.76	0.81
5	A	1.00	3.08	0.95	0.67	0.96	0.45	0.82	0.76	1.49
6	A	1								
7	A	0.67	2.49	0.90			0.70	0.91	0.71	
8	A	0.70	2.53	0.98	0.92	0.92	0.79	0.91	0.69	0.76
9	A	1	2.31	0.99			0.45	0.84	0.76	
10	A	1	2.47	0.98	0.29	0.95	0.83		0.69	3.45
11	A	1	2.29	0.99	1.03	0.98	0.69		0.71	0.97
12	A	1	2.63	0.81	1.18	0.84	1.10		0.66	0.85
13	A	1	2.70	0.95	0.98	0.86	0.73	0.90	0.70	1.02
14	A	0.67	2.21	0.94			0.47	0.86	0.76	
15	A	1	2.20	0.90			0.72	0.91	0.71	
16	A	1	2.81	0.84			0.69	0.84	0.71	
17	A	1	2.51	0.89	1.64	0.90	0.89	0.99	0.68	0.61
18	A	1	2.93	0.87	0.82	0.96	0.61	0.81	0.73	1.22
1	B	1	1.85	0.98			0.37	0.94	0.79	
2	B	0.74	3.25	0.99	1.03	0.96	0.62	0.81	0.72	0.72
3	B	1	2.50	0.96	0.23		0.42	0.92	0.77	4.35
4	B	0.67					0.60	0.84	0.73	

5	B	0.67	2.60	0.87	1.84	0.96	0.35	0.93	0.79	0.36
6	B	1.00	2.72	0.88						
7	B	0.89	3.43	0.99			0.84	1.00	0.69	
8	B	1	3.13	0.98			0.63	0.81	0.72	
9	B	1.00					1.13	0.95	0.65	
10	B	1	2.86	0.99	1.01	0.88	0.68	0.96	0.71	0.99
11	B	1	2.44	0.88			0.89	0.88	0.68	
12	B	1	3.12	0.96	0.66	0.85	0.78	0.95	0.70	1.52
13	B	1	2.40	0.96	1.62	0.99	0.53	0.84	0.74	0.62
14	B	1	2.21	0.85	1.29	0.98	0.70	0.94	0.71	0.78
15	B	0.94	2.36	1.00	0.86	0.98	0.87		0.68	1.09
16	B	0.67	3.37	1.00	0.91	0.94	0.87		0.68	0.73
17	B	0.88	2.33	0.89	1.03	0.94	0.77		0.70	0.85
18	B	0.88	2.89	0.97	1.11	0.80	0.73		0.70	0.79
19	B	0.67	2.55	0.97	1.34	0.97	1.04		0.66	0.50
20	B	0.89	3.76	1.00	0.88	0.94	1.27		0.64	1.01
21	B	1	2.57	0.98	0.90	0.86	0.69	0.90	0.71	1.11
22	B	1.00	2.89	0.97			0.69	0.83	0.71	
23	B	1	2.78	1.00	0.66	0.89				1.52
24	B	1.24	3.73	0.96			0.83	0.91	0.69	
25	B	1	2.69	0.91			0.54	0.85	0.74	
26	B	1	3.30	0.91			0.87		0.68	

4453

4454

Supplementary Appendix 4. Further analyses and supplementary information for Chapter 5. Exploring the drivers of metabolic rate across mammals.

Supplementary Information S2. The scaling of basal metabolic rate for the PanTHERIA and McNab (2008) datasets.

Here I show that the disparity in the scaling of basal metabolic rate (BMR) between uniparous and multiparous eutherian mammal species, as reported by Müller *et al.* (2012), is present for both the BMR database compiled by McNab (2008) (and used in Müller *et al.*) and the online ecological database PanTHERIA (Jones *et al.*, 2009) (Figure S2, Table S7).

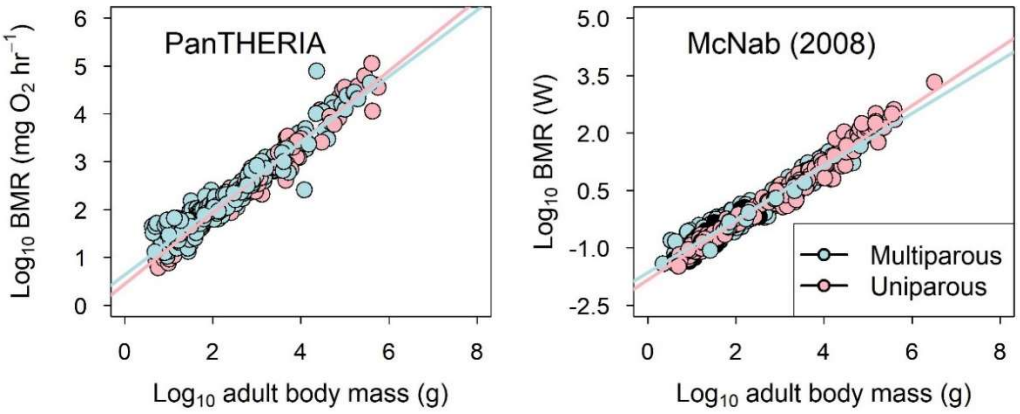

Supplementary Figure 2. Basal metabolic rate (BMR) as a function of adult body size (grams) for uniparous (< 1.5 offspring per litter) and multiparous (≥ 1.5 offspring per litter) eutherian mammal species for the PanTHERIA (Jones *et al.*, 2009) database and the McNab (2008) database. Note the difference in units between PanTHERIA and McNab BMR data.

Supplementary Table 7. The allometric scaling exponents and coefficients for ordinary least squares regression between basal metabolic rate (BMR) and adult body size (grams) for the PanTHERIA (Jones *et al.*, 2009) McNab (2008) databases for

uniparous (< 1.5 offspring per litter) and multiparous (≥ 1.5 offspring per litter) species. BMR is measured in units of mgO_2h^{-1} in the PanTHERIA database and units of watts in the McNab database.

Dataset	Parity	BMR versus adult body mass OLS regression coefficients				
		n	Slope	Intercept	R^2	p
PanTHERIA	Uniparous	128	0.745±0.022	0.447±0.064	0.97	< 0.001
PanTHERIA	Multiparous	336	0.690±0.021	0.644±0.052	0.92	< 0.001
McNab (2008)	Uniparous	158	0.759±0.021	-1.838±0.064	0.97	< 0.001
McNab (2008)	Multiparous	436	0.694±0.015	-1.651±0.037	0.95	< 0.001

Supplementary Information S3. The allometric scaling of maternal production rate and basal metabolic rate.

The disparity in the body mass-scaling of maternal production rate between uniparous (single offspring per litter) and multiparous (more than one offspring per litter) still remained when further distinguishing degree of multiparity parity. It is shown in Supplementary Figure 3 that all bins of multiparity (bins 2-4) had shallower and elevated mass-scaling of total maternal production rate (slopes ± 95% confidence intervals: bin 1 = 0.76±0.03, bin 2 = 0.65±0.05, bin 3 = 0.66±0.04, bin 4 = 0.63±0.29).

The disparity in the body mass-scaling of basal metabolic rate between uniparous (single offspring per litter) and multiparous (more than one offspring per litter) was further examined by distinguishing degree of multiparity parity into three litter size data bins. It is shown in supplementary Supplementary Figure 4 that only species with intermediate litter sizes (bin 3) displayed a different body-mass metabolic scaling exponent to uniparous species (slopes ± 95% confidence intervals : bin 1 = 0.75±0.02, bin 2 = 0.72±0.03, bin 3 = 0.63±0.05, bin 4 = 0.71±0.13).

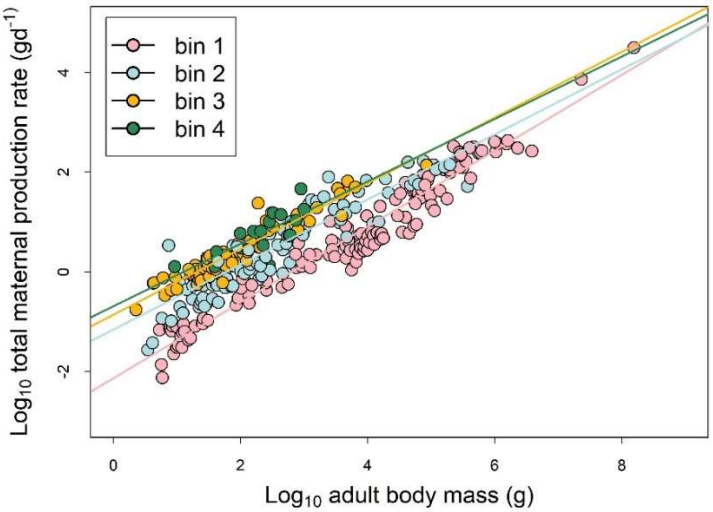

Supplementary Figure 3. The relationship between total maternal production rate and body mass for different degrees of parity using OLS regression. Parity is defined by number of offspring per litter in the following data bins: bin 1: < 1.5, bin 2: 1.5 – 3.99, bin 3: 4 – 6.49, bin 4: 6.5 – 16.89. Data were obtained using the PanTHERIA database (Jones *et al*., 2009).

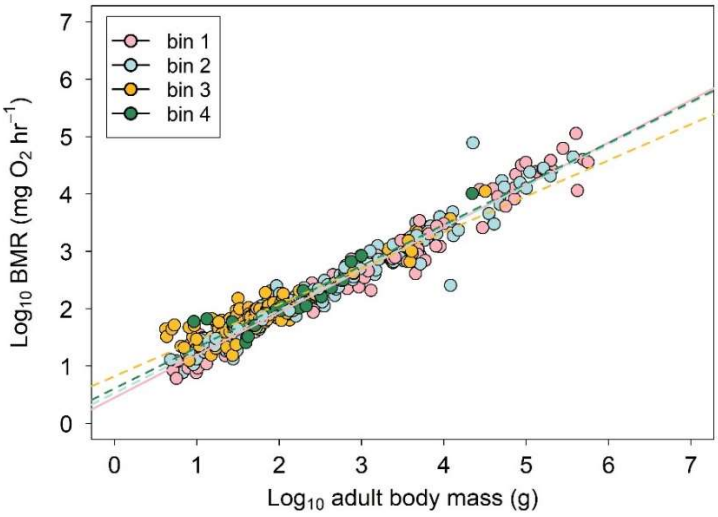

Supplementary Figure 4. The relationship between basal metabolic rate and body mass for different degrees of parity using OLS regression. Parity is defined by number of offspring per litter in the following data bins: bin 1: < 1.5, bin 2: 1.5 – 3.99, bin 3: 4 – 6.49, bin 4: 6.5 – 16.89. Data were obtained using the PanTHERIA database (Jones *et al*., 2009).

Supplementary Appendix 5. Publications.

The publications are presented in the format of the final accepted word document.

(1) Clarke, Villizzi and Lee *et al*. (2019). Identifying potentially invasive non-native marine and brackish water species for the Arabian Gulf and Sea of Oman. *Global Change Biology*, 26(4), 2081-2092.

(2) Lee *et al*. (2020). A new framework for growth curve fitting based on the von Bertalanffy function. *Scientific Reports*, 10(1), 1-12.

Please note publication (1) was authored as a result of research conducted for an ACCE DTP industry internship with the Centre for Environment, Fisheries and Aquaculture Science (Cefas). Whilst this internship was undertaken during my PhD, this publication (1) should not be examined as part of this thesis as stated by the ACCE DTP.

4526

4527 Identifying potentially invasive non-native marine and brackish water species for the Arabian Gulf

4528 and Sea of Oman

4529 Running title: **Marine non-native extant and horizon species**

4530 Stacey A. Clarke[1*], Lorenzo Vilizzi[2], Laura Lee[1,4], Louisa E. Wood[3], Winston J.
4531 Cowie[5], John A. Burt[6], Rusyan J. E. Mamiit[7], Hassina Ali[8], Phil I. Davison[1], Gemma
4532 V. Fenwick[9], Rogan Harmer[1], Michał E. Skóra[10], Sebastian Kozic[2], Luke R.
4533 Aislabie[1], Adam Kennerley[3], Will J. F. Le Quesne[1], Gordon H. Copp[1,2,11] and Paul
4534 D. Stebbing[3,12]

4535 [1] *Centre for Environment, Fisheries and Aquaculture Science, Lowestoft, Suffolk,*
4536 *UK*
4537 [2] *Department of Ecology and Vertebrate Zoology, Faculty of Biology and*
4538 *Environmental Protection, University of Łódź, Łódź, Poland;*
4539 [3] *Centre for Environment, Fisheries and Aquaculture Science, Weymouth, Dorset,*
4540 *UK*
4541 [4] *Department of Evolution, Ecology and Behaviour, Institute of Integrative Biology,*
4542 *University of Liverpool, UK*
4543 [5] *Environment Agency - Abu Dhabi, Abu Dhabi, United Arab Emirates*
4544 [6] *Centre for Genomics and Systems Biology, New York University Abu Dhabi, PO*
4545 *Box 129188, United Arab Emirates*
4546 [7] *Global Green Growth Institute, Abu Dhabi, United Arab Emirates*
4547 [8] *Ministry of Climate Change and Environment, Dubai, United Arab Emirates*
4548 [9] *Lancaster Environment Centre, Lancaster University, Lancashire, UK*
4549 [10] *University of Gdańsk, Faculty of Oceanography and Geography, Institute of*
4550 *Oceanography, Professor Krzysztof Skóra Hel Marine Station, Hel, Poland*
4551 [11] *Department of Life & Environmental Sciences, Bournemouth University, Poole,*
4552 *UK; and Environmental & Life Sciences Graduate Program, Trent University,*
4553 *Peterborough, Canada*

4554 [12] *Present Address: APEM Ltd, A17 Embankment, Business Park, Heaton Mersey,*
4555 *Manchester, SK4 3GN*

4556 *Keywords*: AS-ISK; extant non-native species; horizon species; risk screening;
4557 ROPME

4558 *Corresponding author: Email address: stacey.clarke@cefas.co.uk | Phone number:
4559 +44 (0)1502 524559 | ORCID ID 0000-0003-0332-3959
4560

4561 Abstract

Invasive non-native species (NNS) are internationally recognised as posing a serious threat to global biodiversity, economies and human health. The identification of invasive NNS already established, those that may arrive in the future, their vectors and pathways of introduction and spread, and hotspots of invasion are important for a targeted approach to managing introductions and impacts at local, regional and global scales. The aim of this study was to identify which marine and brackish NNS are already present in marine systems of the northeastern Arabia area (Arabian Gulf and Sea of Oman) and of these which ones are potentially invasive, and which species have a high likelihood of being introduced in the future and negatively affect biodiversity. Overall, 136 NNS were identified, of which 56 are already present in the region and a further 80 were identified as likely to arrive in the future, including fish, tunicates, invertebrates, plants and protists. The Aquatic Species Invasiveness Screening Kit (AS-ISK) was used to identify the risk of NNS being (or becoming) invasive within the region. Based on the AS-ISK basic risk assessment (BRA) thresholds, 36 extant and 37 horizon species (53.7 % of all species) were identified as high risk. When the impact of climate change on the assessment (CCA) was considered, the combined risk score (BRA+CCA) increased for 38.2 % of all species, suggesting higher risk under warmer conditions, including the highest-risk horizon NNS the green crab *Carcinus maenas*, and the extant macro-alga *Hypnea musciformis*. This is the first horizon scanning exercise for NNS in the region, thus providing a vital baseline for future management. The outcome of this study is the prioritisation of NNS to inform decision-making for the targeted monitoring and management in the region to prevent new bio-invasions and to control existing species, including their potential for spread.

Introduction

The increasing degradation of marine and brackish habitats around the globe is drawing attention to the importance of protecting these environments, especially from human-mediated impact. This is especially true for the Arabian Gulf and the Sea of Oman, a region that falls within the area of the Regional Organization for the Protection of the Marine Environment (ROPME), which has the mandate for supporting cooperative management of the ROPME Sea Area (RSA) (Bailey & Munawar, 2015; Van Lavieren & Klaus, 2013). The RSA, which is bordered by the countries of Bahrain, Iran, Iraq, Kuwait, Oman, Qatar, Saudi Arabia and the United

Arab Emirates, has unique environmental features, including a marine environment characterised by extreme oceanographic and meteorological conditions (Riefl *et al*., 2012; Sale *et al*., 2011; Van Lavieren *et al*., 2011; Vaughan, Al-Mansoori & Burt, 2019). Sea surface temperatures (SST) in the RSA regularly exceed 37° C during the extreme summer months (Paparella, Xu, Vaughan & Burt, 2019), and mean salinity is 42 ppt, with > 50 ppt common in the south and up to 70 ppt in coastal lagoons (Vaughan *et al*., 2019; Wabnitz *et al.,* 2018).

Characterised by low species diversity, with many species already living at the margins of survival, the RSA is particularly sensitive to human-generated impacts (Sheppard *et al.*, 2010; Vaughan *et al*., 2019), which are exacerbated by a rapidly-increasing human population and increased use of the marine environment (Bailey & Munawar 2015; Burt, Al-Harthi & Al-Cibahy, 2011; Burt, 2014; Riefl *et al*., 2012; Sale *et al*., 2011; Sheppard *et al*., 2010; United Nations, 2017; Van Lavieren *et al*., 2011; Van Lavieren & Klaus 2013). Particularly detrimental is the rise in temperature and salinity (IPCC, 2007), and the large decrease in input of fresh water from the River Shat Al Arab, which has increased salinity at the northern end of the RSA (UN-ESCWA & BGR, 2013). These are aggravated by extensive use of sea water as a coolant for power stations or directly for desalination – processes that release warmer, more saline water back into the sea (AGEDI, 2016; Elimelech & Phillip, 2011; Jenkins, Paduan, Roberts, Schlenk & Weis, 2012; Le Quesne *et al*., 2019). The original area of coral reef cover in the RSA has declined by 70 %, with most of the remainder either threatened or in a process of severe degradation (Vaughan *et al*., 2019; Wilkinson, 2008).

It is commonly recognised that invasive non-native species (NNS) are one of the greatest threats to global biodiversity and are a key driver in ecosystem change, especially when introduced into sensitive environments (Costello *et al*., 2010; Kideys, 2002; Rockström *et al*., 2009). The International Maritime Organisation (IMO) recognises the introduction of harmful aquatic organisms (including NNS and pathogens) to new environments as one of the four greatest threats to the world's oceans – the other three being land-sourced marine pollution, over-exploitation of living marine resources, and destruction of habitat (IMO, 2009). In recognition of this increasing threat and to manage more effectively the risks posed by invasive NNS, the Convention on Biological Diversity (CBD) has set international targets and

frameworks for global action. Specifically, the CBD has provided Guiding Principles for the Prevention, Introduction and Mitigation of Impacts of Alien Species that Threaten Ecosystems, Habitats and Species (United Nations, 2002). These guidelines include a three-stage hierarchical approach based on: (i) prevention of introduction; (ii) early detection and rapid action (*e.g.* eradication, where feasible) in the event of a new introduction to prevent establishment; (iii) and, where eradication is not feasible, control and containment measures.

Particularly important actions include the identification of potential invasive NNS that could enter a region, early detection of those already there (Chan *et al*., 2019; Ojaveer *et al*., 2018), and prevention of further introductions. On the contrary, post-introduction actions such as eradication, control and containment are generally difficult and unlikely to be successful (Williams & Grosholz, 2008), particularly in the marine environment (Werschkun *et al*., 2014).

Understanding the main vectors and pathways of introduction and spread into, and within, a region enables targeted NNS management by identifying the locations most at risk from introductions (Tidbury, Taylor, Copp, Garnacho & Stebbing, 2016). Within the RSA, key potential vectors of introduction of NNS include ship traffic of which there are the large volumes entering the area from international ports (Sale et al., 2011; Vaughan et al., 2019), especially from India, China and Pakistan (Automatic Identification System (AIS) data obtained on request from Marine Traffic: www.marinetraffic.com/en/p/ais-historical-data). Other introduction vectors include recreational boating, cruise ships and aquaculture, and, to a lesser extent, the aquarium trade (Miza, Majiedt & Sink, 2014). The key vectors involved in marine introduction vectors are ballast water discharge, hull fouling, general fouling, hitchhiking, and release (intentional or accidental: Minchin, Gollasch, Cohen, Hewitt & Olenin, 2009). In terms of aquaculture, this industry is increasing with more than $US 15 billion worth of projects being planned in the RSA for the current decade (Innovation Norway, 2015), and due to limited freshwater resources, most countries in the RSA are actively researching future options for farming marine species.

The present study identifies potentially invasive marine and brackish water NNS in the Arabian Gulf and Sea of Oman. This area also coincides with the Inner and Middle RSA and is referred to hereafter as the risk assessment area (Figure 1). The specific

objectives are to: (i) identify extant NNS in the risk assessment area; (ii) complete a horizon-scanning exercise to determine which marine and brackish NNS are likely to arrive in the risk assessment area in the foreseeable future; (iii) complete risk screenings of both sets of (extant and horizon) species using a widely-tested electronic decision support toolkit with regard to current and future climate conditions; (iv) calibrate and validate the resulting data set, and therefore classify the NNS as being of low-to-medium and high risk of being (or becoming) invasive in the risk assessment area; and (v) evaluate the confidence level of the assessments. Notably, this is the first horizon-scanning and risk-identification exercise for marine and brackish NNS for the RSA, and the outcomes are intended to provide decision makers with evidence upon which to develop informed policy and prioritised management strategies for protection of the area's unique marine and brackish water environments from adverse impacts of NNS.

Materials and Methods

Risk screening

The Aquatic Species Invasiveness Screening Kit (AS-ISK), which is available for free download at www.cefas.co.uk/nns/tools, was used to identify potentially invasive NNS with respect to the risk assessment area. Described in detail in Copp *et al*. (2016), the AS-ISK is fully compliant with the 'minimum standards' (Roy *et al*., 2018) for the assessment of NNS for the European Commission Regulation on the prevention and management of the introduction and spread of invasive alien species (European Commission, 2014). The AS-ISK consists of 55 questions: the first 49 questions cover the biogeography/ historical and biology/ ecology aspects of the species under assessment, including risks of introduction, establishment, dispersal and impact, and comprise the Basic Risk Assessment (BRA). The other six questions require the assessor to predict how future climatic conditions are likely to affect the BRA with respect to risks of introduction, establishment, dispersal and impact, and these comprise the Climate Change Assessment (CCA). In the recently-released AS-ISK v2, which the assessors employed in the current study, the 16 taxonomic groups of aquatic organisms previously accounted for in AS-ISK v1 (Copp *et al*., 2016) have been

4691 expanded to a total of 27 following the classification of living organisms by Ruggiero
4692 *et al*. (2015).

4693 For each question in AS-ISK, the assessor must provide a response, justification
4694 and level of confidence, and the screened species eventually receives both a BRA and
4695 a BRA+CCA (composite) score (respectively ranging from −20.0 to 68.0 and from
4696 −32.0 to 80.0). AS-ISK scores < 1.0 suggest that the species is unlikely to become
4697 invasive in the risk assessment area and is therefore classified as 'low risk'. Higher
4698 scores classify the species as posing either a 'medium risk' or a 'high risk' of becoming
4699 invasive. Distinction between medium and high risk levels depends upon setting a
4700 'threshold' value, which is typically obtained through risk assessment area-specific
4701 'calibration' subject to availability of a representative sample size (*i.e.* number of
4702 screened species), which was recently estimated at n = 15–20 (Vilizzi *et al*., 2019).
4703 For the purposes of this study, with regard to the CCA component of the screening
4704 process, current predictions for the RSA suggest an increase in SST between 0.5 and
4705 1.4° C and salinity increases of up to 18 ppt by 2050 (Vaughan *et al*., 2019; Wabnitz
4706 *et al.,* 2018). The assessors used this scenario to provide a consistent outlook on the
4707 provision of CCA scoring.

4708 The ranked levels of confidence (1 = low; 2 = medium; 3 = high; 4 = very high)
4709 associated with each response in AS-ISK mirror the confidence rankings that the
4710 Intergovernmental Panel on Climate Change recommended (IPCC, 2005; see also
4711 Copp *et al*., 2016). Based on the confidence level (CL) allocated to each response for
4712 a given species, the confidence factor (CF) is calculated as:

4713 $$\sum(CL_{Qi})/(4 \times 55)\ (i = 1, \ldots, 55)$$

4714 where CL_{Qi} is the confidence level (CL) for Question i (Qi), 4 is the maximum
4715 achievable value for certainty of confidence in the response (*i.e*. 'very high') and 55
4716 is the total number of questions comprising the AS-ISK questionnaire. The CF ranges
4717 from a minimum of 0.25 (*i.e.* all 55 questions with CL equal to 1) to a maximum of 1
4718 (*i.e.* all 55 questions with CL equal to 4). Two additional confidence factors were also
4719 computed, namely the CF_{BRA} and the CF_{CCA} based on the 49 questions in the BRA and
4720 the six questions in the CCA, respectively.

4721 NNS selection

Extant – The initial list of NNS recorded in region thus far was compiled using a variety of relevant search terms in Google and Google Scholar, personal bibliographic collections, and NNS databases including the Global Invasive Species Database (GISD, www.iucngisd.org/gisd/), Invasive Species Compendium (CABI, www.cabi.org/isc) and Global Register of Introduced and Invasive Species (Griis, www.griis.org/). These were employed to summarise the existing knowledge of marine and brackish water organisms that are known or suspected to be non-native to any of the countries in the risk assessment area. In-region experts reviewed and validated the initial list through various consultations. For each species identified as potentially being a NNS present, additional information was gathered including: (i) taxonomy; (ii) habitat; (iii) whether the organism has been recorded or suspected to be in the risk assessment area; (iv) whether it is acknowledged to be introduced, established or spreading; (v) the known and potential impacts it may have; (vi) the introduction vector and potential pathway as per CBD groupings, i.e.: intentional release, including biological control, and other releases; escape, including aquaculture, aquarium trade; transport (stowaway), including ballast water, hull fouling, and other transport); (vii) the specific location where it was reported; and (viii) the date it was first recorded. Cryptogenic species (i.e. native/non-native status in the risk assessment area uncertain), or those for which the basis of identification in the risk assessment area was derived from limited records, remained on the list unless expert judgement indicated otherwise. To reduce risk of double-counting the same species under different names, the World Register of Marine Species (WoRMS, www.marinespecies.org/) was used to determine the current and previously accepted genus and species names. Where sources varied in their conclusion of invasiveness of a species in the risk assessment area, the most recent scientific manuscripts were used where available (alongside in-region expert knowledge) to determine the decision to add or not to the list.

Horizon – The assessors generated the horizon list using: (i) a combination of literature searches; (ii) predictions by the CABI Horizon Scanning tool (www.cabi.org/HorizonScanningTool), (iii) refinement of in-region lists where more detailed information obtained during the screening process clarified that the species was not yet present in the risk assessment area (*i.e.* it may be present in Iran, but in the Caspian Sea rather than in the Inner or Middle RSA,); and (iv) a review of aquaculture

in the Inner and Middle RSA (*i.e*. those NNS being used by the industry or being reviewed for future use, but not yet recorded as present outside of cultivation). For the CABI tool, the following search criteria were used: (a) recipient countries selected: only those in-region; (b) source countries selected: neighbouring countries and other countries with matching climate type listed; (c) vectors selected: all, with the exception of those that were considered not applicable to marine species (*i.e.* Containers & packaging; Machinery & equipment; Mulch, straw, baskets & sod; Soil, sand & gravel; Germplasm; Hides, trophies & feathers; Wind-dispersal); and (d) habitats selected: brackish and marine. 'Brackish' was included in the search terms as there is potential for brackish water species to survive in the risk assessment area if they have a marine stage to their life cycle and/or a broad salinity tolerance that enables them to survive in marine habitats. The initial list was then manually reviewed and validated, especially in relation to climate suitability. Despite the climate matching criteria in CABI being selected to restrict to similar climate types, there were some species that were evidently not suited to waters of the temperatures found in the risk assessment area. These were removed from the list unless there was evidence of the species being established in similarly harsh environments elsewhere.

Data processing

Following computation of the BRA and BRA+CCA scores with AS-ISK, Receiver Operating Characteristic (ROC) curve analysis (Bewick, Cheek & Ball, 2004) was used to assess the predictive ability of AS-ISK to discriminate between species posing a high risk and those posing a medium or low risk of being invasive for the risk assessment area. The implementation of the ROC curve analysis requires *a priori* categorisation in terms of documented invasiveness (i.e. non-invasive or invasive) of species. However, unlike fishes and lampreys, for which *a priori* categorisation is facilitated by the availability of online databases providing all required information (*i.e*. FishBase, www.fishbase.org; cf. Bilge, Filiz, Yapici, Tarkan & Vilizzi, 2018; Glamuzina *et al.*, 2017; Li, Chen, Wang & Copp, 2017; Tarkan *et al.*, 2017a,b; Zięba, Vilizzi & Copp, 2019), this study adopted an 'integrated approach' to determine the *a priori* invasiveness status of species in all other aquatic organism groups (other than freshwater and marine fishes and lampreys, as identified in AS-ISK) due to the more limited information available.

The integrated approach followed four steps: (i) similar to fishes and lampreys (cf. FishBase), there was a preliminary consultation of SeaLifeBase (www.sealifebase.org) for any reference to the species' threat to humans, with the species categorised *a priori* as invasive if listed as 'potential pest' and as non-invasive if listed as 'harmless'; (ii) in case the species was listed as either 'not evaluated' or was absent in the above database, then a search was made of the Global Invasive Species Database (GISD - www.iucngisd.org/gisd/), with the species categorised *a priori* as invasive if listed therein; (iii) in case the species was absent from the GISD, then an additional search was made of the continent-level lists for invasive species in Africa, Asia, Europe, North America, South America and Australia, whereby the species was categorised a priori as 'invasive' if it appeared in the generated list; and finally, (iv) in case the species was absent from any of the previous databases, then a Google Scholar (literature) search was performed (using the keywords 'invasive', 'invasiveness' and 'impact' along with that of the species) to check whether at least one peer-reviewed reference in support was found. The latter was then taken as 'sufficient evidence' for categorising the species *a priori* as invasive; whereas, if no evidence was found, then the species was categorised *a priori* as non-invasive. Notably, in case a species was listed as harmless in FishBase or SeaLifeBase but found to be invasive in any of the other steps of the process, then the *a priori* categorisation of the species became that of invasive.

Statistical analysis

A ROC curve is a graph of sensitivity *vs* 1 – specificity (or alternatively, sensitivity *vs* specificity) for each threshold value, where in the present context sensitivity and specificity will be the proportion of *a priori* invasive and non-invasive species, respectively, for the risk assessment area that AS-ISK correctly identified as such. A measure of the accuracy of the calibration analysis is the Area Under the Curve (AUC), which typically ranges from 0.5 to 1, and the closer to 1 the better the ability to differentiate between invasive and non-invasive species. If the AUC is equal to 1, then the test is 100 % accurate, because both sensitivity and specificity are 1, and there are neither 'false positives' (*a priori* non-invasive species classified as high risk, hence false invasive) nor 'false negatives' (*a priori* invasive species classified as low risk, hence false non-invasive). Conversely, if the AUC is equal to 0.5, then the test is 0 % accurate as it cannot discriminate between 'true positives' (*a priori* invasive species

classified as high risk, hence true invasive) and 'true negatives' (*a priori* non-invasive species classified as low risk, hence true non-invasive). Following ROC analysis, the Youden's *J* statistic best determines the AS-ISK threshold value that maximises the true positives rate and minimises the false positives rate; whereas, a 'default' threshold of 1 was set to distinguish between low risk and medium risk species (see *Risk screening*).

ROC curve analysis was carried out with package pROC (Robin *et al.*, 2011) for R x64 v3.2.0 (R Core Team, 2015) using 2 000 bootstrap replicates for the confidence intervals of specificities, which were computed along the entire range of sensitivity points (*i.e.* 0 to 1, at 0.1 intervals). For those groups of aquatic organisms for which a 'representative' sample size was available (*i.e.* $n > 10$), the aquatic organism-specific thresholds could be estimated. However, in case of resulting mean AUC values < 0.5, the corresponding threshold was discarded and the one for the 'nearest' aquatic organism combined group was used. The latter criterion applied also to any group including less than 10 screened species and for which ROC curve analysis was not possible.

Differences between mean CL_{BRA} and CL_{CCA} (see *Risk screening*) depending upon species status (*i.e.* extant or horizon) were tested by permutational (univariate) analysis of variance (PERANOVA) based on a two-factor design (i.e. factor Component, with the two levels BRA and CCA; factor Status, with the two levels Extant and Horizon), with both factors fixed (note that differences between mean CF_{BRA} and CF_{CCA} would lead the same outcomes being the two indices related). The analysis was carried out using PERMANOVA+ for PRIMER v6, with normalisation of the data and using a Bray-Curtis dissimilarity measure, 9 999 unrestricted permutations of the raw data (Anderson, Gorley & Clarke, 2008), and with statistical effects evaluated at $\alpha = 0.05$ including *a posteriori* pair-wise comparisons.

Results

NNS selection

Extant – The final list (Table S1) comprised 56 species from across Chromista (14; 25 % of total), Arthropoda (10; 18 %), Teleostei (10; 18 %), Ascidiacea (seven; 13 %), Plantae (five; 9 %), Mollusca (four; 7 %), Bryozoa (three; 5 %) and Cnidaria (three; 5 %). In total, 35 (63 %) of these species were determined to be introduced, with the

remaining 21 (38 %) being cryptogenic. Native ranges of the 35 species recognised as NNS varied, with 12 (23 %) coming from the Atlantic, seven (13 %) from Southeast Asia, six (11 %) from African waters, three (6 %) from the Pacific, and another three (6 %) from the Indian Ocean, and with the remaining species from a variety of smaller sea regions including the Mediterranean and Caspian seas. The most common suspected vector of introduction (as identified via expert knowledge based on species' characteristics combined with information gathered from literature searches during the risk screening process) was via ballast water (36 instances, 51 %), followed by fouling of equipment, vessel hulls or other hard surfaces (18, 26 %), and aquaculture (10, 14 %). The aquarium trade and mosquito (biological) control introduction vectors made up the remaining 9 % (six instances). It is sometimes difficult to attribute introductions to specific vectors, and therefore the association of vectors to specific species introductions remain speculative. Several species had multiple vectors attributed to their introduction, hence the numbers given here add up to more than the total number of species.

Horizon-scanning – The final list (Table S2) comprised 80 species from across Teleostei (22; 28 % of total), Arthropoda (14; 18 %), Mollusca (14; 18 %), Plantae (seven, 9 %), Annelida (five; 6 %), Ascidiacea (five; 6 %), Cnidaria (five; 6 %), Chromista (three; 4 %), Bryozoa (two; 3 %), Ctenophora (two; 3 %) and Porifera (one; 1 %). Overall, the majority of horizon species are naturally present in Southeast Asia (29, 39 %), followed by those present in the Americas (18, 24 %), European coasts (10, 14 %), central Asia (including the Black and Caspian seas; six, 8 %), Africa (six, 8 %), and with the remainder (five, 7 %) from Australasia and the wider Indo-Pacific or unknown (note that some species have a native range encompassing more than one of the above categories). Vectors (and associated pathways) of introduction were less certain than native origin from the literature available, but based on species characteristics (*e.g.* adhering species) and known introductions elsewhere, the following estimation of potential vectors for horizon species were noted: ballast water (39 potential incidences, 34 %), followed by aquaculture (33, 28 %), biofouling (31, 27 %), aquarium trade (ten, 8 %), and 'other' (three, 3 %).

Outcomes and confidence

Following ROC curve analysis (Table 1) of the AS-ISK scores (Table S3; Species Assessment Reports in S4), BRA thresholds could be computed successfully for all AS-ISK taxonomic groups in the study (namely, brackish and marine fishes and lampreys, tunicates, marine invertebrates, marine Plantae, and marine Protista), with the exception of brackish invertebrates due to low sample size ($n = 4$). Therefore, BRA and BRA+CCA thresholds were estimated for brackish and marine combined. Conversely, reliable calculations of individual BRA+CCA thresholds were not possible for marine Plantae and marine Protista due to their mean AUC values being < 0.5, which was also the case for the combined marine Plantae and Protista threshold (see Section 2.4).

All resulting AUCs (when using combinations of the thresholds described above) were above 0.5 (Table 1), indicating that AS-ISK was able to discriminate reliably between non-invasive and invasive species in the risk assessment area. Youden's *J* provided BRA thresholds ranging from 19.75 (marine fishes) to 34.25 (tunicates), and BRA+CCA thresholds from 20.5 (marine invertebrates and brackish invertebrates – the latter based on the combined groups) and 34.25 (tunicates). These group-specific thresholds were therefore used for calibration of the risk outcomes at the species level, using the appropriate statistical use of interval brackets ("]" and "["; www.mathwords.com/i/interval_notation.htm). Accordingly, the BRA thresholds allowed the distinction of medium-risk species with scores within the interval $[1, \mathrm{Thr}_{\mathrm{BRA}}[$ from high-risk species with scores within $]\mathrm{Thr}_{\mathrm{BRA}}, 68]$; and the BRA+CCA thresholds allowed distinction of medium-risk species with scores within $[1.0, \mathrm{Thr}_{\mathrm{BRA+CCA}}[$, from high-risk species with scores within $]\mathrm{Thr}_{\mathrm{BRA+CCA}}, 80]$. Whereas, species classified as low risk were those with BRA scores within $[-20, 1[$ and BRA+CCA scores within $[-32, 1[$.

Of the 136 NNS assessed in total (i.e. extant and horizon: Table S3), based on the BRA thresholds: 73 (53.7 %) were classified as high risk and 63 (46.3 %) as medium risk (no low-risk species); of the 85 species categorised *a priori* as invasive, 57 (67 %) were classified as high risk (true positives) and 28 (33 %) as medium risk; and of the 51 species categorised *a priori* as non-invasive, 16 (31 %) were classified as high risk (false positives) and 35 (69 %) as medium risk. Based on the BRA+CCA thresholds: 81 (59.6 %) species were classified as high risk, 50 (36.8 %) as medium risk, and five (3.7 %) as low-risk; of the 85 species categorised *a priori* as invasive, 61 (72 %) have a high risk classification (true positives), 22 (26 %) as medium risk and two (2 %) as low risk (false positives: dark doto, *Doto kya* and nimble spray crab, *Percnon gibbesi*); and, of the 51 species categorised *a priori* as non-invasive, 20 (39 %) were classified as high risk species (false positives), 28 (55 %) as medium risk and three (6 %) as low risk (true negatives: charming aeolid *Microchlamylla amabilis*, mysid shrimp *Rhopalophthalmus tattersallae*, and white-crust cuthona *Trinchesia albocrusta*). The overview of AS-ISK scores for species scoring at or above regional threshold for risk of invasiveness are given in Figure 2.

With regard to BRA scores, the highest-scoring (invasive) NNS (score ≥ 45, taken as an *ad hoc* very high risk threshold value) were the green crab, *Carcinus maenas*, crozier weed *Hypnea musciformis*, blue tilapia *Oreochromis aureus*, blackchin tilapia *Sarotherodon melanotheron*, upside down jellyfish *Cassiopea andromeda*, and redbelly tilapia *Coptodon zillii* (from higher to lower scores). As to BRA+CCA scores, the highest-scoring (invasive) species (score ≥ 55, same criterion as per BRA) were *Carcinus maenas*, *S. melanotheron*, *Alexandrium minutum*, *Heterosigma akashiwo*, *Margalefidinium polykrikoides*, titan acorn barnacle *Megabalanus coccopoma*, *Cassiopea andromeda*, and *Karenia selliformis* (from higher to lower scores). There were no low-risk NNS for the BRA, whereas for the BRA+CCA these included mysid shrimp, *R. tattersallae*, *D. kya*, *T. albocrusta*, *Microchlamylla amabilis*, and *P. gibbesi* (from lower to higher scores) (Table S3).

The CCA increased the BRA score for 52 (38.2 %) of the screened species, decreased it for 62 (45.6 %) of them, and remained unchanged for the remaining 22 (16.2 %) (Table S3). Also, 15 (11.0 %) of the screened species achieved the largest possible (positive) change in score of 12, and these included *Carcinus maenas*, the highest-scoring species for both the BRA and BRA+CCA (see above).

Mean CL (*i.e.* over all 55 Qs) was 2.71 ± 0.03 SE, mean CL_{BRA} 2.75 ± 0.03 SE, and mean CL_{CCA} 2.41 ± 0.06 SE (hence, in all cases indicating medium to high confidence). Also, there was a statistically significant Component × Status interaction ($F^{\#}_{1,268}$ = 22.85, $P < 0.001$; $^{\#}$ = permutational value) and this was due to the mean CL_{BRA} being higher than mean CL_{CCA} (*i.e.* 2.78 *vs* 2.07; $t^{\#}$ = 7.81, $P < 0.01$) for the extant NNS, whereas for the horizon NNS, there were no significant differences detected (*i.e.* 2.73 *vs* 2.65; $t^{\#}$ = 0.84, P = 0.400). Mean CF (*i.e*. over all 55Qs) was 0.678 ± 0.007 SE, mean CF_{BRA} = 0.687 ± 0.007 SE, and mean C_{FCCA} = 0.603 ± 0.016 SE. In all cases, the narrow standard errors indicated overall similarity in CLs and CFs across the NNS assessed.

Overall, the highest risk species had a BRA score of >45 or a combined BRA+CCA score of >55. For BRA this included three (5 %) of the extant NNS, and two (2.5 %) of the horizon NNS. For combined BRA+CCA this included five (9 %) of the extant NNS and three (4 %) of the horizon NNS.

Discussion

Of the 56 extant NNS identified in the Inner and Middle RSA, 64 % (36) of species were classified as likely to pose a risk of being invasive, and of the 80 horizon species, 46 % (37) have attributes of risk of invasiveness. Of the species already present, the protozoan Chromista formed a majority at 25 % (14 species) and had a high risk of invasiveness. In contrast to extant species, fish comprised the most common group of aquatic organisms of the horizon NNS forming 28 % (22 species) of the total. Only three Chromista species were identified as horizon NNS, although further representatives of this taxonomic group may be found to be present in the Inner and Middle RSA in the future as they are poorly studied compared to other groups. In general, it is likely the current list of 136 species is only part of the non-native biodiversity present in the risk assessment area and therefore should form a basis before further review by experts in-region. Further study, particularly through field-based monitoring, would likely reveal more NNS to be present.

For both extant and horizon NNS, ballast water was the most common introduction vector providing 51 % of all instances of extant species introductions, and 34 % for horizon species. This is not surprising given the high levels of shipping in the risk assessment area making this a prominent vector for NNS movement. Some 53 000

ships visit the Gulf annually in association with oil transportation alone (Al-Yamani, Skryabin & Durvasula, 2015), and in 2017 a total of 146 671 voyages were received into all ports within the Inner and Middle RSA (AIS data obtained on request from Marine Traffic: www.marinetraffic.com/en/p/ais-historical-data). This may also reflect the high percentage of Chromista identified as extant NNS, as ballast water is a common vector for the movement of these types of organism (Bailey, 2015; Gustaaf, 2015). The prominence of this vector and its link to transporting Chromista further highlights the potential for their low number identified in the horizon scanning to be an artifact of the formulation of the horizon list rather than the actuality. As one of the globally-recognised and most important vectors for the introduction of NNS into aquatic systems, the Ballast Water Management Convention provides some legislative oversight to related activities (Olenin, Minchin, Daunys & Zaiko, 2010). The ballast vector was followed by biofouling and aquaculture, with the latter being responsible for many of the fish species introductions.

The pathways associated with these introduction vectors for horizon species provide an indication of where management efforts should focus to reduce the likelihood of future introduction events. In addition, for those species likely to be transported by ship in ballast water or as hull foulants, the native range may provide an indication of likely ports of entry if matched to shipping pathways. However, this would only apply if the species has not already been introduced elsewhere and many species identified already have a wide Indo-Pacific distribution. The initial vector and pathway analysis undertaken as part of risk screening for species could be strengthened by more in-depth vector/pathway and hotspot analysis, focused particularly on shipping routes (international and regional – the latter important for the spread of NNS once introduced) and aquaculture.

The species identified as posing the highest risk of being invasive under current climatic conditions were the extant macro-algal species, *Hypnea musciformis* and the horizon crab species, *Carcinus maenas*. These species are known to be transported *via* ballast water and to be invasive elsewhere. Also, *C. maenas* is found on several lists of global 'top 100 invasive species' (*e.g.* Lowe, Brown, Boudjelas & De Poorter, 2000; O'Donnel, 2013), and consistent with this, these two species received the highest current (BRA) and future climate (BRA+CCA) scores of all species screened.

Hypnea musciformis is known to form dense floating algal mats (Russell, 1992), which can have socio-economic impacts when they are washed ashore as they release noxious gases whilst decomposing (Russell, 1992). A study on the Hawaiian island of Maui estimated costs for ≈ $US 20 million per year to manage the impacts of *H. musciformis* blooms, such as by cleaning rotting algae off beaches, reduction in property values and lost tourist revenues (Cesar, Vanbeukerling & Prince, 2002). Ecologically, the species can outcompete other macro-algae, and in Hawaii it has become the main food source of the green turtle *Chelonia mydas*. It is uncertain whether or not this alga is as nutritious as native species, and thus a dietary change could affect the fitness of the turtle population (Russell & Balazs, 1994), adding to other pressures affecting turtle populations in the ROPME Sea Area (Pilcher *et al*., 2014).

Carcinus maenas is a generalist known to exert adverse impacts on marine ecosystems, including socially and economically important native species such as crabs and shellfish. A major example includes the collapse of the New England shellfish industry in the 1950s resulting from the introduction of *C. maenas* (Smith, Baptist & Chin, 1995). Its impacts on aquaculture productivity over the west coast of the USA caused severe economic loses at an estimated $US 44 million (Klassen & Locke, 2007). In addition, this shore crab can cause adverse ecological impacts due to habitat degradation, including alterations to the structure of intertidal and subtidal communities (Cohen, Carlton & Fountain, 1955). For example, extensive foraging behaviour of the crab has shown to be a major cause of the significant declines in eelgrass *Zostera marina* beds in the Gulf of St. Lawrence, Nova Scotia (Garbary, Miller, Williams & Seymour, 2014). In another example, *C. maenas* was responsible for the decline of the native Dungeness crab *Metacarcinus magister* on the west coast USA through monopolising prey resources owing to their greater claw strength (Yamada, Davidson & Fisher, 2010). The impacts identified elsewhere for these high-risk species highlight the need for effective management of NNS in the Inner and Middle RSA from environmental, social and economic perspectives.

Climate changes predicted for the ROPME Sea Area, whilst potentially reducing the risk of establishment of many NNS, may benefit coliform bacteria and dinoflagellates (Van Lavieren *et al*., 2011). The BRA+CCA score increased compared to the initial BRA score for 52 species of all 136 screened, suggesting some species

may have a greater risk of invasion with predicted climate change. However, the risk of being invasive was reduced for 62 species, as the naturally extreme conditions of the region are already at the upper end of species' temperature tolerance and increasing temperatures would only exacerbate this stress. In accordance with climate predictions for the ROPME Sea Area (Van Lavieren *et al.*, 2011), the screenings undertaken in this study suggest that the majority of Chromista are likely to pose an increased risk under future conditions (*i.e*. 71 % of all Chromista across extant and horizon species), with increased risk also anticipated for some other taxon groups, namely fish (47 % increase risk of invasion in response to climate change), invertebrates (25 %) and, to a minor degree, plants (4 %). For the other aquatic organism groups, a majority of species would decline in risk as a result of climate change. These contrasting predictions highlight the likelihood of unforeseen responses by species to climate change, and detailed climate modelling for the risk assessment area would enable a more detailed understanding of risks posed by NNS (in particular those species whose BRA+CCA score increased) as well as identifying locations of potentially higher risk based on climate variables. Also, invasiveness risk response to climate change may vary between the Inner and Middle RSA, as these have different climate parameters due to their oceanography (Riefl *et al.*, 2012; Van Lavieren *et al*., 2011; Vaughan *et al.*, 2019).

The present study represents the first application of AS-ISK in the Inner and Middle RSA and the first application of this decision-support tool anywhere to a multi-taxonomic study looking at extant and horizon species. The medium-to-high confidence levels of the screenings and the ability to provide regional thresholds for some taxonomic groups are of particular note, as this highlights the increased specificity to the results, which is important in a region where species are considered generally less likely to establish due to the locally-extreme climatic conditions. Overall, the present results suggest that AS-ISK is a useful and valid decision-support tool for identifying potentially invasive species, both extant and horizon, and assist decision makers in setting priorities for NNS management. The present study complements other AS-ISK based assessments of NNS undertaken in wider Arabia and the eastern Mediterranean (*i.e.* Bilge *et al.*, 2019; Tarkan *et al*., 2017a,b), further highlighting the usefulness of AS-ISK for NNS management in the Inner and Middle RSA. It also provides wider validation of the ability of AS-ISK to identify NNS risk

in a variety of aquatic environments, including those with more specialised and extreme climatic conditions, as well as to assist in NNS management of both extant and horizon species.

The present AS-ISK assessments also helped identify gaps in knowledge with regard to the types and magnitude of adverse impacts that could be imposed on the Inner and Middle RSA. Understanding the impacts already caused in the latter or elsewhere by specific NNS can help to identify where similar impacts may occur in the future, and thus enable preventative steps to be taken to reduce these in advance. An example is the use of early warning systems to monitor algal blooms caused by Chromista to enable the movement or closure of aquaculture farms, or the harvest of their outputs in advance to reduce risk to human health (see FAO, 2017). Such warning systems could be particularly relevant in the Inner and Middle RSA, as in September–October 1999 a harmful algal bloom primarily composed of *K. selliformis* (a cryptogenic NNS) and *Prorocentrum rhathymum* (a definite NNS) caused significant mortality of wild and farmed fish in Kuwait Bay resulting in an estimated economic loss of $US 7 million (Al-Yamani, Saburova & Polikarpov, 2012). Another NNS Chromista *Gymnodinium catenatum* in the Inner and Middle RSA is known elsewhere around the world to have caused paralytic shellfish poisoning, which can have significant human health implications (Hoagland, Anderson & White, 2002).

The present study has also highlighted key species and taxonomic groups with high risk of being/becoming invasive that should provide a focus for further regional study and monitoring. Linked to impact management, two of the key taxonomic groups identified were Chromista and fish (many of which are transported *via* aquaculture). Further study could include in-region surveys to detect the presence and establish the current distribution of extant species, and to monitor for horizon species. Such work could use well-established taxonomic survey methods, environmental DNA methods and regular monitoring of vectors (Trebitz *et al*., 2017), e.g. vessel hulls and ballast water. This will help identify the exact NNS present (*i.e*. provide ground-truthing of species lists) and their current distribution.

In addition to monitoring, NNS vector (and associated pathway) management should be put into place, including ensuring compliance with the Ballast Water Management Convention for vessels entering the Inner and Middle RSA and in wider

port management practices; and implementation of IMO guidelines for the control and management of ships' biofouling to minimise the transfer of invasive aquatic species (Biofouling Guidelines, resolution MEPC.207(62)). This would include ensuring relevant vessels entering the Inner and Middle RSA have ballast water management plans in place, adequate treatment of ballast water to reduce biological organism survival occurring within vessel systems (*e.g.* use of ozone, UV and other forms of filtration), and ballast water exchange occurring in deep waters (away from coastal waters) (IMO, 2009). Further, in-water cleaning of vessel hulls should be minimised where possible or scrapings adequately captured and disposed of on-land (Hopkins & Forrest, 2008).

NNS management in aquaculture should be established within existing and future biosecurity measures including ensuring stock does not come from areas with NNS present that are known to be transported *via* aquaculture (*e.g*. as hitchhikers). Reducing the use of NNS in aquaculture unless they are going to be farmed in enclosed facilities should also be an aim of the management and wider policy regarding the aquaculture vector and its associated pathways. A good overview of existing global regulations, guidelines and methods for reducing the risk and impact of NNS in aquaculture is provided by Hewitt, Campbell & Gollasch (2006).

Surveys and monitoring combined with further vactor/pathway analysis and climate modelling, as suggested within wider discussion above, would enable identification of hotspots of invasion more generally, allowing a geographical as well as species-specific focus to monitoring and management efforts and help to understand better the spread potential within the Inner and Middle RSA for extant NNS. Targeted management of vectors and pathways will help reduce the risk of NNS being introduced in the first instance and combined with monitoring of species themselves, enabling rapid response processes to newly identified introduction events to reduce risk of establishment and spread. This is in line with the CBD guiding principles of prevention of NNS introductions being preferable, followed by early identification and rapid response to reduce establishment and eradication as a last resort. Ensuring NNS are identified and managed before they become established and potentially invasive is especially important in regions where the sensitivity of existing environments to increased pressures is high. Overall, effective NNS management will help provide

another step towards protecting the unique marine and brackish water environments of the RSA alongside existing environmental management measures.

In conclusion, the present study provides baseline knowledge of NNS present in the Inner and Middle RSA and, for the first time, identifies those with the potential to become invasive in the future. This is important as the ROPME Sea Area experiences unique and extreme climatic conditions that are predicted to become harsher to aquatic organisms with climate change. As many species are already at their limits of tolerance, the impacts of invasive NNS combined with existing pressures could increase the risk of species and habitat loss and degradation in the region. Therefore, it is vital to understand the baseline risk that NNS pose to the ROPME Sea Area both now and in the future.

Acknowledgements

This research was funded under the UK-Gulf Marine Environment Partnership (UK-GMEP) Programme. Support for the authors was provided by Cefas in conjunction, where applicable, with host institutions (Lancaster University, UK; University of Gdańsk, Poland; University of Liverpool, UK; University of Łódź, Poland). In-region support was provided by the Environment Agency - Abu Dhabi, with review of initial species lists and vector/pathway analysis undertaken by the following regional and international experts in addition to those listed as co-authors: M. Antonpoulou (Emirates Nature WWF), R. Arthur (American University of Ras Al Khaimah), and J. El Kharraz (Middle East Desalination Research Centre). We would also wish to thank the following who provided support from within Cefas with regards to background information especially on vector/pathways: J. Elphinstone-Davis, D. Murphy and H. Tidbury. The authors of this manuscript have no conflicts of interest to declare. Photo credits for Graphical Abstract go to Dr. Baran Yoğurtçuoğlu for *Coptodon zillii*, Dr. Nurçin Killi for *Cassiopea andromeda,* Professor Jennifer Smith for *Hypnea musciformis,* Pixabay Bluefox-1998 for *Carcinus maenas* and Cefas for jars of algal samples.

Data sharing and data accessibility

The data that supports the findings of this study are available in the supplementary material of this article.

References

AGEDI. (2016). Final Technical Report: Regional Desalination and Climate Change. LNRCCP. CCRG/IO. 105 pp. doi: 10.13140/RG.2.2.33873.53608

Al-Yamani, F. Y., Saburova, M., & Polikarpov, I. (2012). A preliminary assessment of harmful algal blooms in Kuwait's marine environment. *Aquatic Ecosystem Health & Management*, *15*(*S1*), 64–72. doi: 10.1080/14634988.2012.679450

Al-Yamani, F. Y., Skryabin, V. & Durvasula, S. R. V. (2015). Suspected ballast water introductions in the Arabian Gulf. *Aquatic Ecosystem Health & Management 18(3),* 282–289. doi: 10.1080/14634988.2015.1027135

Anderson M. J., Gorley R. N., & Clarke K. R. (2008). PERMANOVA? for PRIMER: Guide to software and statistical methods. PRIMER-E Ltd, Plymouth.

Bailey, S. (2015). An overview of thirty years of research on ballast water as a vector for aquatic invasive species to freshwater and marine environments. *Aquatic Ecosystem Health and Management, 18*, 261–268. doi: 10.1080/14634988.2015.1027129

Bailey, S. A., & Munawar, M. (2015). A synthesis of marine invasive species research and management in the ROPME Sea Area. *Aquatic Ecosystem Health & Management, 18*, 347–354. doi: 10.1080/14634988.2015.1039917

Bewick, V., Cheek, L., & Ball, J. (2004). Statistics review 13: Receiver operating characteristic curves. *Critical Care*, *8*, 508–512. doi: 10.1186/cc3000

Bilge, G., Filiz, H., Yapici, S., Tarkan, A.S., & Vilizzi, L. (2019). A risk screening study on the potential invasiveness of Lessepsian fishes in the south-western coasts of Anatolia. *Acta ichthyologica et Piscatoria, 49*, 23–31. doi: 10.1016/j.marpolbul.2019.110728

Biofouling Guidelines**,** resolution MEPC.207(62): www.imo.org/en/OurWork/ Environment/Biofouling/Documents/RESOLUTION%20MEPC.207[62].pdf

Burt, J. (2014). The environmental costs of coastal urbanization in the Arabian Gulf. City: analysis of urban trends, culture, theory, policy, action. *City, 18*, 760–770. doi: 10.1080/13604813.2014.962889

5195 Burt, J., Al-Harthi, S., & Al-Cibahy, A. (2011). Long-term impacts of bleaching
5196 events on the world's warmest reefs. *Marine Environmental Research, 72*, 225–
5197 229. doi: 10.1016/j.marenvres.2011.08.005
5198 Cesar, H., Vanbeukerling, P., & Prince, S. (2002). An economic valuation of Hawaii's
5199 coral reefs. Hawai'i Coral Reef Initiative Research Program Final Report. 144 pp.
5200 Chan, F., Stanislawczyk, K. C., Sneekes, A., Dvoretsky, A., Gollasch, S., Minchin,
5201 D., … Bailey, S. (2019). Climate change opens new frontiers for marine species in
5202 the Arctic: Current trends and future invasion risks. *Global Change Biology, 25*,
5203 25–38. doi: 10.1111/gcb.14469
5204 Cohen, A. N. Carlton, J. T., & Fountain, M. C. (1955). Introduction, dispersal and
5205 potential impacts of the green crab *Carcinus maenas* in San Francisco Bay,
5206 California. *Marine Biology*, *122*, 225–237. doi: 10.1007/BF00348935
5207 Copp, G. H., Vilizzi, L., Tidbury, H., Stebbing, P. D., Tarkan, A. S., Moissec, L., &
5208 Goulletquer, P. (2016). Development of a generic decision-support tool for
5209 identifying potentially invasive aquatic taxa: AS-ISK. *Management of Biological*
5210 *Invasions*, *7*, 343–350. doi: 10.3391/mbi.2016.7.4.04.
5211 Costello, M. J., Coll, M., Danovaro, R., Halpin, P., Ojaveer, H., & Miloslavich, P.
5212 (2010). A census of marine biodiversity knowledge, resources, and future
5213 challenges. *PloS One, 5*(*8*). doi: 10.1371/journal.pone.0012110
5214 Elimelech, M., & Phillip, W. A. (2011). The future of seawater desalination: energy,
5215 technology, and the environment. *Science, 6043*, 712–717. doi:
5216 10.1126/science.1200488
5217 European Commission. (2014). Regulation (EU) No 1143/2014 of the European
5218 Parliament and of the Council of 22 October 2014 on the prevention and
5219 management of the introduction and spread of invasive alien species. *Official*
5220 *Journal of the European Union.* http://eur-lex.europa.eu/legal-
5221 content/EN/TXT/?uri=OJ:JOL_2014_317_R_0003
5222 FAO. (2017). Developing an Environmental Monitoring System to Strengthen
5223 Fisheries and Aquaculture Resilience and Improve Early Warning in the Lower
5224 Mekong Basin. Bangkok, Thailand, 25–27 March 2015, Workshop led by Virapat,
5225 C., Wilkinson, S. and Soto, D. *FAO Fisheries and Aquaculture Proceedings No.*
5226 *45.* Rome, Italy.
5227 Garbary, D. J., Miller, A. G., Williams, J., & Seymour, N.R. (2014). Drastic decline
5228 of an extensive eelgrass bed in Nova Scotia due to the activity of the invasive green

crab (*Carcinus maenas*). *Marine Biology*, *161*, 3–15. doi: 10.1007/s00227-013-2323-4

Glamuzina, B., Tutman, P., Nikolić, V., Vidović, Z., Pavličević, J., Vilizzi, L., Simonović, P. (2017). Comparison of taxon-specific and taxon-generic risk screening tools for identifying potentially invasive non-native fishes in the River Neretva catchment (Bosnia & Herzegovina and Croatia). *River Research and Applications*, *33*, 670–679. doi: 10.1002/rra.3124

Gustaaf M. H. (2015). Transport of harmful marine microalgae *via* ship's ballast water: Management and mitigation with special reference to the Arabian Gulf region. *Aquatic Ecosystem Health & Management, 18* (*3*), 290–298. doi: 10.1080/14634988.2015.1027138

Hewitt, C. L., Campbell, M. L., & Gollasch, S. (2006). Alien Species in Aquaculture. Considerations for responsible use. IUCN, Gland, Switzerland and Cambridge, UK. 46 pp.

Hoagland, P., Anderson, D. M., & White, A. W. (2002). Economic effects of Harmful algal blooms in the United States: Estimates, assessment Issues, and information needs. *Estuaries*, *25*, 819–837. doi: 10.1007/BF02804908

Hopkins, G., & Forrest, B. (2008). Management options for vessel hull fouling: An overview of risks posed by in-water cleaning. *Ices Journal of Marine Science 65,* 811–815. doi: 10.1093/icesjms/fsn026

IMO. (2009). Ballast Water Management Convention and Guidelines for its implementation. 2009 Edition, The International Maritime Organisation.

Innovation Norway. (2015). Aquaculture in the United Arab Emirates. Report. www.innovasjonnorge.no/contentassets/ eea93bbba18a4a4cb955a36c84159a02/aquaculture-in-uae-apr2015.pdf Accessed date: 26 December 2018.

IPCC. (2005). Guidance Notes for Lead Authors of the IPCC Fourth Assessment Report on Addressing Uncertainties. Intergovernmental Panel on Climate Change, WMO & UNEP. www.ipcc.ch/pdf/assessment-report/ar4/wg1/ar4-uncertaintyguidancenote.pdf Accessed date: 26 September 2018.

IPCC. (2007). Climate change 2007: the physical science basis. In: Solomon, S., Qin, D., Manning, M., Chen, Z., Marquis, M., Avery, K., … Miller, H. L. (Eds), Working Group I Contribution to the Fourth Assessment Report of the IPCC,

Technical Summary (Global Climate Projections), Chapter 10. Intergovernmental Panel on Climate Change.

Jenkins, S., Paduan, J., Roberts, P., Schlenk, D., & Weis, J. (2012). Management of Brine Discharges to Coastal Waters Recommendations of a Science Advisory Panel. Southern California Coastal Water Research Project. State Water Resources Control Board Technical Report 694. 101pp.

Kideys, A. E. (2002). Fall and Rise of the Black Sea Ecosystem. *Science, 297*, 1482–1484. doi: 10.1126/science.1073002

Klassen, G. J., & Locke, A. (2007). A biological synopsis of the European green crab, *Carcinus maenas*. Canadian Manuscript Report of Fisheries and Aquatic Sciences. 2818.

Le Quesne, W. J. F., Fernand, L., Ali, T. S., Andres, O., Antonpoulou, M., Burt, J., … Sheahan, D. (2019). Is the development of desalination compatible with sustainable development of the Arabian Gulf? *Desalination Journal* (in press)

Li, S., Chen, J., Wang, X., & Copp, G. H. (2017). Invasiveness screening of non-native fishes for the middle reach of the Yarlung Zangbo River, Tibetan Plateau, China. *River Research and Applications*, *33*, 1439–1444. doi: 10.1002/rra.3196

Lowe S., Browne M., Boudjelas S., & De Poorter M. (2000). 100 of the World's Worst Invasive Alien Species: A selection from the Global Invasive Species Database. Invasive Species Specialist Group (ISSG), World Conservation Union (IUCN), 12 pp. www.iucn.org/content/100-worlds-worst-invasive-alien-species-a-selection-global-invasive-species-database Accessed date: 13 June 2019.

Minchin, D., Gollasch, S., Cohen, A., Hewitt, C., & Olenin, S., (2009). Characterizing Vectors of Marine Invasion. Chapter 5 of: *Biological Invasions in Marine Ecosystems: Ecological, Management, and Geographic Perspectives*, pp.109-116.

Miza, S., Majiedt, P. & Sink, K., (2014). *Marine alien and invasive species*. Presentation given at the 2014 Biodiversity Planning Forum, 13-16 May, Mpekweni Beach Resort, Eastern Cape, South Africa.

O'Donnel, J. (2013). The Conservation Institute top 100 invasive species list. www.conservationinstitute.org/the-top-100-invasive-species/ Accessed date: 17 June 2019.

Ojaveer, H., Galil, B. S., Carlton, J. T., Alleway, H., Goulletquer, P., Lehtiniemi, M., ... Ruiz, G. M. (2018). Historical baselines in marine bioinvasions: Implications for policy and management. *PloS One*, *13*(*8*). doi: 10.1371%2Fjournal.pone.0202383

5296 Olenin, S.; Minchin, D.; Daunys, D.; Zaiko, A. (2010). Pathways of aquatic invasions
5297 in Europe. In: Settele, J., Penev, L. D., Georgiev, T. A., Grabaum, R., Grobelnik,
5298 V., Hammen, V., Klotz, S., Kotarac, M., Kühn, I., Eds., Atlas of Biodiversity Risk
5299 (pp. 138–139). Pensoft Publishers.
5300 Paparella, F., Xu, C., Vaughan, G. O., & Burt, J. A. (2019). Coral Bleaching in the
5301 Persian/Arabian Gulf is Modulated by Summer Winds. *Frontiers in Marine*
5302 *Science, 6* (205). doi: 10.3389/fmars.2019.00205
5303 Pilcher, N., Antonopoulou, M., Perry, L., Abdel-Moati, M., Zahran Al Abdessalaam,
5304 T., Albeldawi, M., … Willson, A. (2014). Identification of Important Sea Turtle
5305 Areas (ITAs) for hawksbill turtles in the Arabian Region. *Journal of Experimental*
5306 *Marine Biology and Ecology*, *460*, 89–99. doi: 10.1016/j.jembe.2014.06.009
5307 R Core Team. (2015) R: A language and environment for statistical computing. R
5308 Foundation for Statistical Computing, Vienna, Austria.
5309 Riefl, B. M., Purkis, S. J., Al-Cibahy, A. S., Al-Harthi, S., Grandcourt, E., Al-Sulaiti,
5310 K., … Abdel-Moati, A. M. (2012). Coral bleaching and mortality thresholds in the
5311 SE Gulf: highest in the world. *Coral Reefs World, 3*, 95–105. doi: 10.1007/978-94-
5312 007-3008-3_6
5313 Robin X, Turck N, Hainard A, Tiberti N, Lisacek F, Sanchez J. C., & Muller, M.
5314 (2011). pROC: an open-source package for R and S ? to analyze and compare ROC
5315 curves. *BMC Bioinform 12*, 77. doi: 10.1186/1471-2105-12-77
5316 Rockström, J., Steffen, W., Noone, K., Persson, Å., Chapin III, F. S., Lambin, E., ...
5317 Nykvist, B. (2009). Planetary boundaries: exploring the safe operating space for
5318 humanity. *Ecology and Society, 14*(*2*), 32.
5319 Roy, H. E., Rabitsch, W., Scalera, R., Stewart, A., Gallardo, B., Genovesi, P., …
5320 Zenetos, A. (2018). Developing a framework of minimum standards for the risk
5321 assessment of alien species. *Journal of Applied Ecology, 55*, 526–538. doi:
5322 10.1111/1365-2664.13025
5323 Ruggiero M. A., Gordon D. P., Orrell T. M., Bailly N., Bourgoin T., Brusca, R. C., …
5324 Kirk M. P. (2015). Correction: a Higher Level Classification of all Living
5325 Organisms. *PloS One 10*(*6*). doi: 10.1371/journal.pone.0130114
5326 Russell, D. J. (1992). The ecological invasion of Hawaiian reefs by two marine red
5327 algae, *Acanthophora spicifera* (Vahl) Børerg. and *Hypnea musciformis* (Wulfen)
5328 J.Ag., and their association with two native species, *Laurencia nidifica* J.Ag. and
5329 *Hypnea cervicornis* J.Ag. *ICES Marine Science Symposium, 194*, 110–125.

5330 Russell, D. J. & Balazs, G. H. (1994). Colonization by the alien marine alga *Hypnea*
5331 *musciformis* (Wulfen) J. Ag. (Rhodophyta: Gigartinales) in the Hawaiian Islands
5332 and its utilization by the green turtle, *Chelonia mydas*. *Aquatic Botany, 47*(*1*)*,* 53–
5333 60. doi: 10.1016/0304-3770(94)90048-5
5334 Sale, P. F., Feary, D., Burt, J. A., Bauman, A., Cavalcante, G., Drouillard, K., & Van
5335 Lavieren, H. (2011). The growing need for sustainable ecological management
5336 of marine communities of the Persian Gulf. *Ambio, 40*, 4–17. doi:
5337 10.1007%2Fs13280-010-0092-6
5338 Sheppard, C., Al-Husiani, M., Al-Jamali, F., Al-Yamani, F., Baldwin, R., Bishop, …,
5339 Zainal, K. (2010). The Gulf: a young sea in decline. *Marine Pollutution Bulletin,*
5340 *60*, 13–38. doi: 10.1016/j.marpolbul.2009.10.017
5341 Smith, O. R., Baptist, J. P., & Chin, E. (1955). Experimental farming of the soft-shell
5342 clam, *Mya arenaria* in Massachusetts, 1949–1953. *Commercial Fisheries Review,*
5343 *17* (*6*) 1–16.
5344 Tarkan, A. S, Sarı, H. M., İlhan, A., Kurtul, I., & Vilizzi, L. (2017a). Risk screening
5345 of non-native and translocated freshwater fish species in a Mediterranean-type
5346 shallow lake: Lake Marmara (West Anatolia). *Zoology in the Middle East*, *63*, 48–
5347 57. doi: 10.1080/09397140.2017.1269398
5348 Tarkan, A. S., Vilizzi, L., Top, N., Ekmekçi, F. G, Stebbing, P. D., & Copp, G. H.
5349 (2017b). Identification of potentially invasive freshwater fishes, including
5350 translocated species, in Turkey using the Aquatic Species Invasiveness Screening
5351 Kit (AS-ISK). *International Review of Hydrobiology*, *102*, 47–56. doi:
5352 10.1002/iroh.201601877
5353 Tidbury, H. J., Taylor, N. G., Copp, G. H., Garnacho, E., & Stebbing, P. D. (2016).
5354 Predicting and mapping the risk of introduction of marine non-indigenous species
5355 into Great Britain and Ireland. *Biological Invasions, 18*, 3277–3292. doi:
5356 10.1007/s10530-016-1219-x
5357 Trebitz, A. S., Hoffman, J. C., Darling, J. A., Pilgrim, E. M., Kelly, J. R., Brown, E.
5358 A., ... Schardt, J. C. (2017). Early detection monitoring for aquatic non-indigenous
5359 species: Optimizing surveillance, incorporating advanced technologies,
5360 and identifying research needs. *Journal of Environmental Management, 202*(*1*),
5361 299–310. doi: 10.1016/j.jenvman.2017.07.045
5362 United Nations. (2017). United Nations, Department of Economic and Social Affairs,
5363 Population Division. World Population Prospects: The 2017 Revision.

United Nations (2002). Report of the sixth meeting of the Conference of Parties to the Convention on Biological Diversity. Conference of Parties to the Convention on Biological Diversity. The Hague, 7–19 April 2002. UNEP/CBD/COP/6/20.

UN-ESCWA and BGR (United Nations Economic and Social Commission for Western Asia; Bundesanstalt für Geowissenschaften und Rohstoffe), (2013). *Chapter 5 of the Inventory of Shared Water Resources in Western Asia.* (pp. 147-162). Beirut: United Nations Publication.

Vaughan, G.O., Al-Mansoori, N. and Burt, J.A. (2019). World Seas: an Environmental Evaluation (2nd Ed.). pp. 1–23, Chapter 1 In Volume II: the Indian Ocean to the Pacific.

Van Lavieren, H., Burt, J., Feary, D. A., Cavalcante, G., Marquis, E., Benedetti, L., … Sale, P. F. (2011). Managing the growing impacts of development on fragile coastal and marine ecosystems: Lessons from the Gulf. A policy report, UNU-INWEH, Hamilton, ON, Canada.

Van Lavieren, H., & Klaus, R. (2013). An effective regional Marine Protected Area network for the ROPME Sea Area: Unrealistic vision or realistic possibility? *Marine Pollution Bulletin, 72*, 389–405. doi: 10.1016/j.marpolbul.2012.09.004

Vilizzi, L., Copp, G. H., Adamovich, B., Almeida, D., Chan, J., Davison, P. I., … Zeng. Y. (2019). A global review and meta-analysis of applications of the freshwater Fish Invasiveness Screening Kit. *Reviews in Fish Biology and Fisheries*, *29*, 529–568. doi: 10.1007/s11160-019-09562-2

Wabnitz, C. C. C., Lam, V. W. Y., Reygondeau, G., Teh, L. C. L., Al-Abdulrazzak, D., Khalfallah, M., … Cheung, W. W. L. (2018). Climate change impacts on marine biodiversity, fisheries and society in the Arabian Gulf. *PLOS ONE, 13*(*5*). doi: 10.1371/journal.pone.0194537

Werschkun, B., Banerji, S., Basurko, O. C., David, M., Fuhr, F., Gollasch, S., … Höfer, T. (2014). Emerging risks from ballast water treatment: the run-up to the international Ballast water management convention. *Chemosphere*, *112*, 256–266. doi: 10.1016/j.chemosphere.2014.03.135

Wilkinson, C., (2008). Status of Coral Reefs of the World. Australian Institute of Marine Science, Townsville.

Williams, S. L., & Grosholz, E. D. (2008). The invasive species challenge in estuarine and coastal environments: marrying management and science. *Estuaries & Coasts, 31*, 3–20. doi: 10.1007/s12237-007-9031-6

Yamada, S. B., Davidson, T. M., & Fisher, S. (2010). Claw morphology and feeding rates of introduced European green crabs (*Carcinus maenas L*, 1758) and native Dungeness crabs (*Cancer magister* Dana, 1852). *Journal of Shellfish Research*, *29*, 471–477. doi: 10.2983/035.029.0225

Zięba, G., Vilizzi, L. & Copp, G. H. (2019). How likely is pumpkinseed *Lepomis gibbosus* to become invasive in Poland under conditions of climate warming? *Acta Ichthyologica et Piscatoria* (in press).

5406 TABLE 1. TAXONOMIC AQUATIC ORGANISM GROUP-SPECIFIC THRESHOLDS FOR THE
5407 BASIC RISK ASSESSMENT (BRA) AND BRA+CCA (CLIMATE CHANGE ASSESSMENT) OF
5408 THE NON-NATIVE SPECIES (EXTANT AND HORIZON: SEE TABLES S1 AND S2,
5409 RESPECTIVELY) SCREENED WITH AS-ISK FOR THE INNER AND MIDDLE RSA (SEE
5410 TABLE S3). MEAN, LOWER CONFIDENCE INTERVAL (LCI) AND UPPER CONFIDENCE
5411 INTERVAL (UCI) FOR THE AREA UNDER THE CURVE (AUC) ARE PROVIDED.

	BRA				BRA+CCA			
Aquatic organism group	**Thr**	**AUC**	**LCI**	**UCI**	**Thr**	**AUC**	**LCI**	**UCI**
Fishes and lampreys (brackish)	30.50	0.959	0.864	1.000	22.50	0.898	0.710	1.000
Fishes and lampreys (marine)	19.75	0.928	0.811	1.000	21.75	0.792	0.547	1.000
Tunicates	34.25	0.765	0.436	1.000	34.25	0.906	0.701	1.000
Invertebrates (brackish)[1]	26.25	0.717	0.575	0.859	20.50	0.720	0.574	0.867
Invertebrates (marine)	26.25	0.734	0.591	0.878	20.50	0.730	0.576	0.884
Plantae (marine)[2]	27.50	0.785	0.512	1.000	28.25	0.633	0.534	0.731
Protista (marine)[2]	28.50	0.659	0.382	0.937	28.25	0.633	0.534	0.731

5412 [1] BRA AND BRA+CCA THRESHOLDS FROM COMBINED BRACKISH AND MARINE
5413 INVERTEBRATES.

5414 [2] BRA+CCA THRESHOLDS FROM ALL TAXONOMIC GROUPS COMBINED.

5415

Lee *et al*. (2020)

Title: **A new framework for growth curve fitting based on the von Bertalanffy Growth Function.**

Authors: Laura Lee[1*], David Atkinson[1], Andrew G. Hirst[2,3], Stephen J. Cornell[1]

[1]Department of Evolution, Ecology and Behaviour, University of Liverpool, UK

[2]School of Environmental Sciences, University of Liverpool, UK

[3]Centre for Ocean Life, National Institute for Aquatic Resources, Technical University of Denmark, Kemitorvet, 2800 Kgs, Lyngby, Denmark

*Corresponding author: lauralee@liverpool.ac.uk

Abstract

All organisms grow. Numerous growth functions have been applied to a wide taxonomic range of organisms, yet some of these models have poor fits to empirical data and lack of flexibility in capturing variation in growth rate. The von Bertalanffy Growth Function (VBGF) has prevailed for modelling animal growth trajectories, but authors often impose restrictions in the parameterisation which limits the range of possible growth curves. We propose a new VBGF framework that broadens the applicability and increases flexibility of fitting growth curves. This framework offers a curve-fitting procedure for five parameterisations of the VBGF: these allow for different body-size scaling exponents for anabolism (biosynthesis potential), besides the commonly assumed $\frac{2}{3}$ power scaling, and allow for supra-exponential growth, which is at times observed. This procedure is applied to twelve species of diverse aquatic invertebrates, including both pelagic and benthic organisms. We reveal widespread variation in the body-size scaling of biosynthesis potential and consequently growth rate, ranging from isomorphic to supra-exponential growth. This curve-fitting methodology offers improved growth predictions and applies the VBGF to a wider range of taxa that exhibit variation in the scaling of biosynthesis potential. Applying this framework results in reliable growth predictions that are important for assessing individual growth, population production and ecosystem functioning,

including in the assessment of sustainability of fisheries and aquaculture.

[Keywords: growth modelling, von Bertalanffy, aquatic invertebrates, allometry]

Introduction

Body size is a fundamental characteristic of all organisms. Body size has received much attention from biologists owing to its widespread covariation with a plethora of ecological and evolutionary functions and physiological traits[1,2,3,4,5,6,7,8,9]. Understanding growth (i.e. the changes in body size over time) is fundamental to many areas of biology, as well as being crucial for industries based on animal and plant production. Accurate growth predictions are fundamental to aquaculture and production industries, for example, over- or underestimating species growth will result in unreliable predictions of production and hence revenue and profit for producers[10]. For example, modelling the growth rates of farmed tiger prawns, *Penaeus monodon*, under varying environmental conditions including temperature and pond age, allows for predictions of production rates, and hence profitability, in new farming locations[11]. Moreover, gaining knowledge of growth parameters can help to inform management plans, which are required for effective conservation management of target species in aquaculture or reducing pressure on natural populations[12]. For example, growth models have predicted parameter values associated with slow growth and long lifespan in *Stichopus vastus* which has helped inform restrictions on catch quotas to allow natural populations to recover[13]. In addition, understanding growth dynamics has been shown to be important for bivalve species in aquaculture and their use in mitigating eutrophication in coastal areas, for example, gaining accurate growth predictions of soft tissue can help the efficiency of mussel production that is required for eutrophic coastal waters[14].

Methods for fitting growth curves to empirical data are applied extensively[15,16,17,18,19,20,21,22,23,24,25], but many of these approaches can be taxon-specific and lack flexibility to capture variation in growth over ontogeny or between conditions[26]. We propose a new framework for fitting growth curves which applies a set of re-parameterisations of the von Bertalanffy Growth Function (VBGF). This framework improves on existing methods by allowing for growth-curve fitting to a

wide range of taxa which may exhibit variation in rates of growth, including exponential and supra-exponential growers.

The VBGF has been used extensively to model growth for numerous taxa such as fish[27], mammals[28], birds[29], invertebrates[30,31] and dinosaurs[32]. It is a special case of the Richards model[19] and is based on biological principles originally developed by Pütter[33]. The mechanistic interpretation of the VBGF has varied over time, but most commonly growth is argued to occur if the building up of materials prevails over the breakdown of materials[34,35] as denoted by the differential equation:

$$\frac{dm}{dt} = Hm^A - Km^B, \quad (1)$$

where m denotes mass, t is time from birth or hatch, A, B are the mass-scaling exponents of anabolism (synthesis of component materials) and catabolism (breakdown of component materials) respectively, and H and K are the coefficients of anabolism and catabolism, respectively[35]. The Hm^A term in equation (1) can represent the resource availability for growth in an organism, with the mass-scaling exponent A often assumed to relate to the body-mass scaling of surface area available for resource uptake, from which non-growth metabolism (referred to as catabolism by von Bertalanffy[35]) is then subtracted to obtain growth. Therefore, we hereafter refer to 'anabolism' as 'biosynthesis potential'. The Km^B term on the right-hand side of equation (1) represents resource consumption by tissues and is often proposed to scale in proportion to body mass[35], i.e. $B = 1$, though we will discuss potential causes of deviation from this value later.

A common assumption imposed on the VBGF is isomorphic scaling of biosynthesis potential, corresponding to growth without change in body shape, represented by the commonly chosen Euclidean value of $\frac{2}{3}$ for the mass-scaling exponent, A. This assumption is widely imposed despite recognition from von Bertalanffy of the potential range of values for A, for example, rod-like bacteria that grow in one-dimension of length ($A = 1$), with volume increasing proportionally to length and to surface area for resource uptake[35].

The Schnute model is a four-parameter growth model developed by Schnute[36] often applied in aquaculture research[37,38]. The Schnute model has been proposed as

superior to the VBGF for modelling growth of aquaculture species including the spotted rose snapper[39], *Lutjanus guttatus*, and turbot[40], *Scophthalmus maximus*. However, comparisons made between the Schnute model and the VBGF often apply the common parameterisation of $\frac{2}{3}$ scaling of parameter A (equation (1))[40], which limits the range of growth curves that can be captured. Additionally, Yuancai, Maraques & Macedo[41] show through analytical transformation, that the Schnute model and the generalised VBGF (equation (1)) can be formally equivalent despite having different function forms and parameters: the two models gave the same growth predictions for stand density of *Eucalyptus grandis*. Therefore, by considering the flexibility of the VBGF a wide range of growth types can be captured and accurate predictions of growth can be achieved.

Restriction in the parameterisation of the mass-scaling of biosynthesis potential is also present in the Gompertz model[42] which has been used to model growth of plants, birds, fish, mammals, tumour cells and bacteria[43]. Like the VBGF, the Gompertz model is also part of the Richards growth model family[19] where it is a special case of both the VBGF and Richards model where a complementary limit arises when $A \rightarrow 1^{-}$, where $K(A - 1)$ is fixed[19]. As the Gompertz model is achieved by calculating the body-size scaling of biosynthesis potential as a limit ($A \rightarrow 1^{-}$) it assumes an exponential decline in absolute growth rate with body size, making it inappropriate for taxa displaying other growth types that range from isomorphic to supra-exponential. For example, during ontogeny thaliacean organisms, such as salps and doliolids[44], exhibit increasing relative growth rate (RGR), the rate of body mass increase per unit mass per unit time, and thus have potential for supra-exponential growth.

Other well-known models with the same mathematical structure as the VBGF include the Dynamic Energy Budget (DEB) and the ontogenetic growth model (OGM), an extension of the 'West, Brown and Enquist' (WBE) model for metabolic scaling[45], which has been developed and improved over time[46,47,48]. The OGM predicts the rate of energy devoted to growth is equal to the rate of assimilation of metabolic energy (the 'anabolic' term) minus the rate of energy allocated to maintenance (the 'catabolic' term). Although the mathematical structure is the same as the VBGF (equation (1)) the mechanism of growth varies. The OGM assumes a

mass-scaling exponent of biosynthesis potential[48] (assimilation) of $\frac{3}{4}$. As a result, application of the OGM to taxa with differing mass-scaling of resource supply is likely to result in poor-fitting growth curves and inappropriate predictions. Further, Hirst & Forster[49] found poor fit of the WBE to marine invertebrate growth data due to overestimating body size early in ontogeny and underestimating later in ontogeny.

We suggest that parsimonious versions of the VBGF may provide better fits, and incorporate more biologically meaningful parameters, than some other simple equations, such as the logistic model. The logistic model[50] is regarded as the simplest of sigmoidal growth models with its symmetry about the point of inflection as given by the parameterisation[51] $L_t = \frac{L_\infty}{1+e^{-c(t-1)}}$. Shi *et al.*[52] compared the performance of the OGM with the logistic model and a generalised VBGF given by: $L_t = L_\infty[1 - \exp(-KD(t - t_0))]^{1/D}$ where the mass-scaling exponent of biosynthesis potential (A) ranges between 0.5 and 1. Based on Akaike Information Criterion (AIC) scores, the logistic model was found to be best fit for late-larval stage empirical growth data for three fish species. However, for all cases the value for A for the VBGF was 1.0, suggesting that more parsimonious models such as the Gompertz or Exponential model may better fit the data where $A \to 1^-$ and $A = 1$, respectively. Shi *et al.*[52] argue that using a generalised version of the VBGF results in poor predictions of parameters, K and t_0, but this may be resolved by applying the Gompertz or Exponential parameterisation of the VBGF. Additionally, it is unknown what a "good" prediction of t_0 in the generalised VBGF is, considering that t_0 is a mathematical artefact representing time at zero body mass and the biological interpretation of K is debatable[53]. Furthermore, the authors determine goodness of fit of these models through use of R-squared, a method which is inappropriate for non-linear models[54,55].

Despite the numerous debated biological mechanisms underpinning growth models, discussed above, the VBGF (equation (1)) often prevails as a mathematical growth function, which can be parameterised in many ways to capture variation in RGR. Recent studies have highlighted growth curve diversity through the variation in the mass-scaling exponent of biosynthesis potential, A. Insects, for example, seldom grow isomorphically; instead, mass often scales almost in proportion to surface area, and the growth curve is near-exponential[56]. Thus it can be predicted that $\frac{2}{3} < A < 1$ for insect growth. Maino and Kearney[57] found support for this hypothesis, with

reported values of A between $\frac{3}{4}$ and 1 for the mass-scaling exponent of consumption and assimilation in 41 insect species. In addition, if oxygen uptake at rest is considered to be proportional to biosynthesis potential (as oxygen fuels both growth and non-growth, even at rest[58], estimates of values of A may be derived from the mass-scaling of resting or routine metabolic rates. Thus, Killen *et al.*[59] report values between $\frac{2}{3}$ and 1 for the body size scaling of resting metabolic rate for 89 species of teleost fish. The lack of universality in the mass-scaling of biosynthesis potential, if assumed to be proportional to routine metabolic rate, has also been highlighted within invertebrate species, which display a diverse range in the mass-scaling of oxygen consumption[60,61,62]. If the mass-scaling of metabolic rate does not hold universally it is suggestive that neither does the mass-scaling of growth, since growth is fuelled by metabolism (albeit only a component of the total respiration rate may relate to the costs of biosynthesis potential).

The above arguments highlight that when fitting growth curves to empirical data, a single fixed value or limit, for the body mass-scaling exponent of biosynthesis potential is unlikely to hold universally. Therefore, it is proposed that growth-curve fitting methods should not pre-determine this exponent, but instead allow for and test for all plausible possibilities. The importance of applying a multimodel approach to fitting growth curves has been shown by Reynaga-Franco *et al.*[38] where different growth models were favoured by AIC for *Crassostrea gigas* raised under identical conditions. Evidence[62,63] suggests most variation among diverse aquatic taxa relates to scaling of surface area, and hence to the scaling of biosynthesis potential (Hm). By contrast, we argue that the scaling of non-growth metabolism or catabolism (Km) varies less among organisms, and as assumed by von Bertalanffy[35] and Kooijman[64,65], scales approximately linearly with body mass where $B = 1$. We recognise that this assumption is contentious and may require modification for certain taxa, where catabolism (or maintenance) does not necessarily scale in proportion to body volume, such as when the proportion of body composition taken up by non-metabolising fat reserve increases during ontogeny, as reported in some insects[57].

Previous work by Ohnishi *et al.*[66] addressed the need to allow mass-scaling exponents to vary when applying the VBGF to organisms. These authors developed a standardised form of the VBGF which allowed variation in both exponents A and B.

However, the derivation of their solution effectively ensures that the value of exponent A cannot exceed exponent B. Consequently, if we are to fix $B = 1$, we cannot estimate values of A greater than 1. This becomes problematic when organisms have supra-exponential growth ($A > 1$) such as in thaliaceans, as discussed above. In addition, Ohnishi *et al.* do not give methods for calculating confidence intervals or comparing estimates of exponent A to obtain a best-fit value for an organism.

Growth rate has been shown to correlate with many life-history traits, such as fecundity and lifespan for numerous taxa including fish[67,68], reptiles[69], arthropods[70,71], mammals[72,73] and tetrapods[74], making it a key determinant of organism fitness[75]. Therefore, our aim is to improve the flexibility and applicability of current growth-curve fitting methods by offering a new framework, based on the widely known VBGF (equation 1), that allows for diverse growth types (including both isomorphic and non-isomorphic) by applying a set of re-parameterisations that allow variation in the mass-scaling of biosynthesis potential. Marine invertebrates display diverse variation in the mass-scaling of growth and metabolic rate[61,62,76] and thus provide an ideal group to test the applicability of this framework. Further, it has been shown by Glazier[76] that pelagic and benthic invertebrates display marked variation in their metabolic mass-scaling relationships, with pelagic species having significantly greater metabolic mass-scaling exponents than benthic species. By exploring both open-water and bottom-dwelling invertebrate species we are able to capture potential diversity in growth rate that may be attributed by differences in lifestyle and environmental conditions.

Materials and methods

Developing candidate growth models

The solution[19] to the original VBGF (equation (1)) when $B = 1$ is:

$$m = m_0 \left\{ \frac{1 - (1 - Z)\exp\big(K(A-1)(t - t_0)\big)}{Z} \right\}^{-\frac{1}{A-1}} \quad (2)$$

where m_0 represents mass m at time t_0 (time at birth/ hatch). The mass-scaling exponent for biosynthesis potential is given by A and the rate at which final mass is

reached is represented by parameter K. Parameter $Z = \left(\frac{m_\infty}{m_0}\right)^{A-1}$, where $m_\infty = \left(\frac{H}{K}\right)^{1/(1-A)}$, has no simple biological interpretation. While equation (2) represents a valid solution for all $A > 0$, it is not the most suitable form for fitting to data because of collinearity of parameters, and because the expression is singular when $A = 1$. We find that different parameterisations are appropriate for the parameter A, corresponding to the Pure Isomorphy model (VBGF) and four nested non-isomorphic growth models: Exponential, Gompertz, Generalised-VBGF and Supra-exponential. These five parameterisations represent different categories of relative growth rate (RGR) (i.e. the body mass increase per unit mass per unit time)[77], including constant RGR over time (Exponential model), decreasing RGR over time (Gompertz, Generalised-VBGF and Pure Isomorphy models) and increasing RGR over time (Supra-exponential model). For full derivation of equation (2) and further detail of the five parameterisations see Supplementary Appendix I.

(vi) Parameterisation of the Exponential model

When $A = 1$ relative growth rate is constant and growth is purely exponential, which yields the solution

$$m = m_0 \exp\big(k(t - t_0)\big) \tag{3}$$

Where $k = H - K$. Firstly, we fit this model by setting m_0 as the mass at the first time point. This solution involves fitting just one parameter, k. Parameter k is estimated iteratively, after inputting the reasonable start value of 0.1. This estimate is subsequently used as a starting value, along with m_0 as the mass at the first time point, for the subsequent model run where we fit parameter m_0.

(vii) Parameterisation of the Gompertz model

The Gompertz model is a generalisation of the exponential model and a special case of the General-VBGF[35] where RGR decreases over time as the exponent of biosynthesis potential, A, approaches limit $A \to 1^-$, represented by a second parameterisation (b, k) (see Supplementary Appendix 1 for derivation):

$$\lim_{A\to 1^-} m = m_0 \exp\left[-b\left(\exp(-k(t-t_0)-1)\right)\right] \quad (4)$$

When parameter m_0 is initially fixed and t_0 is known, this involves estimating two parameters: b and k. Starting values for k are taken from the estimates of the exponential model, and the starting value for b is chosen so that the asymptotic mass predicted by the model is twice the largest mass in the data. The justification is that the starting value must be larger than the largest mass in the data set for the fitting to work. If this value is too much larger, then the fit will be indistinguishable from an exponential solution and so the fitting will struggle to identify the asymptote, which makes a factor of two a good compromise to ensure the inflection in the model is tested against the data.

(viii) Parameterisation of the Generalised-VBGF

The Generalised-VBGF allows for non-isomorphic growth where RGR decreases over time where the mass-scaling exponent A can hold a value between 0 and 1. We encountered problems when fitting the model by varying the parameters A, Z, and K, because of strong collinearity between A and K, and because of numerical roundoff errors when Z was close to 1. We therefore fitted the model by varying the parameters (A, f, k) where $k = (A-1)K$ and $f = 1 - Z$. In terms of these parameters, equation (2) can be written as:

$$m = m_0 \left\{\frac{1 - f\exp\left(-k(t-t_0)\right)}{1-f}\right\}^{-\frac{1}{A-1}} \quad (5)$$

The parameter range that represents biological growth is $0 < f < 1$, $0 < A < 1$, $k > 0$.

When A is close to 1 we expect k to be similar to its value in the Gompertz model and so we apply the estimates from the Gompertz model as starting values for the Generalised-VBGF. The initial values for the other parameters are given by:

$$(1 - A) = \min\left(a_{max}, \frac{f_{max}}{max(b)}\right) \quad (6)$$

$$f = (1 - A)\max(b) \quad (7)$$

where a_{max}, f_{max} are chosen numbers between 0 and 1, and $\max(b)$ is the largest fitted value of b (amongst all individuals of the species under consideration) from the Gompertz model. This ensures that the initial values of f and A are in the biologically relevant range.

(ix) Parameterisation of the Pure Isomorphy model

Under three-dimensional Euclidean geometry, growth that is purely isomorphic is represented by the fixed value of $\frac{2}{3}$ for the mass-scaling exponent, A, and hence is a reduced version of the Generalised-VBGF where $A = \frac{2}{3}$. This means only two parameters are estimated: f and K from starting values obtained from the estimates given by the Generalised-VBGF.

(x) Parameterisation of the Supra-exponential model

The case $A > 1$ occurs when RGR increases over time and corresponds supra-exponential growth, but the model exhibits biologically unrealistic behaviour, such as infinite mass, unless the parameter values are chosen with care. To avoid this, the optimiser varied parameters Z, α, and s, where $\alpha = \frac{1}{A}$, $s = -(t_{max} - t_0)\frac{K(A-1)}{\log(1-Z)}$ and t_{max} is the largest value of t in the data set for the individual in question. The full biologically relevant parameter space corresponds to each of Z, α, and s being constrained to lie between 0 and 1. To give the original biological parameters we invert the estimates by the transformations:

$$m_\infty = m_0 Z^{\frac{1}{A-1}} \quad (8)$$

$$A = \frac{1}{\alpha} \quad (9)$$

$$K = -\frac{s\log(1 - Z)}{(A - 1)(t_{max} - t_0)} \quad (10)$$

Candidate starting values for these parameters are chosen so that the solution is close to the fitted exponential model. To achieve this, we choose Z to be small, A to be just greater than 1, and $K = kZ$ (where k is taken from the exponential model fit). We then use the above formulae to compute the corresponding values of α, and s.

Fitting and assessing candidate growth models

Model fitting in R

The five candidate models were fitted to empirical mass-time data with log least-squares method of optimisation by using the general-purpose optimisation function *optim()* in R (v3.5.0) (see Supplementary R code and Supplementary Appendix II for user guide). This function was chosen for its robust method of applying Nelder-Mead algorithms. Since optim() does not allow constrained Nelder-Mead optimisation, biological parameters were transformed (using a log or logit transform) so the biologically meaningful range corresponded to $(-\infty, \infty)$ in the space explored by optim().

Optimisation initially fitted the models with the m_0 parameter fixed at the first empirical mass value. Parameter estimates gained from this optimisation were consequently used as starting parameters for optimisation where the m_0 parameter was estimated. It is often unrealistic that the first recorded mass value is the precise mass at time zero (at birth or hatch) and so only the optimised parameter estimates for model fitting where m_0 was estimated were used in subsequent analysis. Hence, the purpose of carrying out optimisation where m_0 is fixed at the first empirical mass value was to produce reasonable starting values for *optim()*.

Log least-squares fitting was chosen over least-squares because it allows for more weighting of error at smaller mass values. This comes from the reasoning that it is biologically realistic to assume fluctuations in growth rate between individuals are proportional to body size, i.e. individuals will grow similarly initially but display more variation in size (mass) later in life. To determine the best fitting value for the mass-scaling exponent of biosynthesis, A, the model with the most negative log likelihood value was taken as the best fit model. Confidence intervals for parameter A were constructed using profile likelihood in R (v3.5.0) (see Supplementary appendix I for

user guide on executing the relevant R code). We use a purely likelihood-based approach, rather than the Akaike Information Criterion, because our focus is on providing a confidence interval for the parameter A rather than in selecting which single model (i.e. value of A) to use for forecasting. The 95% confidence intervals show the range of values of A that would not be rejected as a null model, and hence are consistent with the data.

The data set

Aquatic invertebrates assimilate resources through different body surfaces, for example, integument and/or gills for oxygen uptake. Differences in environmental conditions (e.g. predation) that exist between benthic and pelagic habitats of aquatic invertebrates may affect the mass-scaling of an organism's uptake of resources. For example, high predation risk throughout ontogeny in the sunlit epipelagic zone, which lacks refuges from predators, may lead to the evolution of steeper mass-scaling of resource uptake, compared with more benthic conditions where invertebrates can reduce predation risk by finding refuge[78,79,80]. The diversity in the mass-scaling of biosynthesis potential makes benthic and pelagic invertebrate species two ideal groups to explore variation in the mass-scaling exponent of biosynthesis potential (A) when fitting the VBGF.

Published ontogenetic mass-at-age data were collected for seven pelagic and five benthic invertebrate species using Web of Knowledge. Search terms included "growth AND pelagic AND (lab* OR cultur* OR ontogen* OR development*)" for pelagic species and "growth AND benthic AND (lab* OR cultur* OR ontogen* OR development*)" for benthic species. We chose species based on availability of growth data that conforms to the specific requirements described below. To provide a diverse sample of growth curve fits to empirical data, we chose species comprising both gelatinous and non-gelatinous zooplankton across four phyla: Arthropoda, Cnidaria, Chordata and Mollusca. Species were considered pelagic or benthic based on the zone inhabited by the developmental stage in which growth data was obtained from. For example, for many adult benthic invertebrates the larval stage occurs in the pelagic zone, e.g. many decapod species that occur in the pelagic zone during their zoeal stage before migrating to their benthic habitat. The species used in analysis were as follows.

Pelagic: *Daphnia magna* (Branchiopoda)[81] *Pelagia noctiluca* (Scyphozoa)[82], *Euphausia pacifica* (Euphausiacea)[83], *Oikopleura dioica* (Appendicularia)[84], *Aurelia aurita* (Scyphozoa)[85], *Cyanea capillata* (Scyphozoa)[86] and *Crassostrea gigas* (Bivalvia)[87]. Benthic: *Mytilus edulis* (Bivalvia)[88], *Sepia officinalis* (Cephalopoda)[89], *Echinogammarus marinus* (Amphipoda)[90], *Cherax quadricarinatus* (Decapoda)[91] and *Petrarctus demani* (Decapoda)[92]. Species identities were checked using the World Register of Marine Species (WoRMS) to ensure accepted names were used.

When required, data were extracted from graphs using the software WebPlotDigitizer (Rohatgi, 2017). Data were accepted if collected under controlled and constant environments; field data were therefore excluded. Mass data selected were from time at hatch until reproductive maturity and did not include data from mature animals. We used the time of reproductive maturity determined by the authors themselves, or, when this was unavailable, an approximate age at maturity at the given temperature was obtained from the scientific literature. Data for *C.gigas*, *A.aurita* were from pelagic larvae or juveniles and *M.edulis* data were from benthic juveniles, and did not include growth data up to maturity (incomplete juvenile development) due to lack of available data that conform to our data requirements. Therefore, we recognise that for these three species utilising data across larger parts of life history may result in different model fits. Our data requirements were as follows. Growth data were not collected when conditions included starvation, predation or toxin treatments or temperatures/salinities beyond the normal range encountered by the species in its natural setting. Mass type (either dry, ash-free or wet), treatments, culture conditions, developmental stages, sex and site of origin were also recorded. If only length data were available, we applied published length-mass conversion equations for a given species.

Results

Comparison of models across species

The negative log likelihood values for the five candidate re-parameterisations of the von Bertalanffy Growth Function (VBGF) showed that there was no universal agreement in best-fitting VBGF model across the twelve pelagic and benthic invertebrate species with a range of best-fitting values for the mass-scaling exponent of biosynthesis potential, A, between 0.72 and 1.22 (Table 1) (see Supplementary Appendix I Table S1 for negative log likelihood values). Both pelagic and benthic species displayed the same mixture of best-fitting models including the Generalised-VBGF, Gompertz and the Supra-exponential model (Figures 1 and 2). The Generalised-VBGF was found to be the best fit for 58% (7 out of 12) of species, followed by the Gompertz (25%) and Supra-exponential (17%) model (Table 1). The two models where parameter A remains fixed, the Exponential and Pure Isomorphy model, were not found to be the best fit for any species.

Comparison of models across taxa

Across the arthropods the Generalised-VBGF was the best fit for all four malacostracan species (Table 1), whereas the branchiopod *Daphnia magna* had a growth trajectory best fit by the Gompertz model (Figure 1). Cnidarian species *Pelagia noctiluca* (Figure 1) and *Cyanea capillata* (Figure 2) both displayed decreasing RGR with the Generalised-VBGF model (where A = 0.76 and 0.92, respectively), whereas, during an incomplete juvenile development, the cnidarian *Aurelia aurita* (Figure 2) displayed increasing RGR with the Supra-exponential model as the best fit (A = 1.22) (Table 1). The appendicularian, *Oikopleura dioica*, also displayed supra-exponential growth where A = 1.12 (Figure 1). Across the molluscs, there was no universal agreement in best-fitting model for the incomplete developmental growth of the two bivalve species, *Mytilus edulis* and *Crassostrea gigas* agreeing with the Generalised-VBGF and the Gompertz model, respectively and the benthic cephalopod *Sepia officinalis* agreeing with the Gompertz model (Table 1).

Discussion

A range of values for the mass-scaling exponent of biosynthesis potential, A, ($0.72 < A \leq 1.22$) (Table 1) highlights the diversity of growth curves amongst species (Figures 1 and 2). This proposed framework for fitting growth curves provides improved predictions of growth and increased model validity for species displaying growth curves that differ from commonly fixed values of the mass-scaling of synthesis such as $\frac{2}{3}$ (isomorphic growth) or 1 (pure exponential growth). This includes two cases of supra-exponential growth (where $A > 1$) found in the appendicularian *Oikopleura dioica* (Figure 1) and during part of juvenile development of the scyphozoan *Aurelia aurita* (Figure 2) (Table 1). Widespread diversity in the mass-scaling of biosynthesis potential highlights the range of growth curves present amongst organisms. This brings into question current methods of growth curve-fitting which impose a fixed value, limit or range for exponent A that are unable to capture variation in the mass-scaling of biosynthesis potential, and consequently growth rate.

Both pelagic and benthic species displayed variation in the best-fitting model, suggesting that there is no general difference in pattern of growth between pelagic and benthic species or ontogenetic phases, although a larger sample would be required to test this more definitively. Generally, there was no trend between best-fitting model and taxonomic group, except for the malacostracan crustacean growth curves, which all agreed with the Generalised-VBGF (Table 1). The Generalised-VBGF is a flexible model, allowing A to vary between 0 and 1, so even though all malacostracan species display the same best-fitting model they show diversity in exponent A. This lack of consensus in the best-fitting growth model within taxonomic groups in this study indicates a potentially problematic issue with applying a single growth model when studying specific taxonomic groups.

Gaining accurate predictions of exponent A can aid biological understanding and open up new hypotheses. For example, the steep mass-scaling ($A = 1.12$) of *O.dioica* during ontogenetic growth prompts suggestions about the selective effects on growth of mortality risk in an open-water environment. With no refuges from predators, rapid sustained uptake of resources may be required to reach maturity fast before being consumed[79,80]. The scyphozoan *Pelagia noctiluca* also exists within a high-mortality pelagic environment but instead exhibits a shallower mass-scaling of

biosynthesis potential ($A = 0.76$). This difference in exponent can prompt hypotheses about selective differences in mortality risks, including whether mortality reduces as size increases, or whether energy is invested into functions other than growth such as locomotion and/or buoyancy mechanisms. Furthermore, variation in the mass-scaling of biosynthesis potential was also present amongst benthic species (Table 1). For example, the common cuttlefish, *Sepia officinalis,* exhibits rapid exponential growth where relative growth rate (RGR) is constant ($A = 1$) (Figure 2), whereas the amphipod *Echinogammarus marinus* displays decreasing RGR where $A = 0.79$ (Figure 2). Despite partial covering of sand/seaweed, the predation risk for *S.officinalis* may be high considering the lack of parental care of eggs and high rates of cannibalism[93]. The relatively short lifespan of one to two years for *S.officinalis*[94] supports the idea that sustained rapid growth is required to reach maturity before dying. In contrast, *E.marinus* lives sheltered under algae, mud and/or rocks and exhibits egg development fully within the brood pouch[90]. These features are indicative of low mortality risk throughout development, suggesting that gains in survival may accrue from investing in survival at the expense of sustained rapid feeding and exponential growth. Thus, fitting growth curves under this proposed framework helps formulate specific testable hypotheses about the selective effects of an organism's ecology on their growth.

The lack of universal agreement in the best-fitting growth model suggests applying a single parameterisation is not necessarily the best method of fitting growth curves to data. Instead, using a framework based on a set of parameterisations of a prevailing mathematical function increases flexibility (by allowing for variation in A). Flexibility enables us to find the best-fitting model with reliable predictions of growth and capture variation in growth rate, i.e. isomorphic and non-isomorphic growth. Ultimately, this framework enhances model applicability to a wider range of taxa. To further test and explore this framework, future work should focus on testing the validity of the $B = 1$ assumption for the mass-scaling of maintenance often made in the VBGF. It was assumed by von Bertalanffy[35] that $B = 1$ on the basis that maintenance costs are approximately proportional to body mass. However, for some organisms, body mass composition can change throughout ontogeny, for example, insects have been shown to have increasing energy reserves (non-metabolising body mass) with age, which results in reduced mass-specific maintenance costs[57].

Therefore, we recognise the need for flexibility in parameter B for certain animal groups where maintenance does not scale in proportion to body mass.

To achieve accurate predictions of growth rates, the pattern of growth must be accurately captured by the growth model. The common $\frac{2}{3}$ parameterisation (Pure Isomorphy model) of the VBGF captures sigmoidal growth patterns whereby growth rate declines over time[35]. For organisms where mass-specific growth rate is maintained (exponential growth) or increased (supra-exponential growth) a sigmoidal growth function will predict lower than expected mass-specific rates of growth over time – resulting in poor predictions of growth. Our results show that while the five VBGF models can produce almost indistinguishable growth predictions in some cases, for example the Gompertz and Generalised-VBGF model for larval *Crassostrea gigas* (Figure 1), over the twelve species (Figures 1 and 2) the five models can show great differences in growth predictions for given data. For example, applying the Pure Isomorphy model to *S.officinalis* (Figure 2) would underestimate late juvenile growth whereas the Supra-exponential and Exponential models would overestimate this growth.

Instead, the proposed growth curve fitting procedure for the five parameterisations of the VBGF allows the optimal value for exponent A to be found which results in the most accurate predictions of growth obtained by the VBGF. Hence, this procedure offers application of the VBGF to a wider range of taxa such as marine invertebrates which have previously poorly fitted the VBGF[49]. Modelling growth of marine invertebrates has proved difficult, for example, in sea cucumbers owing to their naturally flaccid bodies and ability to shrink in size (degrow)[95], but accurate growth predictions are key to understanding how well species may survive in specific environmental conditions.

Extensive and successful use of the VBGF occurs for numerous fish species to aid the understanding of growth in relation to reproduction[68], fishing mortality[96] and environmental temperature[97], all of which are relevant to the sustainability of aquaculture. By applying this growth curve-fitting framework, we extend the range of taxa to which the VBGF (equation (1)) can be applied and hence to a wider range of ecological issues, such as the sustainability of marine invertebrate aquaculture.

Data Accessibility

Code to reproduce the fitting of the five VBGF parameterisations can be found at (https://github.com/lauraleemoore/Growth-curve-fitting-).

References

1. Holm, S. *et al*. A comparative perspective on longevity: the effect of body size dominates over ecology in moths. *J. Evol. Biol.*, **29(12),** 2422-2435 (2006).
2. Woodward, G. *et al*. Body size in ecological networks. *Trends Ecol. Evol.*, **20(7),** 402-409 (2005).
3. Kwapich, C.L. Valentini, G. & Hölldobler, B. The non-additive effects of body size on nest architecture in a polymorphic ant. *Philos. Trans. R. Soc. Lon., B, Biol Sci*, **373(1753),** 20170235 (2018).
4. Mayer, M. Shine, R. & Brown, G.P. Bigger babies are bolder: effects of body size on personality of hatchling snakes. *Behaviour*, **153(3),** 313-323 (2016).
5. Mirth, C.K. Frankino, W.A. Shingleton, A.W. Allometry and size control: what can studies of body size regulation teach us about the evolution of morphological scaling relationships? *Curr. Opin. Insect.*, **13,** 93-98 (2016).
6. Gutowsky *et al*. Interactive effects of sex and body size on the movement ecology of adfluvial bull trout (*Salvelinus confluentus*). *Can. J. Zool.*, **94(1),** 31-40 (2015).
7. Green, D.M. Implications of female body-size variation for the reproductive ecology of an anuran amphibian. *Ethol. Ecol. Evol.*, **27(2),** 173-184 (2015).
8. Davies, P.S. Physiological ecology of Patella. I. The effect of body size and temperature on metabolic rate. *J. Mar. Biol. Assoc. UK*, **46(3),** 647-658 (1966).
9. Illius, A.W. & Gordon, I.J. Modelling the nutritional ecology of ungulate herbivores: evolution of body size and competitive interactions. *Oecologia*, **89(3),** 428-434 (1992).
10. González-Wangüemert, M. Valente, S. & Aydin, M. Effects of fishery protection on biometry and genetic structure of two target sea cucumber species from the Mediterranean Sea. *Hydrobiologia*, **743(1),** 65-74 (2015).
11. Jackson, C.J. & Wang, Y.G. Modelling growth rate of *Penaeus monodon* Fabricius in intensively managed ponds: effects of temperature, pond age and stocking density. *Aquac. Res.*, **29(1),** 27-36 (1998).

12. Ansah, Y.B. & Frimpong, E.A. Using model-based inference to select a predictive growth curve for farmed tilapia. *N. Am. J. Aquac.*, **77(3),** 281-288 (2015).
13. Sulardiono, B. Prayitno, S.B. & Hendrarto, I.B. The growth analysis of *Stichopus vastus* (Echinodermata: Stichopodidae) in Karimunjawa waters. *J. Coast. Dev.*, **15,** 315-323 (2012).
14. Petersen, J.K. *et al*. Mussels as a tool for mitigation of nutrients in the marine environment. *Mar. Pollut. Bull.*, **82(1-2),** 137-143 (2014).
15. Bridges, T.C. Turner, L.W. Smith, E.M. Stahly, T.S. & Loewer, O.J. A mathematical procedure for estimating animal growth and body composition. *Trans. ASAE*, **29(5),** 1342-1347 (1986).
16. Kirkwood, G.P. Estimation of von Bertalanffy growth curve parameters using both length increment and age–length data. *Can. J. Fish. Aquat. Sci.*, **40(9),** 1405-1411 (1983).
17. Panik, M.J. *Growth Curve Modelling: Theory and Applications* (John Wiley & Sons, 2014).
18. Potthoff, R.F. & Roy, S.N. A generalized multivariate analysis of variance model useful
especially for growth curve problems. *Biometrika*, **51(3-4),** 313-326 (1964).
19. Richards, F.J. A flexible growth function for empirical use. *J. Exp. Bot.*, **10(2),** 290-301 (1959).
20. Strenio, J.F. Weisberg, H.I. & Bryk, A.S. Empirical Bayes estimation of individual growth curve parameters and their relationship to covariates. *Biometrics*, **39(1),** 71-86 (1983).
21. Higgins, R.M. Diogo, H. & Isidro, E.J. Modelling growth in fish with complex life histories. *Rev. Fish Biol. Fish.*, **25(3),** 449-462 (2015).
22. Chang, Y.J. Sun, C.L. Chen, Y. & Yeh, S.Z. Modelling the growth of crustacean species. *Rev. Fish Biol. Fish.*, **22(1),** 157-187 (2012).
23. Fuentes-Santos, I. Labarta, U. Arranz, K. & Fernández-Reiriz, M.J. From classical to nonparametric growth models: Towards comprehensive modelling of mussel growth patterns. *Mar. Environ. Res.*, **127,** 41-48 (2017).
24. Huchard, E. *et al*. Additive genetic variance and developmental plasticity in growth trajectories in a wild cooperative mammal. *J. Evol. Biol.*, **27(9),** 1893-1904 (2014).

25. Jager, T. & Ravagnan, E. Modelling growth of northern krill (*Meganyctiphanes norvegica*) using an energy-budget approach. *Ecol. Model.*, **325,** 28-34 (2016).
26. Marshall, D.J. & White, C.R. Have we outgrown the existing models of growth? *Trends Ecol. Evol.*, **34(2),** 102-111 (2018).
27. Quince, C. Abrams, P.A. Shuter, B.J. & Lester, N.P. Biphasic growth in fish I: theoretical foundations. *J. Theor. Biol.*, **254(2),** 197-206 (2008).
28. Derocher, A.E. & Wiig, Ø. Postnatal growth in body length and mass of polar bears (*Ursus maritimus*) at Svalbard. *J. Zool. (Lond.)*, **256(3),** 343-349 (2002).
29. Tjørve, K.M.C. & Tjørve, E. Shapes and functions of bird-growth models: how to characterise chick postnatal growth. *Zoology*, **113(6),** 326–333 (2010).
30. Ernsting, G. Zonneveld, C. Isaaks, J.A. & Kroon, A. Size at maturity and patterns of growth and reproduction in an insect with indeterminate growth. *Oikos*, **66,** 17-26 (1993).
31. Siegel, V. Age and growth of Antarctic Euphausiacea (Crustacea) under natural conditions. *Mar. Biol.*, **96(4),** 483-495 (1987).
32. Lehman, T.M. & Woodward, H.N. Modeling growth rates for sauropod dinosaurs. *Paleobiology*, **34(2),** 264–281 (2008).
33. Pütter, A. Studies on the physiological similarity. VI. Similarities in growth. *Eur. J. Physiol.*, **180,** 280 (1920).
34. Bertalanffy, L. von. Problems of organic growth. *Nature*, **163(4135),** 156-158 (1949).
35. Bertalanffy, L. von. A quantitative theory of organic growth (inquiries on growth laws. II). *Hum. Biol.*, **10(2),** 181–213 (1938).
36. Schnute, J. A versatile growth model with statistically stable parameters. *Can. J. Fish. Aquat. Sci.*, **38(9),** 1128-1140 (1981).
37. Góngora-Gómez, A.M. Leal-Sepúlveda, A.L. García-Ulloa, M. Aragón-Noriega, E.A. & Valenzuela-Quiñónez, W. Morphometric relationships and growth models for the oyster *Crassostrea corteziensis* cultivated at the southeastern coast of the Gulf of California Mexico. *Lat. Am. J. Aquat.*, **46(4),** 735-743 (2018).
38. Reynaga-Franco, F.J. *et al*. Multi-model inference as criterion to determine differences in growth patterns of distinct *Crassostrea gigas* stocks. *Aquacul. Int.*, **27,** 1-16 (2019).

6031 39. Castillo-Vargasmachuca, S.G. Ponce-Palafox, J.T. Arámbul-Muñoz, E.
6032 Rodríguez-Domínguez, G. & Aragón-Noriega, E.A. The spotted rose snapper
6033 (*Lutjanus guttatus* Steindachner 1869) farmed in marine cages: review of growth
6034 models. *Rev. Aquacult.*, **10(2),** (2018).
6035 40. Lugert, V. Tetens, J. Thaller, G. Schulz, C. & Krieter, J. Finding suitable growth
6036 models for turbot (*Scophthalmus maximus L.*) in aquaculture 1 (length
6037 application). *Aquac. Res.*, **48(1),** 24-36 (2017).
6038 41. Yuancai, L. Marques, C.P. & Macedo, F.W. Comparison of Schnute's and
6039 Bertalanffy-Richards' growth functions. *Forest Ecol. Manag.*, **96(3),** 283-288
6040 (1997).
6041 42. Gompertz, B. On the nature of the function expressive of the law of human
6042 mortality, and
6043 on a new mode of determining the value of life contingencies. *Phil. Trans. R. Soc.*
6044 *Lon.*, **115,** 513-583 (1825).
6045 43. Tjørve, K.M. & Tjørve, E. The use of Gompertz models in growth analyses, and
6046 new Gompertz-model approach: An addition to the Unified-Richards family. *PLoS*
6047 *ONE*, **12(6),** (2017).
6048 44. Alldredge, A.L. & Madin, L.P. Pelagic tunicates: unique herbivores in the marine
6049 plankton. *Bioscience*, **32(8),** 655-663 (1982).
6050 45. West, G.B. Brown, J.H. & Enquist, B.J. A general model for the origin of
6051 allometric scaling laws in biology. *Science*, **276(5309),** 122-126 (1997).
6052 46. Barneche, D.R. & Allen, A.P. The energetics of fish growth and how it constrains
6053 food-web trophic structure. *Ecol. Lett.*, **21(6),** (2018).
6054 47. West, G.B. Brown, J.H. & Enquist, B.J. A general model for ontogenetic
6055 growth. *Nature*, **413(6856),** 628-631 (2001).
6056 48. Moses, M.E. *et al*. Revisiting a model of ontogenetic growth: estimating model
6057 parameters from theory and data. *Am. Nat.*, **171(5),** 632-645 (2008).
6058 49. Hirst, A.G. & Forster, J. When growth models are not universal: evidence from
6059 marine
6060 invertebrates. *Proc. Biol. Sci.*, **280(1768),** (2013).
6061 50. Verhulst, P.F. Notice sur la loi que la population suit dans son accroissement.
6062 *Corresp. Mathématique Phys.,* **10,** 113-21 (1839).
6063 51. Katsanevakis, S. Modelling fish growth: model selection, multi-model inference
6064 and model selection uncertainty. *Fish. Res.*, **81(2-3),** 229-235 (2006).

52. Shi, P.J. *et al*. On the 3/4-exponent von Bertalanffy equation for ontogenetic growth. *Ecol. Model.*, **276,** 23-28 (2014).
53. Schnute, J. & Fournier, D. A new approach to length–frequency analysis: growth structure. *Can. J. Fish. Aquat. Sci.*, **37(9),** 1337-1351 (1980).
54. Kvålseth, T.O. Cautionary note about R-squared. *Am. Stat.*, **39(4),** 279-285 (1985).
55. Willett, J.B. & Singer, J.D. Another cautionary note about R-squared: Its use in weighted
least-squares regression analysis. *Am. Stat.*, **42(3),** 236-238 (1988).
56. Maino, J.L. & Kearney, M.R. Ontogenetic and interspecific scaling of consumption in
insects. *Oikos*, **124(12),** 695-701 (2015).
57. Maino, J.L. & Kearney, M.R. Testing mechanistic models of growth in insects. *Proc. Soc. Biol. Sci.*, **282(1819),** 20151973 (2015).
58. Rosenfeld, J. Van Leeuwen, T. Richards, J. & Allen, D. (2015). Relationship between growth and standard metabolic rate: measurement artefacts and implications for habitat use and life-history adaptation in salmonids. *J. Anim. Ecol.*, **84(1),** 4-20.
59. Killen, S.S. Atkinson, D. & Glazier, D.S. The intraspecific scaling of metabolic rate with
body mass in fishes depends on lifestyle and temperature. *Ecol. Lett.*, **13(2),** 184-193 (2010).
60. Ellenby, C. Body size in relation to oxygen consumption and pleopod beat in *Ligia oceanica L. J. Exp. Biol.*, **28(4),** 492-507 (1951).
61. Glazier, D.S. Hirst, A.G. & Atkinson, D. Shape shifting predicts ontogenetic changes in
metabolic scaling in diverse aquatic invertebrates. *Proc. Biol. Sci.*, **282(1802),** (2015).
62. Hirst, A.G. Glazier, D.S. & Atkinson, D. Body shape-shifting during growth permits tests that distinguish between competing geometric theories of metabolic scaling. *Ecol. Lett.*, **17(10),** 1274-1281 (2014).
63. Hirst, A.G. Intraspecific scaling of mass to length in pelagic animals: Ontogenetic shape
change and its implications. *Limnol. Oceanogr.*, **57(5),** 1579-1590 (2012).

64. Kooijman, S.A.L.M. *Dynamic Energy Budgets in Biological Systems* (Cambridge University Press, 1993).
65. Kooijman, S.A.L.M. *Dynamic Energy and Mass Budgets in Biological Systems* (Cambridge University Press, 2000).
66. Ohnishi, S. Yamakawa, T. & Akamine, T. On the analytical solution for the Pütter – Bertalanffy growth equation. *J. Theor. Biol.*, **343,** 174–177 (2014).
67. Charnov, E.L. Fish growth: Bertalanffy k is proportional to reproductive effort. *Environ. Biol. Fish.*, **83(2),** 185-187 (2008).
68. Lester, N.P. Shuter, B.J. & Abrams, P.A. Interpreting the von Bertalanffy model of somatic growth in fishes: the cost of reproduction. *Proc. Soc. Biol. Sci.*, **271(1548),** 1625-1631 (2004).
69. Armstrong, D.P. Keevil, M.G. Rollinson, N. & Brooks, R.J. Subtle individual variation in indeterminate growth leads to major variation in survival and lifetime reproductive output in a long lived reptile. *Funct. Ecol.*, **32(3),** 752-761 (2017).
70. Moore, D.W. & Farrar, J.D. Effect of growth on reproduction in the freshwater amphipod, *Hyalella azteca* (Saussure). *Hydrobiologia*, **328(2),** 127-134 (1996).
71. Bouchard, L. & Winkler, G. Life cycle, growth and reproduction of *Neomysis americana* in the St. Lawrence estuarine transition zone. *J. Plankton Res.*, **40(6),** 693-707 (2018).
72. Quesnel, L. King, W.J. Coulson, G. & Festa-Bianchet, M. Tall young females get ahead: size-specific fecundity in wild kangaroos suggests a steep trade-off with growth. *Oecologia*, **186(1),** 59-71 (2018).
73. Rollo, C.D. Growth negatively impacts the life span of mammals. *Evol. Dev.*, **4(1),** 55-61 (2002).
74. Bruce, R.C. Relative growth rates in three species of *Desmognathus* (Amphibia: Plethodontidae). *Herpetologica*, **72(3),** 174-180 (2016).
75. Pardo, S.A. Cooper, A.B. & Dulvy, N.K. Avoiding fishy growth curves. *Methods Ecol. Evol.*, **4(4),** 353-360 (2013).
76. Glazier, D.S. The 3/4-power law is not universal: evolution of isometric, ontogenetic metabolic scaling in pelagic animals. *BioScience*, **56(4),** 325-332 (2006).
77. Bhowmick, A.R. Chattopadhyay, G. & Bhattacharya, S. Simultaneous identification of growth law and estimation of its rate parameter for biological growth data: a new approach. *J. Biol. Phys.*, **40(1),** 71-95 (2014).

78. L'Abée-Lund, J.H. Langeland, A. Jonsson, B. & Ugedal, O. Spatial segregation by age and size in Arctic charr: a trade-off between feeding possibility and risk of predation. *J. Anim. Ecol.*, **62,** 160-168 (1993).
79. Tan, H. Hirst, A.G. Glazier, D.S. & Atkinson, D. Ecological pressures and the contrasting scaling of metabolism and body shape in coexisting taxa: cephalopods versus teleost fish. *Philos. Trans. R. Soc. Lon., B, Biol. Sci.*, **374(1778),** 20180543 (2019).
80. Seibel, B.A. Thuesen, E.V. Childress, J.J. & Gorodezky, L.A. Decline in pelagic cephalopod metabolism with habitat depth reflects differences in locomotory efficiency. *Biol. Bull.*, **192(2),** 262-278 (1997).
81. Mitchell, S.F. Trainor, F.R. Rich, P.H. & Goulden, C.E. Growth of *Daphnia magna* in the
laboratory in relation to the nutritional state of its food species, *Chlamydomonas reinhardtii*. *J. Plankton Res.*, **14(3),** 379-391 (1992).
82. Lilley, M.K. *et al*. Culture and growth of the jellyfish *Pelagia noctiluca* in the laboratory.
Mar. Ecol. Prog. Ser., **510,** 265-273 (2014).
83. Ross, R.M. Energetics of *Euphausia pacifica*. II. Complete carbon and nitrogen budgets at 8 and 12°C throughout the life span. *Mar. Biol.*, **68(1),** 15-23 (1982).
84. Lombard, F. Renaud, F. Sainsbury, C. Sciandra, A. & Gorsky, G. Appendicularian ecophysiology I: Food concentration dependent clearance rate, assimilation efficiency, growth and reproduction of *Oikopleura dioica*. *J. Mar. Sys.*, **78(4),** 606-616 (2009).
85. Båmstedt, U. Wild, B. & Martinussen, M. Significance of food type for growth of ephyrae *Aurelia aurita* (Scyphozoa). *Mar. Biol.,* **139(4),** 641-650 (2001).
86. Båmstedt, U. Ishii, H. & Martlnussen, M.B. Is the scyphomedusa *Cyanea capillata* (l.) dependent on gelatinous prey for its early development? *Sarsia*, **82(3),** 269-273 (1997).
87. Kheder, R.B. Quéré, C. Moal, J. & Robert, R. Effect of nutrition on *Crassostrea gigas* larval development and the evolution of physiological indices. Part A: Quantitative and qualitative diet effects. *Aquaculture*, **305(1-4),** 165-173 (2010).
88. Thomsen, J. Casties, I. Pansch, C. Körtzinger, A. & Melzner, F. Food availability outweighs ocean acidification effects in juvenile *Mytilus edulis*: laboratory and field experiments. *Glob. Chang. Biol.*, **19(4),** 1017-1027 (2013).

89. Domingues, P.M. Sykes, A. & Andrade, J.P. The effects of temperature in the life cycle of two consecutive generations of the cuttlefish *Sepia officinalis* (Linnaeus, 1758), cultured in the Algarve (South Portugal). *Aquacult. Int.*, **10(3),** 207-220 (2002).
90. Maranhão, P. & Marques, J.C. The influence of temperature and salinity on the duration of embryonic development, fecundity and growth of the amphipod *Echinogammarus marinus* Leach (Gammaridae). *Acta Oecol.*, **24(1),** 5-13 (2003).
91. Stumpf, L. Tropea, C. & Greco, L.S.L. Recovery growth of *Cherax quadricarinatus*
juveniles fed on two high-protein diets: Effect of daily feeding following a cyclic feeding
period on growth, biochemical composition and activity of digestive enzymes. *Aquaculture*, **433,** 404-410 (2014).
92. Ito, M. & Lucas, J.S. The Complete Larval Development of the Scyllarid Lobster, *Scyllarus demani holthuis*, 1946 (Decapoda, Scyllaridae), in the Laboratory. *Crustaceana*, **58(2),** 144-167 (1990).
93. Ibánez, C.M. & Keyl, F. Cannibalism in cephalopods. *Rev. Fish Biol. Fish.*, **20(1),** 123-136 (2010).
94. Pérez-Losada, M.A.R.C.O.S. Nolte, M.J. Crandall, K.A. & Shaw, P.W. Testing hypotheses of population structuring in the Northeast Atlantic Ocean and Mediterranean Sea using the common cuttlefish *Sepia officinalis*. *Mol. Ecol.*, **16(13),** 2667-2679 (2007).
95. Olaya-Restrepo, J. Erzini, K. & González-Wangüemert, M. Estimation of growth parameters for the exploited sea cucumber *Holothuria arguinensis* from South Portugal. *Fish. Bull.*, **116(1),** 1-8 (2018).
96. Taylor, N.G. Walters, C.J. & Martell, S.J. A new likelihood for simultaneously estimating
von Bertalanffy growth parameters, gear selectivity, and natural and fishing mortality.
Can. J. Fish. Aquat. Sci., **62(1),** 215-223 (2005).
97. Pauly, D. On the interrelationships between natural mortality, growth parameters, and mean environmental temperature in 175 fish stocks. *ICES J. Mar. Sci.*, **39(2),** 175-192 (1980).

Acknowledgements

We thank the Natural Environment Research Council (NERC) for funding the studentship as part of the ACCE Doctoral Training Partnership.

Author contributions

LL, DA and AGH conceived the aims of this study. Mathematical derivations and model parameterisations were produced and written by SJC, with R code written by both SJC and LL. LL performed the analysis and drafted the manuscript. All authors contributed to the draft and gave approval for final draft submission.

Additional information

The authors declare no competing interests.

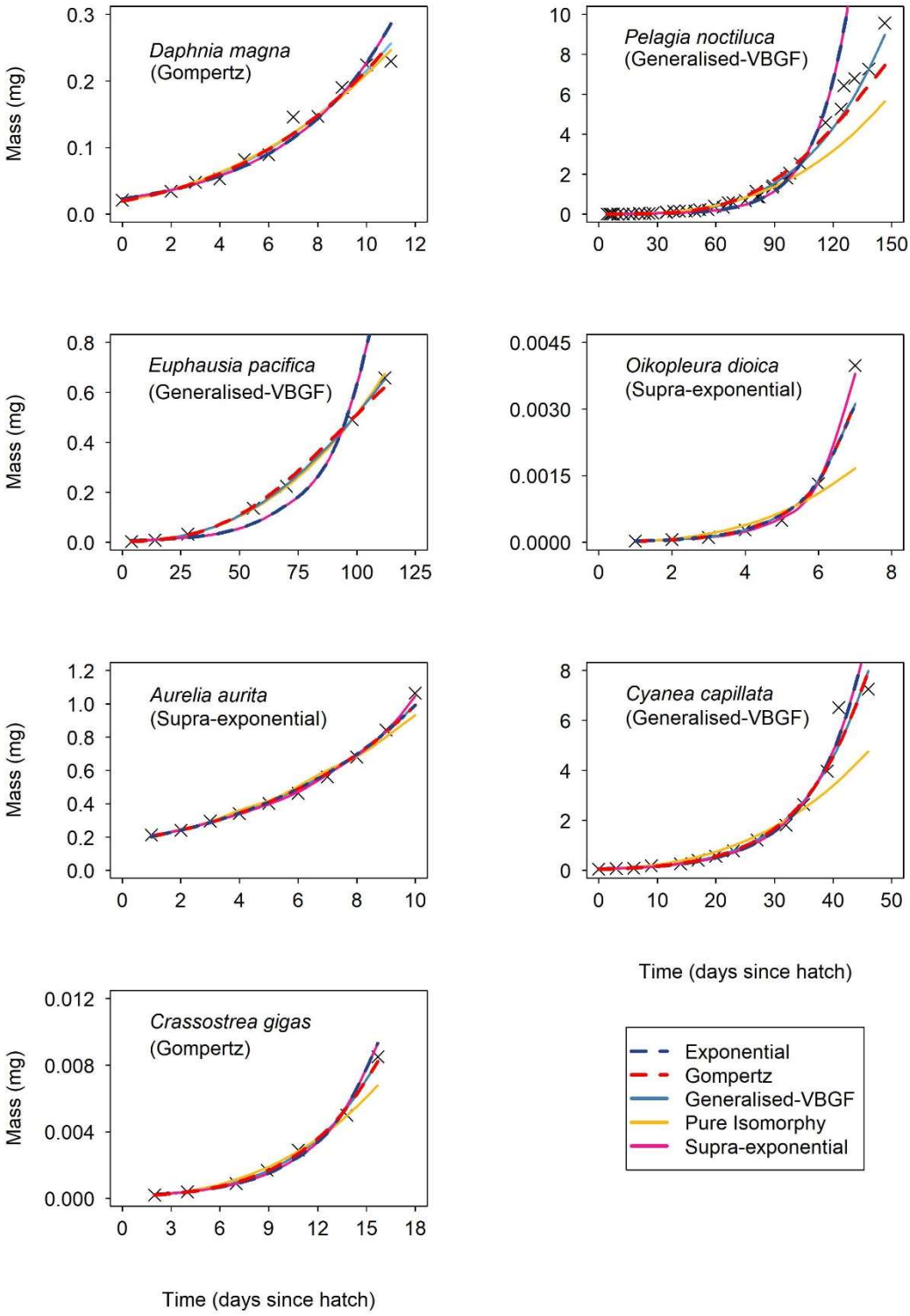

Figure 1. Model fits for the five von Bertalanffy growth function (VBGF) (equation 1) parameterisations (equation 1) for empirical mass versus time data for seven species of pelagic invertebrates with the best fit model given in brackets. From top left: *Daphnia magna* (Gompertz), *Pelagia noctiluca* (Generalised-VBGF), *Euphausia pacifica* (Generalised-VBGF), *Oikopleura dioica* (Supra-exponential), *Aurelia aurita*

(Supra-exponential), *Cyanea capillata* (Generalised-VBGF) and *Crassostrea gigas* larvae (Gompertz).

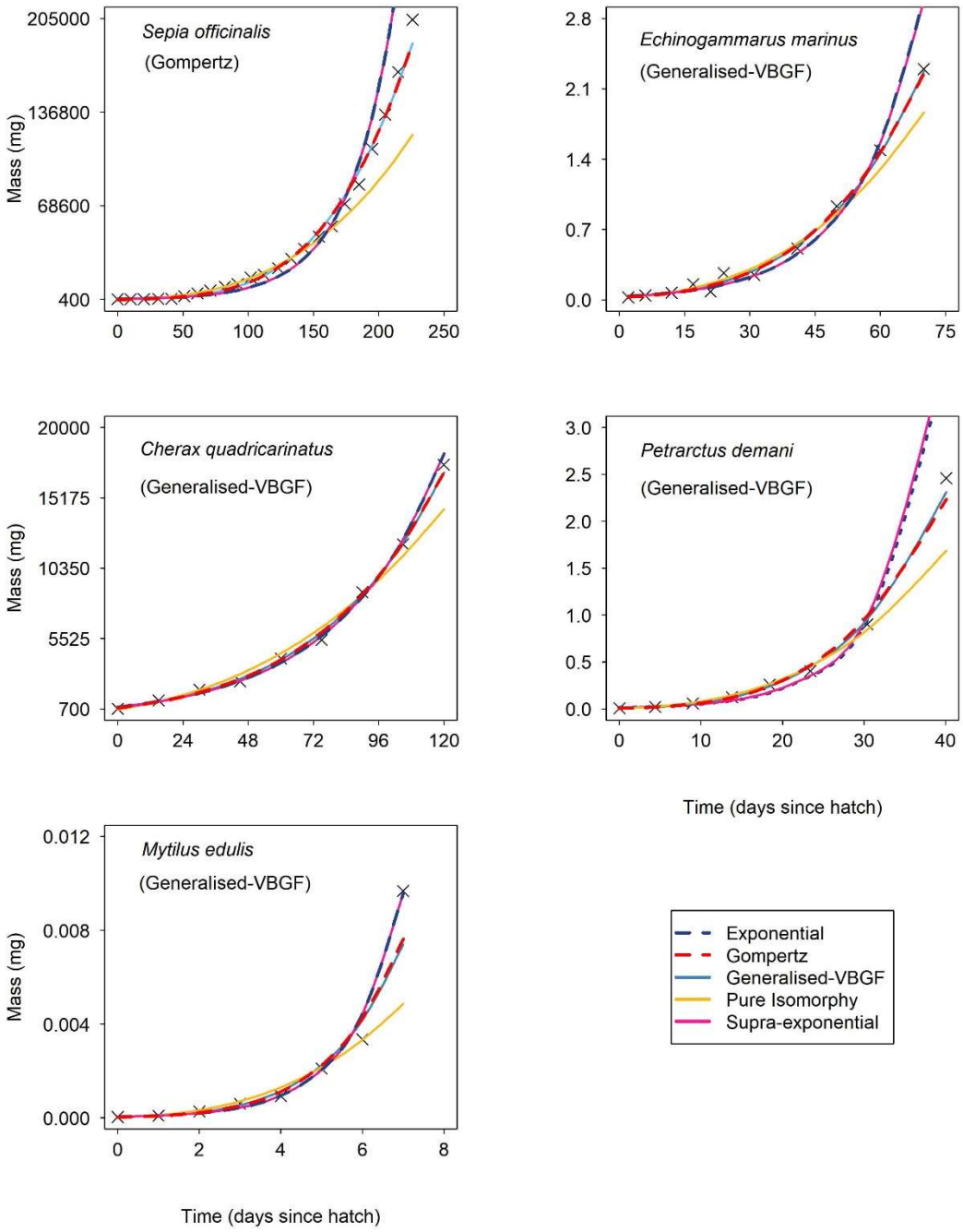

Figure 2. Model fits for the five von Bertalanffy growth function (VBGF) (equation 1) parameterisations for empirical mass versus time data for five species of benthic invertebrates with the best fit model given in brackets. From top left: *Sepia officinalis* (Gompertz), *Echinogammarus marinus* (Gompertz), *Cherax quadricarinatus* (Exponential), *Petrarctus demani* (Generalised-VBGF) and *Mytilus edulis* (Generalised-VBGF).

Table 1. The best-fitting values for the mass-scaling exponent for biosynthesis potential, *A*, as determined by the most negative log-likelihood between the five parameterisations of the VBGF: Exponential, Gompertz, Generalised-VBGF, Pure Isomorphy and Supra-exponential for empirical mass versus time data for twelve pelagic and benthic invertebrate species. The zone (pelagic or benthic) represents the zone inhabited during the development phase in which growth data was obtained for. The number of datapoints is represented by N. The 95% confidence intervals for parameter *A* were calculated using profile likelihood.

Habitat	Zone	Phylum	Class	Species	N	Best fit model	*d.f.*	***A*** estimate	95% confidence intervals
Freshwater	Pelagic	Arthropoda	Branchiopoda	*Daphnia magna*	11	VBGF-Gompertz	7	1.0	0.58 – 1
Marine	Pelagic	Arthropoda	Malacostraca	*Euphausia pacifica*	7	Generalised-VBGF	2	0.79	0.68 – 0.91
Marine	Pelagic	Cnidaria	Scyphozoa	*Pelagia noctiluca*	39	Generalised-VBGF	34	0.76	0.73 – 0.78
Marine	Pelagic	Chordata	Appendicularia	*Oikopleura dioica*	7	VBGF-Supra-exponential	2	1.12	1.06 – 1.16
Marine	Pelagic	Cnidaria	Scyphozoa	*Aurelia aurita*	10	VBGF-Supra-exponential	5	1.22	1.21 – 1.32
Marine	Pelagic	Cnidaria	Scyphozoa	*Cyanea capillata*	14	Generalised-VBGF	9	0.92	0.88 – 0.96
Marine	Pelagic	Mollusca	Bivalvia	*Crassostrea gigas*	7	VBGF-Gompertz	3	1	0.80 – 1
Marine	Benthic	Arthropoda	Malacostraca	*Echinogammarus marinus*	11	Generalised-VBGF	7	0.79	0.64 – 0.93
Freshwater	Benthic	Arthropoda	Malacostraca	*Cherax quadricarinatus*	9	Generalised-VBGF	4	0.89	0.81 – 0.95
Marine	Benthic	Arthropoda	Malacostraca	*Petrarctus demani*	8	Generalised-VBGF	3	0.79	0.76 – 0.93
Marine	Benthic	Mollusca	Bivalvia	*Mytilus edulis*	8	Generalised-VBGF	3	0.87	0.79 – 0.95
Marine	Benthic	Mollusca	Cephalopoda	*Sepia officinalis*	23	VBGF-Gompertz	19	1.0	0.80 – 1

6237 **References**

6238 Alldredge, A.L. and Madin, L.P. (1982). Pelagic tunicates: unique herbivores in the
6239 marine plankton. *Bioscience*, 32(8), 655-663.

6240 Andrews, R.M. and Pough, F.H. (1985). Metabolism of squamate reptiles: allometric
6241 and ecological relationships. *Physiological Zoology*, 58(2), 214-231.

6242 Anger, K. (1996). Physiological and biochemical changes during lecithotrophic larval
6243 development and early juvenile growth in the northern stone crab, *Lithodes maja*
6244 (Decapoda: Anomura). *Marine Biology*, 126(2), 283-296.

6245 Anger, K. and Schultze, K. (1995). Elemental composition (CHN), growth and exuvial
6246 loss in the larval stages of two semiterrestrial crabs, *Sesarma curacaoense* and
6247 *Armases miersii* (Decapoda: Grapsidae). *Comparative Biochemistry and Physiology*
6248 *Part A: Physiology*, 111(4), 615-623.

6249 Anger, K. and Schultze, K. (1997). Larval growth patterns in the aesop shrimp
6250 *Pandalus montagui*. *Journal of Crustacean Biology*, 17(3), 472-479.

6251 Anninsky, B.E. Finenko, G.A. Abolmasova, G.I. and Romanova, Z.A. (2007).
6252 Somatic organic content of the ctenophores *Mnemiopsis leidyi* (Ctenophora: Lobata)
6253 and *Beroe ovata* (Ctenophora: Beroida) in early ontogenetic stages. *Russian Journal*
6254 *of Marine Biology*, 33(6), 417-424.

6255 Ansah, Y.B. and Frimpong, E.A. (2015). Using model-based inference to select a
6256 predictive growth curve for farmed tilapia. *North American Journal of*
6257 *Aquaculture*, 77(3), 281-288.

6258 Armstrong, D.P. Keevil, M.G. Rollinson, N. and Brooks, R.J. (2017). Subtle
6259 individual variation in indeterminate growth leads to major variation in survival and
6260 lifetime reproductive output in a long-lived reptile. *Functional Ecology*, 32(3), 752-
6261 761.

6262 Astorga, D. Ruiz, J. and Prieto, L. (2012). Ecological aspects of early life stages of
6263 *Cotylorhiza tuberculata* (Scyphozoa: Rhizostomae) affecting its pelagic population
6264 success. *Hydrobiologia*, 690(1), 141-155.

6265 Atkinson, D. (1994). Temperature and Organism Size—A Biological Law for
6266 Ectotherms? *Advances in Ecological Research*, 25, 1-58.

6267 Atkinson, D. and Sibly, R.M. (1997). Why are organisms usually bigger in colder
6268 environments? Making sense of a life history puzzle. *Trends in Ecology and Evolution*,
6269 12(6), 235-239.

6270 Atkinson, D. Morley, S.A. Weetman, D. and Hughes, R.N. (2001). Offspring size
6271 responses to maternal temperature in ectotherms. *Animal Developmental Ecology*,
6272 269-285.

6273 Atkinson, D. Ciotti, B.J. and Montagnes, D.J.S. (2003). Protists decrease in size
6274 linearly with temperature: ca. 2.5% °C $^{-1}$. *Proceedings of the Royal Society of London.*
6275 *Series B: Biological Sciences*, 270(1533), 2605-2611.

6276 Baillieul, M. Smolders, R. and Blust, R. (2005). The effect of environmental stress on
6277 absolute and mass-specific scope for growth in *Daphnia magna* Strauss. *Comparative*
6278 *Biochemistry and Physiology Part C: Toxicology & Pharmacology*, 140(3), 364-373.

6279 Baker, L.D. and Reeve, M.R. (1974). Laboratory culture of the lobate ctenophore
6280 *Mnemiopsis mccradyi* with notes on feeding and fecundity. *Marine biology*, 26(1), 57-
6281 62.

6282 Balavoine, G. (2014) Segment formation in annelids: Patterns, processes and
6283 evolution. *International Journal of Developmental Biology*, 58(6-8), 469-483.

6284 Ballesteros, F.J. *et al*. (2018). On the thermodynamic origin of metabolic scaling.
6285 *Scientific Reports*, 8(1), 1-10.

6286 Båmstedt, U. Ishii, H. and Martlnussen, M.B. (1997). Is the scyphomedusa *Cyanea*
6287 *capillata* (L.) dependent on gelatinous prey for its early development? *Sarsia*, 82(3),
6288 269-273.

6289 Båmstedt, U. Lane, J. and Martinussen, M.B. (1999). Bioenergetics of ephyra larvae
6290 of the scyphozoan jellyfish *Aurelia aurita* in relation to temperature and salinity.
6291 *Marine Biology*, 135(1), 89-98.

6292 Båmstedt, U. Wild, B. and Martinussen, M. (2001). Significance of food type for
6293 growth of ephyrae *Aurelia aurita* (Scyphozoa). *Marine Biology*, 139(4), 641-650.

6294 Banavar, J.R. Damuth, J. Maritan, A and Rinaldo, A. (2002). Modelling universality
6295 and scaling. *Nature*, 420(6916), 626.

Banavar, J.R. Cooke, T.J. Rinaldo, A. and Maritan, A. (2014). Form, function, and evolution of living organisms. *Proceedings of the National Academy of Sciences*, 111(9), 3332-3337.

Banavar, J.R. *et al*. (2010). A general basis for quarter-power scaling in animals. *Proceedings of the National Academy of Science*, 107(36), 15816-15820.

Barneche, D.R. and Allen, A.P. (2018). The energetics of fish growth and how it constrains food-web trophic structure. *Ecology Letters*, 21(6), 836-844.

Barnett, C.M. Bengough, A.G. and Mckenzie, B.M. (2009). Quantitative image analysis of earthworm-mediated soil displacement. *Biology and Fertility of Soils*, 45(8), 821-828.

Begum, S. *et al*. (2009). A metabolic model for the ocean quahog *Arctica islandica* – effects of animal mass and age, temperature, salinity, and geography on respiration rate. *Journal of Shellfish Research*, 28(3), 533-539.

Bertalanffy, L.V. (1938). A quantitative theory of organic growth (inquiries on growth laws. II). *Human Biology*, 10(2), 181-213.

Bertalanffy, L.V. (1949). Problems of organic growth. *Nature*, 163(4135), 156-158.

Bertalanffy, L.V. (1957). Quantitative laws in metabolism and growth. *The Quarterly Review of Biology*, 32(3), 217-231.

Bertha, E.L.E. (1992). Growth and larval development of *Nyctiphanes simplex* in laboratory conditions. *California Cooperative Oceanic Fisheries Investigations*, 33, 162-171.

Bhowmick, A.R. Chattopadhyay, G. and Bhattacharya, S. (2014). Simultaneous identification of growth law and estimation of its rate parameter for biological growth data: a new approach. *Journal of Biological Physics*, 40(1), 71-95.

Bjærke, O. Andersen, T. and Titelman, J. (2014). Predator chemical cues increase growth and alter development in nauplii of a marine copepod. *Marine Ecology Progress Series*, 510, 15-24.

Bokma, F. (2004). Evidence against universal metabolic allometry. *Functional Ecology*, 18(2), 184-187.

6325 Bonnet, X. Bradshaw, D. and Shine, R. (1998). Capital versus Income Breeding: An
6326 Ectothermic Perspective. *Oikos*, 2, 333-342.

6327 Bouchard, L. and Winkler, G. (2018). Life cycle, growth and reproduction of
6328 *Neomysis americana* in the St. Lawrence estuarine transition zone. *Journal of*
6329 *Plankton Research*, 40(6), 693-707.

6330 Bridges, T.C. *et al*. (1986). A mathematical procedure for estimating animal growth
6331 and body composition. *Transactions of the American Society of Agricultural and*
6332 *Biological Engineers*, 29(5), 1342-1347.

6333 Brody, S. and Procter, R. C. (1932). Relation between basal metabolism and mature
6334 body-weight in different species of mammals and birds. *University of Missouri*
6335 *College of Agriculture, Food and Natural Resources*, 89-101.

6336 Brown, J.H. Gillooly, J.F. Allen, A.P. Savage V.M. and West, G.B. (2004). Toward a
6337 metabolic theory of ecology. *Ecology*, 85(7), 1771-1789.

6338 Brown, J.H. West, G.B. and Enquist, B.J. (2005). Yes, West, Brown and Enquist's
6339 model of allometric scaling is both mathematically correct and biologically relevant.
6340 *Functional Ecology*, 19(4), 735-738.

6341 Bruce, R.C. (2016). Relative growth rates in three species of *Desmognathus*
6342 (Amphibia: Plethodontidae). *Herpetologica*, 72(3), 174-180.

6343 Bueno, J. and López-Urrutia, Ã. (2014). Scaling up the curvature of mammalian
6344 metabolism. *Frontiers in Ecology and Evolution*, 2, 61.

6345 Burns, C.W. (1969). Relation between filtering rate, temperature, and body size in
6346 four species of *Daphnia*. *Limnology and Oceanography*, 14(5), 693-700.

6347 Calder, W.A. (1985). *Size, function, and life history*. Dover Publications, Inc. Mineola,
6348 New York.

6349 Campbell, R.G. Wagner, M.M. Teegarden, G.J. Boudreau, C.A. and Durbin, E.G.
6350 (2001). Growth and development rates of the copepod *Calanus finmarchicus* reared in
6351 the laboratory. *Marine Ecology Progress Series*, 221, 161-183.

6352 Capellini, I. Venditti, C. and Barton, R.A. (2010). Phylogeny and metabolic scaling in
6353 mammals. *Ecology*, 91(9), 2783-2793.

6354 Carlotti, F. and Nival, P. (1992). Model of copepod growth and development:
6355 Moulting and mortality in relation to physiological processes during an individual
6356 moult cycle. *Marine ecology progress series,* 84(3), 219-233.

6357 Carnevali, M.C. (2006). Regeneration in Echinoderms: repair, regrowth,
6358 cloning. *Invertebrate Survival Journal*, 3(1), 64-76.

6359 Castillo-Vargasmachuca, *et al*. (2018). The spotted rose snapper (*Lutjanus guttatus*
6360 Steindachner 1869) farmed in marine cages: review of growth models. *Reviews in*
6361 *Aquaculture*, 10(2), 376-384.

6362 Chang, Y.J. Sun, C.L. Chen, Y. and Yeh, S.Z. (2012). Modelling the growth of
6363 crustacean species. *Reviews in Fish Biology and Fisheries*, 22(1), 157-187.

6364 Charnov, E.L. Turner, T.F. and Winemiller, K.O. (2001). Reproductive constraints
6365 and the evolution of life histories with indeterminate growth. *Proceedings of the*
6366 *National Academy of Sciences*, 98(16), 9460-9464.

6367 Charnov, E.L. (2008). Fish growth: Bertalanffy *k* is proportional to reproductive effort.
6368 *Environmental Biology of Fishes*, 83(2), 185-187.

6369 Clarke, A. (2019). Energy Flow in Growth and Production. *Trends in Ecology and*
6370 *Evolution*, 34(6), 502-509.

6371 Clarke, A. and Johnston, N.M. (1999). Scaling of metabolic rate with body mass and
6372 temperature in teleost fish. *Journal of Animal Ecology*, 68(5), 893-905.

6373 Clarke, A. and O'Connor, M.I. (2014). Diet and body temperature in mammals and
6374 birds. *Global Ecology and Biogeography*, 23(9), 1000-1008.

6375 Clarke, A. and Rothery, P. (2008). Scaling of body temperature in mammals and
6376 birds. *Functional Ecology*, 22(1), 58-67.

6377 Clarke, A. Rothery, P. and Isaac, N.J.B. (2010). Scaling of basal metabolic rate with
6378 body mass and temperature in mammals. *Journal of Animal Ecology*, 79(3), 610-619.

6379 Clutter, R.I. and Theilacker, G.H. (1971). Ecological efficiency of a pelagic mysid
6380 shrimp, estimates from growth, energy budget, and mortality studies. *Fishery Bulletin*,
6381 69(1), 93-114.

6382 Colin, S.P. and Dam, H.G. (2005). Testing for resistance of pelagic marine copepods

to a toxic dinoflagellate. *Evolutionary Ecology*, 18(4), 355-377.

O'Connor, M.I. Piehler, M.F. Leech, D.M. Anton, A. and Bruno, J.F. (2009). Warming and Resource Availability Shift Food Web Structure and Metabolism. *Public Library of Science Biology*, 7(9).

Cuesta, J.A. Guerao, G. Schubart, C.D. and Anger, K. (2011). Morphology and growth of the larval stages of *Geograpsus lividus* (Crustacea, Brachyura), with the descriptions of new larval characters for the Grapsidae and an undescribed setation pattern in extended developments. *Acta Zoologica*, 92(3), 225-240.

Daan, R. (1986). Food intake and growth of *Sarsia tubulosa* (Sars, 1835), with quantitative estimates of predation on copepod populations. *Netherlands Journal of Sea Research*, 20(1), 67-74.

Dagg, M.J. and Littlepage, J.L. (1972). Relationships between growth rate and RNA, DNA, protein and dry weight in *Artemia salina* and *Euchaeta elongata*. *Marine Biology*, 17(2), 162-170.

Davies, P.S. (1966). Physiological ecology of Patella. I. The effect of body size and temperature on metabolic rate. *Journal of the Marine Biology Association of the United Kingdom*, 46(3), 647-658.

Dawirs, R.R. (1985). Temperature and larval development of *Carcinus maenas* (Decapoda) in the laboratory; predictions of larval dynamics in the sea. *Marine Ecology Progress Series*, 24(3), 297-302.

Degen, A.A. Kam, M. Khokhlova, I.S. Karsnov, B.R. and Barraclough, T.G. (1998). Average daily metabolic rate of rodents: Habitat and dietary comparisons. *Functional Ecology*, 12(1), 63-73.

Deibel, D. (1982). Laboratory-measured grazing and ingestion rates of the salp, *Thalia democratica* Forskal, and the doliolid, *Dolioletta gegenbauri* Uljanin (Tunicata, Thaliacea). *Journal of Plankton Research*, 4(2), 189-201.

DeLong, J.P. Okie, J.G. Moses, M.E. Sibly, R.M. and Brown, J.H. (2010). Shifts in metabolic scaling, production, and efficiency across major evolutionary transitions of life. *Proceedings of the National Academy of Sciences*, 107(29), 12941-12945.

Demetrius, L. Legendre, S.rremöes, P. (2009). Evolutionary entropy: A predictor of

6413 body size, metabolic rate and maximal life Span. *Bulletin of Mathematical Biology*,
6414 71(4), 800-818.

6415 Derocher, A.E. & Wiig, Ø. (2002). Postnatal growth in body length and mass of polar
6416 bears (*Ursus maritimus*) at Svalbard. *Journal of Zoology*, 256(3), 343-349.

6417 Dmitriew, C.M. (2011). The evolution of growth trajectories: what limits growth rate?
6418 *Biological Reviews*, 86, 97 – 116.

6419 O'Dor, R.K. and Hoar, J.A. (2000). Does geometry limit squid growth? *Journal of*
6420 *Marine Science*, 57(1), 8-14.

6421 Dodds, P.S. (2010). Optimal form of branching supply and collection networks.
6422 *Physical Review Letters*, 104(4), 048702.

6423 Domingues, P.M. Sykes, A. and Andrade, J.P. (2002). The effects of temperature in
6424 the life cycle of two consecutive generations of the cuttlefish *Sepia officinalis*
6425 (Linnaeus, 1758), cultured in the Algarve (South Portugal). *Aquaculture International*,
6426 10(3), 207-220.

6427 Doostmohammadi, A. Stocker, R. and Ardekani, A.M. (2012). Low-Reynolds-number
6428 swimming at pycnoclines. *Proceedings of the National Academy of Sciences*, 109(10),
6429 3856-3861.

6430 Drewes, C.D. and Zoran, M. J. (1989). Neurobehavioral specializations for respiratory
6431 movements and rapid escape from predators in posterior segments of the tubificid
6432 *Branchiura sowerbyi*. *Aquatic Oligochaete Biology*, 51, 65-71.

6433 Ehnes, R.B. Rall, B. C. and Brose, U. (2011). Phylogenetic grouping, curvature and
6434 metabolic scaling in terrestrial invertebrates. *Ecology Letters*, 14(10), 9930-1000.

6435 Ellenby, C. (1951). Body size in relation to oxygen consumption and pleopod beat in
6436 *Ligia oceanica* L. *Journal of Experimental Biology*, 28(4), 492-507.

6437 Enquist, B.J. *et al*. (2007). Does the exception prove the rule? *Nature*, 445(7127), E9-
6438 E10.

6439 Epelbaum, A.B. and Kovatcheva, N.P. (2005). Daily food intakes and optimal food
6440 concentrations for red king crab (*Paralithodes camtschaticus*) larvae fed A*rtemia*
6441 *nauplii* under laboratory conditions. *Aquaculture nutrition*, 11(6), 455-461.

6442 Ernsting, G. Zonneveld, C. Isaaks, J.A. and Kroon, A. (1993). Size at maturity and
6443 patterns of growth and reproduction in an insect with indeterminate growth. *Oikos*, 66,
6444 17-26.

6445 Escribano, R. Rodriguez, L. and Irribarren, C. (1998). Temperature-dependent
6446 development and growth of *Calanus chilensis* Brodsky from Northern Chile. *Journal*
6447 *of Experimental Marine Biology and Ecology*, 229(1), 19-34.

6448 Flores, A.A. Negreiros-Fransozo, M.L. and Fransozo, A. (1998). The megalopa and
6449 juvenile development of Pachygrapsus transversus (Gibbes, 1850)(Decapoda,
6450 Brachyura) compared with other grapsid crabs. *Crustaceana*, 71(2), 197-222.

6451 Franco, S.C. Augustin, C.B. Geffen, A.J. and Dinis, M.T. (2017). Growth, egg
6452 production and hatching success of *Acartia tonsa* cultured at high densities.
6453 *Aquaculture*, 468, 569-578.

6454 Fryd, M. Haslund, O.H. and Wohlgemuth, O. (1991). Development, growth and egg
6455 production of the two copepod species *Centropages hamatus* and *Centropages typicus*
6456 in the laboratory. *Journal of plankton research*, 13(4), 683-689.

6457 Fuentes-Santos, I. Labarta, U. Arranz, K. and Fernández-Reiriz, M.J. (2017). From
6458 classical to nonparametric growth models: Towards comprehensive modelling of
6459 mussel growth patterns. *Marine Environment Research*, 127, 41-48.

6460 Geiser, F. (2004). Metabolic rate and body temperature reduction during hibernation
6461 and daily torpor. *Annual Reviews of Physiology*, 66, 239-274.

6462 Gillooly, J.F. Brown, J.H. West, G.B. Savage, V.M. and Charnov, E.L. (2001). Effects
6463 of size and temperature on metabolic rate. *Science*, 293(5538), 2248-2251.

6464 Gillooly, J.F. *et al*. (2006). Response to Clarke and Fraser: effects of temperature on
6465 metabolic rate. *Functional Ecology*, 20(2), 400-404.

6466 Glazier, D.S. (2005). Beyond the '¾-power law': variation in the intra- and
6467 interspecific scaling of metabolic rate in animals. *Biological Review*, 80(04), 611.

6468 Glazier, D.S. (2006). The ¾-power law is not universal: evolution of isometric,
6469 ontogenetic metabolic scaling in pelagic animals. *BioScience*, 56(4), 325.

6470 Glazier, D.S. (2008). Effects of metabolic level on the body size scaling of metabolic

rate in birds and mammals. *Proceedings of the Royal Society B: Biological Sciences*, 275(1641), 1405-1410.

Glazier, D.S. (2010). A unifying explanation for diverse metabolic scaling in animals and plants. *Biological Review*, 85(1), 111-138.

Glazier, D.S. (2014a). Metabolic Scaling in Complex Living Systems. *Systems*, 2(4), 451-540.

Glazier, D.S. (2014b). Scaling of Metabolic Scaling within Physical Limits. *Systems*, 2(4), 425-450.

Glazier, D.S. (2018). Rediscovering and Reviving Old Observations and Explanations of Metabolic Scaling in Living Systems. *Systems,* 6(1), 4.

Glazier, D.S. (2020). Activity alters how temperature influences intraspecific metabolic scaling: testing the metabolic-level boundaries hypothesis. *Journal of Comparative Physiology B: Biochemical, Systemic, and Environmental Physiology*, 190, 445-454.

Glazier, D.S. *et al*. (2011). Ecological effects on metabolic scaling: amphipod responses to fish predators in freshwater springs. *Ecological Monographs*, 81(4), 599-618.

Glazier, D.S. Hirst, A.G. and Atkinson, D. (2015). Shape shifting predicts ontogenetic changes in metabolic scaling in diverse aquatic invertebrates. *Proceedings of the Royal Society B: Biological Sciences,* 282(1802), 20142302-20142302.

Gompertz, B. (1825). On the nature of the function expressive of the law of human mortality, and on a new mode of determining the value of life contingencies. *Philosophical transactions of the Royal Society of London*, 115, 513-583.

Góngora-Gómez, A.M. *et al*. (2018). Morphometric relationships and growth models for the oyster *Crassostrea corteziensis* cultivated at the southeastern coast of the Gulf of California Mexico. *Latin American Journal of Aquatic Research*, 46(4), 735-743.

González-Wangüemert, M. Valente, S. and Aydin, M. (2015). Effects of fishery protection on biometry and genetic structure of two target sea cucumber species from the Mediterranean Sea. *Hydrobiologia*, 743(1), 65-74.

6500 Graham, J.B. (1988). Ecological and evolutionary aspects of integumentary
6501 respiration: body size, diffusion and the Invertebrata. *American Zoologist*, 28(3),
6502 1031-1045.

6503 Graham, J.B. (1990). Ecological, evolutionary, and physical factors influencing
6504 aquatic animal respiration. *American Zoologist*, 30(1), 137-146.

6505 Green, D.M. (2015). Implications of female body-size variation for the reproductive
6506 ecology of an anuran amphibian. *Ethology, Ecology & Evolution*, 27(2), 173-184.

6507 Greve, W. (1970). Cultivation experiments on North Sea ctenophores. *Helgoländer*
6508 *wissenschaftliche Meeresuntersuchungen*, 20(1-4), 304-317.

6509 Griebeler, E.M. and Werner, J. (2016). Mass, phylogeny, and temperature are
6510 sufficient to explain differences in metabolic scaling across mammalian orders?
6511 *Ecology and Evolution*, 6(23), 8352–8365.

6512 Guerin, C. and Giani, N. (1996). Analytical study of the locomotor and respiratory
6513 movements of tubificid worms by means of video recording. *Hydrobiologia*, 333(1),
6514 63-69.

6515 Gunadi, B. and Edwards, C.A. (2003). The effects of multiple applications of different
6516 organic wastes on the growth, fecundity and survival of *Eisenia fetida*
6517 (Savigny)(Lumbricidae). *Pedobiologia*, 47(4), 321-329.

6518 Gutowsky *et al*. (2015). Interactive effects of sex and body size on the movement
6519 ecology of adfluvial bull trout (*Salvelinus confluentus*). *Canadian Journal of Zoology*,
6520 94(1), 31-40.

6521 Hansen, B.W. (1999). Cohort growth of planktotrophic polychaete larvae--are they
6522 food limited? *Marine Ecology Progress Series*, 178, 109-119.

6523 Harrison, J.F. (2017). Do performance–safety tradeoffs cause hypometric metabolic
6524 scaling in animals? *Trends in Ecology and Evolution*, 32(9), 653-664.

6525 Haukka, J.K. (1987). Growth and survival of *Eisenia fetida* (Sav.)(Oligochaeta:
6526 Lumbricidae) in relation to temperature, moisture and presence of *Enchytraeus*
6527 *albidus* (Henle)(Enchytraeidae). *Biology and Fertility of Soils*, 3(1-2), 99-102.

6528 Hayssen, V. and Lacy, R.C. (1985). Basal metabolic rates in mammals: Taxonomic

differences in the allometry of BMR and body mass. *Comparative Biochemistry and Physiology, Part A: Physiology*, 81(4), 741-754.

Haywood, G.J. and Burns, C.W. (2003). Growth of *Nyctiphanes* (Euphausiacea) on different diets. *Journal of Experimental Marine Biology and Ecology*, 289(1), 139-151.

Higgins, R.M. Diogo, H. and Isidro, E.J. (2015). Modelling growth in fish with complex life histories. *Reviews in Fish Biology and Fisheries*, 25(3), 449-462.

Hillman, S.S. and Withers, P.C. (1979). An analysis of respiratory surface area as a limit to activity metabolism in anurans. *Canadian Journal of Zoology*, 57(11) ,2100-2105.

Hirst, A.G. (2012). Intraspecific scaling of mass to length in pelagic animals: Ontogenetic shape change and its implications. *Limnology and oceanography*, 57(5), 579-1590.

Hirst, A.G. and Forster, J. (2013). When growth models are not universal: evidence from marine invertebrates. *Proceedings of the Royal Society B: Biological Sciences*, 280(1768), 20131546.

Hirst, A.G. Glazier, D.S. and Atkinson, D. (2014). Body shape shifting during growth permits tests that distinguish between competing geometric theories of metabolic scaling. *Ecology Letters*, 17(10), 1274-1281.

Hirst, A.G. Lilley, M.K.S. Glazier, D.S. and Atkinson, D. (2017). Ontogenetic body-mass scaling of nitrogen excretion relates to body surface area in diverse pelagic invertebrates. *Limnology and Oceanography*, 62(1), 311-319.

Hoefnagel, K.N. and Verberk, W.C. (2015). Is the temperature-size rule mediated by oxygen in aquatic ectotherms? *Journal of Thermal Biology*, 54, 56-65.

Holm, S. *et al*. (2006). A comparative perspective on longevity: the effect of body size dominates over ecology in moths. *Journal of Evolutionary Biology*, 29(12), 2422-2435.

Huchard, E. *et al*. (2014). Additive genetic variance and developmental plasticity in growth trajectories in a wild cooperative mammal. *Journal of Evolutionary Biology*, 27(9), 1893-1904.

6559 Hudson, L.N. Isaac, N.J.B. and Reuman, D.C. (2013). The relationship between body
6560 mass and field metabolic rate among individual birds and mammals. *Journal of Animal*
6561 *Ecology*, 82(5), 1009-1020.

6562 Ibánez, C.M. and Keyl, F. (2010). Cannibalism in cephalopods. *Reviews in Fish*
6563 *Biology & Fisheries*, 20(1), 123-136.

6564 Ikeda, T. (1995). Distribution, growth and life cycle of the mesopelagic amphipod
6565 *Primno abyssalis* (Hyperiidea: Phrosinidae) in the southern Japan Sea. *Marine*
6566 *Biology*, 123(4), 789-798.

6567 Illius, A.W. and Gordon, I.J. (1992). Modelling the nutritional ecology of ungulate
6568 herbivores: evolution of body size and competitive interactions. *Oecologia*, 89(3),
6569 428-434.

6570 Ito, M. and Lucas, J.S. (1990). The Complete Larval Development of the Scyllarid
6571 Lobster, *Scyllarus demani holthuis*, 1946 (Decapoda, Scyllaridae), in the Laboratory.
6572 *Crustaceana*, 58(2), 144-167.

6573 Ivleva, I.V. (1980). The dependence of crustacean respiration rate on body mass and
6574 habitat temperature. *Internationale Revue der gesamten Hydrobiologie und*
6575 *Hydrographie*, 65(1), 1-47.

6576 Jackson, C.J. and Wang, Y.G. (1998). Modelling growth rate of *Penaeus monodon*
6577 Fabricius in intensively managed ponds: effects of temperature, pond age and stocking
6578 density. *Aquatic Research*, 29(1), 27-36.

6579 Jacobi, C.C. and Anger, K. (1985). Growth and respiration during the larval
6580 development of *Hyas coarctatus* (Decapoda: Majidae). *Marine Biology*, 87(2), 173-
6581 180.

6582 Jager, T. and Ravagnan, E. (2016). Modelling growth of northern krill
6583 (*Meganyctiphanes norvegica*) using an energy-budget approach. *Ecological*
6584 *Modelling*, 325, 28-34.

6585 Jensen, M.A. Carter, C.G. Adams, L.R. and Fitzgibbon, Q.P. (2013). Growth and
6586 biochemistry of the spiny lobster *Sagmariasus verreauxi* cultured at low and high
6587 density from hatch to puerulus. *Aquaculture*, 376, 162-170.

6588 Jespersen, H. and Olsen, K. (1982). Bioenergetics in veliger larvae of *Mytilus edulis*
6589 L., *Ophelia*, 21(1), 101-113.

6590 Jones, K.E. *et al*. (2009). PanTHERIA: a species-level database of life history,
6591 ecology, and geography of extant and recently extinct mammals. *Ecology*, 90(9),
6592 2648-2648.

6593 Jung-Madsen, S. and Nielsen, T.G. (2015). Early development of *Calanus glacialis*
6594 and *C.finmarchicus*. *Limnology and Oceanography*, 60(3), 934-946.

6595 Kang, H.K. and Kang, Y.J. (1998). Growth and development of *Acartia steueri*
6596 (Copepoda: Calanoida) in the laboratory. *Korean Journal of Fisheries and Aquatic*
6597 *Sciences*, 31(6), 842-851.

6598 Kaonga, C.C. Kumwenda, J. and Mapoma, H.T. (2010). Accumulation of lead,
6599 cadmium, manganese, copper and zinc by sludge worms; *Tubifex tubifex* in sewage
6600 sludge. *International Journal of Environmental Science and Technology*, 7(1), 119-
6601 126.

6602 Karasov, W.H. and Diamond, J.M. (1985.) Digestive adaptations for fueling the cost
6603 of endothermy. *Science*, 228(4696), 202-204.

6604 Karkach, A.S. (2006). Trajectories and models of individual growth. *Demographic*
6605 *Research*, 15(12), 347-400.

6606 Kaster, J. and Wolff, R.J. (1982). A Convoluted Respiratory Exchange Surface in
6607 *Tubifex tubifex* (Tubificidae). *Transactions of the American Microscopical Society*,
6608 101(1), 91-95.

6609 Katsanevakis, S. (2006). Modelling fish growth: model selection, multi-model
6610 inference and model selection uncertainty. *Fisheries Research*, 81(2-3), 229-235.

6611 Kearney, M.R. and White, C.R. (2012). Testing metabolic theories. *American*
6612 *Naturalist*, 180(5), 546-565.

6613 Kheder, R.B. Quere, C. Moal, J. and Robert, R. (2010). Effect of nutrition on
6614 *Crassostrea gigas* larval development and the evolution of physiological indices. Part
6615 A: Quantitative and qualitative diet effects. *Aquaculture*, 305(1), 165-173.

6616 Killen, S.S., Atkinson, D. and Glazier, D.S. (2010). The intraspecific scaling of

6617 metabolic rate with body mass in fishes depends on lifestyle and temperature. *Ecology*
6618 *Letters*, 13(2), 184-193.

6619 Killen, S.S. Marras, S. and McKenzie, D.J. (2011). Fuel, fasting, fear: routine
6620 metabolic rate and food deprivation exert synergistic effects on risk-taking in
6621 individual juvenile European sea bass. *Journal of Animal Ecology*, 80(5), 1024-1033.

6622 Kimoto, K. Uye, S. and Onbé, T. (1986). Egg production of a brackish-water calanoid
6623 copepod *Sinocalanus tenellus* in relation to food abundance and temperature. *Bulletin*
6624 *of Plankton Society of Japan.*

6625 Kingma, B. Frijns, A. and van Marken Lichtenbelt, (2012). The thermoneutral zone:
6626 implications for metabolic studies. *Frontiers in bioscience*, 4, 1975-1985.

6627 Kirkwood, G.P. (1983). Estimation of von Bertalanffy growth curve parameters using
6628 both length increment and age–length data. *Canadian Journal of Fisheries & Aquatic*
6629 *Sciences*, 40(9), 1405-1411.

6630 Kleiber, M. (1932). Body size and metabolism. *Hilgardia*, 6(11), 315-353.

6631 Koivisto, S. and Ketola, M. (1995). Effects of copper on life-history traits of *Daphnia*
6632 *pulex* and *Bosmina longirostris*. *Aquatic Toxicology*, 32(2-3), 255-269.

6633 Kolokotrones, T. Savage, V. Deeds, E.J. and Fontana, W. (2010). Curvature in
6634 metabolic scaling. *Nature*, 464(7289), 753-756.

6635 Kooijman, S.A.L.M. (1986). Energy Budgets Can Explain Body Size Relations,
6636 Journal of Theoretical Biology, 121(3), 269-282.

6637 Kooijman, S.A.L.M. (1993). *Dynamic Energy Budgets in Biological Systems*
6638 Cambridge University Press.

6639 Kooijman, S.A.L.M. (2000). *Dynamic Energy and Mass Budgets in Biological*
6640 *Systems* Cambridge University Press.

6641 Kooijman, S.A.L.M. (2010) *Dynamic energy budget theory for metabolic*
6642 *organisation.* Cambridge University Press.

6643 Koop, J.H. Winkelmann, C. Becker, J. Hellmann, C. and Ortmann, C. (2011).
6644 Physiological indicators of fitness in benthic invertebrates: a useful measure for
6645 ecological health assessment and experimental ecology. *Aquatic Ecology*, 45(4), 547-

559.

Kozlowski, J. (1992). Optimal Allocation of Resources to Growth and Reproduction: Implications for Age and Size at Maturity. *Trends in Ecology & Evolution*, 7(1), 15-19.

Kozlowski, J. Czarnoleski, M. and Danko, M. (2004). Can optimal resource allocation models explain why ectotherms grow larger in cold? *Integrative & Comparative Biology*, 44(6), 480-93.

Kozlowski, J. and Konarzewski, M. (2004). Is West, Brown and Enquist's model of allometric scaling mathematically correct and biologically relevant? *Functional Ecology*, 18(2), 283-289.

Kozlowski, J. and Konarzewski, M. (2005). West, Brown and Enquist's model of allometric scaling again: the same questions remain. *Functional Ecology*, 19(4), 739-743.

Kozłowski, J. Konarzewski, M. and Czarnoleski, M. (2020). Coevolution of body size and metabolic rate in vertebrates: a life-history perspective. *Biological Reviews*.

Krimsky, L.S. and Epifanio, C.E. (2010). Growth of juvenile stone crabs, *Menippe mercenaria*, reared in the laboratory. *Journal of Crustacean Biology*, 30(2), 336-338.

Kuklinski, P. *et al*. (2013). Seasonality of occurrence and recruitment of Arctic marine benthic invertebrate larvae in relation to environmental variables. *Polar Biology*, 36(4), 549-560.

Kvålseth, T.O. (1985). Cautionary note about R-squared. *American Statistician*, 39(4), 279-285.

Kwapich, C.L. Valentini, G. and Hölldobler, B. (2018). The non-additive effects of body size on nest architecture in a polymorphic ant. *Philosophical Transitions of the Royal Society London. B: Biological Sciences*, 373(1753), 20170235.

L'Abée-Lund, J.H. Langeland, A. Jonsson, B. and Ugedal, O. (1993). Spatial segregation by age and size in Arctic charr: a trade-off between feeding possibility and risk of predation. *Journal of Animal Ecology*, 62, 160-168.

Leandro, S.M. Queiroga, H. Rodríguez-Graña, L. and Tiselius, P. (2006).

6675 Temperature-dependent development and somatic growth in two allopatric
6676 populations of *Acartia clausi* (Copepoda: Calanoida). *Marine Ecology Progress*
6677 *Series*, 322, 189-197.

6678 Lee, H.W. Ban, S. Ikeda, T. and Matsuishi, T. (2003). Effect of temperature on
6679 development, growth and reproduction in the marine copepod *Pseudocalanus*
6680 *newmani* at satiating food condition. *Journal of Plankton Research*, 25(3), 261-271.

6681 Lee, K.E. and Foster, R.C. (1991). Soil fauna and soil structure. *Australian Journal of*
6682 *Soil Research*, 29(6), 745-775.

6683 Lee, L. Atkinson, D. Hirst, A.G. and Cornell, S.J. (2020). A new framework for growth
6684 curve fitting based on the von Bertalanffy growth function. *Scientific Reports*, 10(1),
6685 1-12.

6686 Lehman, T.M. and Woodward, H.N. (2008). Modeling growth rates for sauropod
6687 dinosaurs. *Paleobiology*, 34(2), 264-281.

6688 Lemaître, J.F. Müller, D.W.H. and Clauss, M. (2014). A test of the metabolic theory
6689 of ecology with two longevity data sets reveals no common cause of scaling in
6690 biological times. *Mammal Review*, 44(3-4), 204-214.

6691 Lemke, A.M. and Benke, A.C. (2003). Growth and reproduction of three cladoceran
6692 species from a small wetland in the south-eastern USA. *Freshwater biology*, 48(4),
6693 589-603.

6694 Lesniowski, T.J. *et al*. (2015). Effects of food and CO2 on growth dynamics of
6695 polyps of two scyphozoan species (*Cyanea capillata* and *Chrysaora hysoscella*).
6696 *Marine Biology*, 162(6), 1371-1382.

6697 Lester, N.P. Shuter, B.J. and Abrams, P.A. (2004). Interpreting the von Bertalanffy
6698 model of somatic growth in fishes: the cost of reproduction. *Proceedings of the Royal*
6699 *Society of London. Series B: Biological Sciences*, 271(1548), 1625-1631.

6700 Levine, D.M. and Sulkin, S.D. (1979). Partitioning and utilization of energy during
6701 the larval development of the xanthid crab, *Rhithropanopeus harrisii* (Gould). *Journal*
6702 *of Experimental Marine Biology and Ecology*, 40(3), 247-257.

6703 Li, C. Luo, X. Huang, X. and Gu, B. (2009). Influences of temperature on development
6704 and survival, reproduction and growth of a calanoid copepod (*Pseudodiaptomus*

6705 *dubia*). *The Scientific World Journal*, 9, 866-879.

6706 Li, J. *et al.* (2010). Resistance reduction by bionic coupling of the earthworm
6707 lubrication function. *Science China Technological Sciences*, 53, 2989-2995.

6708 Li, Y. *et al*. (2016). Effects of different ratios of sewage sludge and cattle manure on
6709 growth and propagation of *Eisenia fetida*. *Public Library of Science*, 11(6), e0156492.

6710 Lilley, M.K. *et al*. (2014). Culture and growth of the jellyfish *Pelagia noctiluca* in the
6711 laboratory. *Marine Ecology Progress Series*, 510, 265-273 (2014).

6712 Loman, B.L.J. (2003). Growth or reproduction? Resource allocation by female frogs
6713 *Rana temporaria*. *Oecologia*, 442, 541-546.

6714 Lombard, F. Renaud, F. Sainsbury, C. Sciandra, A. and Gorsky, G. (2009).
6715 Appendicularian ecophysiology I: Food concentration dependent clearance rate,
6716 assimilation efficiency, growth and reproduction of *Oikopleura dioica*. *Journal of*
6717 *Marine Systems*, 78(4), 606-616.

6718 Lovegrove, B.G. (2000). The Zoogeography of Mammalian Basal Metabolic Rate.
6719 *The American Naturalist*, 156(2), 201-219.

6720 Lovegrove, B.G. (2003). The influence of climate on the basal metabolic rate of small
6721 mammals: A slow-fast metabolic continuum. *Journal of Comparative Physiology B:*
6722 *Biochemical, Systemic, and Environmental Physiology*, 173(2), 87-112.

6723 Lugert, V. Tetens, J. Thaller, G. Schulz, C. and Krieter, J. (2017). Finding suitable
6724 growth models for turbot (*Scophthalmus maximus L*.) in aquaculture 1 (length
6725 application). *Aquatic Research*, 48(1), 24-36.

6726 MacKay, N.J. (2011). Mass scale and curvature in metabolic scaling. Comment on: T.
6727 Kolokotrones *et al*., Curvature in metabolic scaling, Nature 464 (2010) 753-756.
6728 *Journal of Theoretical Biology*, 280(1), 194-196.

6729 Maino, J.L. and Kearney, M.R. (2015a). Ontogenetic and interspecific scaling of
6730 consumption in insects. *Oikos*, 124(12), 1564-1570.

6731 Maino, J.L. and Kearney, M.R. (2015b). Testing mechanistic models of growth in
6732 insects. *Proceedings of the Royal Society London. B: Biological Sciences*, 282(1819),
6733 20151973.

6734 Maino, J.L. Kearney, M.R. Nisbet, R.M. and Kooijman, S.A.L.M. (2014). Reconciling
6735 theories for metabolic scaling. *Journal of Animal Ecology*, 83(1), 20-29.

6736 Makarievaw, A.M. Gorshkovw, V.G. and Li, B.L. (2003). A note on metabolic rate
6737 dependence on body size in plants and animals. *Journal of Theoretical Biology*, 221,
6738 301-307.

6739 Maranhão, P. and Marques, J.C. (2003). The influence of temperature and salinity on
6740 the duration of embryonic development, fecundity and growth of the amphipod
6741 *Echinogammarus marinus* Leach (Gammaridae). *Acta Oecologica*, 24(1), 5-13.

6742 Marian, M.P. and Pandian, T.J. (1984). Culture and harvesting techniques for *Tubifex*
6743 *tubifex*. *Aquaculture*, 42(3-4), 303-315.

6744 Marques, J.C. and Nogueira, A. (1991). Life cycle, dynamics, and production of
6745 *Echinogammarus marinus* (Leach (Amphipoda)) in the Mondego estuary (Portugal).
6746 *Oceanologica Acta*, 11.

6747 Marschall, H.P. and Hirche, H.J. (1984). Development of eggs and nauplii of
6748 *Euphausia superba*. *Polar biology*, 2(4), 245-250.

6749 Marshall, D.J. and White, C.R. (2019). Have We Outgrown the Existing Models of
6750 Growth? *Trends in Ecology and Evolution*, 34(2), 102-111.

6751 Massel, S.R. (2012). *Fluid Mechanics for Marine Ecologists*. Springer Science.

6752 Mayer, M. Shine, R. and Brown, G.P. (2016). Bigger babies are bolder: effects of body
6753 size on personality of hatchling snakes. *Behaviour*, 153(3), 313-323.

6754 McHenry, M.J. and Jed, J. (2003). The ontogenetic scaling of hydrodynamics and
6755 swimming performance in jellyfish (*Aurelia aurita*). *Journal of Experimental Biology*,
6756 206(22), 4125-4137.

6757 McNab, B.K. (2000). Energy constraints on carnivore diet. *Nature*, 407(6804), 584.

6758 McNab, B.K. (2008). An analysis of the factors that influence the level and scaling of
6759 mammalian BMR. *Comparative Biochemistry and Physiology - A Molecular and*
6760 *Integrative Physiology*, 151(1), 5-28.

6761 Mcnab, B.K. (2010). Geographic and temporal correlations of mammalian size
6762 reconsidered: A resource rule. *Oecologia*, 164(1), 13-23.

6763 McNab, B.K. (2019). What determines the basal rate of metabolism? *Journal of*
6764 *Experimental Biology*, 222(15), jeb205591.

6765 McPeek, M.A. Grace, M. and Richardson, J.M.L. (2001). Physiological and
6766 behavioral responses to predators shape the growth/predation risk trade-off in
6767 damselflies. *Ecology*, 82(6), 1535-1545.

6768 Meeh, K. (1879). Oberflächenmessungen des menschlichen Körpers, *Ztschr f Biol*, 15,
6769 425-458.

6770 Meehan, T.D. (2006). Mass and temperature dependence of metabolic rate in litter and
6771 soil invertebrates. *Physiological & Biochemical Zoology*, 79(5), 878-884.

6772 Metcalfe, N.B. and Monaghan, P. (2003). Growth versus lifespan: Perspectives from
6773 evolutionary ecology. *Experimental Gerontology*, 38(9), 935-940.

6774 Mileikovsky, S.A. and Shirshov, P.P. (1973). Speed of active movement of pelagic
6775 larvae of marine bottom dwelling invertebrates and their ability to regulate their
6776 vertical position. *Marine Biology*, 23, 11-17.

6777 Mirth, C.K. Frankino, W.A. and Shingleton, A.W. (2016). Allometry and size control:
6778 what can studies of body size regulation teach us about the evolution of morphological
6779 scaling relationships? *Current Opinion in Insect Science*, 13, 93-98.

6780 Mitchell, S.F. Trainor, F.R. Rich, P.H. and Goulden, C.E. (1992). Growth of *Daphnia*
6781 *magna* in the laboratory in relation to the nutritional state of its food species,
6782 *Chlamydomonas reinhardtii*. *Journal of Plankton Research*, 14(3), 379-391.

6783 Miyake, H. Iwao, K. and Kakinuma, Y. (1997). Life History and Environment of
6784 *Aurelia aurita*. *South Pacific Study*, 17(2), 273-285.

6785 Moore, D.W. and Farrar, J.D. (1996). Effect of growth on reproduction in the
6786 freshwater amphipod, *Hyalella azteca* (Saussure). *Hydrobiologia*, 328(2), 127-134.

6787 Moses, M.E. *et al*. (2008). Revisiting a model of ontogenetic growth: estimating model
6788 parameters from theory and data. *The American Naturalist*, 171(5), 632-645.

6789 Müller, D.W.H. *et al*. (2012). Dichotomy of eutherian reproduction and metabolism.
6790 *Oikos*, 121(1), 102-115.

6791 Mullin, M.M. and Brooks, E.R. (1970). Growth and metabolism of two planktonic,

6792 marine copepods as influenced by temperature and type of food. *Marine food chains*,
6793 74-95.

6794 Nelder, J.A. and Mead, R. (1965). A simplex method for function minimization.
6795 *The Computer Journal*, **7**, 308–313.

6796 Ohnishi, S. Yamakawa, T. and Akamine, T. (2014). On the analytical solution for the
6797 Pütter – Bertalanffy growth equation. *Journal of Theoretical Biology*, 343, 174-177.

6798 Okie, J.G. (2013). General models for the spectra of surface area scaling strategies of
6799 cells and organisms: fractality, geometric dissimilitude, and internalization. *The*
6800 *American Naturalist*, 181(3), 421-439.

6801 Olaya-Restrepo, J. Erzini, K. and González-Wangüemert, M. (2018). Estimation of
6802 growth parameters for the exploited sea cucumber *Holothuria arguinensis* from South
6803 Portugal. *Fisheries Bulletin*, 116(1), 1-8.

6804 Olsen, A.I. Mæland, A. Waagbø, R. and Olsen, Y. (2000). Effect of algal addition on
6805 stability of fatty acids and some water-soluble vitamins in juvenile *Artemia*
6806 *franciscana*. *Aquaculture Nutrition*, 6(4), 263-273.

6807 Omori, M. (1979). Growth, feeding, and mortality of larval and early postlarval stages
6808 of the oceanic shrimp *Sergestes similis* Hansen. Limnol. *Oceanography*, 24(2), 273-
6809 288.

6810 Oplinger, R.W. and Wagner, E.J. (2011). Culture of *Tubifex tubifex*: Effect of Feed
6811 Type, Ration, Temperature, and Density on Juvenile Recruitment. *North American*
6812 *Journal of Aquaculture*, 73, 68-75.

6813 Ortiz, D.O. Muxagata, E. and Bersano, J.G.F. (2017). *Notodiaptomus incompositus*
6814 (Brian, 1925)(Copepoda, Calanoida) reared in the laboratory: growth experiments and
6815 reproductive aspects. *Crustaceana*, 90(5), 517-533.

6816 Oyugi, D.O. *et al*. (2011). Effects of temperature on the foraging and growth rate of
6817 juvenile common carp, *Cyprinus carpio*. *Journal of Thermal Biology*, 37(1), 89-94.

6818 Packard, G.C. (2012). Is non-loglinear allometry a statistical artifact? *Biological*
6819 *Journal of the Linnaean Society*, 107(4), 764-773.

6820 Packard, G.C. (2015). Quantifying the curvilinear metabolic scaling in mammals.

Journal of Experimental Zoology Part A: Ecological Genetics and Physiology, 323(8), 540-546.

Paffenhöfer, G.A. (1976). On the biology of Appendicularia of the southeastern North Sea. *Proceedings of the 10th European Symposium on Marine Biology*.

Paffenhöfer, G.A. and Harris, R.P. (1976). Feeding, growth and reproduction of the marine planktonic copepod *Pseudocalanus elongatus* Boeck. *Journal of the Marine Biological Association of the United Kingdom*, 56(2), 327-344.

Painter, P.R. (2005). Data from necropsy studies and in vitro tissue studies lead to a model for allometric scaling of basal metabolic rate. *Theoretical Biology and Medical Modelling. BioMed Central*, 2(1), 39.

Panik, M.J. (2014). *Growth Curve Modelling: Theory and Applications*. John Wiley & Sons.

Pardo, S.A. Cooper, A.B. and Dulvy, N.K. (2013). Avoiding fishy growth curves. *Methods in Ecology and Evolution*, 4(4), 353-360.

Patefield, W.M. (1985). Information from the maximized likelihood function. *Biometrika*, 72(3), 664-668.

Pauly, D. (1980). On the interrelationships between natural mortality, growth parameters, and mean environmental temperature in 175 fish stocks. *Journal of Marine Science*, 39(2), 175-192.

Pequeno, P.A.C.L. *et al*. (2017). Ecology shapes metabolic and life history scalings in termites. *Ecological Entomology*, 42(2), 115–124.

Pérez-Losada, M.A.R.C.O.S. Nolte, M.J. Crandall, K.A. and Shaw, P.W. (2007). Testing hypotheses of population structuring in the Northeast Atlantic Ocean and Mediterranean Sea using the common cuttlefish *Sepia officinalis*. *Molecular Ecology*, 16(13), 2667-2679.

Pernet, B. (2000). Reproduction and development of three symbiotic scaleworms (Polychaeta: Polynoidae). *Invertebrate Biology*, 119(1), 45-57.

Petersen, J.K. *et al*. (2014). Mussels as a tool for mitigation of nutrients in the marine environment. *Marine Pollution Bulletin*, 82(1-2), 137-143.

6850 Peterson, W.T. (1986). Development, growth and survivorship of the copepod
6851 *Calanus marshallae* in the laboratory. *Marine Ecology Progress Series*, 29(1), 61-72.

6852 Pillar, S. (1985). Laboratory studies on the larval growth and development of
6853 *Nyctiphanes capensis* (Euphausiacea). *Journal of plankton research*, 7(2), 223-240.

6854 PJ, O. (1985). Physiological adaptations and the concepts of optimal reproductive
6855 strategy and physiological constraint in marine invertebrates. *Symposia of the Society*
6856 *for Experimental Biology*, 39, 267–300.

6857 Potthoff, R.F. and Roy, S.N. (1964). A generalized multivariate analysis of variance
6858 model useful especially for growth curve problems. *Biometrika*, 51(3-4), 313-326.

6859 Price, C.A. *et al*. (2012). Testing the metabolic theory of ecology. *Ecology Letters*,
6860 1465-1474.

6861 Promboon, P. Nabhitabhata, J. and Duengdee, T. (2011). Life cycle of the marbled
6862 octopus, *Amphioctopus aegina* (Gray) (Cephalopoda: Octopodidae) reared in the
6863 laboratory. *Scientia Marina*, 75(4), 811-821.

6864 Pütter, A. (1920). Studies on the physiological similarity. VI. Similarities in growth.
6865 *European Journal of Physiology*, 180, 280.

6866 Quesnel, L. *et al*. (2004). Tall young females get ahead: size-specific fecundity in wild
6867 kangaroos suggests a steep trade-off with growth. *Oecologia*, 186(1), 59-71.

6868 Quillin, K.J. (2000). Ontogenetic scaling of burrowing forces in the earthworm
6869 *Lumbricus terrestris*. *Journal of Experimental Biology*, 203(18), 2757-2770.

6870 Quince, C. Abrams, P.A. Shuter, B.J. and Lester, N.P. (2008). Biphasic growth in fish
6871 I: theoretical foundations. *Journal of Theoretical Biology*, 254(2), 197-206.

6872 Rasmussen, T. and Tande, K. (1995). Temperature-dependent development, growth
6873 and mortality in larvae of the deep-water prawn *Pandalus borealis* reared in the
6874 laboratory. *Marine Ecology Progress Series*, 118(1), 149-157.

6875 Rathore, R.S. and Khangarot, B.S. (2002). Effects of temperature on the sensitivity of
6876 sludge worm *Tubifex tubifex* Müller to selected heavy metals. *Ecotoxicology and*
6877 *Environmental Safety*, 53(1), 27-36.

6878 Reeve, M.R. and Walter, M.A. (1972). Conditions of culture, food-size selection, and

the effects of temperature and salinity on growth rate and generation time in *Sagitta hispida* Conant. *Journal of Experimental Marine Biology and Ecology*, 9(2), 191-200.

Rey, C. Harris, R. Irigoien, X. Head, R. and Carlotti, F. (2001). Influence of algal diet on growth and ingestion of *Calanus helgolandicus* nauplii. *Marine Ecology Progress Series*, 216, 151-165.

Reynaga-Franco, F.J. *et al*. (2019). Multi-model inference as criterion to determine differences in growth patterns of distinct *Crassostrea gigas* stocks. *Aquaculture International*, 27, 1-16.

Richards, F.J. (1959). A flexible growth function for empirical use. *Journal of Experimental Botany*, 10(2), 290-301.

Ricklefs, R.E. (2003). Is rate of ontogenetic growth constrained by resource supply or tissue growth potential? A comment on West *et al*.'s model. *Functional Ecology*, 17(3), 384-393.

Rodríguez, A. and Spivak, E.D. (2001). The larval development of *Panopeus margentus* (Decapoda: Brachyura: Panopeidae) reared in the laboratory. *Journal of Crustacean Biology*, 21(3), 806-820.

Roff, D.A. (2002). *Life history evolution*. Sinauer Associates, Inc.

Rollo, C.D. (2002). Growth negatively impacts the life span of mammals. *Evolution & Development*, 4(1), 55-61.

Rosa, S. Pansera, M. Granata, A. and Guglielmo, L. (2013). Interannual variability, growth, reproduction and feeding of *Pelagia noctiluca* (Cnidaria: Scyphozoa) in the Straits of Messina (Central Mediterranean Sea): Linkages with temperature and diet. *Journal of Marine Systems*, 111, 97-107.

Rosenfeld, J. van Leeuwen, T. Richards, J. and Allen, D. (2015). Relationship between growth and standard metabolic rate: measurement artefacts and implications for habitat use and life-history adaptation in salmonids. *Journal of Animal Ecology*, 84(1), 4-20.

Ross, R.M. (1982). Energetics of *Euphausia pacifica*: II. Complete carbon and nitrogen budgets at 8° C and 12°C throughout the life span. *Marine Biology*, 68, 15-23.

6909 Rubner, M. (1883). Ueber den einfluss der korpergrosse auf stoffund kaftwechsel.
6910 *Zeitschrift fur Biologie*, 19, 535–562.

6911 Sabatini, M. and Kiørboe, T. (1994). Egg production, growth and development of the
6912 cyclopoid copepod *Oithona similis*. *Journal of Plankton Research*, 16(10), 1329-1351.

6913 Saiz, E. and Alcaraz, M. (1991). Effects of small-scale turbulence on development
6914 time and growth of *Acartia grani* (Copepoda: Calanoida). *Journal of Plankton*
6915 *Research*, 13(4), 873-883.

6916 Sato, R. Tanaka, Y. and Ishimaru, T. (2001). House Production by *Oikopleura dioica*
6917 (Tunicata, Appendicularia) Under Laboratory Conditions. *Journal of Plankton*
6918 *Research*, 23(4), 415-423.

6919 Savage, V.M. Deeds, E.J. and Fontana, W. (2008). Sizing up allometric scaling theory.
6920 *Public Library of Science: Computational Biology*, 4(9), e1000171.

6921 Schiffer, M. *et al*. (2013). Tolerance of *Hyas araneus* zoea I larvae to elevated
6922 seawater PCO2 despite elevated metabolic costs. *Marine biology*, 160(8), 1943-1953.

6923 Schleucher, E. and Withers, P. C. (2002). Metabolic and Thermal Physiology of
6924 Pigeons and Doves. *Physiological and Biochemical Zoology*, 75(5), 439-450.

6925 Schnute, J. and Fournier, D. (1980). A new approach to length–frequency analysis:
6926 growth structure. *Canadian Journal of Fish and Aquatic Science*, 37(9), 1337-1351.

6927 Schnute, J. (1981). A versatile growth model with statistically stable
6928 parameters. *Canadian Journal of Fish and Aquatic Science*, 38(9), 1128-1140.

6929 Seebacher, F. White, C.R. and Franklin, C.E. (2015). Physiological plasticity increases
6930 resilience of ectothermic animals to climate change. *Nature Climate Change*, 5(1), 61-
6931 66.

6932 Seibel, B.A. Thuesen, E.V. Childress, J.J. and Gorodezky, L.A. (1997). Decline in
6933 pelagic cephalopod metabolism with habitat depth reflects differences in locomotory
6934 efficiency. *The Biological Bulletin*, 192(2), 262-278.

6935 Seidl, M.D. Pirow, R. and Paul, R.J. (2002). Water fleas (*Daphnia magna*) provide a
6936 separate ventilatory mechanism for their brood. *Zoology*, 105(1), 15-23.

6937 Shi, P.J. *et al*. (2014). On the ¾-exponent von Bertalanffy equation for ontogenetic
6938 growth. *Ecological Modelling*, 276, 23-28.

6939 Sibly, R.M. Collett, D. Promislow, D.E.L. Peacock, D.J. and Harvey, P.H. (1997).
6940 Mortality rates of mammals. *Journal of Zoology*, 243(1), 1-12.

6941 Sibly, R.M. and Atkinson, D. (1994). How rearing temperature affects optimal adult
6942 size in ectotherms. *Functional Ecology*, 8(4), 486-493.

6943 Sibly, R.M. and Brown, J.H. (2007). Effects of body size and lifestyle on evolution of
6944 mammal life histories. *Proceedings of the National Academy of Sciences of the United*
6945 *States of America*, 104(45), 17707-17712.

6946 Sibly, R.M. and Brown, J.H. (2009). Mammal reproductive strategies driven by
6947 offspring mortality-size relationships. *The American Naturalist*, 173(6), E185-E199.

6948 Sibly, R.M. *et al*. (2015). Fundamental insights into ontogenetic growth from theory
6949 and fish. *Proceedings of the National Academy of Sciences of the United States of*
6950 *America*, 112(45), 13934-13939.

6951 Siegel, V. (1987). Age and growth of Antarctic Euphausiacea (Crustacea) under
6952 natural conditions. *Marine Biology*, 96(4), 483-495.

6953 Slater, L.M. and Hopcroft, R.R. (2005). Development, growth and egg production of
6954 *Centropages abdominalis* in the eastern subarctic Pacific. *Journal of plankton*
6955 *Research*, 27(1), 71-78.

6956 Smaers, J.B. *et al*. (2018). A cerebellar substrate for cognition evolved multiple times
6957 independently in mammals. *eLife*, 7, e35696.

6958 Smith, R.J. (2009). Use and misuse of the reduced major axis for line-fitting. *American*
6959 *Journal of Physical Anthropology*, 140, 476-486.

6960 Speakman, J.R. (1999). The cost of living: field metabolic rates of small mammals.
6961 *Advances in Ecological Research*, 30, 177–297.

6962 Speakman, J.R. and Król, E. (2010a). Maximal heat dissipation capacity and
6963 hyperthermia risk: neglected key factors in the ecology of endotherms. *Journal of*
6964 *Animal Ecology*, 79(4), 726-746.

6965 Speakman, J.R. and Król, E. (2010b). The heat dissipation limit theory and evolution

of life histories in endotherms - time to dispose of the disposable soma theory? *Integrative and Comparative Biology*, 50(5), 793-807.

Speakman, J.R. and McQueenie, J. (1996). Limits to sustained metabolic rate: The link between food intake, basal metabolic rate, and morphology in reproducing mice, *Mus musculus*. *Physiological Zoology*, 69(4), 746-769.

Speakman, J. Krol, E. and Johnson, M.S. (2004). The functional significance of individual variation in basal metabolic rate. *Physiological and Biochemical Zoology*, 77(6), 900-915.

Spiess, A. and Neumeyer, N. (2010). An evaluation of R^2 as an inadequate measure for nonlinear models in pharmacological and biochemical research: a Monte Carlo approach. *BMC Pharmacology*, **10(**6).

Sprung, M. (1984). Physiological energetics of mussel larvae (*Mytilus edulis*). I. Shell growth and biomass. *Marine Ecology Progress Series*, 17(3), 283-293.

Stephens, P.A. *et al*. (2009). Capital breeding and income breeding: their meaning, measurement, and worth. *Ecology*, 90(8), 2057-2067.

Streicher, J.W. Cox, C.L. and Birchard, G.F. (2012). Non-linear scaling of oxygen consumption and heart rate in a very large cockroach species (*Gromphadorhina portentosa*): Correlated changes with body size and temperature. *Journal of Experimental Biology*, 215(7), 1137-1143.

Strenio, J.F. Weisberg, H.I. and Bryk, A.S. (1983). Empirical Bayes estimation of individual growth curve parameters and their relationship to covariates. *Biometrics*, 39(1), 71-86.

Stumpf, L. Tropea, C. and Greco, L.S.L. (2014). Recovery growth of *Cherax quadricarinatus* period on growth, biochemical composition and activity of digestive enzymes. *Aquaculture*, 433, 404-410.

Sulardiono, B. Prayitno, S.B. and Hendrarto, I.B. (2012). The growth analysis of *Stichopus vastus* (Echinodermata: Stichopodidae) in Karimunjawa waters. *Journal of Coastal Development*, 15, 315-323.

Svetlichny, L. *et al*. (2010). Salinity tolerance of *Calanus euxinus* in the Black and Marmara Seas. *Marine Ecology Progress Series*, 404, 127-138.

6996 Symonds, M.R. and Elgar, M.A. (2002). Phylogeny affects estimation of metabolic
6997 scaling in mammals. *Evolution*, 56(11), 2330-2333.

6998 Tan, H. Hirst, A.G. Glazier, D.S. and Atkinson, D. (2019). Ecological pressures and
6999 the contrasting scaling of metabolism and body shape in coexisting taxa: Cephalopods
7000 versus teleost fish. *Philosophical Transactions of the Royal Society B: Biological*
7001 *Sciences*, 374(1778).

7002 Tang, H. *et al*. (2016). Earthworm (*Eisenia fetida*) behavioral and respiration
7003 responses to sublethal mercury concentrations in an artificial soil substrate. *Applied*
7004 *Soil Ecology*, 104, 48-53.

7005 Taylor, N.G. Walters, C.J. and Martell, S.J. (2005). A new likelihood for
7006 simultaneously estimating von Bertalanffy growth parameters, gear selectivity, and
7007 natural and fishing mortality. *Canadian Journal of Fisheries and Aquatic Science*,
7008 62(1), 215-223.

7009 Thomsen, J. Casties, I. Pansch, C. Körtzinger, A. and Melzner, F. (2013). Food
7010 availability outweighs ocean acidification effects in juvenile *Mytilus edulis*: laboratory
7011 and field experiments. *Global Change Biology*, 19(4), 1017-1027.

7012 Tjørve, K.M.C. and Tjørve, E. (2010). Shapes and functions of bird-growth models:
7013 how to characterise chick postnatal growth. *Zoology*, 113(6), 326-333.

7014 Tjørve, K.M.C. and Tjørve, E. (2017). The use of Gompertz models in growth
7015 analyses, and new Gompertz-model approach: An addition to the Unified-Richards
7016 family. *Public Library of Science,* 12(6), e0178691.

7017 Tripathi, G. and Bhardwaj, P. (2004). Comparative studies on biomass production, life
7018 cycles and composting efficiency of *Eisenia fetida* (Savigny) and *Lampito mauritii*
7019 (Kinberg). *Bioresource Technology*, 92(3), 275-283.

7020 Troedsson, C. *et al*. (2002). Resource allocation between somatic growth and
7021 reproductive output in the pelagic chordate *Oikopleura dioica* allows opportunistic
7022 response to nutritional variation. *Marine Ecology Progress Series*, 243, 83-91.

7023 Tunberg, B.G. and Creswell, R.L. (1991). Development, growth, and survival in the
7024 juvenile Caribbean king crab *Mithrax spinosissimus* (Lamarck) reared in the
7025 laboratory. *Journal of Crustacean Biology*, 11(1), 138-149.

7026 Uvarov, A.V. and Scheu, S. (2004). Effects of temperature regime on the respiratory
7027 activity of developmental stages of *Lumbricus rubellus* (Lumbricidae). *Pedobiologia*,
7028 48(4), 365-371.

7029 Uye, S. (1991). Temperature-dependent development and growth of the planktonic
7030 copepod *Paracalanus* sp. In the laboratory. *Bulletin of Plankton Society of Japan*, 627-
7031 636.

7032 Uye, S. Iwai, Y. and Kasahara, S. (1983). Growth and production of the inshore marine
7033 copepod *Pseudodiaptomus marinus* in the central part of the Inland Sea of Japan.
7034 *Marine Biology*, 73, 91-98.

7035 Uye, S.I. (1988). Temperature-dependent development and growth of *Calanus sinicus*
7036 (Copepoda: Calanoida) in the laboratory. *Hydrobiologia*, 167(1) 285-293.

7037 van der Bijl, W. (2018). Phylopath: Easy phylogenetic path analysis in R. *PeerJ*, 6,
7038 e4718.

7039 van Der Meer, J. (2006a). Metabolic theories in ecology. *Trends in Ecology and*
7040 *Evolution*, 21(3), 136-140.

7041 van der Meer, J. (2006b). An introduction to Dynamic Energy Budget (DEB) models
7042 with special emphasis on parameter estimation. *Journal of Sea Research*, 56(2), 85-
7043 102.

7044 van der Most, P.J. *et al*. (2011). Trade-off between growth and immune function: a
7045 meta-analysis of selection experiments. *Functional Ecology*, 25(1), 74-80.

7046 Venter, J. and Reinecke, A. (1988). The life-cycle of the compost worm *Eisenia fetida*
7047 (Oligochaeta). *South African Journal of Zoology*, 23(3), 161-165.

7048 Verhulst, P.F. (1839). Notice sur la loi que la population suit dans son accroissement.
7049 *Correspondence Mathématique et Physique,* 10, 113-21.

7050 Vidal, J. (1980). Physioecology of zooplankton. I. Effects of phytoplankton
7051 concentration, temperature, and body size on the growth rate of *Calanus pacificus* and
7052 *Pseudocalanus* sp. *Marine Biology*, 56(2), 111-134.

7053 Vijverberg, J. and Koelewijn, H.P. (2004). Effect of temperature on development and
7054 growth of the raptorial cladoceran *Leptodora kindtii* under laboratory conditions.

7055 *Freshwater Biology*, 49(11), 1415-1422.

7056 Vincenzi, S. *et al*. (2016). Trade-offs between accuracy and interpretability in von
7057 Bertalanffy random-effects models of growth. *Ecological Applications*, 26(5), 1535-
7058 1552.

7059 West, G.B. Brown, J.H. and Enquist, B.J. (1997). A general model for the origin of
7060 allometric scaling laws in biology. *Science*, 276(5309), 122-126.

7061 West, G.B. Brown, J.H. and Enquist, B.J. (1999). The fourth dimension of life: Fractal
7062 geometry and allometric scaling of organisms. *Science*, 284(5420), 1677-1679.

7063 West, G.B. Brown, J.H. and Enquist, B.J. (2001). A general model for ontogenetic
7064 growth. *Nature*, 413(6856), 628-631.

7065 White, C.R. (2011). Allometric estimation of metabolic rates in animals. *Comparative*
7066 *Biochemistry and Physiology. A: Molecular and Integrative Physiology*, 158(3), 346-
7067 357.

7068 White, C.R. Blackburn, T.M. and Seymour, R.S. (2009). Phylogenetically informed
7069 analysis of the allometry of mammalian basal metabolic rate supports neither
7070 geometric nor quarter-power scaling. *Evolution*, 63(10), 2658-2667.

7071 White, C.R. and Seymour, R.S. (2003). Mammalian basal metabolic rate is
7072 proportional to body mass$^{2/3}$. *Proceedings of the National Academy of Sciences of the*
7073 *United States of America*, 100(7), 4046-4049.

7074 White, C.R. Cassey, P. and Blackburn, T.M. (2007). Allometric exponents do not
7075 support a universal metabolic allometry. *Ecology*, 88(2), 315-323.

7076 White, C.R. Phillips, N.F. and Seymour, R.S. (2006). The scaling and temperature
7077 dependence of vertebrate metabolism. *Biology Letters*, 2(1), 125-127.

7078 Wilhelm, F.M. (2002). Estimating reproductive effort in small aquatic invertebrates
7079 from lipid dynamics. *Journal of Freshwater Ecology*, 17(4), 595-599.

7080 Willett, J.B. and Singer, J.D. (1988). Another cautionary note about R-squared: Its use
7081 in weighted least-squares regression analysis. *The American Statistician*, 42(3), 236-
7082 238.

Woodward, G. *et al*. (2005). Body size in ecological networks. *Trends in Ecology & Evolution*, 20(7), 402-409.

Yamada, Y. and Ikeda, T. (2000). Development, maturation, brood size and generation length of the mesopelagic amphipod *Cyphocaris challengeri* (Gammaridea: Lysianassidae) off southwest Hokkaido, Japan. *Marine Biology*, 137(5), 933-942.

Yamada, Y. and Ikeda, T. (2000). Development, maturation, brood size and generation length of the mesopelagic amphipod *Cyphocaris challengeri* (Gammaridea: Lysianassidae) off southwest Hokkaido, Japan. *Marine Biology*, 137(5-6), 933-942.

Yan, Y.Y. *et al*. (2007). Numerical modelling of electro-osmotically driven flow within the microthin liquid layer near an earthworm surface-a biomimetic approach. *Proceedings of the Institution of Mechanical Engineers, Part C: Journal of Mechanical Engineering Science*, 221(10), 1201-1210.

Yuancai, L. Marques, C.P. and Macedo, F.W. (1997). Comparison of Schnute's and Bertalanffy-Richards' growth functions. *Forest Ecology & Management*, 96(3), 283-288.